

Final Report

**Development, Application, and Evaluation of an
Advanced Photochemical Air Toxics Modeling System**

CRC Project A-42-2

Prepared for:

Coordinating Research Council, Inc.
3650 Mansell Road, Suite 140
Alpharetta, Georgia 30022

and

US Department of Energy
Office of Heavy Vehicle Technologies

funded through

National Renewable Energy Laboratory
1617 Cole Blvd.
Golden, Colorado 80401

Prepared by

ENVIRON International Corporation
101 Rowland Way
Novato, California 94945

September 27, 2002

ACKNOWLEDGEMENTS

This report represents the cumulating of research and input from several different groups. The Coordinating Research Council (CRC) Atmospheric Impacts Committee headed by Mr. Brent Bailey provided numerous valuable inputs. Dr. Doug Lawson of the Department of Energy (DOE) National Renewable Energy Laboratory also provided valuable comments. The MATES-II application could not have been performed without the data from the groundbreaking work of the South Coast Air Quality Management District (SCAQMD). Finally, the extension of CAMx to treat air toxics is possible due to the previous work of the ENVIRON CAMx development team. The CAMx air toxics model development study was led by Ralph Morris of ENVIRON with participation of several ENVIRON staff including Greg Yarwood, Gary Wilson, Ed Tai, and Steven Lau.

TABLE OF CONTENTS

| | Page |
|--|-------------|
| EXECUTIVE SUMMARY | ES-1 |
| Introduction | ES-1 |
| Approach | ES-2 |
| Application and Evaluation Using the MATES-II Annual Database | ES-6 |
| Application and Evaluation Using the August 1997 SCOS Database | ES-20 |
| Conclusions..... | ES-25 |
| 1. INTRODUCTION | 1-1 |
| Background..... | 1-1 |
| CRC/DOE Review of Air Toxics Modeling | 1-2 |
| Objectives | 1-3 |
| Overview of Approach | 1-3 |
| 2. DEVELOPMENT OF MODEL INPUTS | 2-1 |
| Modeling Domain | 2-1 |
| Meteorological Inputs..... | 2-1 |
| Air Quality Data..... | 2-2 |
| Initial and Boundary Conditions | 2-3 |
| Emissions | 2-6 |
| 3. IMPLEMENTATION OF AIR TOXICS MODELING CAPABILITY INTO CAMx | 3-1 |
| CAMx Reactive Tracer Implementation | 3-1 |
| Subgrid-scale Near-Source Modeling | 3-7 |
| 4. CAMx AIR TOXICS MODELING RESULTS USING THE MATES-II DATABASE | 4-1 |
| Model Performance Evaluation | 4-2 |
| Spatial Distribution of Air Toxic Concentrations | 4-8 |
| Summary of Model Performance | 4-11 |
| Risk Calculation and Exposure Modeling | 4-12 |

| | |
|---|------------|
| 5. SUBGRID-SCALE NEAR-SOURCE IMPACTS | 5-1 |
| Demonstration of the Subgrid-Scale Near-Source Treatment Using the Mates-II Database | 5-1 |
| 6. CAMx AIR TOXICS TESTS USING THE AUGUST 1997 SCOS EPISODE..... | 6-1 |
| PAMS Observations Database..... | 6-2 |
| August 1997 CAMx/RTRAC Air Toxics Simulation..... | 6-4 |
| Model Performance Evaluation | 6-4 |
| CB-IV Versus SAPRC99 Chemistry Comparisons | 6-12 |
| Risk Comparisons | 6-19 |
| 7. SUMMARY, CONCLUSIONS, AND RECOMMENDATIONS | 7-1 |
| Summary | 7-1 |
| Conclusions..... | 7-1 |
| Recommendations | 7-4 |
| 8. REFERENCES | 8-1 |
| 9. GLOSSARY OF ABBREVIATIONS/ACRONYMS | 9-1 |

APPENDICES

| |
|--|
| Appendix A: Scatter Plots of Predicted and Observed 24-Hour Concentrations from the MATES-II Database |
| Appendix B: Spatial Distribution of Annual Average Concentrations Estimated by CAMx/EMFAC2000 |

TABLES

| | |
|--|------|
| Table ES-1. Emissions adjustment factors used to update the MATES-II EMFAC7G on-road mobile source emissions to EMFAC2000 levels. | ES-4 |
| Table ES-2. Summary of annual air toxics emission totals (lb/day) for the South Coast Air Basin (SoCAB) from MATES-II using EMFAC7G and updated using EMFAC2000..... | ES-4 |
| Table ES-3. Summary air toxics model performance statistics using the MATES-II database..... | ES-8 |

| | | |
|-------------|--|-------|
| Table ES-4. | Average risk across the 10 MATES-II sites calculated in MATES-II (all toxic compounds with no indoor/outdoor effect) and by this study (missing some MATES-II air toxic compounds that accounted for 10% of the risk) with no indoor/outdoor (I/O) effects and accounting for indoor/outdoor effects on an annual average and hourly basis. | ES-17 |
| Table ES-5. | Comparison of the estimated exposure to air toxics using the 10-site average risk and basin-wide population versus using spatially varying risk and spatially varying population with and without accounting for indoor/outdoor (I/O) effects. | ES-18 |
| Table ES-6. | Summary of CAMx/RTRAC subgrid-scale point source modeling annual results for the MATES-II air toxics point sources. | ES-20 |
| Table ES-7. | Comparison of the 10 station average one in a million risks using the benzene, 1,3-butadiene, acetaldehyde, and formaldehyde average concentration estimates by the CAMx/CB4 and CAMx/S99 RTRAC modeling of the August 1997 SCOS episode. | ES-24 |
| Table ES-8. | Comparison of the 10 station average one in a million risks by major source category from the 4-day average organic air toxic concentration estimates by the CAMx/CB4 and CAMx/S99 RTRAC modeling of the August 1997 SCOS episode. | ES-25 |
| Table 2-1. | Initial and boundary conditions used for the CAMx/RTRAC air toxics modeling | 2-3 |
| Table 2-2. | Emissions adjustment factors used to update the MATES-II EMFAC7G on-road mobile source emissions to EMFAC2000 levels..... | 2-7 |
| Table 2-3. | Summary of annual air toxics emission totals (lb/day) for the South Coast Air Basin (SoCAB) from MATES-II using EMFAC7G and updated using EMFAC2000..... | 2-8 |
| Table 4-1. | Summary model performance evaluation statistics for benzene (predicted minus observed, positive bias implies overprediction)..... | 4-3 |
| Table 4-2. | Summary model performance evaluation statistics for 1,3-butadiene (predicted minus observed, positive bias implies overprediction)..... | 4-4 |
| Table 4-3. | Summary model performance evaluation statistics for acetaldehyde (predicted minus observed, positive bias implies overprediction)..... | 4-5 |
| Table 4-4. | Summary model performance evaluation statistics for formaldehyde (predicted minus observed, positive bias implies overprediction)..... | 4-5 |
| Table 4-5. | Summary model performance evaluation statistics for chromium PM _{2.5} (predicted minus observed, positive bias implies overprediction). | 4-6 |
| Table 4-6. | Summary model performance evaluation statistics for hexavalent Chromium PM _{2.5} (predicted minus observed, positive bias implies overprediction). | 4-7 |
| Table 4-7. | Summary model performance evaluation statistics for elemental Carbon PM _{2.5} (predicted minus observed, positive bias implies overprediction). | 4-7 |

| | | |
|------------|---|------|
| Table 4-8. | Average risk across the 10 MATES-II sites calculated in MATES-II (no indoor/outdoor effect) and by this study with no indoor/outdoor (I/O) effects and accounting for indoor/outdoor effects on an annual average and hourly. | 4-14 |
| Table 4-9. | Comparison of the estimated number of premature deaths due to exposure to air toxics using the 10-site average risk and basin-wide population versus using spatially varying risk and spatially varying population with and without accounting for indoor/outdoor (I/O) effects. | 4-15 |
| Table 5-1. | Location, stack parameters, and emissions for the five point source complexes in the MATES-II modeling database that had air toxics emissions. | 5-2 |
| Table 5-2. | Summary of CAMx/RTRAC subgrid-scale near-source modeling annual results for the MATES-II air toxics point sources | 5-5 |
| Table 6-1. | Locations of the six PAMS sites operating in the SoCAB during summer 1997. | 6-2 |
| Table 6-2. | Comparison of the 10 station average one in a million risks using the benzene, 1,3-butadiene, acetaldehyde, and formaldehyde average concentration estimates by the CAMx/CB4 and CAMx/S99 RTRAC modeling of the August 1997 SCOS episode. | 6-20 |
| Table 6-3. | Comparison of the 10 station average one in a million risks by major source category from the 4-day average organic air toxic concentration estimates by the CAMx/CB4 and CAMx/S99 RTRAC modeling of the August 1997 SCOS episode. | 6-21 |

FIGURES

| | | |
|---------------|---|-------|
| Figure ES-1a. | Scatter plot of predicted and observed 24-hour benzene concentrations (ug/m3) for the SoCAB and MATES-II April 1998 – March 1999 period and the UAM-Tox /7G (top) and CAMx/7G (bottom) models. | ES-9 |
| Figure ES-1b. | Scatter plot of predicted and observed 24-hour formaldehyde concentrations (ug/m3) for the SoCAB and MATES-II April 1998 – March 1999 period and the UAM-Tox /7G (top) and CAMx/7G (bottom) models | ES-10 |
| Figure ES-1c. | Scatter plot of predicted and observed 24-hour hexavalent chromium concentrations (ug/m3) for the SoCAB and MATES-II April 1998 – March 1999 period and the UAM-Tox /7G (top) and CAMx/7G (bottom) models. | ES-11 |
| Figure ES-2a. | Annual average benzene (top) and 1,3-butadiene (bottom) concentrations (ppm) in the SoCAB estimated by the CAMx/EMFAC2000 | ES-13 |

| | |
|--|-------|
| Figure ES-2b. Annual average primary formaldehyde (top) and secondary formaldehyde (bottom) concentrations (ppm) in the SoCAB estimated by the CAMx/EMFAC2000. | ES-14 |
| Figure ES-2c. Ratio of annual average primary to total formaldehyde concentrations (top) and annual average diesel PM _{2.5} concentrations (ug/m ³) (bottom) concentrations (ppm) in the SoCAB estimated by the CAMx/EMFAC2000. | ES-15 |
| Figure ES-2d. Annual average hexavalent chromium PM _{2.5} (top) and hexavalent chromium PM _{2.5-10} (bottom) concentrations (ppm) in the SoCAB estimated by the CAMx/EMFAC2000. | ES-16 |
| Figure ES-3a. Time series of observed and estimated hourly benzene concentrations during August 3-7, 1997 at the Pico Rivera (top) and Upland (bottom) PAMS sites using the CAMx air toxics modeling system with the CB-IV (CB4) and SAPRC99 (S99) chemistry mechanisms. | ES-22 |
| Figure ES-3b. Time series of observed and estimated hourly acetaldehyde (top) and formaldehyde (bottom) concentrations during August 3-7, 1997 at the Pico Rivera PAMS site using the CAMx air toxics modeling systems with the CB-IV (CB4) and SAPRC99 (S99) chemistry mechanisms. | ES-23 |
| Figure 2-1. Location of surface meteorological (red x), upper-air meteorological (blue diamonds), and precipitation (green boxes) sites in the SoCAB used for the April 1998 – March 1999 CALMET modeling. | 2-4 |
| Figure 2-2. Location of the 10 MATES-II fixed sites air toxics samplers | 2-5 |
| Figure 3-1. Example RTRAC chemistry input file for modeling the MATES toxic species using CB4 as the host mechanism. | 3-5 |
| Figure 3-2. Example RTRAC chemistry input file for modeling toxic species with SAPRC99 as the host mechanism. | 3-6 |
| Figure 3-3. Example RTRAC receptor input file identifying the grid cells with locations of point source complexes where hourly decay rates will be output for subgrid-scale point source modeling. | 3-7 |
| Figure 4-1a. Spatial distribution of estimated risk (out of a million) not accounting for indoor/outdoor effects. | 4-16 |
| Figure 4-1b. Spatial distribution of estimated risk (out of a million) accounting for indoor/outdoor effects on an annual basis. | 4-17 |
| Figure 4-1c. Spatial distribution of estimated risk (out of a million) accounting for indoor/outdoor effects on an hourly basis. | 4-18 |
| Figure 4-2a. Spatial distribution of mortalities (people) not accounting for indoor/outdoor effects. | 4-19 |
| Figure 4-2b. Spatial distribution of mortalities (people) accounting for indoor/outdoor effects on an annual basis. | 4-20 |
| Figure 4-2c. Spatial distribution of mortalities (people) accounting for indoor/outdoor effects on an hourly basis. | 4-21 |
| Figure 5-1. Location of point source complexes treated by the subgrid-scale plume model. | 5-3 |

| | | |
|--------------|--|------|
| Figure 6-1. | Location of PAMS monitors in the SoCAB operating during the August 1997 SCOS episode. | 6-3 |
| Figure 6-2a. | Comparison of predicted and observed benzene concentrations on August 3-7, 1997 at the Azusa (top) and Banning (bottom) PAMS sites using CAMx/CB4 and CAMx/SAPRC99 (S99) model configurations. | 6-7 |
| Figure 6-2b. | Comparison of predicted and observed benzene concentrations on August 3-7, 1997 at the Hawthorne (top) and Los Angeles – North Main (bottom) PAMS sites using CAMx/CB4 and CAMx/SAPRC99 (S99) model configurations. | 6-8 |
| Figure 6-2c. | Comparison of predicted and observed benzene concentrations on August 3-7, 1997 at the Pico Rivera (top) and Upland (bottom) PAMS sites using CAMx/CB4 and CAMx/SAPRC99 (S99) model configurations. | 6-9 |
| Figure 6-3. | Comparison of predicted and observed acetaldehyde concentrations on August 3-7, 1997 at the Pico Rivera PAMS site using CAMx/CB4 and CAMx/SAPRC99 (S99) model configurations. | 6-10 |
| Figure 6-4. | Comparison of predicted and observed formaldehyde concentrations on August 3-7, 1997 at the Pico Rivera PAMS site using CAMx/CB4 and CAMx/SAPRC99 (S99) model configurations. | 6-11 |
| Figure 6-5a. | Scatter plot of CAMx/CB-IV (CB4) and CAMx/SAPRC99 (S99) predicted 24-hour average benzene concentrations (ppb) on August 5-7, 1997 at the 10 MATES-II monitoring sites (see Figure 2-2 for locations). | 6-13 |
| Figure 6-5b. | Scatter plot of CAMx/CB-IV (CB4) and CAMx/SAPRC99 (S99) predicted 24-hour average 1,3-butadiene concentrations (ppb) on August 5-7, 1997 at the 10 MATES-II monitoring sites (see Figure 2-2 for locations). | 6-14 |
| Figure 6-5c. | Scatter plot of CAMx/CB-IV (CB4) and CAMx/SAPRC99 (S99) predicted 24-hour average primary acetaldehyde concentrations (ppb) on August 5-7, 1997 at the 10 MATES-II monitoring sites (see Figure 2-2 for locations). | 6-15 |
| Figure 6-5d. | Scatter plot of CAMx/CB-IV (CB4) and CAMx/SAPRC99 (S99) predicted 24-hour average primary formaldehyde concentrations (ppb) on August 5-7, 1997 at the 10 MATES-II monitoring sites (see Figure 2-2 for locations). | 6-16 |
| Figure 6-5e. | Scatter plot of CAMx/CB-IV (CB4) and CAMx/SAPRC99 (S99) predicted 24-hour average secondary acetaldehyde concentrations (ppb) on August 5-7, 1997 at the 10 MATES-II monitoring sites (see Figure 2-2 for locations). | 6-17 |
| Figure 6-5f. | Scatter plot of CAMx/CB-IV (CB4) and CAMx/SAPRC99 (S99) predicted 24-hour average secondary formaldehyde concentrations (ppb) on August 5-7, 1997 at the 10 MATES-II monitoring sites (see Figure 2-2 for locations). | 6-18 |

| | | |
|-------------|---|------|
| Figure 6-6. | Estimated risk due to organic air toxic compounds at the 10 MATES-II sites (see Figure 2-2 for locations), by species estimated by the CAMx/CB-VI (CB4) and CAMx/SAPRC99 (S99) simulations of the August 1997 SCOS episode..... | 6-22 |
| Figure 6-7. | Estimated risk due to organic air toxic compounds at the 10 MATES-II sites (see Figure 2-2 for locations), by major source categories estimated by the CAMx/CB-VI (CB4) and CAMx/SAPRC99 (S99) simulations of the August 1997 SCOS episode | 6-23 |
| Figure 6-8. | Spatial distribution of risks in the SoCAB (in millions) estimated by CAMx/CB-IV (top) and CAMx/SAPRC99 (bottom). | 6-25 |
| Figure 6-9. | Differences in risk (in millions) between the CAMx/CB-IV (CB4) and CAMx/SAPRC99 (S99) air toxics simulations (S99 – CB4). | 6-26 |

EXECUTIVE SUMMARY

INTRODUCTION

Exposure to air toxics and associated risk is an increasing concern in urban areas across the United States (US). Urban air toxics include compounds that have been traditionally associated with gasoline and diesel combustion (mobile sources), such as diesel particles, benzene, 1,3-butadiene, formaldehyde, and acetaldehyde, compounds associated with other industrial activities, such as carbon tetrachloride and hexavalent chromium, and heavy metals (e.g., mercury and cadmium). The US Environmental Protection Agency (EPA) has several programs underway to assess exposure to air toxics and to develop mitigation strategies. The evaluation of alternative control strategies for air toxics is performed using air quality modeling.

Currently EPA recommends that the ISC air quality model be used to assess the impacts of urban air toxic compounds (EPA, 1999). ISC is a steady-state Gaussian plume model that treats transport and dispersion assuming instantaneous transport of pollutants from the source to the receptor and treats chemistry through a constant half-life decay rate. However, such a modeling approach has several limitations for simulating urban air toxics:

- The steady-state Gaussian plume model formulation is not valid for longer downwind distances of over a few kilometers;
- The chemical decay of organic air toxic compounds (e.g., benzene and 1,3-butadiene) depends on atmospheric photochemistry so varies spatially (both horizontally and vertically) and temporally and can not be accurately treated using a single half-life decay;
- The secondary formation of air toxics (e.g., formaldehyde and acetaldehyde) can not be adequately treated by such models; and
- Such models can not address regional-scale and mesoscale air toxics issues.

More recently there have been significant advances in regional/mesoscale photochemical and particulate matter (PM) models. Multi-scale photochemical grid models have been developed that can treat many scales and pollutants addressing both urban and regional-scale ozone, PM, and visibility issues within one modeling framework. When combined with a near-source treatment, such modeling platforms would be ideal for simulating air toxic compounds.

The Coordinating Research Council (CRC) and the Department of Energy (DOE) are interested in advancing the state-of-science for air toxics modeling. CRC/DOE funded Project A-42-1 to review air toxics modeling techniques and make recommendations for improvements (Seigneur, Lohman, and Pun, 2001). This was followed by CRC/DOE Project A-42-2 to implement air toxics modeling capability into a state-of-science multi-scale photochemical grid model, which is the subject of this report.

Objective

The objective of the CRC/DOE Project A-42-2 Air Toxics Modeling Study is to advance the state-of-science for air toxics modeling by implementing an air toxics modeling capability into a current state-of-science multi-scale grid model, the Comprehensive Air-quality Model with extensions (CAMx). This implementation accounts for the full chemistry of organic air toxic species, retains the CAMx two-way grid nesting capability so that linked regional-scale and urban-scale modeling can be performed, and accounts for near-source local-scale impacts using a subgrid-scale plume model. The model is tested and evaluated using observed air toxic compound and surrogate species concentrations from the 1998-1999 Multiple Air Toxics and Exposure Study (MATES-II, SCAQMD, 2000) and for the August 1997 Southern California Ozone Study (SCOS) episode in the South Coast (Los Angeles) Air Basin (SoCAB).

APPROACH

The development and testing of the advanced air toxics modeling system involved the following activities:

- Implementation of the reactive tracer (RTRAC) modeling capability in the CAMx “Probing Tools” infrastructure including an air toxics chemistry module to treat the formation and destruction of reactive air toxic compounds;
- Implementation of code to extract CAMx-estimated hourly air toxic compound decay rates at each vertical layer for user selected receptor locations for use with a near-source model;
- Modification of an existing near-source plume model to accept the hourly air toxic compound decay rates generated by the CAMx air toxics module;
- Development of a three-dimensional hourly air toxics modeling database for the SoCAB and the MATES-II annual (April 1998 – March 1999) sampling period;
- Application and evaluation of the CAMx air toxics modeling system for the SoCAB and the April 1998-March 1999 year using the MATES-II monitoring database and comparison of model performance with the MATES-II UAM-Tox application;
- Development of air toxics modeling inputs for the August 3-7, 1997 SCOS episode and application and evaluation of the CAMx air toxics modeling system including testing of the air toxics modeling capability using both the CB-IV and SAPRC99 photochemical mechanisms;
- Calculation of risk and exposure using both outdoor exposures as well as a simple accounting for indoor/outdoor effects; and
- Documentation of the results in a final report (this document) and delivery of the modeling system and database to CRC/DOE.

Multiple Air Toxics Exposure Study (MATES-II)

During April 1998 to March 1999 an air toxics sampling field study was conducted for the SoCAB as part of the Multiple Air Toxics Exposure Study (MATES-II). The South Coast Air Quality Management District (SCAQMD) applied the UAM-Tox photochemical air toxics grid

model for the MATES-II April 1998-March 1999 annual period. Air toxic concentration estimates were obtained across the SoCAB at 10 fixed sites for approximately 50 air toxic compounds. The UAM-Tox modeling was performed on a 210-km by 120-km modeling domain covering the SoCAB using a horizontal resolution of 2-km and five vertical layers up to a region top of 2-km above ground level (AGL). Hourly three-dimensional meteorological inputs for April 1, 1998 through March 31, 1999 were generated using the CALMET diagnostic meteorological model and surface and upper-air meteorological observations that were then mapped to the UAM format using the CALMETUAM processor. The UAM-Tox emissions inventory inputs were generated by the SCAQMD for the expanded CB-IV chemical mechanism (the TOX mechanism). The TOX mechanism explicitly treats several organic air toxics including benzene, 1,3-butadiene, acetaldehyde, and formaldehyde. The UAM-Tox model was then applied and evaluated against the MATES-II air toxics observations and modeled and observed risk and exposure calculations were made (SCAQMD, 2000). The MATES-II study calculated outdoor or front yard exposure and risk. That is, no indoor effects on exposure was accounted for nor any effects due to the spatial distribution on movement of the population.

Development of CAMx Air Toxics Modeling Inputs for the MATES-II Year

The MATES-II CALMET surface and upper-air meteorological inputs and the UAM-Tox emission inputs for the April 1, 1998 through March 31, 1999 period were requested and acquired from the SCAQMD. The UAM-Tox model was also requested, but the SCAQMD stated that they could not provide the model as it is proprietary. The SCAQMD did provide the MATES-II observations and concurrent UAM-Tox model predictions. Thus, the UAM-Tox model performance was carried through in this study and compared with the CAMx air toxic estimates and performance.

CALMET was run for the April 1998 – March 1999 year to generate hourly three-dimensional meteorological fields. A CALMET-CAMx converter program was acquired from the California Air Resources Board (ARB) and was used to convert the CALMET output to the meteorological variables and formats required by CAMx. CAMx was configured on the same 210-km by 120-km modeling domain with a 2-km horizontal resolution as used by the UAM-Tox. CAMx was set up with 6 vertical layers of spatially and temporally constant thickness up to a region top of 2,000-m AGL. The UAM-Tox TOX chemical mechanism includes several explicit organic air toxic compounds that were combined to generate standard CB-IV chemical mechanism input. Air toxics compounds for the following species were extracted from the MATES-II emissions database for separate modeling by the CAMx reactive tracers (RTRAC):

- Benzene
- 1,3-Butadiene
- Acetaldehyde
- Formaldehyde
- Chromium
- Hexavalent chromium [Cr(VI)]
- Diesel Particulate Matter

- Elemental Carbon

Note that elemental carbon (EC) and chromium are not air toxic compounds, however they are carried as a separate species to assist in the model performance evaluation.

The MATES-II mobile source emissions were updated from EMFAC7G to EMFAC2000. The DTIM traffic demand model output that provides the gridded Vehicles Miles Traveled (VMT) activity data that is used with EMFAC to generate modeling inventories was not available. Thus, the MATES-II EMFAC7G mobile source emission estimates were updated to EMFAC2000 using the seasonal SoCAB-wide adjustment factors given in Table ES-1.

Table ES-1. Emissions adjustment factors used to update the MATES-II EMFAC7G on-road mobile source emissions to EMFAC2000 levels.

| Species | Summer | Winter | Spring/Fall |
|-----------------|--------|--------|-------------|
| VOC | 1.544 | 1.417 | 1.481 |
| NO _x | 1.260 | 1.374 | 1.317 |
| CO | 1.937 | 1.465 | 1.701 |
| PM | 1.081 | 1.081 | 1.081 |

The resultant total air toxics emissions for the EMFAC7G and EMFAC2000 emissions databases are shown in Tables ES-2. The total primary air toxics emissions for the organic species (i.e., benzene, 1,3-butadiene, acetaldehyde and formaldehyde) are 20% to 35% higher using EMFAC2000 over EMFAC7G due to the ~50% increase in emissions from on-road mobile sources (see Table ES-1), whereas the increases in total PM air toxics species (e.g., diesel PM, Cr(VI), etc.) is less than 5% (Table ES-2).

Table ES-2 . Summary of annual air toxics emission totals (lb/day) for the South Coast Air Basin (SoCAB) from MATES-II using EMFAC7G and updated using EMFAC2000.

| Pollutant | On-Road | Off-Road | Point | AB2588 | Area | Total |
|--|---------|----------|-------|--------|---------|---------|
| <i>MATES-II Emissions Based on EMFAC7G</i> | | | | | | |
| Benzene | 21308.8 | 6338.1 | 245.7 | 267.4 | 2379.9 | 30540.0 |
| 1,3-Butadiene | 3852.8 | 1557.0 | 9.7 | 2.0 | 369.9 | 5791.5 |
| Acetaldehyde | 5242.4 | 5403.1 | 45.8 | 57.1 | 185.2 | 10933.6 |
| Formaldehyde | 16270.2 | 15780.1 | 581.2 | 674.4 | 1075.4 | 34381.2 |
| Chromium | 2.3 | 2.6 | 5.0 | 2.2 | 291.1 | 303.3 |
| Hexavalent Chromium | 0.4 | 0.4 | 0.5 | 1.0 | 0.0 | 2.3 |
| Diesel PM | 23042.1 | 18249.6 | 0.0 | 5.4 | 806.0 | 42103.2 |
| Elemental Carbon | 26669.5 | 5586.6 | 762.9 | 0.0 | 25326.7 | 58345.6 |
| <i>Updated Emissions Using EMFAC2000</i> | | | | | | |
| Benzene | 31547.7 | 6338.1 | 245.7 | 267.4 | 2379.9 | 40778.9 |
| 1,3-Butadiene | 5704.1 | 1557.0 | 9.7 | 2.0 | 369.9 | 7642.8 |
| Acetaldehyde | 7761.4 | 5403.1 | 45.8 | 57.1 | 185.2 | 13452.6 |
| Formaldehyde | 24088.0 | 15780.1 | 581.2 | 674.4 | 1075.4 | 42199.1 |
| Chromium | 2.5 | 2.6 | 5.0 | 2.2 | 291.1 | 303.5 |
| Hexavalent Chromium | 0.4 | 0.4 | 0.5 | 1.0 | 0.0 | 2.3 |
| Diesel PM | 24908.5 | 18249.6 | 0.0 | 5.4 | 806.0 | 43969.6 |
| Elemental Carbon | 28829.7 | 5586.6 | 762.9 | 0.0 | 25326.7 | 60505.8 |

Hybrid CAMx Air Toxics Modeling System

The hybrid CAMx air toxics modeling systems consists of two main components:

- The CAMx photochemical grid model with the reactive tracer (RTRAC) treatment of air toxics accounting for full photochemistry effects on air toxics within the grid modeling framework; and
- A new source air quality model to treat the near-source subgrid-scale impacts of air toxics due to local point, area, volume, and line sources using the CAMx estimated hourly chemical delay rates for reactive air toxics.

The CAMx photochemical grid model is first applied to obtain the mesoscale/regional impacts of air toxics. The near-source model is then applied for user selected emission complexes to obtain the near-source air toxics impacts within 1-2-km of the source. The results of the near-source and mesoscale/regional impact of air toxics are then combined using procedures that avoids double counting.

Implementation of Reactive Tracers in CAMx

The CAMx model was modified to treat reactive tracers (RTRAC). The reactive tracers operate in parallel to the host photochemical grid model extracting information on chemical transformation and deposition that are applied to the air toxic reactive tracers. There were several objectives in the implementation of an air toxics modeling capability into CAMx:

- Implement state-of-science (SOS) treatment of air toxic compounds including full atmospheric chemistry of reactive air toxics and species-dependent and size resolved deposition;
- Ability to treat both the regional and urban-scale impacts of air toxics using a flexible two-way nested-grid photochemical grid model modeling framework;
- Ability to treat the near-source impacts of air toxic fence-line or hot-spot impacts using a subgrid-scale near-source model;
- Ease of use and ease of extension to additional air toxics; and
- Demonstrate the advanced air toxics modeling system using the 1998/1999 annual MATES-II database for the South Coast Air Basin (SoCAB).

The extension of the CAMx modeling system to treat air toxics including the following activities:

- Implementation of the reactive tracer (RTRAC) approach in CAMx that carries air toxic compounds in parallel to the host photochemical grid model, extracts information on chemical formation and decay of air toxics from the host model chemistry, and deposits the air toxics using gaseous or particle deposition rules.
- Extraction of hourly air toxics decay rates from the CAMx chemical mechanism at selected locations that can be used with a near-source model.

- Modification of a near-source model to use the CAMx generated air toxic hourly decay rates.
- Develop pre- and post-processing software to combine air toxics for different families of tracers, compare results with observations, and combine the grid model and near-source modeling results.

APPLICATION AND EVALUATION USING THE MATES-II ANNUAL DATABASE

The CALMET meteorological model was applied for the April 1998 – March 1999 period and used with the CAMx air toxics modeling system to simulate air toxic concentrations. There were numerous problems with the CALMET meteorological fields because the winds, temperature, pressure, and density were frequently inconsistent with each other so that they were not dynamically balanced producing unrealistic vertical velocities.

Model estimated air toxics concentrations for the April 1998-March 1999 period and the SoCAB region were evaluated against the MATES-II 24-hour air toxics observations for three photochemical grid model configurations:

- The MATES-II UAM-Tox results provided by the SCAQMD using EMFAC7G emissions (UAM-Tox/7G)
- CAMx/RTRAC results using EMFAC7G emissions (CAMx/7G); and
- CAMx/RTRAC results using EMFAC2000 emissions (CAMx/2000).

Statistical Performance Evaluation

There are no recommended performance goals for air toxic compounds. EPA has published performance goals for ozone modeling (EPA, 1991), however the ozone performance goals and measures are inappropriate for air toxics. Seigneur, Lohman, and Pun (2001) have noted that the accuracy of the emissions for organic air toxics compounds is around a factor of 2 or 3.

Table ES-3 provides summary model performance evaluation measures for the seven “air toxic” species measured in MATES-II and modeled using the CAMx/RTRAC and the UAM-Tox. Scatter plots of the predicted and observed 24-hour benzene, formaldehyde, and hexavalent chromium concentrations and the UAM-Tox/7G and CAMx/7G model configurations are shown in Figure ES-1. All three model configurations estimate the average observed benzene within a factor of 2, with UAM-Tox exhibiting a near zero bias and CAMx/EMFAC7G and CAMx/EMFAC2000 exhibiting an overestimation tendency of approximately 20 and 55 percent, respectively.

All three model configurations underestimate the average observed 1,3-butadiene concentrations by 40% to 55%, with the UAM-Tox/7G and CAMx/2000 approximate 40% underprediction bias being lower than CAMx/7G bias (55%). However, all three models underestimate the average observed 1,3-butadiene concentrations by approximately a factor of 2.

The UAM-Tox and CAMx exhibit very different performance for carbonyls. UAM-Tox/7G underestimates acetaldehyde and formaldehyde by 65% and 30%, respectively, whereas CAMx exhibits an overprediction tendency of approximately 60% to 50%, respectively. The higher mobile source VOC emissions from EMFAC2000 (Tables ES-1 and ES-2) exacerbate the CAMx carbonyl overestimation tendency. Figure ES-1b displays the UAM-Tox/7G and CAMx/7G scatter plots of predicted and observed formaldehyde concentrations that illustrate the different tendencies of the two models toward under- and over-prediction, respectively. UAM-Tox/7G never estimates 24-hour formaldehyde concentrations greater than 10 ppb although there are numerous (~ 30) observed values, whereas CAMx/7G estimates several (~ 10) 24-hour formaldehyde concentrations greater than 20 ppb although no such observations ever occur. Formaldehyde and acetaldehyde in the CB-IV chemical mechanism are lumped species so contains mass associated with other species than pure formaldehyde or acetaldehyde, thus one would expect the model to overestimate the observed carbonyls concentrations.

Chromium and hexavalent chromium [Cr(VI)] are severely overestimated by all three model configurations. UAM-Tox/7G overestimates the average chromium and Cr(VI) concentrations by approximately a factor of 4, whereas the CAMx overprediction tendency is a factor of 2-2.5 on average. The scatter plot of predicted and observed 24-hour Cr(VI) concentrations (Figure ES-1c) reveals that many of the observed values are reproduced by a factor of 2, but there are some observed values that are overestimated by over a factor of 10.

Much better model performance is seen for the three model's ability to predict the observed elemental carbon (EC) concentrations (Table ES-3). On average the models reproduce EC to within 20% and most of the 24-hour average EC observations are estimated to within a factor of 2.

Table ES-3. Summary air toxics model performance statistics using the MATES-II database.

| | UAM-Tox | CAMx 7G | CAMx 2000 |
|---|---------|---------|-----------|
| <i>Benzene Concentrations</i> | | | |
| N | 499 | 499 | 499 |
| Average Observed ($\mu\text{g}/\text{m}^3$) | 3.5793 | 3.5793 | 3.5793 |
| Average Predicted ($\mu\text{g}/\text{m}^3$) | 3.5715 | 4.3340 | 5.5540 |
| Bias ($\mu\text{g}/\text{m}^3$) | -0.0078 | 0.7546 | 1.9747 |
| Gross Error ($\mu\text{g}/\text{m}^3$) | 1.6544 | 2.0886 | 2.8501 |
| Ratio Avg Pred/Avg Obs | 0.998 | 1.211 | 1.552 |
| <i>1,3-Butadiene Concentrations</i> | | | |
| N | 499 | 499 | 499 |
| Average Observed ($\mu\text{g}/\text{m}^3$) | 0.9987 | 0.9987 | 0.9987 |
| Average Predicted ($\mu\text{g}/\text{m}^3$) | 0.6238 | 0.4508 | 0.6081 |
| Bias ($\mu\text{g}/\text{m}^3$) | -0.3749 | -0.5479 | -0.3906 |
| Gross Error ($\mu\text{g}/\text{m}^3$) | 0.5585 | 0.6436 | 0.5983 |
| Ratio Avg Pred/Avg Obs | 0.625 | 0.451 | 0.609 |
| <i>Acetaldehyde Concentrations</i> | | | |
| N | 490 | 490 | 490 |
| Average Observed ($\mu\text{g}/\text{m}^3$) | 3.0470 | 3.0470 | 3.0470 |
| Average Predicted ($\mu\text{g}/\text{m}^3$) | 1.0776 | 4.9222 | 5.5758 |
| Bias ($\mu\text{g}/\text{m}^3$) | -1.9695 | 1.8751 | 2.5287 |
| Gross Error ($\mu\text{g}/\text{m}^3$) | 2.1534 | 2.4679 | 2.9601 |
| Ratio Avg Pred/Avg Obs | 0.354 | 1.615 | 1.830 |
| <i>Formaldehyde Concentrations</i> | | | |
| N | 502 | 502 | 502 |
| Average Observed ($\mu\text{g}/\text{m}^3$) | 4.8413 | 4.8413 | 4.8413 |
| Average Predicted ($\mu\text{g}/\text{m}^3$) | 3.3549 | 7.4321 | 9.1052 |
| Bias ($\mu\text{g}/\text{m}^3$) | -1.4864 | 2.5908 | 4.2639 |
| Gross Error ($\mu\text{g}/\text{m}^3$) | 2.6984 | 4.0573 | 5.2589 |
| Ratio Avg Pred/Avg Obs | 0.693 | 1.535 | 1.881 |
| <i>Chromium Concentrations $\text{PM}_{2.5}$</i> | | | |
| N | 429 | 429 | 429 |
| Average Observed ($\mu\text{g}/\text{m}^3$) | 4.8157 | 4.8157 | 4.8157 |
| Average Predicted ($\mu\text{g}/\text{m}^3$) | 18.1940 | 12.5408 | 12.5488 |
| Bias ($\mu\text{g}/\text{m}^3$) | 13.3783 | 7.7251 | 7.7331 |
| Gross Error ($\mu\text{g}/\text{m}^3$) | 13.8582 | 9.7482 | 9.7548 |
| Ratio Avg Pred/Avg Obs | 3.778 | 2.604 | 2.606 |
| <i>Hexavalent Chromium Concentrations $\text{PM}_{2.5}$</i> | | | |
| N | 486 | 486 | 486 |
| Average Observed ($\mu\text{g}/\text{m}^3$) | 0.1807 | 0.1807 | 0.1807 |
| Average Predicted ($\mu\text{g}/\text{m}^3$) | 0.7334 | 0.3820 | 0.3874 |
| Bias ($\mu\text{g}/\text{m}^3$) | 0.5527 | 0.2013 | 0.2067 |
| Gross Error ($\mu\text{g}/\text{m}^3$) | 0.6175 | 0.2903 | 0.2944 |
| Ratio Avg Pred/Avg Obs | 4.059 | 2.114 | 2.144 |
| <i>Elemental Carbon Concentrations $\text{PM}_{2.5}$</i> | | | |
| N | 426 | 426 | 426 |
| Average Observed ($\mu\text{g}/\text{m}^3$) | 3.3912 | 3.3912 | 3.3912 |
| Average Predicted ($\mu\text{g}/\text{m}^3$) | 3.9072 | 3.9214 | 3.9496 |
| Bias ($\mu\text{g}/\text{m}^3$) | 0.5161 | 0.5302 | 0.5584 |
| Gross Error ($\mu\text{g}/\text{m}^3$) | 1.5177 | 1.7196 | 1.7332 |
| Ratio Avg Pred/Avg Obs | 1.152 | 1.156 | 1.165 |

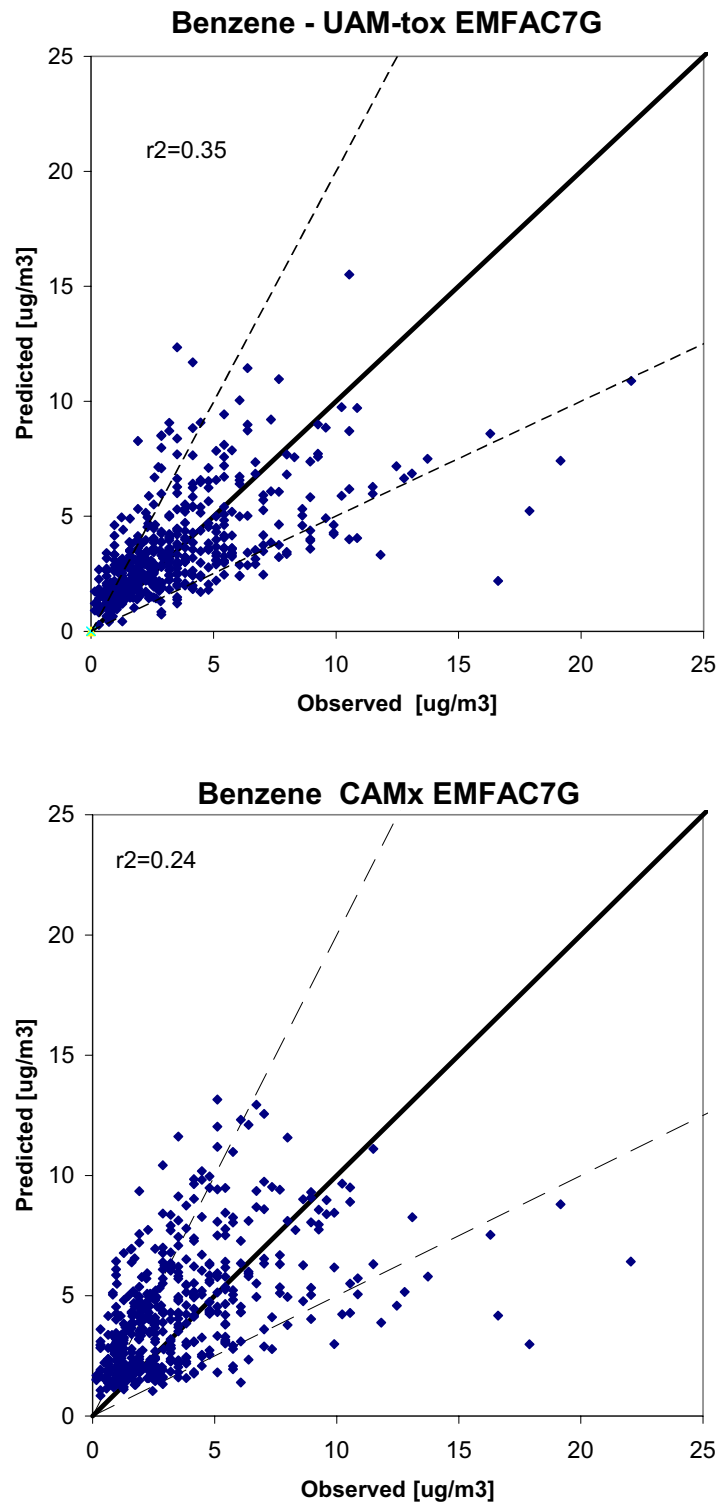


Figure ES-1a. Scatter plot of predicted and observed 24-hour benzene concentrations ($\mu\text{g}/\text{m}^3$) for the SoCAB and MATES-II April 1998 – March 1999 period and the UAM-Tox/7G (top) and CAMx/7G (bottom) models.

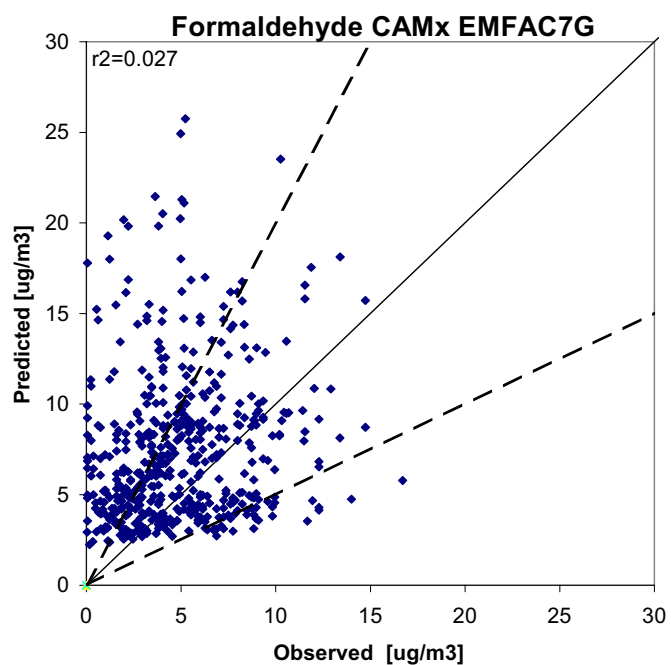
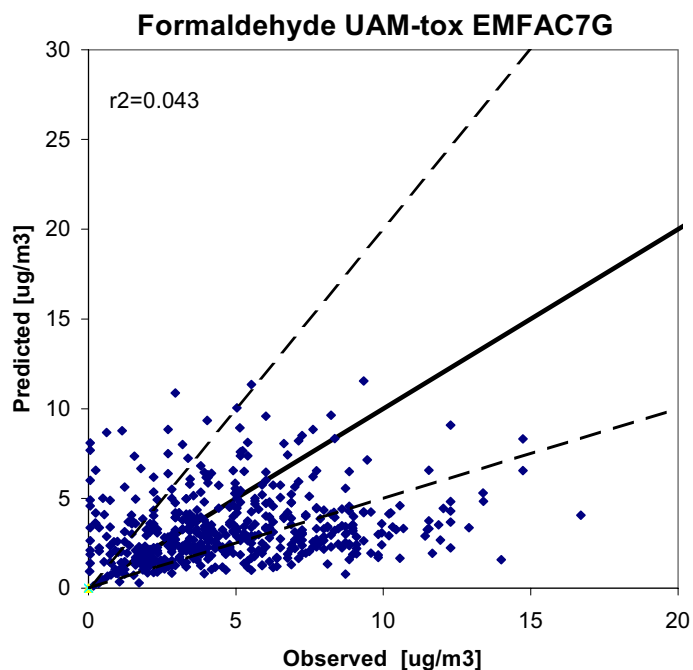


Figure ES-1b. Scatter plot of predicted and observed 24-hour formaldehyde concentrations ($\mu\text{g}/\text{m}^3$) for the SoCAB and MATES-II April 1998 – March 1999 period and the UAM-Tox/7G (top) and CAMx/7G (bottom) models

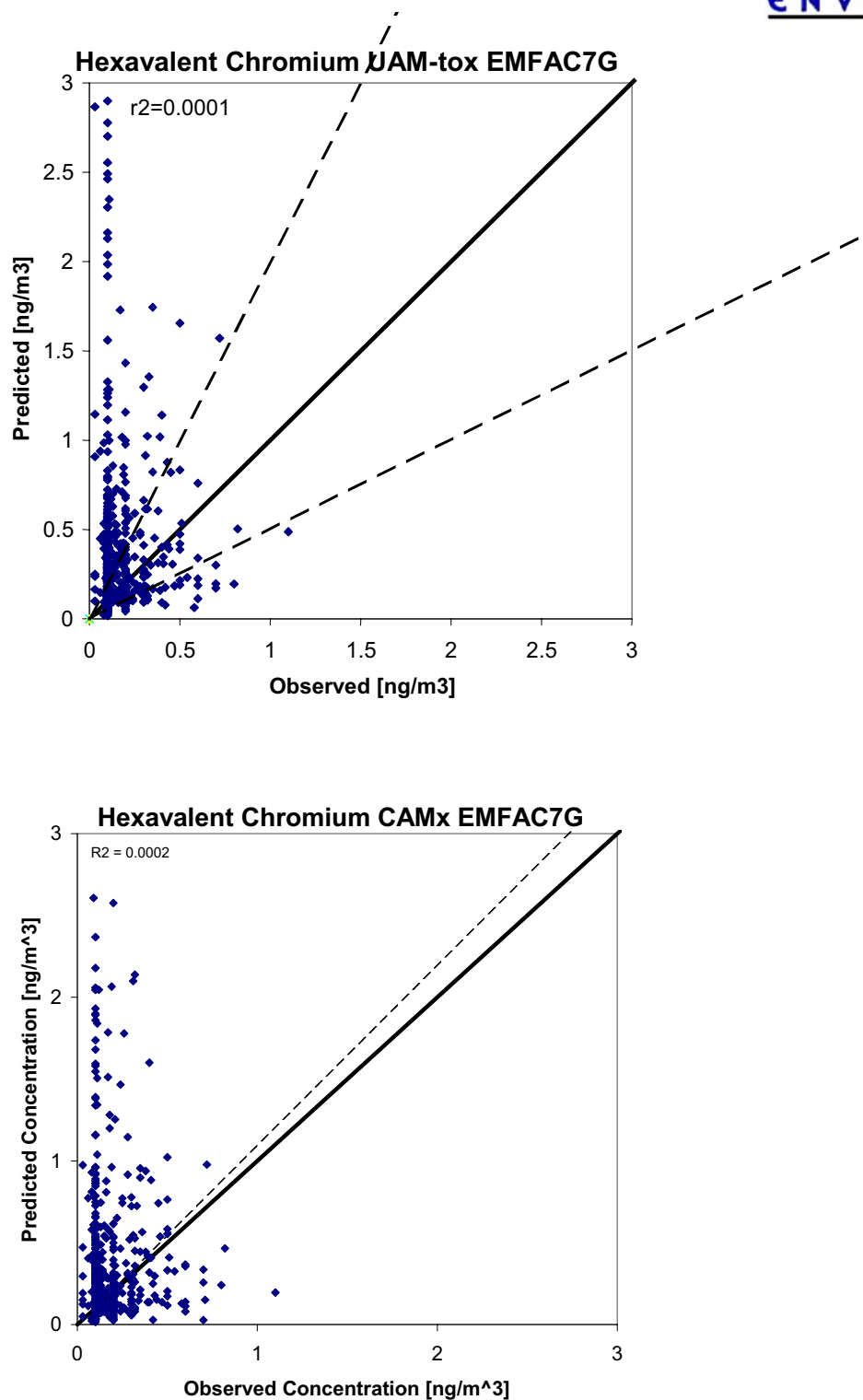


Figure ES-1c. Scatter plot of predicted and observed 24-hour hexavalent chromium concentrations ($\mu\text{g}/\text{m}^3$) for the SoCAB and MATES-II April 1998 – March 1999 period and the UAM-Tox/7G (top) and CAMx/7G (bottom) models.

Spatial Distribution of Air Toxic Compound Estimates

Figure ES-2a displays the spatial distribution of the annual average CAMx/2000 estimated benzene and 1,3-butadiene concentrations. The footprint of the major roadways is clearly evident in the spatial distribution of the benzene concentrations. The highest estimated benzene concentrations occur in downtown Los Angeles and Anaheim, as well as at the LAX airport. This is in contrast to the spatial distribution of 1,3-butadiene where by far the largest concentrations occur at the LAX airport.

Figure ES-2b and ES-2c display the spatial distribution of primary formaldehyde, secondary formaldehyde, and the ratio of primary to secondary formaldehyde concentrations. There are two major hot spots of primary formaldehyde concentrations (> 3 ppb) that occur at the LAX airport (maximum of 7.7 ppb) on the coast near El Segundo and at the port area near Long Beach. Lower hot spots of primary formaldehyde, in the 1-3 ppb range, occur over the downtown areas of Los Angeles and Anaheim. Over most of the rest of the domain, primary formaldehyde concentrations are much less than 1 ppb. Except for the two hot spot locations, secondary formaldehyde has a higher contribution to the total formaldehyde concentrations, with a maximum concentration of 8.8 ppb occurring over the San Bernardino Mountains.

The spatial distribution of the roadways are clearly evident in the annual average diesel fine particulate matter concentrations (Figure ES-2c, bottom). However, by far the largest diesel $PM_{2.5}$ source area is the port area near Long Beach. Diesel PM emissions from marine vessels are believed to be the largest contributor at this location although trucks, cranes and other sources associated with the port operations also contribute.

Finally, Figure ES-2d shows the spatial distribution of Cr(VI) concentrations in the fine (top) and coarse (bottom) PM modes. Unlike the other air toxics, whose spatial distributions followed roadways and or were associated with the airport or port areas, the spatial distribution of Cr(VI) concentrations are highly localized spikes, that are likely associated with local chrome plating operations. The coarse mode Cr(VI) concentrations are higher than the fine mode Cr(VI) and the coarse mode Cr(VI) spikes are more prevalent than the fine mode Cr(VI) spikes. As the MATES-II monitoring only analyzed fine mode Cr(VI), the fine mode is much lower than the coarse mode, then this raises questions on the adequacy of the MATES-II fine model only Cr(VI) observation database for model evaluation and risk assessment.

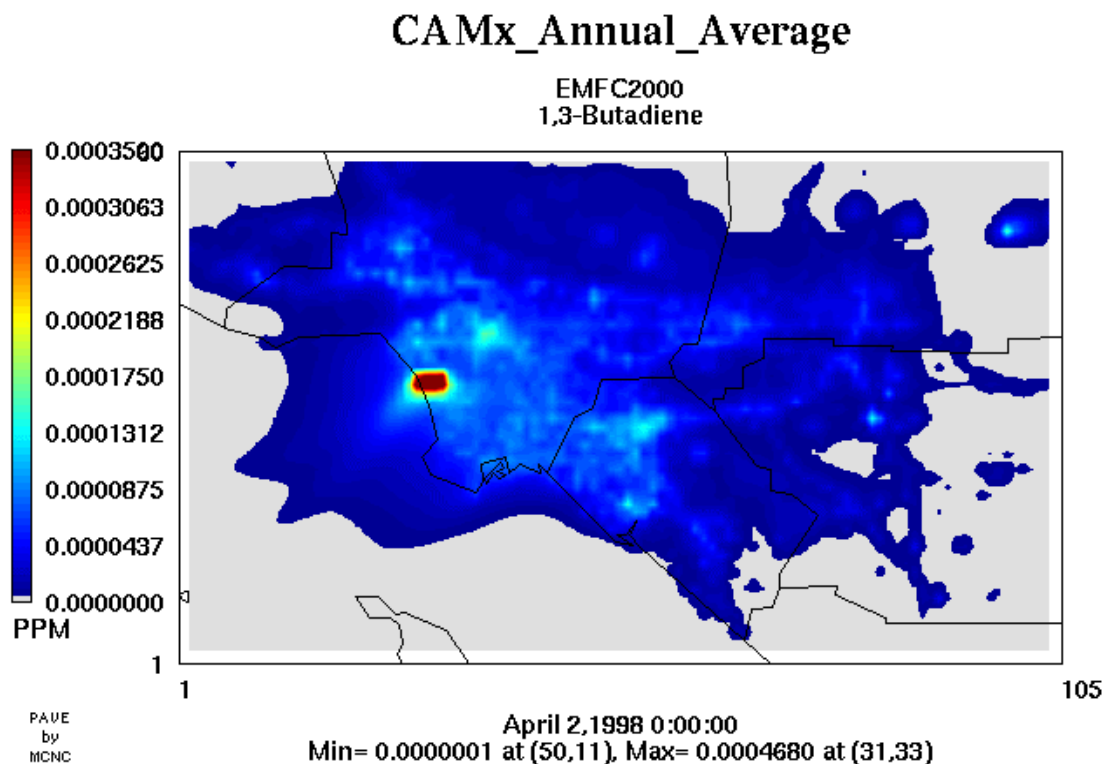
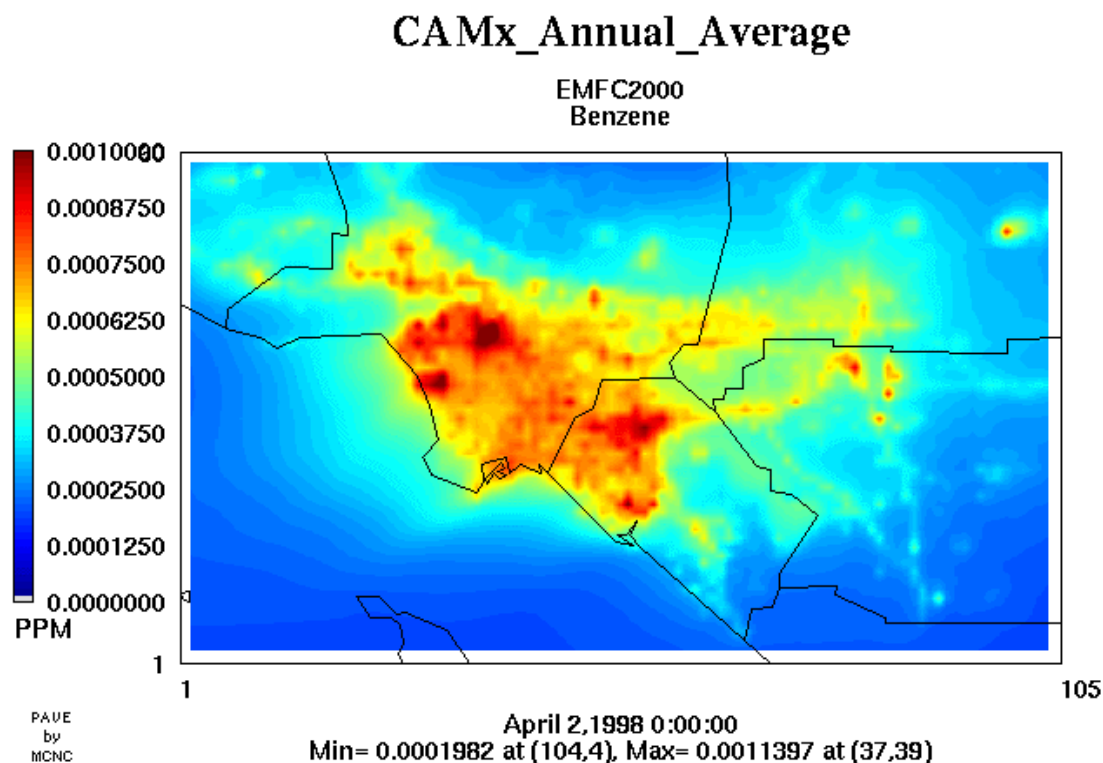


Figure ES-2a. Annual average benzene (top) and 1,3-butadiene (bottom) concentrations (ppm) in the SoCAB estimated by the CAMx/EMFAC2000.

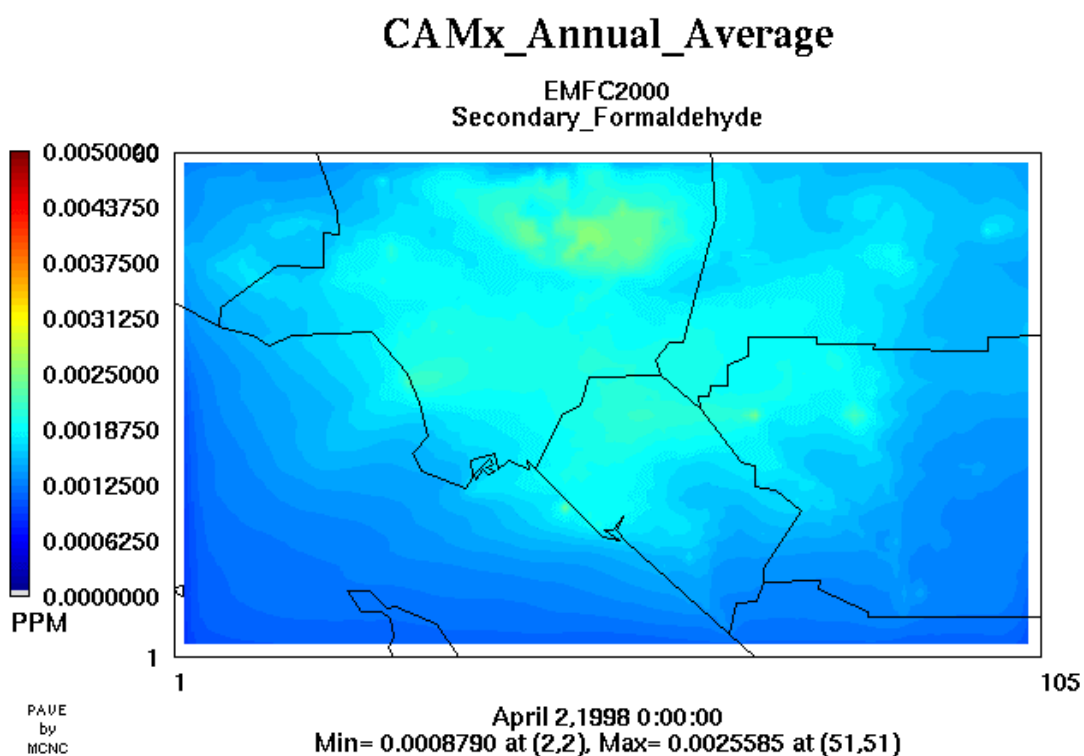
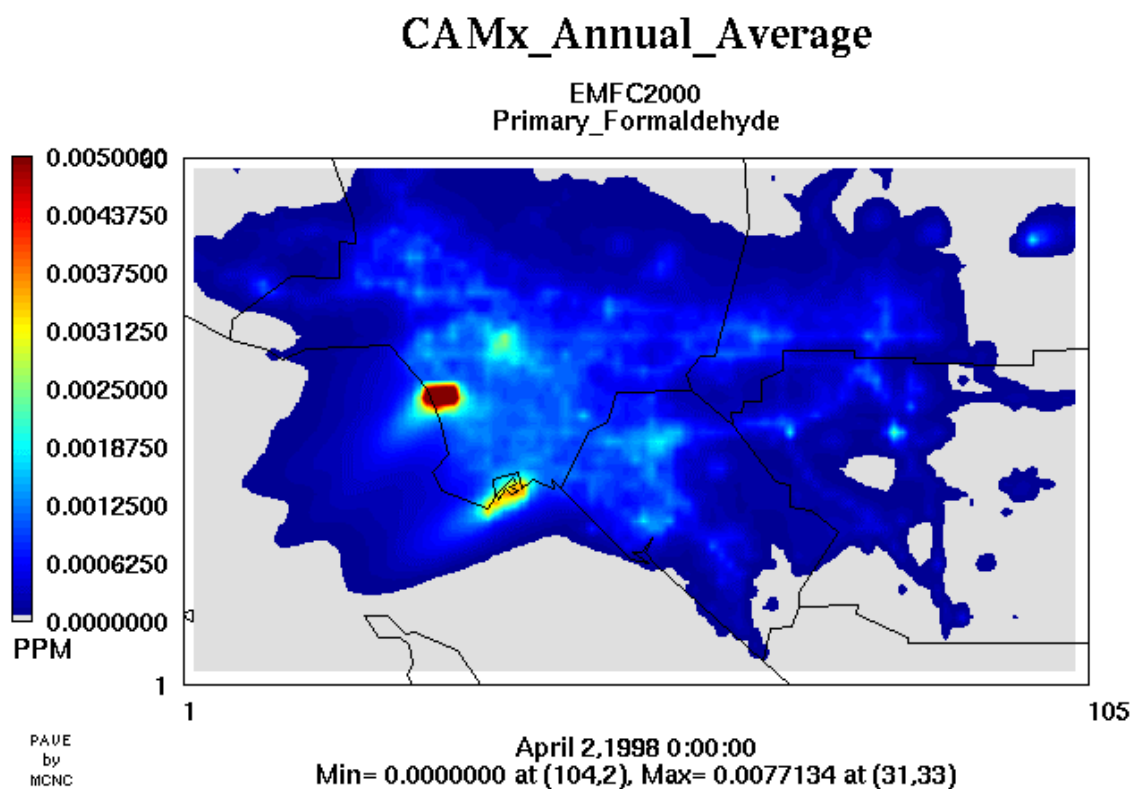
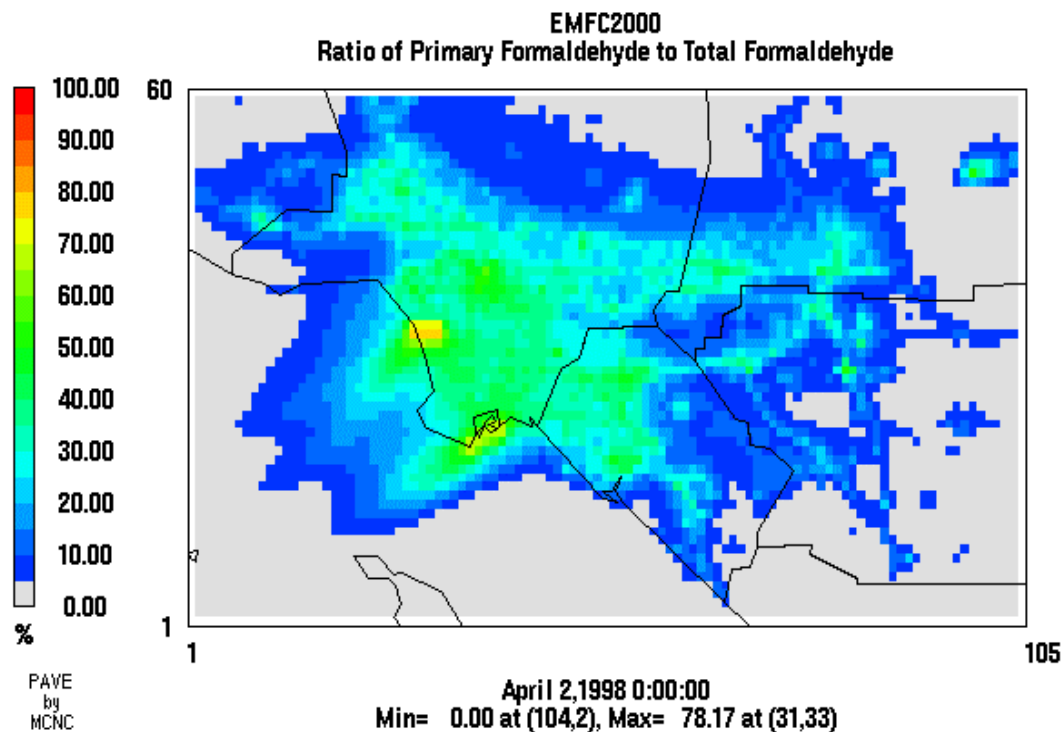


Figure ES-2b. Annual average primary formaldehyde (top) and secondary formaldehyde (bottom) concentrations (ppm) in the SoCAB estimated by the CAMx/EMFAC2000.

CAMx Annual Average



CAMx Annual Average

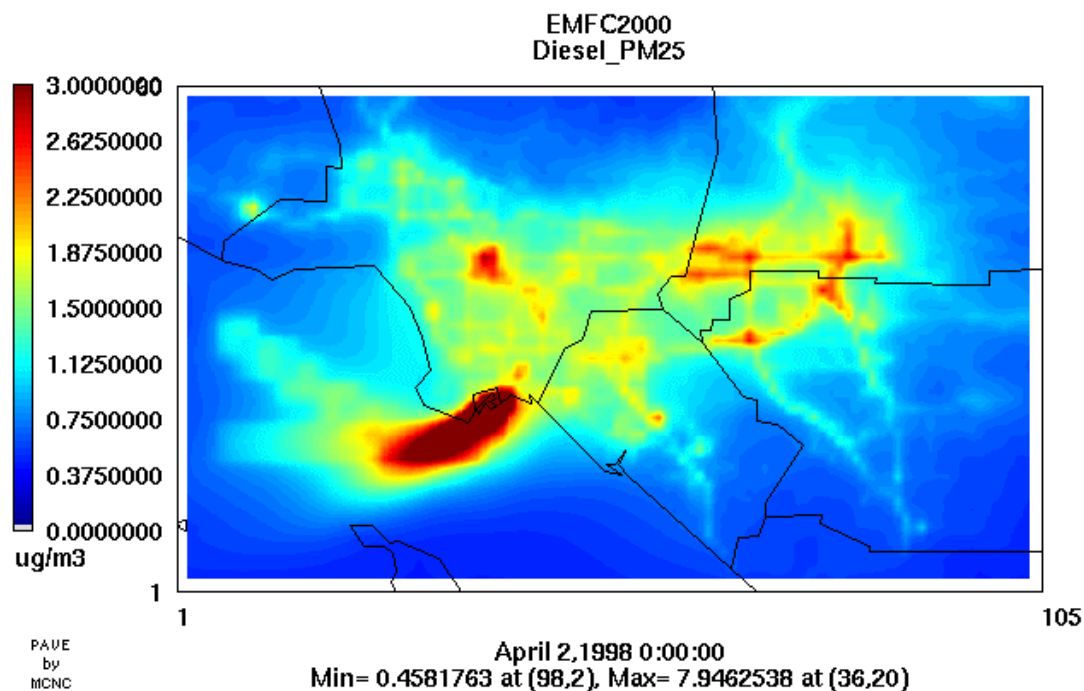


Figure ES-2c. Ratio (%) of annual average primary to total formaldehyde concentrations (top) and annual average diesel PM_{2.5} concentrations (µg/m³) (bottom) concentrations (ppm) in the SoCAB estimated by the CAMx/EMFAC2000.

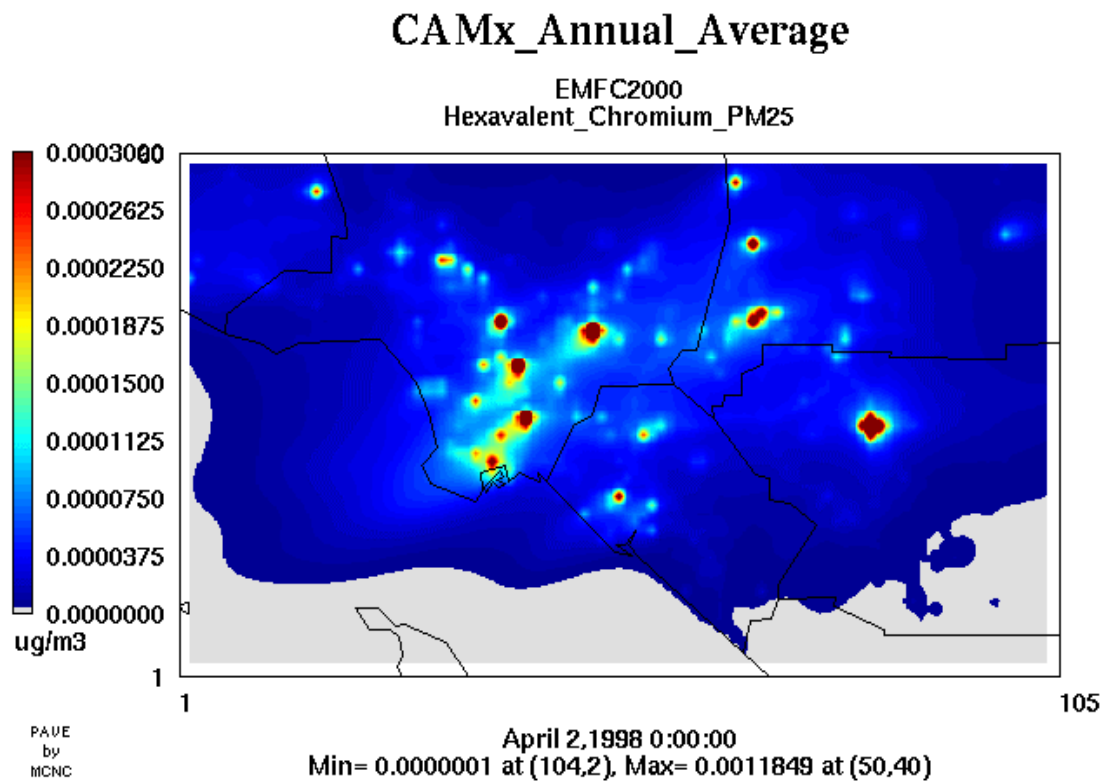
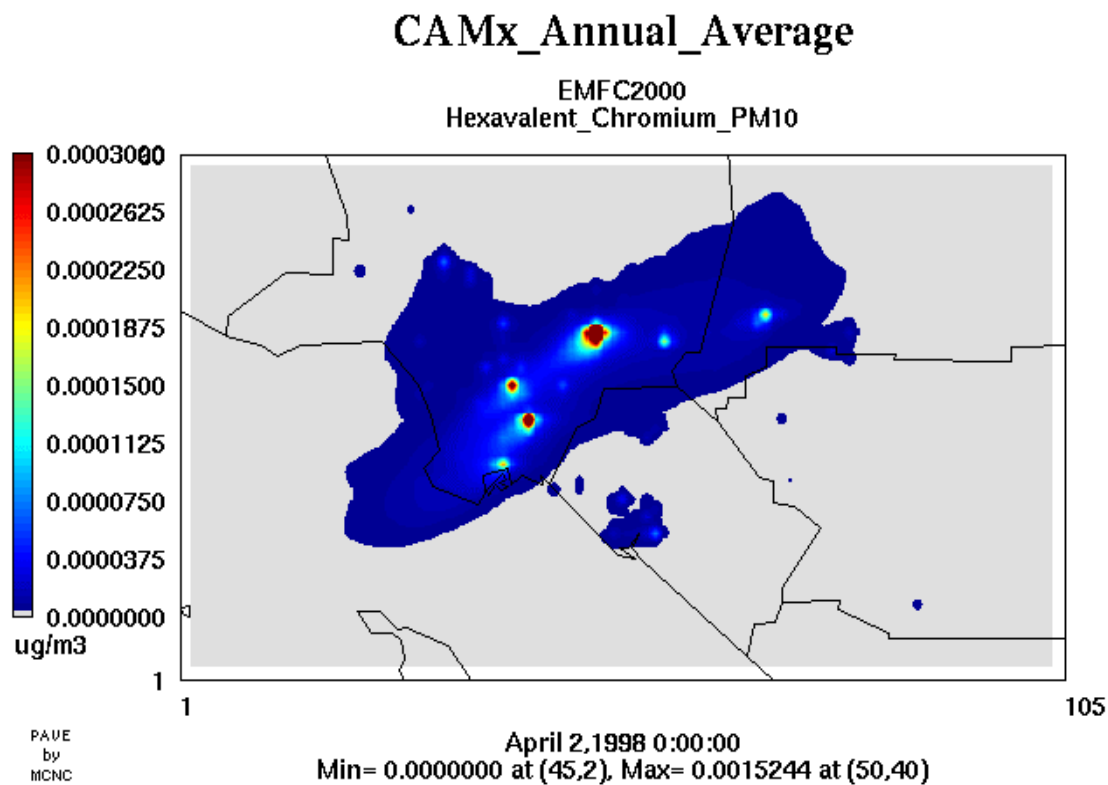


Figure ES-2d. Annual average hexavalent chromium PM_{2.5} (top) and hexavalent chromium PM_{2.5-10} (bottom) concentrations ($\mu\text{g}/\text{m}^3$) in the SoCAB estimated by the CAMx/EMFAC2000.

Risk and Exposure Calculations using the CAMx MATES-II Results

The MATES-II study used species-dependent unit risk factors (URFs) that are applied to the annual average air toxics concentrations and summed to estimate the one in a million risk of premature death due to exposure to air toxics. In MATES-II, risk was calculated in terms of outdoor exposures. That is, the long-term rate of cancer incidence due to exposure to air toxics assumed that a person was outdoors 24 hours/day 365 days/year. In this study we accounted for indoor/outdoor effects on risk and exposure several different ways:

- 10 site average using annual average concentrations and no indoor/outdoor ratio (i.e., the method used in MATES-II, SCAQMD, 2000);
- 10 site average using annual average concentrations and constant (0.59) indoor/outdoor ratio; and
- 10 site average using hourly concentrations and hourly indoor/outdoor ratio.

These approaches are very simplistic ways for accounting for indoor/outdoor effects on risk and exposure, but do represent an improvement over the MATES-II “outdoor” exposure approach. The results of these risk calculations using the CAMx air toxics modeling results are displayed in Table ES-4, where the risk results of the MATES-II modeling and monitoring are also listed (SCAQMD, 2000). The estimated risk calculated in this study is actually greater than the risks calculated in MATES-II even though this study did not simulate all of the MATES-II air toxic compounds (which accounted for approximately 10% of the MATES-II risk estimates). This study’s risk, without accounting for indoor/outdoor effects, is 35%-60% higher than the average risks reported in MATES-II. The higher aldehyde and benzene concentrations estimated by CAMx/RTRAC than UAM-Tox (see Table ES-3) account for most of these differences (although diesel particles may also play a role). When accounting for indoor/outdoor effects on diesel particles only, the estimated risk is reduced by approximately one-third. Note that there is little difference (within 2%) in the calculated risk whether a composite annual average indoor/outdoor factor is used or if hourly indoor/outdoor values are applied to the hourly air toxics concentrations.

Table ES-4. Average risk across the 10 MATES-II sites calculated in MATES-II (all toxic compounds with no indoor/outdoor effect) and by this study (missing some MATES-II air toxic compounds that accounted for 10% of the risk) with no indoor/outdoor (I/O) effects and accounting for indoor/outdoor effects on an annual average and hourly basis.

| Scenario | Risk (Number in a million) | Percent different from no indoor/outdoor ratio. |
|--|-------------------------------|--|
| <i>MATES-II Study Results No Indoor/Outdoor Effects (SCAQMD, 2000)</i> | | |
| Modeled Average, no I/O | 1,230 | |
| Monitored Average, no I/O | 1,414 | |
| <i>This Study’s Modeling Risk with and without Accounting for Indoor/Outdoor Effects</i> | | |
| No Indoor/Outdoor Effects | 1,950 | |
| Annual Indoor/Outdoor Ratio | 1,284 | -34.1 |
| Hourly Indoor/Outdoor Ratios | 1,257 | -35.5 |

Combining the risk factors with population gives the exposure to air toxics. In MATES-II, the average risk across the basin or in a county was compared with the basin-average or countywide population. In this study exposure was calculated several ways:

- The 10-site average risks in Table ES-4 were applied to the basin-wide population of 14,404,993 people (similar to the MATES-II approach);
- An annual average gridded risk with and without indoor/outdoor effects was applied to a gridded population field and totaled to accounting for the spatial distribution of the air toxics and population; and
- The exposure was accumulated throughout the year using the gridded hourly air toxics concentrations, the gridded population, and the hourly indoor/outdoor ratios.

Again these are simple approaches for accounting for indoor/outdoor effects and the spatially distribution of population on exposure, but are marginal improvements over the MATES-II approach that did not account for such effects. The results of the exposure calculation accounting for and not accounting for the spatial distribution of the air toxics and populations and accounting for and not accounting for the indoor/outdoor (I/O) effects are shown in Table ES-5. When accounting for the spatial variations in air toxics concentrations and population, the estimated exposure is reduced by 16%. As seen for risk, accounting for indoor/outdoor effects on exposure, whether hourly or on an annual composite basis, reduces the exposure to air toxics by 34-36%. Combining the spatially varying and indoor/outdoor effects, we see almost a factor of 2 reduction in the estimated exposures due to air toxics over the “outdoor” exposure 10-site average approach used in MATES-II.

Table ES-5. Comparison of the estimated exposure to air toxics using the 10-site average risk and basin-wide population versus using spatially varying risk and spatially varying population with and without accounting for indoor/outdoor (I/O) effects.

| Scenario | 10-Site Average | | Spatially Varying | | % 10-site vs. Spat. Varying |
|----------------|-----------------|------------|-------------------|------------|-----------------------------|
| | Exposure | (% no I/O) | Exposure | (% no I/O) | |
| No I/O Effects | 28,087 | | 23,519 | | (-16) |
| Constant I/O | 18,496 | (-34) | 15,624 | (-34) | (-16) |
| Hourly I/O | 18,112 | (-36) | 15,258 | (-35) | (-16) |

Subgrid-Scale Near-Source Impact Assessment

The implementation of air toxics modeling capability into the CAMx modeling system contained provisions for interfacing with a subgrid-scale near-source model. The MATES-II emissions databases were analyzed and all point sources that contained emissions for any one of the seven air toxics being analyzed were extracted for use with the subgrid scale near-source algorithm. There were 13 point sources in the MATES-II modeling emission input files that had air toxics compound emissions for benzene, acetaldehyde, and formaldehyde. These 13 point sources consisted of five different point source complex locations. Emissions from each of the five point source complexes were treated as a separate family of reactive air toxics tracer emissions in the CAMx RTRAC tracer run using the EMFAC2000 inputs. This results in the model tracking air toxic concentrations for six separate families of tracers, the five point

source complex emissions and the remainder of the emissions. The CAMx/RTRAC simulation generated gridded hourly air toxic concentration impacts for each of the six families of tracers, as well as a vertical profile of hourly air toxic compound decay rates extracted from the CAMx chemistry module to be used with the near-source model.

The ISC steady-state Gaussian plume model was selected for the subgrid-scale plume model as it is the current near-source model recommended in EPA's UATMG (EPA, 1999). ISC treats the chemical decay of pollutants through input of a constant half-life decay factor. The ISC model was modified to read in the CAMx/RTRAC vertical sounding of hourly decay rates for the April 1998 through March 1999 year. Different air toxic compound decay rates were used for each hour of each day of the year and potentially for each point source in the point source complex being modeled. After calculation of the point source plume rise, the air toxic decay rate at the effective stack height of the source is extracted from the array of CAMx estimated decay rates for the day and hour being simulated and used in the ISC point source impact calculation. Note that ISC could also be used to estimate the near-source impacts from area, volume, and line sources, however such data were not available.

The ISC model was used to estimate the subgrid-scale near-source impacts of the 5 point source complexes. Thus, receptors were specified on rings of receptors around the point source complex at distances of 100-m, 200-m, etc. out to 1-km. Beyond 1-km, the CAMx grid model estimates are used (i.e., ISC is just used to estimate the near-source impacts of air toxics within ≤ 1 -km of the source).

Table ES-6 summarizes the results of the subgrid-scale point source modeling using the MATES-II database. A couple comments on Table ES-6:

- The point sources with air toxics emissions in the MATES-II emissions file generally have small impacts compared to the regional "background" concentration estimated by the grid model;
- With one exception, the ISC maximum estimated near-source air toxic concentration is greater than the CAMx/RTRAC grid cell average value;
- The ISC estimated maximum value with decay is either the same or less than the maximum estimated value without decay; and
- The ISC estimated maximum near-source benzene and formaldehyde concentrations due to a point source complex are as much as respectively 20 and 10 times higher than the corresponding CAMx grid cell volume estimate.

Table ES-6. Summary of CAMx/RTRAC subgrid-scale near-source modeling annual results for the MATES-II air toxics point sources.

| IX | IY | Species | CAMx Total ($\mu\text{g}/\text{m}^3$) | CAMx Point ($\mu\text{g}/\text{m}^3$) | ISC Point W/ Decay ($\mu\text{g}/\text{m}^3$) | ISC Point No Decay ($\mu\text{g}/\text{m}^3$) | CAMx Total – Point (Backgrnd) ($\mu\text{g}/\text{m}^3$) | ISC Point w/ Decay + Backgrnd ($\mu\text{g}/\text{m}^3$) | ISC Point No Decay + Backgrnd ($\mu\text{g}/\text{m}^3$) |
|----|----|---------|---|---|--|--|--|--|--|
| 34 | 48 | BENZ | 3.879316 | 0.000063 | 0.000090 | 0.000090 | 3.879253 | 3.879343 | 3.879343 |
| 39 | 36 | BENZ | 5.282383 | 0.001360 | 0.001710 | 0.001720 | 5.281023 | 5.282733 | 5.282743 |
| 41 | 36 | BENZ | 5.799652 | 0.002099 | 0.003900 | 0.003900 | 5.797553 | 5.801453 | 5.801453 |
| 42 | 44 | BENZ | 5.865131 | 0.001506 | 0.007010 | 0.007010 | 5.863625 | 5.870635 | 5.870635 |
| 50 | 43 | BENZ | 5.978545 | 0.000071 | 0.001360 | 0.001360 | 5.978474 | 5.979834 | 5.979834 |
| 34 | 48 | FORM | 3.502453 | 0.000107 | 0.000170 | 0.000180 | 3.502346 | 3.502516 | 3.502526 |
| 39 | 36 | FORM | 5.617651 | 0.002453 | 0.003260 | 0.003430 | 5.615198 | 5.618458 | 5.618628 |
| 41 | 36 | FORM | 5.655835 | 0.003790 | 0.007130 | 0.007800 | 5.652045 | 5.659175 | 5.659845 |
| 42 | 44 | FORM | 5.001340 | 0.002465 | 0.013410 | 0.014020 | 4.998875 | 5.012285 | 5.012895 |
| 50 | 43 | FORM | 4.982802 | 0.000270 | 0.002730 | 0.002730 | 4.982532 | 4.985262 | 4.985262 |
| 42 | 44 | ACET | 1.277799 | 0.000000 | 0.000000 | 0.000000 | 1.277799 | 1.277799 | 1.277799 |

APPLICATION AND EVALUATION USING THE AUGUST 1997 SCOS DATABASE

To provide an additional test of the new CAMx RTRAC air toxics capability, it was also applied for the August 3-7, 1997 Southern California Ozone Study (SCOS) episode and the air toxics modeling results compared against data from the PAMS network. In this application, the CAMx air toxics simulations were performed using both the CB4 and SAPRC99 chemical mechanisms to assure that the air toxics capability worked with both chemical mechanism and to provide an estimate of the sensitivity of the reactive air toxics estimates to the choice of chemical mechanism. The August 3-7, 1997 CAMx meteorological modeling database was based on the MM5 prognostic meteorological model. Thus, it is of much higher quality and won't have the mass inconsistent meteorological fields that were present in the MATES-II period modeling that used CALMET meteorology.

Model Performance Evaluation

Six Photochemical Assessment Monitoring Stations (PAMS) sites were in operation during the August 1997 SCOS episode that collected hourly concentrations of benzene. In addition, one PAMS site also collected hourly formaldehyde and acetaldehyde concentrations. Figure ES-3a displays example predicted and observed time series of hourly benzene concentrations at two of the PAMS sites (Upland and Pico Rivera). Figure ES-3b displays hourly time series of hourly formaldehyde and acetaldehyde concentrations at Pico Rivera. CAMx air toxics modeling results are presented using both CB-IV and SAPRC99 as the host model photochemical mechanism. The estimated benzene concentrations are generally lower than the observed values but agree reasonably well, including reproducing the peak morning observed benzene concentration on August 5 (Julian day 217) at Pico Rivera as well as the observed values during the last two days of the episode (August 6-7). The CAMx/CB-IV and CAMx/SAPRC estimated benzene concentrations are nearly identical, with the CAMx/CB-IV

estimates being slightly higher in the afternoons at Upland due to the higher photochemical activity in the SAPRC99 chemistry that decays the benzene slightly faster.

There are larger differences in the CAMx/CB-IV and CAMx/SAPRC99 acetaldehyde and formaldehyde concentration estimates. The CAMx/SAPRC99 carbonyl concentrations are greater than observed, whereas there is better agreement using CAMx/CB-IV. The hotter chemistry in SAPRC99 generates more secondary acetaldehyde and formaldehyde than the CB-IV chemistry.

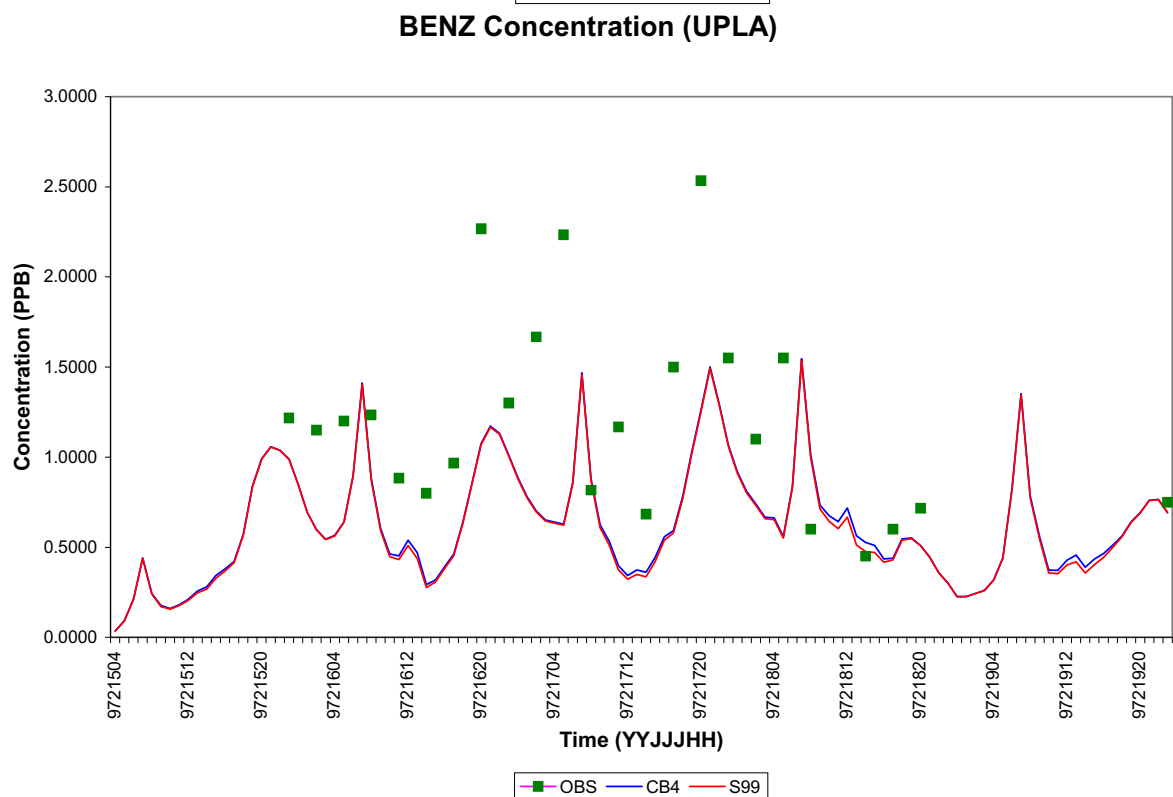
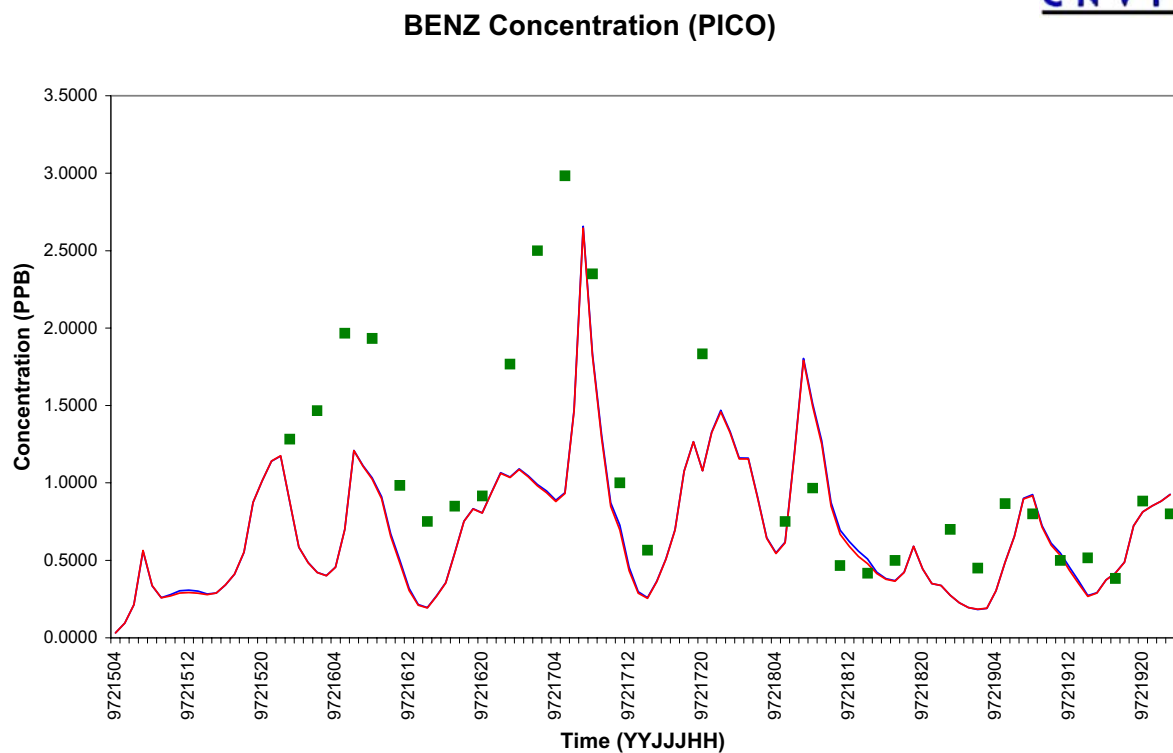
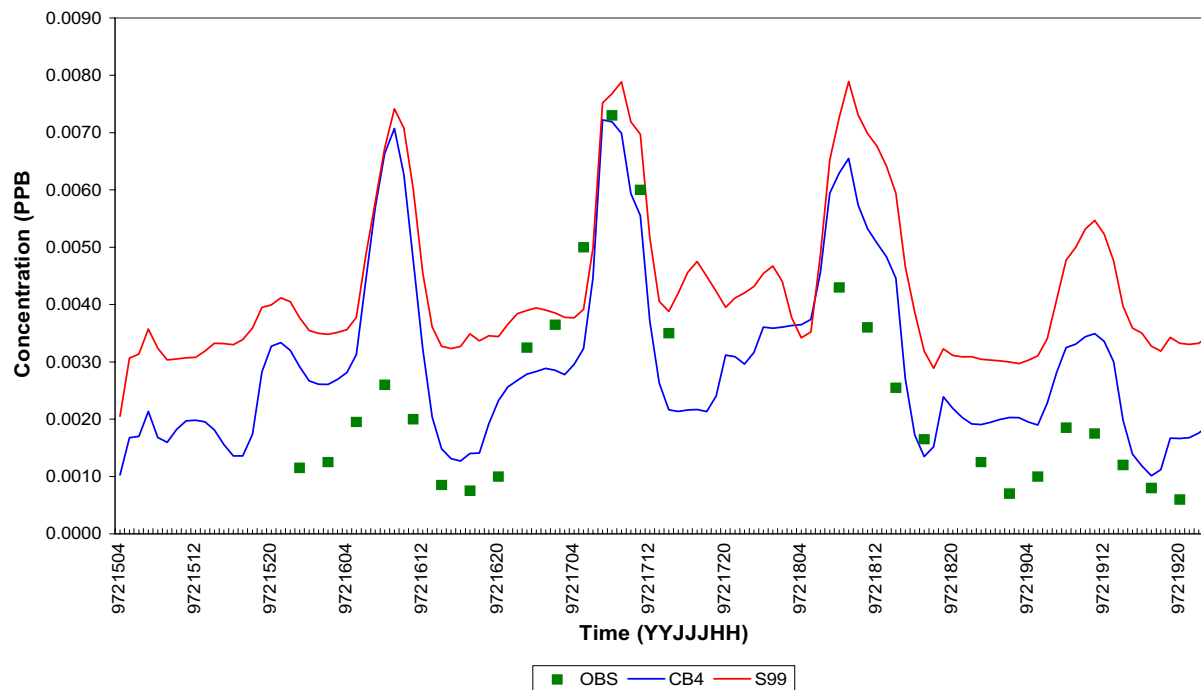


Figure ES-3a. Time series of observed and estimated hourly benzene concentrations during August 3-7, 1997 at the Pico Rivera (top) and Upland (bottom) PAMS sites using the CAMx air toxics modeling system with the CB-IV (CB4) and SAPRC99 (S99) chemistry mechanisms.

ACET Concentration (PICO)



FORM Concentration (PICO)

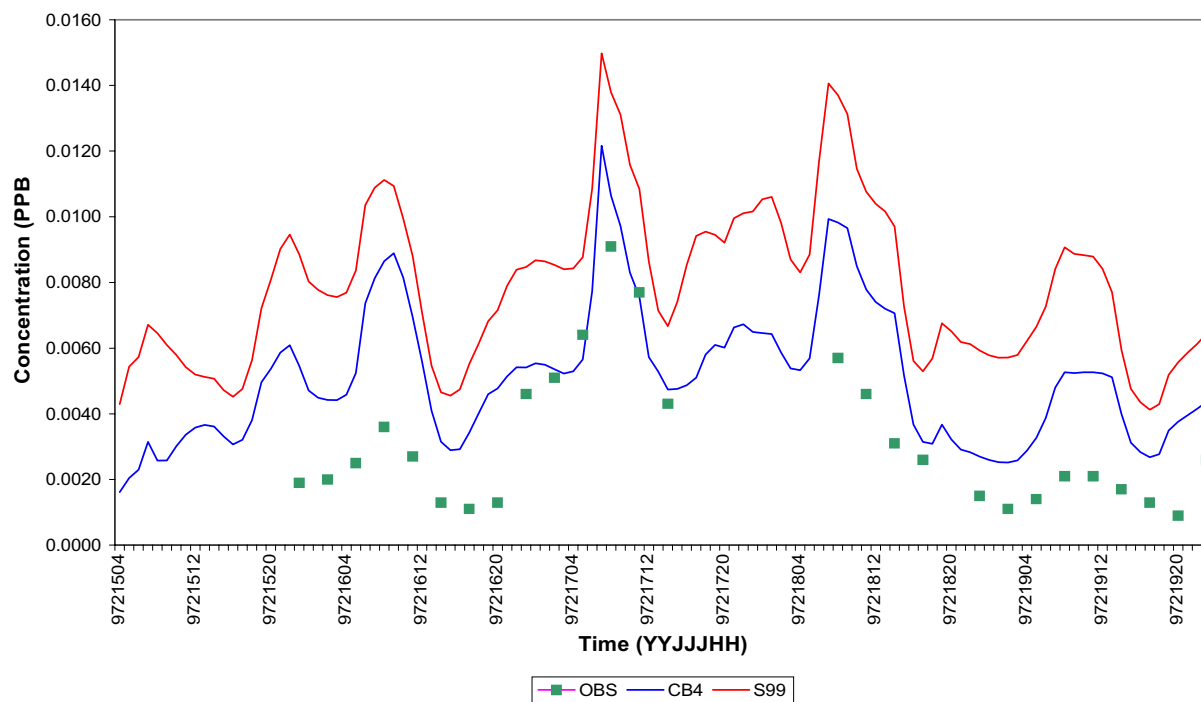


Figure ES-3b. Time series of observed and estimated hourly acetaldehyde (top) and formaldehyde (bottom) concentrations during August 3-7, 1997 at the Pico Rivera PAMS site using the CAMx air toxics modeling systems with the CB-IV (CB4) and SAPRC99 (S99) chemistry mechanisms.

Risk and Exposure Calculations

Table ES-7 presents the estimated risks from the August 1997 episode average benzene, 1,3-butadiene, acetaldehyde, and formaldehyde concentrations averaged across the 10 MATES-II sites for the CAMx/CB-IV (CB4) and CAMx/SAPRC99 (S99) RTRAC simulations. These four organic compounds accounted for approximately 20% of the total risk due to air toxics in the MATES-II study. Note that risks are typically calculated for an annual period or longer and these comparisons for an episodic average period is made solely to illustrate the differences the CB-IV and SAPRC99 chemistry will have on risk calculations. Although the total risk due to the four organic air toxics estimates by S99 (157 in a million) is only 10% higher than that estimated by CB4 (144 in a million), there are significant differences in the contributions of the different organic air toxic compounds to the total risk. The CB4 simulation estimates that primary benzene (40%), and primary 1,3-butadiene (24%) are the two biggest risk contributors, with secondary formaldehyde (21%) and secondary acetaldehyde (12%) being next most important. The S99 simulation also estimates that primary benzene is the most important contributor to total risk (36%), but secondary formaldehyde is now comparable (34%), followed by 1,3-butadiene (15%) and secondary acetaldehyde (12%) whose risks are also now comparable using S99. Table ES-7 clearly shows the competing effects of the more reactive S99 chemistry that decays primary emitted air toxics faster than the CB4 chemistry (e.g., a 33 percent reduction in risk due to 1,3-butadiene), yet forms more secondary air toxic compounds (e.g., 74% increase in risk due to secondary formaldehyde).

Table ES-7. Comparison of the 10 station average one in a million risks using the benzene, 1,3-butadiene, acetaldehyde, and formaldehyde average concentration estimates by the CAMx/CB4 and CAMx/S99 RTRAC modeling of the August 1997 SCOS episode.

| Species | CB-IV Chemistry | | SAPRC99 Chemistry | | % Difference S99-CB4 |
|--------------------|-----------------|-----|-------------------|-----|-------------------------|
| | Risk | (%) | Risk | (%) | |
| Benzene | 57.5 | 40 | 56.4 | 36 | -2 |
| 1,3-Butadiene | 34.7 | 24 | 23.3 | 15 | -33 |
| Prim. Acetaldehyde | 0.7 | 0 | 0.5 | 0 | -28 |
| Prim. Formaldehyde | 6.0 | 4 | 4.5 | 3 | -25 |
| Sec. Acetaldehyde | 14.0 | 10 | 19.1 | 12 | +36 |
| Sec. Formaldehyde | 30.6 | 21 | 53.3 | 34 | +74 |
| Total | 143.5 | | 157.1 | | +10 |

Table ES-8 displays the 10-site average risks by major source category whose contributions were tracked separately in the CAMx/RTRAC simulations (another useful feature of the reactive tracer modeling approach). The CB4 and S99 simulations both estimate that air toxics emitted from on-road mobile sources and formed as secondary species are the highest contributors to the total risk due to organic air toxic compounds. However, the CB4 simulation estimates that primary emissions from mobile sources (55%) contribute substantially more risk than secondary species (31%), whereas S99 estimates they have about equivalent contributions (44% and 46%). Both simulations estimate that other low-level anthropogenic emissions are minor contributors to total risk due to organic air toxics (~10%) and that the point source contribution is negligible (~1%).

Table ES-8. Comparison of the 10 station average one in a million risks by major source category from the 4-day average organic air toxic concentration estimates by the CAMx/CB4 and CAMx/S99 RTRAC modeling of the August 1997 SCOS episode.

| Species | CB-IV Chemistry | | SAPRC99 Chemistry | | % Difference S99-CB4 |
|---------------|-----------------|-----|-------------------|-----|-------------------------|
| | Risk | (%) | Risk | (%) | |
| Mobile | 79.6 | 55 | 69.6 | 44 | -13 |
| Point | 3.2 | 2 | 1.5 | 1 | -55 |
| Other Anthro. | 16.0 | 11 | 13.7 | 9 | -15 |
| Secondary | 44.5 | 31 | 72.4 | 46 | +63 |
| Total | 143.5 | | 157.1 | | +10 |

CONCLUSIONS

There are several conclusions from the study related to the MATES-II database, the new hybrid CAMx air toxics modeling system, air toxics model evaluation, and risk and exposure calculations.

MATES-II Databases

- The MATES-II emissions inventories are suspect and have allocated too much point source air toxics emissions to the low-level gridded emissions rather than leaving them in the point source files.
- The CALMET generated hourly meteorological fields for the SoCAB are highly suspect and likely introduce spurious vertical velocities.
- For several species (e.g., chromium and hexavalent chromium $PM_{2.5}$) the MATES-II measured concentrations were frequently below the detection limit so were set to half of the detection limit that affected the model performance evaluation.
- Chromium and hexavalent chromium were measured only in the fine PM mode ($PM_{2.5}$), yet the emissions inventory and modeling suggest a majority of these compounds are in the coarse mode so the model performance evaluation for these species is limited and incomplete.

CAMx Air Toxics Modeling System

- The CAMx reactive tracer (RTRAC) treatment of air toxics has been demonstrated to be an effective, accurate, flexible, and efficient methodology for treating both inert and reactive, gaseous and particulate, and primary and secondary air toxic compounds.
- The near-source subgrid-scale plume treatment, that is coupled with CAMx through the CAMx chemistry and RTRAC reactive tracers as background concentrations, has proven to be an efficient and flexible approach for estimating maximum fence-line or hot-spot air toxics impacts in a mass consistent fashion with a grid model.

- The CAMx air toxics modeling system is applicable to many scales, from local plume impacts using the subgrid-scale near-source plume models, to the urban-scale and region-scale using the CAMx two-way nested-grid formulation.
- The update of the MATES-II emissions from EMFAC7G to EMFAC2000 results in substantial increases (approximately 50%) in on-road mobile source organic air toxics emissions (e.g., benzene, 1,3-butadiene, and aldehydes).
- The use of the subgrid-scale near-source model produced maximum concentrations due to the point sources near the source that were as much as 10-20 times greater than the CAMx/RTRAC estimated 2-km by 2-km grid cell average concentration.

Model Performance Evaluation using the MATES-II Annual Database

- The UAM-Tox and CAMx models both exhibit some skill in estimating the MATES-II observed benzene concentrations, with UAM-Tox exhibiting almost zero bias on average and CAMx exhibiting a slight (20%) overprediction bias. When the emissions are updated with EMFAC2000, the CAMx overprediction bias is increased. However, both UAM-Tox and CAMx are reproducing the observed benzene concentrations to within the uncertainties of the emissions inventory that is approximately a factor of 2 (Seigneur, Lohman, and Pun, 2002). The spatial distribution of the estimated benzene concentrations in the SoCAB follow the major roadways in the region.
- CAMx and UAM-Tox both underestimate the observed 1,3-butadiene by approximately a factor of 2 on average. The very highest annual average estimated 1,3-butadiene concentrations occur over the LAX airport, with lower 1,3-butadiene concentrations in the remainder of the domain that follow the roadways in the SoCAB.
- The UAM-Tox underestimates the observed acetaldehyde concentrations by approximately a factor of 3, whereas CAMx is within a factor of 2 with an overestimation bias on average of 60% (EMFAC7G) and 80% (EMFAC2000).
- Both UAM-Tox and CAMx estimate the average observed formaldehyde concentrations within a factor of 2 with UAM-Tox exhibiting a 30% underprediction tendency and CAMx exhibiting a 50% (EMFAC7G) and 90% (EMFAC2000) overprediction tendency.
- Both models overestimate the observed chromium and hexavalent chromium concentrations with the UAM-Tox overestimation being quite severe (factor of 4 to 4.5), whereas the CAMx overestimation tendency being not as severe (factor of 2 to 2.5). The spatial distribution of chromium follows the roadways with the coarse mode chromium being much higher than the fine mode chromium. The spatial distribution of the hexavalent chromium is very spotty. The coarse mode hexavalent chromium concentrations are greater than their fine mode counterparts. The MATES-II monitoring only measured fine mode chromium and hexavalent chromium, thus as a majority of these species are in the coarse mode the evaluation for these two species is incomplete.

Model Evaluation Using the August 1997 SCOS Episode Database

- The observed benzene concentrations during the August 3-7, 1997 SCOS episode are reproduced by the CAMx model fairly well using both the CB-IV and SAPRC99 chemical mechanisms.
- The observed formaldehyde and acetaldehyde concentrations are also replicated fairly well by the CAMx model, with much better model performance being exhibited by the CAMx using the CB-IV chemistry than using the SAPRC99 chemistry.
- The SAPRC99 chemistry is more reactive than the CB-IV chemistry, so it decays primary emitted organic air toxic species much faster (e.g., 1,3-butadiene) and forms more secondary air toxic compounds (e.g., formaldehyde and acetaldehyde) than CB-IV.

Risk and Exposure Calculations

- The CAMx air toxics modeling in this study estimated higher risk than estimated by UAM-Tox in the MATES-II due to increased concentration estimates of primary air toxics, which was partly due to the EMFAC2000 update, and increased concentrations in the secondary air toxics due to higher aldehyde estimates.
- Accounting for indoor/outdoor effects on the risk and exposure calculations reduced the risk and exposure by approximately one-third.
- Very similar risk and exposure estimates were obtained whether an annual composite indoor/outdoor ratio was used with annual average air toxics concentrations or whether hourly indoor/outdoor factors and concentrations were used.
- Use of the SAPRC99 chemistry decreases the risk due to primary air toxics and increases the risk due to secondary air toxics for a net increase in total toxic risk of approximately 10% over using the CB-IV chemistry.
- The two highest areas of risk are the port area near Long Beach and downtown Los Angeles, whereas downtown Los Angeles has much higher exposure due to the higher population.

1. INTRODUCTION

BACKGROUND

Many different approaches are being used or are planned to be used for air toxics modeling to support a number of regulatory requirements. Section 112 of the 1990 Clean Air Act Amendments (CAAA) requires EPA to address a number of air toxics issues ranging from reducing exposure to urban air toxics, reducing the deposition of toxic compounds that accumulate in water bodies, and the Residual Risk Program. Thus, air toxic modeling needs to address modeling from the micro-scale up to the regional-scale. Most air toxics modeling applications to date have applied steady-state Gaussian plume models, such as the ISC model as recommended in EPA's urban air toxic modeling guidance (UATMG, EPA, 1999) and whose algorithms are used in EPA's ASPEN model (SAI, 1999) that was applied in the Cumulative Exposure Project (CEP). More recently, the Urban Airshed Model, a photochemical grid model, has been extended to include explicit treatment of organic air toxics (UAM-Tox) and has been applied to estimate urban air toxics in the Los Angeles region (SCAQMD, 2000). The Regional Modeling System for Aerosols and Deposition (REMSAD; ICF, 2001) is a regional-scale grid model designed to simulate the fate and transport of specific air toxics related to deposition that reaches the Great Waters (e.g., Cadmium, Mercury, POMs, etc.). Each of the modeling approaches has its strengths and weaknesses:

Steady-state Gaussian plume models proposed for use in the EPA UATMG (e.g., ISC and ASPEN) are computationally efficient and are appropriate for modeling near-source "fence line" or "hot spot" impacts of inert or semi-inert air toxics from point and area sources. However, they have poor treatment of chemistry (constant half-life decay) and are not reliable for impacts at farther downwind distances;

The UAM-Tox model has good treatment of photochemistry and air toxics chemistry but has poor treatment of near-source impacts as its resolution is limited to the grid spacing used (typically 1-4-km) and does not include grid-nesting so can only be applied to limited (e.g., urban) areas; and

The REMSAD model treats regional-scale transport and has detailed treatment of regional/rural chemistry for selected air toxics. It does include two-way grid nesting, but has poor treatment of urban chemistry and does not treat many air toxics important for urban air toxics issues.

The weaknesses in the current air toxic modeling approaches are either not addressed or are treated in a simplistic fashion using highly questionable technical approaches. For example, to treat secondary formaldehyde and acetaldehyde formation, the EPA UATMG proposes that the OZIPR photochemical box model be used to develop ratios of secondary formaldehyde to primary formaldehyde that are then applied to the ISC-estimated primary formaldehyde predictions to obtain secondary formaldehyde estimates. As shown in this study, secondary formaldehyde and acetaldehyde dominates the total formaldehyde and acetaldehyde over most of an urban area. The errors introduced by this technically questionable and unjustifiable technique are impossible to quantify.

The treatment of exposure in air toxics modeling is also frequently oversimplified. For example, the most common practice is to assume “front-yard exposures” whereby the population is assumed to be always outside at their place of residence for a long period of time (e.g., 70 years). Such simplifications are likely to greatly overstate the exposure and subsequent risks. More detailed exposure models account for microenvironments, such as whether people are indoors or outdoors, the amount of ventilation of the building with the outside (e.g., air conditioning), and when people are on the street or in their cars that would enhance their exposure to some air toxics (e.g., diesel particulate). Detailed exposure models also account for the movement of the population through the daily cycle (activity). Some also use probability theory to model the human contact with the air toxics. Most exposure studies assume that the only pathway of air toxics into the human body is through inhalation ignoring the multimedia and multi-pathway exposures (e.g., exposure of air toxics through inhalation and through the skin, and through the ingestion of food and water).

CRC/DOE REVIEW OF AIR TOXICS MODELING

The Coordinating Research Council (CRC) and the Department of Energy (DOE) through the National Research Energy Laboratory (NREL) sponsored Project A-42-1 to review air toxics modeling approaches and applications to identify the current key issues (Seigneur, Lohman, and Pun, 2002). Some of the key findings of the Project A-42-1 study were as follows:

- Most air toxics modeling applications failed to account for the contributions of indoor air toxics to exposure and many also did not account for the changes in outdoor air toxics levels when exposed to people indoors.
- Most air toxics modeling studies relied on emission inventories and/or ambient air concentrations of surrogate species (e.g., CO, EC, etc.). Most of the time the models are not even evaluated against air toxic compound observations.
- There are significant uncertainties associated with emissions of air toxics from both mobile and stationary sources. Studies in the South Coast (Los Angeles) Air Basin (SoCAB) suggest uncertainties on the order of a factor of 2 or 3 for individual VOC species such as benzene, 1,3-butadiene, formaldehyde, and acetaldehyde, whereas diesel PM appears to be underestimated.
- Routine measurements of air toxics are pretty much limited to Photochemical Assessment Monitoring Stations (PAMS) sites that are located in ozone nonattainment areas and include benzene, formaldehyde, and acetaldehyde (the 1,3-butadiene measurements are less reliable). Some special study data are also available.
- Chemical transformation of most VOCs needs to be taken into account as they can oxidize rapidly and several air toxics are formed secondarily (e.g., formaldehyde and acetaldehyde). Chemical transformation of trace metals is important for chromium and mercury.
- Wet and dry removal of gaseous air toxics are not well known and default values tend to be used. The deposition of particulate air toxics depends on their size distribution and needs to be characterized.

- Indoor sources are poorly characterized and may dominate exposure. For example the ratio of indoor to outdoor formaldehyde concentrations has been reported to be a factor of 6-7.
- For exposure modeling, local population activity patterns are needed along with local microenvironment information.
- There is a need to combine regional/urban-scale modeling with local-scale modeling to properly predict air toxics concentrations at the neighborhood level.

OBJECTIVE

The objective of the CRC/DOE Project A-42-2 Air Toxics Modeling Study is to advance the science for air toxics modeling by implementing an air toxics modeling capability into a current state-of-science multi-scale photochemical grid model, the Comprehensive Air-quality Model with extensions (CAMx). This implementation will account for the full chemistry of organic air toxic species, retain the CAMx two-way grid nesting capability so that linked regional-scale and urban-scale modeling can be performed, and account for near-source local-scale impacts using a subgrid-scale plume model. The model will be tested and evaluated using observed air toxics and surrogate concentrations from the 1998-1999 Multiple Air Toxics and Exposure Study (MATES-II, SCAQMD, 2000 in the South Coast (Los Angeles) Air Basin (SoCAB) of California.

OVERVIEW OF APPROACH

As part of the Multiple Air Toxics Exposure Study (MATES-II), the South Coast Air Quality Management District (SCAQMD) applied the UAM-Tox photochemical and air toxics grid model for a year (April 1998-March 1999). Air toxic concentration estimates were obtained across the South Coast (Los Angeles) Air Basin (SoCAB) for approximately 50 toxic compounds. The UAM-Tox used a 105 by 60 horizontal array of 2-km by 2-km grid cells to cover the SoCAB and five vertical layers up to a region top of 2-km AGL. The UAM-Tox vertical layer structure is defined by the input mixing height with two layers below and 3 layers above the mixing height and minimum thickness of 25 and 150 m, respectively. Hourly three dimensional meteorological inputs were generated for April 1, 1998 through March 31, 1999 using the CALMET diagnostic meteorological model and surface and upper-air meteorological observations. The UAM-Tox emissions inventory inputs were generated by the SCAQMD for the expanded CB-IV chemical mechanism (TOX mechanism) that explicitly treats several organic air toxics including benzene, 1,3-butadiene, acetaldehyde, and formaldehyde.

The MATES-II hourly CALMET meteorological inputs and UAM-Tox emission for April 1, 1998 through March 31, 1999 were acquired from the SCAQMD. The UAM-Tox model was also requested, but the SCAQMD responded that they could not provide the model as it is proprietary. They did provide the MATES-II observations and concurrent UAM-Tox model predictions. Thus, the UAM-Tox model performance was carried through in this study and compared with the CAMx air toxic estimates and performance.

The CALMET diagnostic meteorological model was run for the April 1998 – March 1999 year and a CALMET-CAMx converter program was used to convert the CALMET output to the meteorological variables and formats needed by CAMx. CAMx was configured on the same 105 by 60 2-km by 2-km horizontal grid as UAM-Tox. CAMx was set up with 6 vertical layers of spatially and temporally constant thickness up to a region top of 2,000-m AGL. The UAM-Tox TOX chemical mechanism species emissions were combined to generate standard CB4 mechanism input. Air toxics compounds for the following species were extracted from the MATES-II emissions database for separate modeling:

- Benzene
- 1,3-Butadiene
- Acetaldehyde
- Formaldehyde
- Chromium
- Hexavalent chromium
- Diesel Particulate Matter
- Elemental Carbon

Note that elemental carbon (EC) is not an air toxic, but is carried as a separate species to aid in the model performance evaluation. Similarly, chromium is not an air toxic, but is included to enhance the model evaluation.

The CAMx model was modified to treat reactive tracers (RTRAC). The reactive tracers operate in parallel to the host photochemical grid model extracting chemical transformation, decay, and deposition information for each toxic species from the host model.

The CAMx model was then run for the April 1998 – March 1999 period and the modeled air toxics estimates were compared against the observed values as well as the MATES-II UAM-Tox model performance. The mobile source emissions inventory was then updated using EMFAC2000 and the base case simulation and model performance evaluation was conducted again.

To provide an additional test of the new CAMx RTRAC air toxics capability, it was also applied for the August 3-7, 1997 Southern California Ozone Study (SCOS) episode and the air toxics modeling results compared against observed data from the Photochemical Assessment Monitoring Stations (PAMS) network. In this application, the CAMx air toxics simulation was performed using both the CB4 and SAPRC99 chemical mechanisms to assure that the air toxics capability is also working with the SAPRC99 chemical mechanism and to provide an estimate of the sensitivity of the reactive air toxics estimates to the choice of chemical mechanism.

2. DEVELOPMENT OF MODEL INPUTS

Inputs for the Comprehensive Air-quality Model with extensions (CAMx, www.camx.com) were developed for two South Coast (Los Angeles) Air Basin (SoCAB) modeling periods:

- The MATES-II April 1, 1998 through March 31, 1999 annual modeling period; and
- The August 3-7, 1997 Southern California Ozone Study (SCOS) episode.

The 1998/1999 annual database was built off of the MATES-II UAM-Tox modeling (SCAQMD, 1999) and is described below. The August 1997 SCOS CAMx database has been used extensively for ozone modeling of the SoCAB and its development is described elsewhere (Morris et al., 2002; Yarwood et al., 2002; Morris et al., 2001).

MODELING DOMAIN

CAMx was operated on the same 210-km by 120-km modeling domain that covered the SoCAB as used by the UAM-Tox model in MATES-II. The horizontal grid consisted of an array of 105 by 60 2-km by 2-km grid cells. CAMx was operated with six vertical layers up to a 2,000-m above ground level (AGL) region top with vertical layer interface heights as follows (m AGL):

- 0-m
- 20-m
- 100-m
- 500-m
- 1000-m
- 1500-m
- 2000-m

METEOROLOGICAL INPUTS

The CALMET meteorological model (Scire et al., 1999) was used to develop hourly three-dimensional meteorological inputs for the SoCAB and the 1998/1999 year. CALMET employs a diagnostic wind model (DWM) that uses surface and aloft meteorological observations and empirical algorithms to diagnose several wind flow features due to complex terrain, such as slope flows, blocking/deflection, channeling, etc. Other meteorological variables, including temperatures, pressure, relative humidity, mixing heights, etc., are interpolated from the observations. Since CALMET is a diagnostic meteorological model, the meteorological variables are not necessarily balanced by the governing equations of motion. Any balance comes from the observed upper-air meteorological variables that are interpolated in CALMET.

The CALMET input files for April 1998 through March 1999 and SoCAB were obtained from the SCAQMD. These files included observations for approximately 90 surface meteorological sites and 4 to 11 upper-air meteorological observation sites. Figure 2-1 displays the locations of these sites in the SoCAB.

The CALMET output was processed to the variables and formats needed by CAMx using the CALMET-CAMx converter program that was obtained from the California Air Resources Board (ARB). A key input to CAMx is the vertical turbulent exchange coefficients (i.e., level of mixing). The ARB CALMET-CAMx converter program used algorithms from the CALGRID photochemical grid model to define the vertical diffusivities. A test run of CAMx for April 1998 was initiated and the model stopped after a few days with an error in the vertical transport step. The problem was traced to the CALMET meteorological variables that were not in balance with each other. These problems tended to occur at an upper-air meteorological site where an incomplete hourly sounding was taken, such as a radar profiler that measured winds but not temperatures. In this case the temperatures at the site location are interpolated from other sites so were not necessarily in balance with the local radar profiler winds. For hours in which the CALMET meteorological variables were so out of balance that the CAMx vertical transport algorithm failed to converge, the wind fields were replaced by interpolated ones from the previous and subsequent hours. This resulted in a laborious process of running CALMET, running the CALMET-CAMx converter, and then running CAMx to identify problems in the meteorological fields that caused the model to abort. The problems in the meteorological fields would then be fixed using the procedures above and the process was repeated over again. There were approximately 40 instances of this problem occurring throughout the April 1998 – March 1999 year.

Note that although the interpolated wind fields fixed the cases when CALMET meteorological variables were so out of balance with each other that the CAMx vertical transport algorithm failed to converge, this occurrence points to fundamental problems in the CALMET meteorological fields when used with mass conservative and consistent models, such as CAMx. Although the model appears to be running, there will always be questions whether the CALMET wind fields adequately characterize transport due to their technical deficiencies.

AIR QUALITY DATA

The MATES-II field study program collected up to 30 gaseous and particulate species at 10 fixed sites as follows (see Figure 2-2):

- Burbank
- Los Angeles
- Huntington Park
- Pico Rivera
- Compton
- Long Beach
- Wilmington
- Anaheim
- Rubidoux
- Fontana

The MATES-II period of interest was April 1998 through March 1999. Collection of ambient data at all of the sites was terminated on March 31, 1999. The starting dates varied by site: 6 were started in April 1998, Rubidoux started in May 1998, Huntington Park started in June 1998, and Wilmington and Compton started in July 1998.

Laboratories at the SCAQMD and the California Air Resources Board (ARB) performed the analysis of the samples. When a measured air toxic species was below the detection limit, it was set to half of the detection limit. Note that the SCAQMD and ARB laboratories sometimes had different detection limits.

INITIAL AND BOUNDARY CONDITIONS

The same initial concentrations and boundary conditions (IC/BC) as reported in the MATES-II UAM-Tox modeling was used for the CAMx/RTRAC air toxics modeling (SCAQMD, 1999). The air toxic boundary conditions used in this study are shown in Table 2-1.

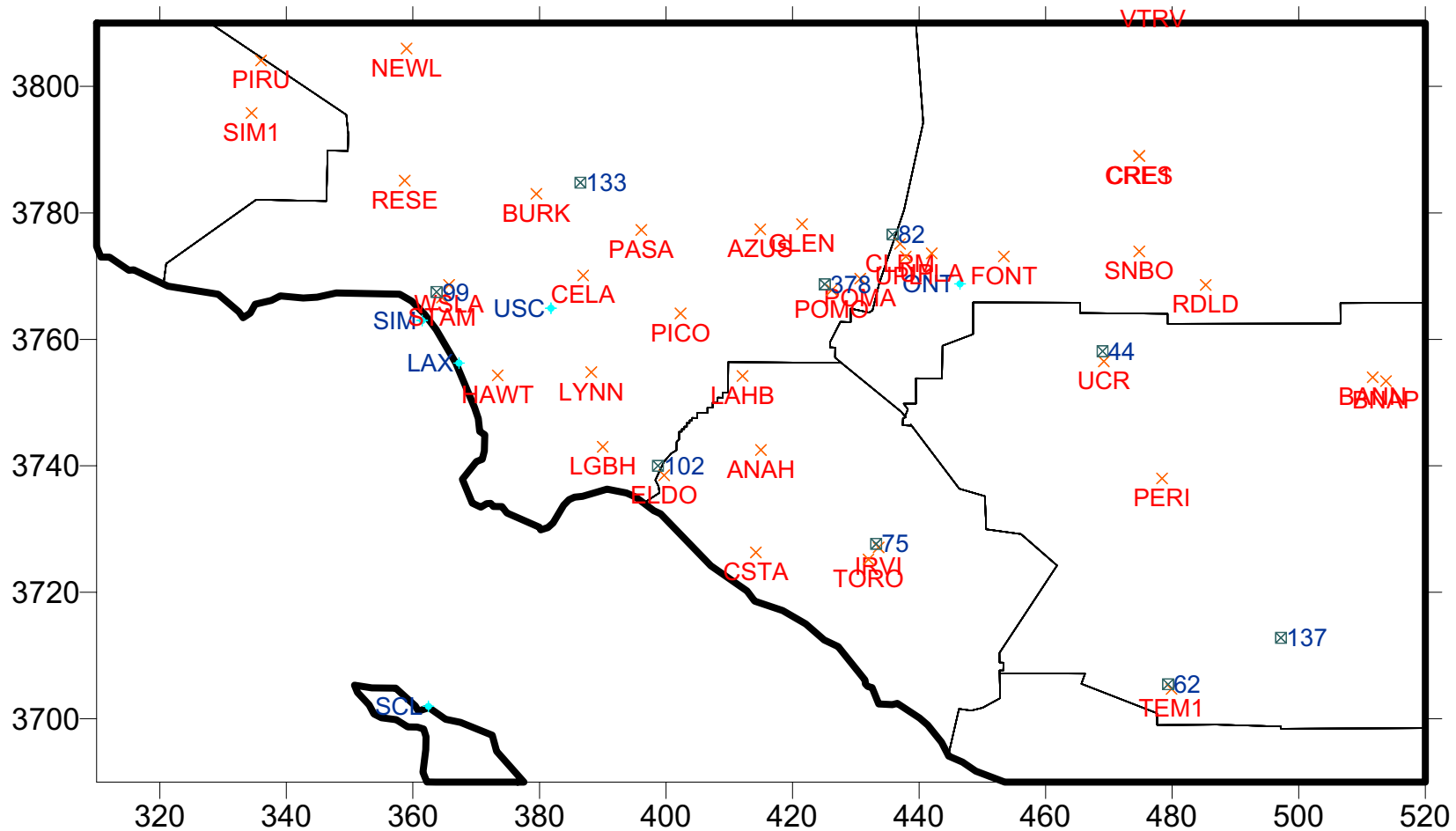
Table 2-1. Initial and boundary conditions used for the CAMx/RTRAC air toxics modeling (Source: SCAQMD 2000).

| Species | IC/BC ($\mu\text{g}/\text{m}^3$) |
|--|---------------------------------------|
| Benzene | 0.640 |
| 1,3-Butadiene | 0.008 |
| Acetaldehyde ¹ | 0.008 |
| Formaldehyde ¹ | 0.540 |
| Chromium | 0.000041 |
| Hexavalent Chromium | 8.2E-14 |
| Diesel Particulate Matter ² | 0.450 |
| Elemental Carbon | 0.450 |

¹Primary and secondary acetaldehyde and formaldehyde were modeled as separate species with a zero IC/BC for the primary species and values in Table 2-1 for the secondary species.

²Elemental Carbon (EC) is also called Light Absorbency Carbon (LAC) or Soot may consist of other compounds besides EC depending on the measurement technique utilized.

For the photochemical host model, fairly clean initial and boundary conditions were used of 40 ppb ozone, 1.5 ppb NO_x, and approximately 30 ppbC VOC.



Mates Terrain and Met Station Map
 Surface Sites in Red; Upper Air Sites in Blue; Precip Sites in Green

Figure 2-1. Location of surface meteorological (red x), upper-air meteorological (blue diamonds), and precipitation (green boxes) sites in the SoCAB used for the April 1998 – March 1999 CALMET modeling.

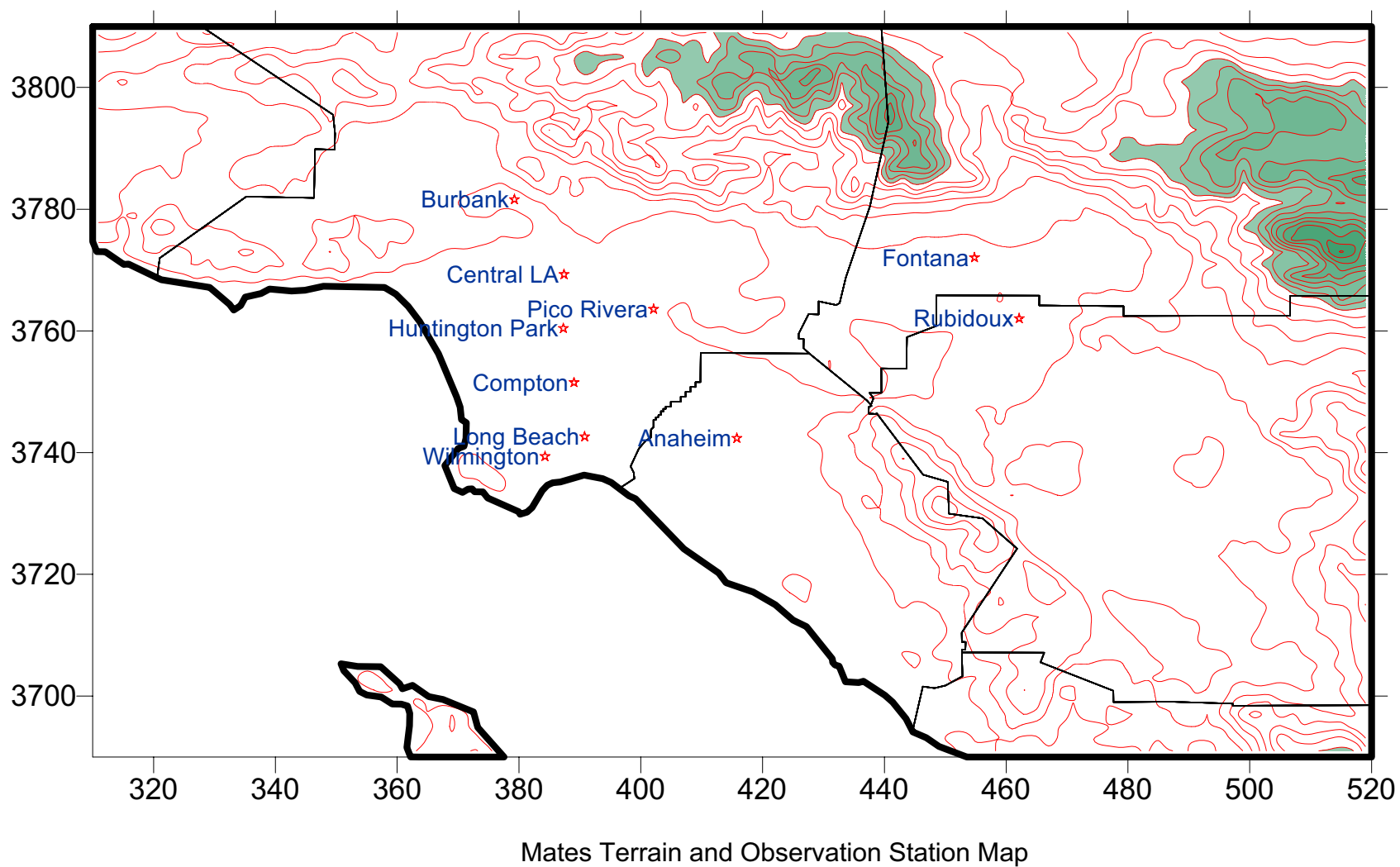


Figure 2-2. Location of the 10 MATES-II fixed sites air toxics samplers.

EMISSIONS

The SCAQMD provided the MATES-II UAM-Tox hourly emissions files for the 98/99 year in two forms:

- Gaseous species speciated for the UAM-Tox extended CB4 air toxics chemical mechanism (the TOX mechanism); and
- Particulate Matter species that were separated into the fine ($< 2.5\mu\text{m}$) and the coarse ($2.5\text{--}20\mu\text{m}$) fractions.

The gaseous TOX chemical mechanism emission species were mapped into the standard CB4 mechanism species using the carbon bond mechanism mapping rules. Selected air toxic compounds species were extracted from the gaseous and particulate MATES-II emissions databases for treatment by the CAMx reactive tracer modeling as follows:

- BENZ – benzene
- BUTA – 1,3-butadiene
- PACET – primary acetaldehyde
- PFORM – primary formaldehyde
- CRC – chromium $\text{PM}_{2.5}$
- CRF – chromium $\text{PM}_{2.5-10}$
- CR6F – hexavalent chromium $\text{PM}_{2.5}$
- CR6C – hexavalent chromium $\text{PM}_{2.5-10}$
- DSLF – diesel particulate matter $\text{PM}_{2.5-10}$
- DSLC – diesel particulate matter $\text{PM}_{2.5-10}$
- ECF – elemental carbon $\text{PM}_{2.5}$
- ECC – elemental carbon $\text{PM}_{2.5-10}$

Note that when performing the CAMx reactive tracer simulation two additional air toxic compound tracers are simulated that are tracked separately:

- SACET – secondary acetaldehyde
- SFORM – secondary formaldehyde

In each grid cell and at each integration time step, the amount of acetaldehyde and formaldehyde that is formed by chemistry in the host photochemical grid model is added to the SACET and SFORM reactive tracer species. Note that when tracking separate families of air toxics (e.g., mobile, point, and area source), the secondarily formed compounds are allocated to their own family (i.e., they are not attributed to any specific emissions source category or geographic region).

EMFAC2000 Emissions Update

The MATES-II emissions data mobile source emissions estimates were based on the EMFAC7G mobile source emissions model. More recently, the ARB has released the EMFAC2000 emissions model that contains many updates and improvements. The MATES-II EMFAC7G mobile source emission estimates were updated using EMFAC2000. However, the

DTIM2 traffic output for the 1998/1999 year used to develop the MATES-II EMFAC7G mobile source emissions were not available. Thus, the MATES-II EMFAC7G mobile source emissions were updated to EMFAC2000 by applying basin-wide adjustment factors to all on-road mobile source emissions using EMFAC2000 and EMFAC7G simulations for summer and winter periods. For spring and fall, an average of the summer and winter adjustment factors were used. Table 2-2 summarizes the EMFAC2000/EMFAC7G mobile source emissions adjustment factors that were used.

Table 2-2. Emissions adjustment factors used to update the MATES-II EMFAC7G fleet average on-road mobile source emissions to EMFAC2000 levels.

| Species | Summer | Winter | Spring/Fall |
|----------------|---------------|---------------|--------------------|
| VOC | 1.544 | 1.417 | 1.481 |
| NOx | 1.260 | 1.374 | 1.317 |
| CO | 1.937 | 1.465 | 1.701 |
| PM | 1.081 | 1.081 | 1.081 |

Emission Totals

Table 2-3 summarizes the annual average emissions in the SoCAB for the air toxic compounds being modeled in this study. Emission totals are presented for both the MATES-II emissions inventories based on EMFAC7G and the emissions updated to EMFAC2000. The EMFAC2000 emissions update increases the on-road mobile source contributions to all air toxics. For example, the mobile source benzene contribution is increased from 70% using EMFAC7G to 77% using EMFAC2000 due to the almost 50% higher VOC emissions in EMFAC2000 as compared to EMFAC7G. There were smaller changes in the PM species, with on-road diesel PM increasing by approximately 8% for a basin-wide increase of approximately 4%.

The host model CB4 photochemical emissions inventory inputs were also updated to EMFAC2000 using the adjustment factors listed in Table 2-2.

Table 2-3. Summary of annual air toxics emission totals (lb/day) for the South Coast Air Basin (SoCAB) from MATES-II using EMFAC7G and updated using EMFAC2000.

| Pollutant | On-Road | Off-Road | Point | AB2588 | Area | Total |
|---|----------------|-----------------|--------------|---------------|-------------|--------------|
| <i>MATES-II Emissions Based on EMFAC7G</i> | | | | | | |
| Benzene | 21308.8 | 6338.1 | 245.7 | 267.4 | 2379.9 | 30540.0 |
| 1,3-Butadiene | 3852.8 | 1557.0 | 9.7 | 2.0 | 369.9 | 5791.5 |
| Acetaldehyde | 5242.4 | 5403.1 | 45.8 | 57.1 | 185.2 | 10933.6 |
| Formaldehyde | 16270.2 | 15780.1 | 581.2 | 674.4 | 1075.4 | 34381.2 |
| Chromium | 2.3 | 2.6 | 5.0 | 2.2 | 291.1 | 303.3 |
| Hexavalent Chromium | 0.4 | 0.4 | 0.5 | 1.0 | 0.0 | 2.3 |
| Diesel PM | 23042.1 | 18249.6 | 0.0 | 5.4 | 806.0 | 42103.2 |
| Elemental Carbon | 26669.5 | 5586.6 | 762.9 | 0.0 | 25326.7 | 58345.6 |
| <i>Updated Emissions Using EMFAC2000</i> | | | | | | |
| Benzene | 31547.7 | 6338.1 | 245.7 | 267.4 | 2379.9 | 40778.9 |
| 1,3-Butadiene | 5704.1 | 1557.0 | 9.7 | 2.0 | 369.9 | 7642.8 |
| Acetaldehyde | 7761.4 | 5403.1 | 45.8 | 57.1 | 185.2 | 13452.6 |
| Formaldehyde | 24088.0 | 15780.1 | 581.2 | 674.4 | 1075.4 | 58469.2 |
| Chromium | 2.5 | 2.6 | 5.0 | 2.2 | 291.1 | 303.5 |
| Hexavalent Chromium | 0.4 | 0.4 | 0.5 | 1.0 | 0.0 | 2.3 |
| Diesel PM | 24908.5 | 18249.6 | 0.0 | 5.4 | 806.0 | 43969.6 |
| Elemental Carbon | 28829.7 | 5586.6 | 762.9 | 0.0 | 25326.7 | 60505.8 |

3. IMPLEMENTATION OF AIR TOXICS MODELING CAPABILITY INTO CAMx

There were several objectives in the implementation of an air toxics modeling capability into CAMx:

- Implement state-of-science (SOS) treatment of air toxic compounds including full atmospheric chemistry of reactive air toxics and species-dependent and size resolved deposition;
- Ability to treat both the regional and urban-scale impacts of air toxics using a flexible two-way nested-grid photochemical grid model modeling framework;
- Ability to treat the near-source impacts of air toxic point source fence-line or hot-spot impacts using a subgrid-scale plume model/module;
- Ease of use and ease of extension to additional air toxics; and
- Demonstrate the advanced air toxics modeling system using the 1998/1999 annual MATES-II database for the South Coast Air Basin (SoCAB).

The extension of the CAMx modeling system to treat air toxics included the following activities:

- Implementation of the reactive tracer (RTRAC) approach in CAMx that carries air toxic compounds in parallel to the host photochemical grid model, extracts information on chemical formation and decay of air toxics from the host model chemistry, and deposits the air toxics using gaseous or particle deposition rules.
- Extraction of hourly air toxics decay rates from the CAMx chemical mechanism at selected locations where near-source point source modeling will be performed.
- Modify a near-source plume or puff model to accept the CAMx air toxic hourly decay rates.
- Develop pre- and post-processing software to combine air toxics for different families of tracers, compare results with observations, and combine the grid model and point source model estimates.

CAMx REACTIVE TRACER IMPLEMENTATION

The CAMx reactive tracer (RTRAC) algorithms are designed to provide a flexible approach for tracking the emission, dispersion/transport, deposition, and chemical reaction of multiple gas and particle tracers. In this study, the tracers are used to model air toxics, but RTRAC is not limited to this purpose and can be used to simulate a variety of different organic and inorganic gaseous and particulate species. RTRAC is implemented as a CAMx “Probing Tool” and shares model data structures with other Probing Tools such as the Ozone Source Apportionment Technology (OSAT), Decoupled Direct Method (DDM), OSAT, DDM and Process Analysis. This streamlines the CAMx code and improves efficiency, but means that RTRAC cannot be used simultaneously with other Probing Tools. However, we do not view this as a limitation as in practice the different Probing Tools are applied in separate CAMx simulations. RTRAC tracers are defined for each CAMx run via an input file such as the examples shown in Figures 3-1 and 3-2. This provides complete flexibility in the selection of

tracers to be included in each analysis. You are not locked into a pre-determined set of tracers. This allows easy extension of the method to additional air toxic compound tracers as needed.

The RTRAC calculations for emissions, transport, and deposition use the existing CAMx algorithms. The emissions are specified through an extra set of emission files (surface and/or point source) for the reactive tracer species. Emissions of gases are in moles per emission time period (normally moles/hour), whereas particles are in micro-grams per emission time period. The emissions file format is the same as for a regular CAMx emissions file (i.e., the UAM-IV format) as described in the CAMx User's Guide (ENVIRON, 2002).

The RTRAC transport uses same horizontal advection algorithm as selected for the host CAMx simulation. The advection algorithms currently available in CAMx are the Piecewise Parabolic Method (PPM), the Bott scheme, or Smolarkiewicz scheme (ENVIRON, 2002). The PPM or Bott schemes are recommended because they have less numerical diffusion than the Smolarkiewicz scheme. In fact, the Smolarkiewicz advection solver will be dropped from CAMx on the next public release of CAMx that should include the version of CAMx with the RTRAC air toxics capability

Deposition of reactive tracers uses the CAMx algorithms which are described in the CAMx User's Guide (ENVIRON, 2002). Deposition of gases is modeled based on the resistance model of Wesely (1989) and particle deposition occurs via diffusion, impaction, and/or gravitational settling using the resistance approach of Slinn and Slinn (1980). Physical characteristics must be provided for each reactive tracer (see Figure 3-1) for the deposition calculations. For gaseous species, the required parameters are Henry's Law constant and diffusivity ratio relative to water:

$$\text{Diffusivity Ratio} = (\text{Molecular Weight}/18)^{0.5}.$$

The deposition calculation for gaseous species that react in plant tissue also uses a reactivity parameter that describes whether a species reacts when dissolved inside leaf tissues (Wesely, 1989). This parameter is intended for modeling the deposition of reactive species, such as ozone, and should be set to zero for air toxics. The deposition calculation for particles requires the particle density and size associated with each species. The particle size is calculated as the geometric mean of the lower and upper cut points (see Figure 3-1). If possible, the particle size and density should be based on the measured size of particles associated with each toxic species.

Gas Phase Chemistry

The RTRAC chemistry calculations use a special chemistry module that was added to CAMx for this study. Chemical change may be modeled for gases that are primary or secondary species. There is no chemistry for the tracer Particulate Matter (PM) species in this version of RTRAC.

The chemical decay of gaseous tracers accounts for thermal reactions with ozone (O₃), hydroxyl radical (OH) and nitrate radical (NO₃) and photolysis. The algorithms are coded so

that all chemical decay pathways are zero by default and only become non-zero if decay rates are explicitly specified in the input file (see Figure 3-1). The example RTRAC chemistry input file in Figure 3-1 shows how thermal reactions are specified by naming the tracer and oxidant that react and providing reaction rate parameters. Note that the RTRAC air toxic chemical reaction rates depend on the rates and parameters provided in the RTRAC input file (e.g., Figures 3-1 and 3-2) not the rates in the host model chemical mechanism, but the host model provides the oxidizing species (i.e., O₃, OH, and NO₃).

Thermal Reactions

Thermal reactions with oxidants are modeled as second order reactions:

$$\text{decay rate} = k [\text{tracer}] [\text{oxidant}]$$

The rate constant (k) is defined using the generalized temperature dependent rate expression:

$$k = A \exp(E_a/T) \times (T/300)^B$$

The Arrhenius factor (A) must be in units (ppm⁻¹min⁻¹), the activation energy (E_a) must be Kelvin and B is dimensionless. Oxidant concentrations for the decay calculation are obtained from the CAMx photochemical simulation for each grid cell at each time step. RTRAC can be used with either the CB4 or SAPRC99 chemical mechanisms that are available in the current version of CAMx (ENVIRON, 2002). Choosing the CB4 or SAPRC99 mechanism will influence the RTRAC chemical decay rates by changing the oxidant concentrations in the host model.

Photolysis

Photolysis reactions are specified (see Figure 3-1) by naming the tracer undergoing photolysis and providing a ratio of the tracer photolysis rate to one of the photolysis reactions in the host photochemical mechanism (i.e., CB4 or SAPRC99). For example, Figure 3-1 shows that there are both primary and secondary acetaldehyde reactive tracers in the MATES toxics modeling (PACET and SACET) and the photolysis rate for both species is set equal to reaction 45. Reaction 45 in the CB4 mechanisms is photolysis of ALD2, which is based on acetaldehyde. Figure 3-1 also shows that there are two types of formaldehyde in the MATES toxics modeling (PFORM and SFORM). Modeling the photolysis of formaldehyde with RTRAC is complicated by the fact that the CB4 mechanism includes two photolysis reactions for formaldehyde (reactions 38 and 39). The solution shown in Figure 3-1 is to model formaldehyde photolysis as 1.6 times the rate of CB4 reaction 39.

The RTRAC photolysis rate treatment is explicitly linked to the host model chemistry by setting photolysis rates relative to host model reactions. For example, in Figure 3-1 the SACET photolysis rate is set relative to CB4 reaction 45, but in Figure 3-2 for the SAPRC99 mechanism the SACET photolysis is set relative to reaction 131. This is because acetaldehyde photolysis is reaction number 45 for CB4 and 131 for SAPRC99. The CAMx host

mechanisms are defined by the ASCII chemistry parameters files and mechanism listings distributed with CAMx and available from the CAMx web page (www.camx.com).

Secondary Species

Secondary species are formed in the atmosphere through chemical reactions. For example, secondary formation is an important source of formaldehyde and acetaldehyde. RTRAC allows tracers to be defined to track the secondary formation of any species that is included in the host chemical mechanism (CB4 or SAPRC99). For example, in Figure 3-1 the species SFORM is used to track secondary formaldehyde, and so SFORM is defined as a secondary species and identified with the host species FORM. This means that the RTRAC chemistry module will identify the chemical production of FORM in each grid cell at each time step, and add this chemical production to the SFORM tracer. Since SFORM is intended to track only secondary formaldehyde, no primary emissions were included for SFORM.

Secondary species can be subject to chemical decay just like primary species. Therefore, the RTRAC chemistry module allows decay reactions (thermal and photolysis) to be specified for secondary species using the same method as for primary species. In this way, the concentration of a secondary species is determined by the balance between chemical production and destruction plus other model processes (transport, diffusion, and deposition).

The treatment of secondary species is explicitly linked to the host model chemistry by relating RTRAC species to host model species. For example, in Figure 3-1 the SFORM is declared to be secondary to the host species FORM, but in Figure 3-2 for the SAPRC99 mechanism the SFORM is declared to be secondary to the host species HCHO. This is because formaldehyde is called FORM in CB4 and HCHO in SAPRC99. The CAMx host mechanisms are defined by the ASCII chemistry parameters files and mechanism listings distributed with CAMx and available from the CAMx web page (www.camx.com).

Chemical Rate Data for Air Toxics

Reaction rate data for many gases can be found in rate constant compilations such as IUPAC (2001), JPL (2001) and Calvert et al. (2000, 2002). For this study, rate constants for the RTRAC air toxics chemistry were obtained from a study by Harley and Cass (1995) that modeled detailed VOCs for Los Angeles. Photolysis rates were calculated using the Tropospheric Ultra-violet Visible (TUV) model (Madronich, 2002) that is available as a CAMx pre-processor. TUV includes photolysis data (cross-sections and quantum yields) for many species and data for other species are included in IUPAC (2001), JPL (2001) and Calvert et al. (2002).

| | | | | | | | | |
|-----------------------------|-------|-----------------------------------|------|-------------|----------|---------|-----------|-----------|
| CAMx Version | | VERSION3.1 | | | | | | |
| Description | | MATES Toxics for CRC project A-42 | | | | | | |
| No of gas tracers | | 6 | | | | | | |
| No of aero tracers | | 8 | | | | | | |
| No photolysis rxns | | 4 | | | | | | |
| No thermal rxns | | 12 | | | | | | |
| Gas Tracers | | | | | | | | |
| No. | Name | P/S | SNAM | lower bnd | H-law | T-fact | Diffrat | Reactivty |
| 1 | PACET | PRIM | | 1.00E-12 | 6.30e+03 | -6492. | 1.56 | 0.0 |
| 2 | HCHO | PRIM | | 1.00E-12 | 6.30e+03 | -6492. | 1.29 | 0.0 |
| 3 | BENZ | PRIM | | 1.00E-12 | 1.80e-01 | 0. | 2.08 | 0.0 |
| 4 | BUTA | PRIM | | 1.00E-12 | 1.00e-02 | 0. | 1.73 | 0.0 |
| 5 | SACET | SEC | ALD2 | 1.00E-12 | 6.30e+03 | -6492. | 1.56 | 0.0 |
| 6 | SFORM | SEC | FORM | 1.00E-12 | 6.30e+03 | -6492. | 1.29 | 0.0 |
| Aero Tracers | | | | | | | | |
| No. | Name | lower bnd | | mol wt | Density | Low cut | Upper cut | |
| 7 | DSLFF | 1.00E-09 | | 1. | 1.5 | 0.10 | 2.50 | |
| 8 | ECF | 1.00E-09 | | 1. | 1.5 | 0.10 | 2.50 | |
| 9 | CRF | 1.00E-09 | | 1. | 1.5 | 0.10 | 2.50 | |
| 10 | CR6F | 1.00E-09 | | 1. | 1.5 | 0.10 | 2.50 | |
| 11 | DSLCL | 1.00E-09 | | 1. | 1.5 | 2.50 | 10.00 | |
| 12 | ECC | 1.00E-09 | | 1. | 1.5 | 2.50 | 10.00 | |
| 13 | CRC | 1.00E-09 | | 1. | 1.5 | 2.50 | 10.00 | |
| 14 | CR6C | 1.00E-09 | | 1. | 1.5 | 2.50 | 10.00 | |
| Photolysis reactions | | | | | | | | |
| Toxic | Rxn # | Factor | | | | | | |
| PACET | 45 | 1.0 | | | | | | |
| SACET | 45 | 1.0 | | | | | | |
| HCHO | 39 | 1.6 | | | | | | |
| SFORM | 39 | 1.6 | | | | | | |
| Thermal reactions and rates | | | | | | | | |
| Toxic | React | A(ppm-lmin-1) | | Ea(K) | B | Tref | | |
| PACET | OH | 8.2015E+03 | | 3.1099E+02 | 0.0 | 300.0 | | |
| PACET | NO3 | 2.0689E+03 | | -1.8599E+03 | 0.0 | 300.0 | | |
| HCHO | OH | 1.6699E+03 | | 6.4815E+02 | 2.0 | 300.0 | | |
| HCHO | NO3 | 4.1377E+03 | | -2.5161E+03 | 0.0 | 300.0 | | |
| BENZ | OH | 3.6944E+03 | | -1.9978E+02 | 0.0 | 300.0 | | |
| BUTA | OH | 2.1871E+04 | | 4.4787E+02 | 0.0 | 300.0 | | |
| BUTA | O3 | 4.8766E+01 | | -2.5000E+03 | 0.0 | 300.0 | | |
| BUTA | NO3 | 2.1871E+04 | | -1.4890E+03 | 0.0 | 300.0 | | |
| SACET | OH | 8.2015E+03 | | 3.1099E+02 | 0.0 | 300.0 | | |
| SACET | NO3 | 2.0689E+03 | | -1.8599E+03 | 0.0 | 300.0 | | |
| SFORM | OH | 1.6699E+03 | | 6.4815E+02 | 2.0 | 300.0 | | |
| SFORM | NO3 | 4.1377E+03 | | -2.5161E+03 | 0.0 | 300.0 | | |

Figure 3-1. Example RTRAC chemistry input file for modeling the MATES toxic species using CB4 as the host chemical mechanism.

| | | | | | | | | |
|-----------------------------|---|---------------|-------------|-----------|----------|--------|----------|-----------|
| CAMx Version | VERSION3.1 | | | | | | | |
| Description | Toxics for CRC project A-42 with SAPRC99 host mechanism | | | | | | | |
| No of gas tracers | 14 | | | | | | | |
| No of aero tracers | 0 | | | | | | | |
| No photolysis rxns | 8 | | | | | | | |
| No thermal rxns | 28 | | | | | | | |
| Gas Tracers | | | | | | | | |
| No. | Name | P/S | SNAM | lower bnd | H-law | T-fact | Difftrat | Reactivty |
| 1 | mPACET | PRIM | | 1.00E-12 | 6.30e+03 | -6492. | 1.56 | 0.0 |
| 2 | mPFORM | PRIM | | 1.00E-12 | 6.30e+03 | -6492. | 1.29 | 0.0 |
| 3 | mBENZ | PRIM | | 1.00E-12 | 1.80e-01 | 0. | 2.08 | 0.0 |
| 4 | mBUTA | PRIM | | 1.00E-12 | 1.00e-02 | 0. | 1.73 | 0.0 |
| 5 | SACET | SEC | CCHO | 1.00E-12 | 6.30e+03 | -6492. | 1.56 | 0.0 |
| 6 | SFORM | SEC | HCHO | 1.00E-12 | 6.30e+03 | -6492. | 1.29 | 0.0 |
| 7 | oPACET | PRIM | | 1.00E-12 | 6.30e+03 | -6492. | 1.56 | 0.0 |
| 8 | oPFORM | PRIM | | 1.00E-12 | 6.30e+03 | -6492. | 1.29 | 0.0 |
| 9 | oBENZ | PRIM | | 1.00E-12 | 1.80e-01 | 0. | 2.08 | 0.0 |
| 10 | oBUTA | PRIM | | 1.00E-12 | 1.00e-02 | 0. | 1.73 | 0.0 |
| 11 | pPACET | PRIM | | 1.00E-12 | 6.30e+03 | -6492. | 1.56 | 0.0 |
| 12 | pPFORM | PRIM | | 1.00E-12 | 6.30e+03 | -6492. | 1.29 | 0.0 |
| 13 | pBENZ | PRIM | | 1.00E-12 | 1.80e-01 | 0. | 2.08 | 0.0 |
| 14 | pBUTA | PRIM | | 1.00E-12 | 1.00e-02 | 0. | 1.73 | 0.0 |
| Photolysis reactions | | | | | | | | |
| Toxic | Rxn # | Factor | | | | | | |
| mPACET | 131 | 1.0 | | | | | | |
| oPACET | 131 | 1.0 | | | | | | |
| pPACET | 131 | 1.0 | | | | | | |
| SACET | 131 | 1.0 | | | | | | |
| mPFORM | 123 | 1.6 | | | | | | |
| oPFORM | 123 | 1.6 | | | | | | |
| pPFORM | 123 | 1.6 | | | | | | |
| SFORM | 123 | 1.6 | | | | | | |
| Thermal reactions and rates | | | | | | | | |
| Toxic | React | A(ppm-lmin-1) | Ea(K) | B | Tref | | | |
| mPACET | OH | 8.2015E+03 | 3.1099E+02 | 0.0 | 300.0 | | | |
| mPACET | NO3 | 2.0689E+03 | -1.8599E+03 | 0.0 | 300.0 | | | |
| oPACET | OH | 8.2015E+03 | 3.1099E+02 | 0.0 | 300.0 | | | |
| oPACET | NO3 | 2.0689E+03 | -1.8599E+03 | 0.0 | 300.0 | | | |
| pPACET | OH | 8.2015E+03 | 3.1099E+02 | 0.0 | 300.0 | | | |
| pPACET | NO3 | 2.0689E+03 | -1.8599E+03 | 0.0 | 300.0 | | | |
| mPFORM | OH | 1.6699E+03 | 6.4815E+02 | 2.0 | 300.0 | | | |
| mPFORM | NO3 | 4.1377E+03 | -2.5161E+03 | 0.0 | 300.0 | | | |
| oPFORM | OH | 1.6699E+03 | 6.4815E+02 | 2.0 | 300.0 | | | |
| oPFORM | NO3 | 4.1377E+03 | -2.5161E+03 | 0.0 | 300.0 | | | |
| pPFORM | OH | 1.6699E+03 | 6.4815E+02 | 2.0 | 300.0 | | | |
| pPFORM | NO3 | 4.1377E+03 | -2.5161E+03 | 0.0 | 300.0 | | | |
| mBENZ | OH | 3.6944E+03 | -1.9978E+02 | 0.0 | 300.0 | | | |
| oBENZ | OH | 3.6944E+03 | -1.9978E+02 | 0.0 | 300.0 | | | |
| pBENZ | OH | 3.6944E+03 | -1.9978E+02 | 0.0 | 300.0 | | | |
| mBUTA | OH | 2.1871E+04 | 4.4787E+02 | 0.0 | 300.0 | | | |
| mBUTA | O3 | 4.8766E+01 | -2.5000E+03 | 0.0 | 300.0 | | | |
| mBUTA | NO3 | 2.1871E+04 | -1.4890E+03 | 0.0 | 300.0 | | | |
| oBUTA | OH | 2.1871E+04 | 4.4787E+02 | 0.0 | 300.0 | | | |
| oBUTA | O3 | 4.8766E+01 | -2.5000E+03 | 0.0 | 300.0 | | | |
| oBUTA | NO3 | 2.1871E+04 | -1.4890E+03 | 0.0 | 300.0 | | | |
| pBUTA | OH | 2.1871E+04 | 4.4787E+02 | 0.0 | 300.0 | | | |
| pBUTA | O3 | 4.8766E+01 | -2.5000E+03 | 0.0 | 300.0 | | | |
| pBUTA | NO3 | 2.1871E+04 | -1.4890E+03 | 0.0 | 300.0 | | | |
| SACET | OH | 8.2015E+03 | 3.1099E+02 | 0.0 | 300.0 | | | |
| SACET | NO3 | 2.0689E+03 | -1.8599E+03 | 0.0 | 300.0 | | | |
| SFORM | OH | 1.6699E+03 | 6.4815E+02 | 2.0 | 300.0 | | | |
| SFORM | NO3 | 4.1377E+03 | -2.5161E+03 | 0.0 | 300.0 | | | |

Figure 3-2. Example RTRAC chemistry input file for modeling toxic species with SAPRC99 as the host chemical mechanism.

Chemical Decay Rates for Near-Source Modeling

The chemical decay rate of organic air toxics compounds in the CAMx RTRAC reactive tracers is based on the host model photolysis rates, ozone, OH, and NO₃ concentrations and the user input a species-specific reaction rates and temperature dependencies (see Figures 3-1 and 3-2). If subgrid-scale near-source impacts are to be calculated, then the user inputs the locations of each of the near-source emission complexes using the CAMx Probing Tools receptor file input format. Figure 3-3 displays an example RTRAC receptor input file for the five point source complex locations for which subgrid-scale point source modeling was performed in the MATES-II test simulations (see Chapter 5). At each grid cell, hourly decay rates for each air toxic compound are output for each CAMx vertical layer that will be interfaced with the user-selected subgrid-scale near-source model.

| | | | | |
|-------------|-----------|---|----|----|
| SINGLE CELL | Test Cell | 1 | 42 | 44 |
| SINGLE CELL | Test Cell | 1 | 41 | 36 |
| SINGLE CELL | Test Cell | 1 | 39 | 36 |
| SINGLE CELL | Test Cell | 1 | 50 | 43 |
| SINGLE CELL | Test Cell | 1 | 34 | 48 |

Figure 3-3. Example RTRAC receptor input file identifying the grid cells with locations of point source complexes where hourly decay rates will be output for subgrid-scale point source modeling (see CAMx User's Guide for format, www.com).

SUBGRID-SCALE NEAR-SOURCE MODELING

Initially, a non-steady-state Gaussian Puff Model (GPM) was planned to be embedded inside of CAMx to calculate near-source point source impacts. The GPM would track emissions from a point source using a Gaussian distribution that would impact a user-defined receptor grid. At farther downwind distances, the GPM air toxic tracer mass would be released to the grid model for further tracking. However a review of the air toxic near-source models revealed that many have specialized cavity and building effects and downwash algorithms that are undergoing continuous development (e.g., the PRIME downwash algorithms). Thus, any GPM subgrid-scale point source model embedded inside of CAMx would be based on older near-source model formulation and would have to constantly play catch up with the latest plume model developments. Furthermore, there are emerging state-of-the-art exposure models based on Large Eddy Simulation (LES) models using a high-resolution grid that model the air toxics concentrations explicitly from the source to the person (e.g., street corner). The flexibility to ultimately link the CAMx air toxics model with an LES approach is desirable. Thus, it was decided to decouple the subgrid-scale near-source model from CAMx and run the models in a separate hybrid mode extracting the needed chemistry information from CAMx but using the latest point source modeling techniques for the near-source plume impacts. Because the CAMx RTRAC capability is able to run families of tracer representing different sources, then we are able to avoid double counting when two models are used to model the same sources (e.g., CAMx for regional/mesoscale and ISC for subgrid-scale near-source impacts). That is, the air toxics emissions for a near-source complex are modeled as a

separate family in CAMx RTRAC that is excluded when summing up the families of air toxics from CAMx RTRAC simulation that is used as “background” to combine with the subgrid-scale near-source model estimates.

For subgrid-scale near-source modeling using the CAMx RTRAC air toxics modeling system the user performs the following activities:

- Identify the N separate near-source complex locations to be modeled.
- Separate the air toxic emissions into N + 1 families of tracers (each family contains a complete set of all emitted air toxics) that represent the N near-source complexes plus the remainder of all the air toxics emissions.
- Define an RTRAC receptor file corresponding to the locations of the N near-source complexes (see Figure 3-3).
- Perform a CAMx RTRAC air toxics reactive tracer grid model simulations.
- Modify the user-selected near-source plume model to accept the CAMx output hourly species-dependent chemical decay rates.
- Run the near-source plume model separately for each near-source complex using the CAMx decay rates output file and a user-defined receptor file.
- Combine the CAMx/RTRAC estimated air toxics concentrations for all sources but the near-source complex under study with the near-source plume model estimates of the near-source complex under study to get the combined near-source fence-line/hot-spot plus regional background concentration impact.

The CAMx RTRAC air toxics reactive tracer simulation provides a vertical “sounding” of hourly air toxic compound decay rates for each air toxic compound at each location specified by the user. These decay rate results are designed to interface with a user-selected near-source plume model for near-source impacts modeling. There are several different types of near-source models that can be selected for the subgrid-scale impacts:

- A steady-state Gaussian plume model (e.g., ISC or AERMOD).
- A non-steady-state Gaussian plume model (e.g., CALPUFF).
- A high-resolution Large Eddy Simulation (LES) grid model.
- Other model as selected by the user.

For the MATES-II April 1998 through March 1999 CAMx/RTRAC application, the ISC steady-state Gaussian plume model was selected to demonstrate the subgrid-scale near-source treatment. These results are discussed in Section 5.

4. CAMx AIR TOXICS MODELING RESULTS USING THE MATES-II DATABASE

This section presents the results for the CAMx/RTRAC annual air toxics model simulations for the MATES-II April 1998 through March 1999 year. The regional modeling results are presented without the subgrid-scale plume modeling for three model configurations:

- The MATES-II UAM-Tox results using EMFAC7G emissions;
- CAMx/RTRAC results using EMFAC7G emissions; and
- CAMx/RTRAC results using EMFAC2000 emissions.

The three model configurations were evaluated against the measured air toxic compound concentrations at the 10 MATES-II monitoring sites (Figure 1-2) for the following species:

- Benzene;
- 1,3-Butadiene
- Acetaldehyde;
- Formaldehyde;
- Chromium;
- Hexavalent chromium; and
- Elemental carbon¹

Note that elemental carbon (EC) is not an air toxic compound. A large fraction of diesel Particulate Matter (PM) is emitted as EC. Thus, the EC evaluation is used as a surrogate to provide an indication of the performance of the modeling system for diesel PM. Since diesel PM consists of several different components that cannot be measured separately in the atmosphere, it cannot be measured as a separate compound. However, it should be pointed out that gasoline combustion, vegetative burning, charboiling, and other sources also emit EC. Thus, EC is not a unique tracer species for diesel combustion. The MATES-II study estimated that 67% of the EC in the SoCAB is due to diesel PM emissions (SCAQMD, 2000). If this is true then EC performance is a reasonable but imperfect indication of diesel PM₁₀ performance. Thus, care should be taken in using the EC performance as a quantitative measure of the model's ability to simulate diesel PM.

Model performance statistics were calculated for the seven air pollutants and three model configurations under study. Currently there are no model performance goals or objectives for air toxic species. The EPA UATMG Houston and Phoenix air toxic modeling demonstration studies exhibited fairly poor model performance (EPA, 1999). Whereas, the performance of the MATES-II UAM-Tox modeling ranged from fair to poor (SCAQMD, 2000). The following model performance measures were calculated in this study using the 24-hour average MATES-II observation database:

¹ Elemental Carbon (EC) may consist of other species and varies depending on the measurement technique used.

Number of Predicted/Observed Pairs: The number of predicted and observed pairs matched by time (day) and location (10 MATES-II) sites provide a measure of the robustness of the model performance statistics.

Average Predicted and Observed: A comparison of the average predicted and observed values provides a measure of how well the model agrees with the observations on average.

Bias, Gross Error, and Root Mean Squared Error (RMSE): The bias, gross error, and RMSE are the average signed and unsigned (absolute value) difference and the square root of the square of the average difference in the predicted and observed concentrations in terms of $\mu\text{g}/\text{m}^3$ (or ng/m^3 for chromium and hexavalent chromium).

Fractional Bias and Error: The fractional bias and error are presented in terms of percent and are the bias and gross error of the predicted and observed concentrations normalized by the average of the predicted and observed values.

Normalized Bias and Error: The normalized bias and error are also presented in terms of percent and are the bias and gross error normalized by the observed value.

In calculating these performance statistics, no concentration thresholds were used (i.e., all predicted and observed pairs were used). Note that EPA has published ozone model performance goals for the normalized bias ($\leq \pm 15\%$) and gross error ($\leq 35\%$) (EPA, 1991). However, the EPA ozone performance measures use an observed cutoff level that is typically 60 ppb to avoid dividing by an observed concentration near zero. As many of the air toxics compound measurements are near or close to the detection limit, then normalized and fractional bias measures are going to exhibit much higher percentage differences than seen for ozone. Thus, we place more emphasis on the absolute measures of model performance (e.g., bias and gross error) and visual aids (e.g., scatter plots) and less on statistical measures that divide by a concentration (fractional and normalized measures).

MODEL PERFORMANCE EVALUATION

Scatter plots of predicted and observed 24-hour concentrations of the seven pollutants under study and the three model configurations are shown in Appendix A. Summary model performance statistics are shown in Tables 4-1 through 4-7. Note that for the PM species (chromium, hexavalent chromium, and elemental carbon), only the fine component of the PM ($\text{PM}_{2.5}$) was compared with the observed fine components because there were no observations available for the coarse ($\text{PM}_{2.5-10}$) components of the species in the MATES-II observation database provided by the SCAQMD.

Benzene

The first three scatter plots in Appendix A are comparisons of 24-hour average predicted and observed benzene concentrations for the UAM-Tox/EMFAC7G (UAM-Tox/7G), CAMx/EMFAC7G (CAMx/7G), and CAMx/EMFAC2000 (CAMx/2000) model

configurations, respectively. The two EMFAC7G model configurations exhibit scatter centered on the 1:1 line with CAMx/7G exhibiting more scatter and a lower correlation coefficient ($r^2=0.24$) than UAM-Tox/7G ($r^2=0.35$). The model performance statistics suggest a near zero bias for UAM-Tox/7G ($-0.008 \mu\text{g}/\text{m}^3$) and close to zero bias for CAMx/7G ($0.755 \mu\text{g}/\text{m}^3$). The CAMx/7G exhibits an overprediction tendency that is reflected in the scatter plot (Appendix A). The update of the emissions inventory from EMFAC7G to EMFAC2000 increases the benzene emissions by approximately 30% (see Table 2-3). Thus, the CAMx/7G benzene overprediction tendency is increased when the EMFAC2000 emissions are used so that the benzene bias is now approaching $2 \mu\text{g}/\text{m}^3$ for CAMx/2000. The fractional bias for benzene ranges from 13% (UAM-Tox/7G) to 66% (CAMx/2000). When EMFAC7G emissions are used, almost all of the predicted/observed data points in the scatter plot are within a factor of 2 of each other (the dotted lines in Appendix A) whereas the CAMx/2000 estimates are always within a factor of 3. UAM-Tox is performing slightly better than CAMx/7G which is performing better than CAMx/2000. Seigneur and co-workers have reported uncertainties in the benzene emissions on the order of 2 or 3 (Seigneur, Lohman, and Pun, 2002). Thus, all three models appear to be predicting benzene within the uncertainties of the emissions inventory.

Table 4-1. Summary model performance evaluation statistics for benzene (predicted minus observed, positive bias implies overprediction).

| | UAM-Tox EMFAC7G | CAMx EMFAC7G | CAMx EMFAC2000 |
|--|--------------------|-----------------|-------------------|
| N | 499 | 499 | 499 |
| Average Observed ($\mu\text{g}/\text{m}^3$) | 3.5793 | 3.5793 | 3.5793 |
| Average Predicted ($\mu\text{g}/\text{m}^3$) | 3.5715 | 4.3340 | 5.5540 |
| Bias ($\mu\text{g}/\text{m}^3$) | -0.0078 | 0.7546 | 1.9747 |
| Gross Error ($\mu\text{g}/\text{m}^3$) | 1.6544 | 2.0886 | 2.8501 |
| RMSE($\mu\text{g}/\text{m}^3$) | 2.4431 | 2.8769 | 3.7184 |
| Fractional Bias (%) | 13.3055 | 31.0123 | 51.6827 |
| Fractional Error (%) | 47.0972 | 56.6317 | 66.5515 |
| Normalized Bias (%) | 43.1722 | 82.9322 | 133.0869 |
| Normalized Error (%) | 69.2531 | 102.6754 | 144.8457 |

1,3-Butadiene

All three models exhibit an underestimation tendency of observed 1,3-butadiene concentrations. The average observed value is approximately $1 \mu\text{g}/\text{m}^3$ and the average predicted values are 0.6, 0.5, and $0.6 \mu\text{g}/\text{m}^3$ for UAM-Tox/7G, CAMx/7G, and CAMx/2000, respectively. In general, the model performance of the three models is comparable, with UAM-Tox/7G performing a little better than CAMx/2000 which is performing a little better than CAMx/7G. All three models fail to estimate the very highest observed values $> 3 \mu\text{g}/\text{m}^3$ as the model predictions are always under $3 \mu\text{g}/\text{m}^3$. The model predictions are well within the emissions inventory uncertainties of a factor of 2-3 reported by Seigneur and co-workers (2002).

Table 4-2. Summary model performance evaluation statistics for 1,3-butadiene (predicted minus observed, positive bias implies overprediction).

| | UAM-Tox EMFAC7G | CAMx EMFAC7G | CAMx EMFAC2000 |
|--|--------------------|-----------------|-------------------|
| N | 499 | 499 | 499 |
| Average Observed ($\mu\text{g}/\text{m}^3$) | 0.9987 | 0.9987 | 0.9987 |
| Average Predicted ($\mu\text{g}/\text{m}^3$) | 0.6238 | 0.4508 | 0.6081 |
| Bias ($\mu\text{g}/\text{m}^3$) | -0.3749 | -0.5479 | -0.3906 |
| Gross Error ($\mu\text{g}/\text{m}^3$) | 0.5585 | 0.6436 | 0.5983 |
| RMSE($\mu\text{g}/\text{m}^3$) | 0.9244 | 1.0430 | 0.9602 |
| Fractional Bias (%) | -14.9472 | -55.9368 | -30.0836 |
| Fractional Error (%) | 59.8067 | 80.6696 | 71.5459 |
| Normalized Bias (%) | 16.9421 | -17.9995 | 12.5738 |
| Normalized Error (%) | 69.8195 | 69.6343 | 80.1203 |

Acetaldehyde

UAM-Tox underestimates the observed acetaldehyde by approximately a factor of 3 with predicted and observed average concentration of 1 and $3\mu\text{g}/\text{m}^3$, respectively (Appendix A and Table 4-3). Both CAMx/7G and CAMx/2000 overestimate the observed acetaldehyde concentrations by approximately 60 ($\sim 5\mu\text{g}/\text{m}^3$) and 80 ($\sim 5\text{--}6\mu\text{g}/\text{m}^3$) percent, respectively. CAMx/7G is exhibiting the best model performance and both CAMx runs estimate a majority of the observed 24-hour acetaldehyde concentrations are reproduced to within a factor of 2. This is in contrast to the UAM-Tox that underestimates most of the observed acetaldehyde concentrations by over a factor of 2. It is interesting to note that most of the UAM-Tox acetaldehyde estimates are below $2\mu\text{g}/\text{m}^3$, whereas most of the CAMx acetaldehyde estimates are above $2\mu\text{g}/\text{m}^3$. The CAMx simulations were performed using a $0.008\mu\text{g}/\text{m}^3$ boundary condition, which is reported to be the same one as used by UAM-Tox and is well below $2\mu\text{g}/\text{m}^3$. Thus, the CAMx acetaldehyde concentrations are mainly emitted or formed within the SoCAB domain, rather than transported from the boundary conditions. There are a fair amount of observed acetaldehyde concentrations below $2\mu\text{g}/\text{m}^3$ so the CAMx $2\mu\text{g}/\text{m}^3$ predicted minimum is not a desirable model performance attribute. On the other hand, there are even more observed values above $2\mu\text{g}/\text{m}^3$ so the UAM-Tox $2\mu\text{g}/\text{m}^3$ maximum is even more undesirable. CAMx is clearly exhibiting better model performance for acetaldehyde than UAM-Tox.

Note that in the CB4 chemical mechanism the secondarily produced ALD2 species that is allocated to the RTRAC secondary acetaldehyde species is a lumped species that includes other higher aldehydes than acetaldehyde. The fraction of acetaldehyde in ALD2 will vary. This introduces an uncertainty in the CAMx/CB4 RTRAC acetaldehyde estimates. This issue is addressed in Chapter 6 where air toxics modeling results using CAMx with the CB4 and SAPRC99, which has acetaldehyde as an explicit species, chemical mechanisms we compared.

Table 4-3. Summary model performance evaluation statistics for acetaldehyde (predicted minus observed, positive bias implies overprediction).

| | UAM-Tox EMFAC7G | CAMx EMFAC7G | CAMx EMFAC2000 |
|--|--------------------|-----------------|-------------------|
| N | 490 | 490 | 490 |
| Average Observed ($\mu\text{g}/\text{m}^3$) | 3.0470 | 3.0470 | 3.0470 |
| Average Predicted ($\mu\text{g}/\text{m}^3$) | 1.0776 | 4.9222 | 5.5758 |
| Bias ($\mu\text{g}/\text{m}^3$) | -1.9695 | 1.8751 | 2.5287 |
| Gross Error ($\mu\text{g}/\text{m}^3$) | 2.1534 | 2.4679 | 2.9601 |
| RMSE($\mu\text{g}/\text{m}^3$) | 2.8001 | 3.2317 | 3.9127 |
| Fractional Bias (%) | -76.6732 | 53.6722 | 63.0566 |
| Fractional Error (%) | 96.2067 | 66.4057 | 71.8629 |
| Normalized Bias (%) | -11.0903 | 283.1744 | 328.8876 |
| Normalized Error (%) | 99.5018 | 293.4599 | 336.0885 |

Formaldehyde

The UAM-Tox exhibits a net underprediction tendency of the observed formaldehyde concentrations of approximately 30%, whereas the two CAMx simulations exhibit an overprediction tendency that is approximately 50% (EMFAC7G) and 90% (EMFAC2000) (Appendix A and Table 4-4). As was seen for acetaldehyde, the CAMx simulation formaldehyde estimates appear to not go below approximately $2\mu\text{g}/\text{m}^3$.

Table 4-4. Summary model performance evaluation statistics for formaldehyde (predicted minus observed, positive bias implies overprediction).

| | UAM-Tox EMFAC7G | CAMx EMFAC7G | CAMx EMFAC2000 |
|--|--------------------|-----------------|-------------------|
| N | 502 | 502 | 502 |
| Average Observed ($\mu\text{g}/\text{m}^3$) | 4.8413 | 4.8413 | 4.8413 |
| Average Predicted ($\mu\text{g}/\text{m}^3$) | 3.3549 | 7.4321 | 9.1052 |
| Bias ($\mu\text{g}/\text{m}^3$) | -1.4864 | 2.5908 | 4.2639 |
| Gross Error ($\mu\text{g}/\text{m}^3$) | 2.6984 | 4.0573 | 5.2589 |
| RMSE($\mu\text{g}/\text{m}^3$) | 3.5861 | 5.4102 | 6.9849 |
| Fractional Bias (%) | -25.5018 | 44.9967 | 60.5307 |
| Fractional Error (%) | 64.1063 | 67.8014 | 75.2718 |
| Normalized Bias (%) | 155.0187 | 427.9297 | 576.5912 |
| Normalized Error (%) | 218.2940 | 445.6601 | 588.2816 |

Chromium PM_{2.5})

All three models estimate much higher average fine particulate chromium values than observed. As seen in the scatter plots (Appendix A), there are numerous observed PM_{2.5} chromium values near zero that have been set to half the detection limit when it was below the instrument detection limit. Note that because of their low concentrations, chromium and

hexavalent chromium results are presented in terms of nanograms per cubic meter (ng/m^3) rather than the usual micrograms per cubic meter ($\mu\text{g}/\text{m}^3$) that is used for the other species ($1000 \text{ ng}/\text{m}^3 = 1 \mu\text{g}/\text{m}^3$). The UAM-Tox average chromium concentration ($18 \text{ ng}/\text{m}^3$) is approximately 4.5 times the observed value ($4.8 \text{ ng}/\text{m}^3$), whereas the CAMx estimated average chromium concentration ($12.5 \text{ ng}/\text{m}^3$) is approximately 2.5 times the average observed value (Table 4-5). The EMFAC2000 update has little effect on the chromium concentration estimates as the difference in EMFAC7G and EMFAC2000 emissions is smaller (8%) than for organic emissions ($\sim 50\%$) and on-road mobile is a smaller fraction to total chromium emissions than the organic air toxics. Clearly the overprediction tendency is partly an emissions and/or measurement issue. Although model performance for both models is poor, the CAMx overprediction (factor of 2.5) is not as severe as UAM-Tox over prediction (factor of 4.5) for chromium $\text{PM}_{2.5}$.

Table 4-5. Summary model performance evaluation statistics for chromium $\text{PM}_{2.5}$ (predicted minus observed, positive bias implies overprediction).

| | UAM-Tox EMFAC7G | CAMx EMFAC7G | CAMx EMFAC2000 |
|--|--------------------|-----------------|-------------------|
| N | 429 | 429 | 429 |
| Average Observed (ng/m^3) | 4.8157 | 4.8157 | 4.8157 |
| Average Predicted (ng/m^3) | 18.1940 | 12.5408 | 12.5488 |
| Bias (ng/m^3) | 13.3783 | 7.7251 | 7.7331 |
| Gross Error (ng/m^3) | 13.8582 | 9.7482 | 9.7548 |
| RMSE(ng/m^3) | 17.5245 | 12.7672 | 12.7754 |
| Fractional Bias (%) | 117.8772 | 88.0246 | 88.0641 |
| Fractional Error (%) | 121.0043 | 110.8439 | 110.8636 |
| Normalized Bias (%) | 943.3663 | 620.3307 | 620.7668 |
| Normalized Error (%) | 945.9296 | 636.7145 | 637.1380 |

Hexavalent Chromium

The two models also overestimate hexavalent chromium (CrVI). For CrVI , the SCAQMD and ARB laboratory equipment had two different detection limits that are readily apparent in the scatter plots as vertical lines (Appendix A). As shown in Table 4-6, the average observed CrVI ($0.18 \text{ ng}/\text{m}^3$) is overestimated by the UAM-Tox by a factor of 4 ($0.73 \text{ ng}/\text{m}^3$). The CAMx average CrVI estimates ($0.38 \text{ ng}/\text{m}^3$) overestimate the average observed values by approximately a factor of 2.

Table 4-6. Summary model performance evaluation statistics for Hexavalent Chromium $PM_{2.5}$ (predicted minus observed, positive bias implies overprediction).

| | UAM-Tox EMFAC7G | CAMx EMFAC7G | CAMx EMFAC2000 |
|--------------------------------|----------------------------|-------------------------|---------------------------|
| N | 486 | 486 | 486 |
| Average Observed (ng/m^3) | 0.1807 | 0.1807 | 0.1807 |
| Average Predicted (ng/m^3) | 0.7334 | 0.3820 | 0.3874 |
| Bias (ng/m^3) | 0.5527 | 0.2013 | 0.2067 |
| Gross Error (ng/m^3) | 0.6175 | 0.2903 | 0.2944 |
| RMSE(ng/m^3) | 1.4518 | 0.5085 | 0.5162 |
| Fractional Bias (%) | 59.2450 | 33.0777 | 34.1689 |
| Fractional Error (%) | 86.8649 | 79.2191 | 79.4204 |
| Normalized Bias (%) | 473.6166 | 198.7015 | 202.9212 |
| Normalized Error (%) | 493.9665 | 231.2150 | 234.8527 |

Elemental Carbon

The evaluation of elemental carbon (EC) is presented as a surrogate for diesel particles. However, not all EC is due to diesel combustion and not all diesel particles is EC so the evaluation link between EC and diesel particles is purely qualitative.

On average, the three models have similar fairly good model performance for EC, overpredicting the average observed EC value ($3.4 \mu g/m^3$) by approximately $0.5 \mu g/m^3$ (15%) (Table 4-7). The model performance for EC is better than for the other species examined with fractional bias of about 14% (CAMx) and 22% (UAM-Tox). EMFAC2000 has little effect on the EC model estimates.

Table 4-7. Summary model performance evaluation statistics for Elemental Carbon $PM_{2.5}$ (predicted minus observed, positive bias implies overprediction).

| | UAM-Tox EMFAC7G | CAMx EMFAC7G | CAMx EMFAC2000 |
|-----------------------------------|----------------------------|-------------------------|---------------------------|
| N | 426 | 426 | 426 |
| Average Observed ($\mu g/m^3$) | 3.3912 | 3.3912 | 3.3912 |
| Average Predicted ($\mu g/m^3$) | 3.9072 | 3.9214 | 3.9496 |
| Bias ($\mu g/m^3$) | 0.5161 | 0.5302 | 0.5584 |
| Gross Error ($\mu g/m^3$) | 1.5177 | 1.7196 | 1.7332 |
| RMSE($\mu g/m^3$) | 2.0378 | 2.3286 | 2.3485 |
| Fractional Bias (%) | 22.4869 | 13.8016 | 14.4090 |
| Fractional Error (%) | 44.3902 | 48.1519 | 48.3003 |
| Normalized Bias (%) | 48.5975 | 41.2235 | 42.1979 |
| Normalized Error (%) | 66.4768 | 67.9416 | 68.5887 |

SPATIAL DISTRIBUTION OF AIR TOXIC CONCENTRATIONS

The spatial distribution of the estimated air toxic concentrations were examined for the CAMx/7G and CAMx/2000 simulations. As the UAM-Tox predictions were available only at the monitoring sites, the UAM-Tox spatial distributions were not analyzed. CAMx using EMFAC7G or EMFAC2000 estimated very similar spatial distributions of pollutants, thus only the CAMx/2000 results are presented in Appendix B.

Benzene

The spatial distribution of the CAMx estimated annual benzene concentrations follow the major roadways in the SoCAB (Appendix B). The maximum concentration of 1.1 ppb (0.0011 ppm) occurs in downtown Los Angeles at the confluence of the 5, 10, 60, and 110 freeways. From downtown Los Angeles, there are high estimated benzene concentrations heading directly west toward the coast following the 10 freeway to Santa Monica. South of Santa Monica is a more isolated benzene maximum that is centered over the LAX airport. Heading east from downtown Los Angeles, freeways 10 and 60 are clearly evident in the benzene concentration patterns as the two freeways come together in Riverside. There are also estimated elevated benzene concentrations in northern Orange County centered over Anaheim and then a trail heading east from Anaheim following freeway 91 to Riverside. The fact that the estimated benzene concentrations follow the major roadways is not surprising given that almost 80% of the benzene emissions in the SoCAB are attributable to on-road mobile sources (see Table 2-3).

1,3-Butadiene

Although on-road mobile sources also dominate the 1,3-butadiene emissions in the SoCAB, contributing approximately 75% (See Table 2-3), the spatial patterns of the 1,3-butadiene concentration estimates are very different from benzene. The major feature of the CAMx estimated annual distribution of 1,3-butadiene concentrations is the presence of a blob of highest 1,3-butadiene concentrations centered over the LAX airport where annual average concentrations approaching 0.5 ppb occur. Although elevated 1,3-butadiene concentrations are seen over downtown Los Angeles and Anaheim, the peaks appear to be under 0.15 ppb and are much lower than the elevated blob over LAX of 0.25-0.50 ppb. When using a lower scale in the spatial plot (not shown), the roadways begin to appear in the 1,3-butadiene concentration distribution, but the presence of the LAX airport is still the dominant feature. The reasons why LAX is so dominant in the 1,3-butadiene concentrations distributions are unclear but are believed to be due to the following:

- Highly concentrated emissions of 1,3-butadiene from on-road and non-road (e.g., aircraft) sources;
- Coastal environment with very little vertical and horizontal mixing that limits the dispersal of pollutants;
- A highly reactive compound that decays quickly so is not transported far; and

- Relatively lower photochemical oxidants on the coast as compared to further in the interior of the domain that result in slower 1,3-butadiene decay rates at LAX compared to farther inland.

Acetaldehyde

Appendix B contains spatial plots of primarily emitted and secondarily formed annual average acetaldehyde concentrations. Primary acetaldehyde concentrations have two major hot spots where annual average concentrations exceed 1 ppb: the LAX airport on the west coast near El Segundo; and the Ports of Long Beach and Los Angeles down by Long Beach. Over the rest of the SoCAB, the primary acetaldehyde concentrations are 0.5 ppb or less.

The spatial distribution of secondary acetaldehyde concentrations is very different from primary acetaldehyde. Secondary acetaldehyde increases in concentrations going inland from west to east across the domain and peaking at 1-2 ppb in the Riverside/Ontario area and in the San Gabriel Mountains north of Glendora. Not surprisingly, the pattern of secondary acetaldehyde is somewhat similar to what is sometimes seen for ozone, another secondary pollutant. Appendix B also has ratios of the annual average primary to total acetaldehyde concentrations. Except for the LAX airport and port areas near Long Beach, secondary acetaldehyde accounts for over 70 percent of the total acetaldehyde concentration. Eliminating LAX, the Port, and the downtown centers of Los Angeles and some of the other major cities, secondary acetaldehyde contributes 90 percent or more to the total acetaldehyde concentrations over a majority of the SoCAB.

Formaldehyde

LAX and the Port areas are also two hot spots for primary formaldehyde concentrations where annual average concentrations of 3-8 ppb are estimated to occur (Appendix B). The city centers of Los Angeles and Anaheim are also clearly evident in the annual average primary formaldehyde spatial distributions. The gradient of secondary formaldehyde concentrations going west to east is not as pronounced as seen for acetaldehyde. The peak formaldehyde over the San Gabriel Mountains north of Glendora appears to be higher than over the Riverside/Ontario area, whereas for secondary acetaldehyde the reverse was true. This is believed to be due to the higher formaldehyde yields from biogenic VOC emissions (isoprene) compared to acetaldehyde yields and the fact that biogenic VOCs that are more prevalent in the San Gabriel Mountains.

The amount of primary formaldehyde to total formaldehyde is greater than seen for acetaldehyde. This is mainly because there are 4 times as much primary formaldehyde emissions as primary acetaldehyde emissions (see Table 2-3).

Primary formaldehyde accounts for over 60 percent of the total formaldehyde over the LAX airport and Port regions. Away from those areas in the populated regions of the basin, primary formaldehyde accounts for 25-50% and secondary formaldehyde accounts for 50-75% of the total formaldehyde. Secondary formaldehyde dominates the total formaldehyde concentrations in the more rural and remote areas of the SoCAB.

Chromium

Spatial maps of annual average fine and coarse PM chromium concentrations are contained in Appendix B. The distribution of the chromium appears to follow the roadways. The coarse mode chromium appears to be higher than the fine mode with very high concentrations out in the Riverside/Ontario/San Bernardino areas, whereas the fine mode has higher concentrations in the downtown Los Angeles area. The reasons for these differences in the spatial distribution of fine versus coarse model chromium estimates are unclear as only model-ready gridded emissions were provided so we cannot go back to the raw emissions data to identify the source categories that cause these differences. However, we do know that, as currently formulated, the fate of whether chromium resides in the fine or coarse mode is based on how it is split in the emissions inventory. The current implementation of chromium in CAMx does not allow the particles to grow and transfer from the fine to coarse modes or vice versa. The relatively high amounts of coarse mode chromium estimates raises questions regarding the adequacy of the MATES-II procedures to evaluate just the fine mode of these species.

Hexavalent Chromium

The spatial distribution of hexavalent chromium (CrVI) is very spotty and not at all related to the distributions of roadways in the SoCAB. There appears to be six isolated fine mode CrVI hot spots, five in Los Angeles and one in San Bernardino County. However, there appears to be many more (> 20) coarse mode CrVI hot spot locations. The coarse mode CrVI estimates are much greater than the fine mode CrVI estimates over most of the domain. Again, these results raise questions regarding using the MATES-II fine mode measurements to evaluate a model for predicting a species that resides mainly in the coarse mode.

Diesel Particles

The estimated diesel particle concentrations reside almost completely within the fine PM mode (Appendix B). There are high estimated concentrations of diesel PM due to emissions from the Ports of Long Beach and Los Angeles, downtown Los Angeles, Anaheim, and areas in the Ontario/Riverside/San Bernardino area. The major roadways are evident in the diesel particle concentration estimates. However, by far the largest source region is the Port area near Long Beach where annual average concentrations in excess of $2\mu\text{g}/\text{m}^3$ stretch from the Ports to the west out to sea. The marine vessels, loading/unloading apparatus, and trucking equipment all contribute to these high diesel PM concentrations. Again, since only fully merged emissions were available, the relative contributions of these sources to the total diesel PM in the Port area could not be obtained, but we suspect marine vessels to be a major contributor.

“Elemental” Carbon

“Elemental” Carbon (EC) is also mainly in the fine PM mode. The spatial distributions of estimated annual average fine EC concentrations consist of five major elevated EC regions

superimposed on top of elevated EC concentrations that follow the roadway distribution. The five elevated EC regions are as follows:

- The Port area near Long Beach, where the EC is likely primarily due to the diesel engines in the marine vessels and support equipment;
- Downtown Los Angeles where the high EC concentrations are likely due to motor vehicle emissions from the confluence of several freeways and congestion;
- An area up in the San Gabriel Mountains that we suspect may be due to forest fires;
- Around Ontario; and
- Around San Bernardino.

Although there is lots of motor vehicle traffic at these latter two high EC concentration locations, it is unclear why the annual average at these two locations are higher than other major cities (e.g., Anaheim). It maybe due to a combination of high emissions, prevailing westerly winds from upwind source regions, and stagnation. Vegetative burning (wild fires) may also have played a role in these two high EC locations.

The spatial distribution of the coarse EC estimates is quite different and lower than the fine EC estimates. With one notable exception, the distribution of elevated coarse EC follows the roadways. The exception is a bull's eye annual average coarse EC approaching $2\mu\text{g}/\text{m}^3$ that appears to occur in Upland on freeway 10 just northwest of Ontario. As only model-ready emissions files were provided by the SCAQMD, we could not investigate the details as to what in the emissions is causing this coarse EC spike at this location.

SUMMARY OF MODEL PERFORMANCE

The three model configurations (UAM-Tox/7G, CAMx/7G, and CAMx/2000) exhibit some skill in estimating the MATES-II benzene observations. Although UAM-Tox exhibited slightly better model performance for benzene than CAMx, the differences were well below the uncertainties in the emissions inventory.

The three models exhibit a similar 40-55% underprediction tendency for 1,3-butadiene. None of the models estimated a 24-hour 1,3-butadiene concentration $> 2\mu\text{g}/\text{m}^3$, whereas there were over 50 observed occurrences throughout the modeling year.

The UAM-Tox and CAMx exhibit very different model performance characteristics for acetaldehyde. UAM-Tox underpredicts on average by a factor of 3, whereas CAMx is within a factor of 2 on average (overprediction of 60% and 80% for CAMx/7G and CAMx/2000).

The three models estimate the observed average formaldehyde within a factor of 2, but UAM-Tox/7G exhibits an underprediction tendency (-30%), when CAMx/7G (+60%) and CAMx/2000 (+80%) exhibit an overprediction tendency. The performance statistics suggest UAM-Tox is performing a little better than CAMx.

For fine particulate chromium and hexavalent chromium (CrVI), the models severely overestimate the observed concentration. The UAM-Tox overestimation tendency is much

more severe with chromium and CrVI that are overestimated by a factor of approximately 4.5 and 4, respectively. Whereas the CAMx average overprediction is by a factor of approximately 2.5 and 2, respectively.

The three models exhibit much more skill in estimating the observed elemental carbon (EC) concentrations with a bias that is within 15% of the average observed value. The CAMx simulation EC model performance statistics are slightly better than those for UAM-Tox.

RISK CALCULATION AND EXPOSURE MODELING

The MATES-II study used species-dependent unit risk factors (URFs) that are applied to the annual average air toxics concentrations and summed to estimate the one in a million risk of premature death due to exposure to air toxics. MATES-II calculated monitored and modeled risk at the 10 MATES-II monitoring sites and averaged them to obtain the SoCAB basin-wide risk estimate. The URFs used in the MATES-II study, that are also used in this study, are as follows:

- Benzene: $2.9 \times 10^{-5} (\mu\text{g}/\text{m}^3)^{-1}$
- 1,3-Butadiene: $1.7 \times 10^{-4} (\mu\text{g}/\text{m}^3)^{-1}$
- Acetaldehyde: $2.7 \times 10^{-6} (\mu\text{g}/\text{m}^3)^{-1}$
- Formaldehyde: $6.0 \times 10^{-6} (\mu\text{g}/\text{m}^3)^{-1}$
- Diesel Particles: $3.0 \times 10^{-4} (\mu\text{g}/\text{m}^3)^{-1}$

In MATES-II, risk was calculated in terms of outdoor frontyard exposures. That is, the long-term rate of cancer incidence due to exposure to air toxics assumed that a person was outdoors 24 hours/day 365 days/year. The exposure to air toxics is going to vary greatly indoors versus outdoors by pollutant. For example, there are indoor sources of formaldehyde that increase indoor exposure to that pollutant. On the other hand, diesel PM will be greater outdoors than indoor and greater still on and near major roadways.

Ideally to estimate risk and exposure the effects of population movement by population charts, effects of indoor effects by different building types (e.g., air conditioning), and population location to emissions (e.g., on street corner) should be accounted for. In this study we analyzed several simplistic representations of indoor effects and population distribution on exposure that represents an improvement over the MATES-II front yard outdoor exposure approach.

We reviewed available literature to identify indoor/outdoor ratios that could be applied in a simple fashion to estimate the exposure of people to outdoor air toxics. The only pollutant that was characterized sufficient by well was diesel particles, which according to MATES-II accounted for 70% of the risk in the SoCAB.

Using work as reported by Hayes and co-workers (1994) we developed indoor/outdoor ratios by month and time of day that represented the following factors:

- Indoor at home;
- Indoor at work;
- Outdoors; and
- In a car.

The resultant annual average indoor/outdoor ratio was 0.59, which agreed fairly well with the Hayes and co-workers (1994) 0.55 for adults and 0.60 for children factors.

Exposure was then calculated several different ways as follows:

- 10 site average using annual average concentrations and no indoor/outdoor ratio;
- 10 site average using annual average concentrations and constant (0.59) indoor/outdoor ratio; and
- 10 site average using hourly concentrations and hourly indoor/outdoor ratio.

The results of these risk calculations are displayed in Table 4-8. The risk results of the MATES-II modeling and monitoring are also shown in Table 4-8. Even though this study did not simulate all air toxic compounds, this study's risks are greater than estimated by MATES-II. According to MATES-II, the air toxics not accounted for in this study account for approximately 10% of the risk. This study's risk, without accounting for indoor/outdoor effects, is 35-60% higher than the average risks reported in MATES-II. The higher aldehyde and benzene concentrations estimated by CAMx/RTRAC than UAM-Tox account for most of these differences (although diesel particles may also play a role).

When accounting for indoor/outdoor effects on diesel particles only, the estimated risk is reduced by approximately one-third. Note that there is little difference (within 2%) in the calculated risk whether a composite annual average indoor/outdoor factor is used or if hourly values are applied to the hourly air toxics concentrations.

Figure 4-1 displays the spatial distribution of annual risk with and without accounting for indoor/outdoor effects. The highest risks occur in Los Angeles County with large areas of risk exceeding 2,000 in a million (Figure 4-1a). When indoor/outdoor effects are accounted for there are only two isolated areas with risk exceeding 2,000 in a million, downtown Los Angeles and the port area near Long Beach. The risk at the location of the maximum risk (port area) without indoor/outdoor effects (4,519 in a million) is reduced approximately 40% when indoor/outdoor (I/O) effects are accounted for (2,776 and 2,703 in a million) applying I/O effects on an annual versus hourly basis, respectively.

Table 4-8. Average risk across the 10 MATES-II sites calculated in MATES-II (no indoor/outdoor effect) and by this study with no indoor/outdoor (I/O) effects and accounting for indoor/outdoor effects on an annual average and hourly.

| Scenario | Risk (Number in a million) | Percent different from no indoor/outdoor ratio. |
|--|-------------------------------|--|
| <i>MATES-II Study Results No Indoor/Outdoor Effects (SCAQMD, 2000)</i> | | |
| Modeled Average, no I/O | 1,230 | |
| Monitored Average, no I/O | 1,414 | |
| This Study's Modeling Risk with and without Accounting for Indoor/Outdoor Effects | | |
| No Indoor/Outdoor Effects | 1,950 | |
| Annual Indoor/Outdoor Ratio | 1,284 | -34.1 |
| Hourly Indoor/Outdoor Ratios | 1,257 | -35.5 |

Combining the risk factors with population gives the exposure to air toxics. In MATES-II, the average risk across the basin or in a county was compared with the basin-average or countywide population. Exposure was calculated several ways in this study:

- The 10-site average risks in Table 4-8 were applied to the basin-wide population of 14,404,993 people (similar to the MATES-II approach);
- An annual average gridded risk with and without indoor/outdoor effects was applied to a gridded population field and totaled to accounting for the spatial distribution of the air toxics and population; and
- The exposure was accumulated throughout the year using the gridded hourly air toxics concentrations, the gridded population, and the hourly indoor/outdoor ratios.

Note that the gridded population used when calculating spatially varying exposure totaled to the same amount as the basin-wide calculations using the 10-site average (around 14 million people).

The results of the exposure calculation accounting for and not accounting for the spatial distribution of the air toxics and populations and accounting for and not accounting for the indoor/outdoor (I/O) effects are shown in Table 4-9. When accounting for the spatial variations in air toxics concentrations and population, the estimated exposure is reduced by 16%. As seen for risk, accounting for indoor/outdoor effects on exposure, whether hourly or on an annual composite basis, reduces the exposure to air toxics by 34-36%. Combining the spatially varying and indoor/outdoor effects, we see almost a factor of 2 reduction in the estimated exposures due to air toxics. That is using a simple representation of the effects of population distribution and indoor/outdoor effects on risk and exposure reduces them by approximately a factor of 2 over what was reported in MATES-II (SCAQMD, 2000).

Figure 4-2 displays the spatial distribution of exposure with no indoor/outdoor effects and accounting for them on an annual and hourly basis. Note that even though the magnitude of the risk was higher in the port area near Long Beach than in downtown Los Angeles, the exposure in downtown Los Angeles is higher than in the port area due to the higher population. Accounting for indoor/outdoor effects reduces the exposure at any location by approximately one-third, which was also seen for the basin-wide exposure (Table 4-9).

Table 4-9. Comparison of the estimated exposure to air toxics using the 10-site average risk and basin-wide population versus using spatially varying risk and spatially varying population with and without accounting for indoor/outdoor (I/O) effects.

| Scenario | 10-Site Average | | Spatially Varying | | % 10-site vs. Spat. Varying |
|----------------|-----------------|------------|-------------------|------------|-----------------------------|
| | Exposure | (% no I/O) | Exposure | (% no I/O) | |
| No I/O Effects | 28,087 | | 23,519 | | (-16) |
| Constant I/O | 18,496 | (-34) | 15,624 | (-34) | (-16) |
| Hourly I/O | 18,112 | (-36) | 15,258 | (-35) | (-16) |

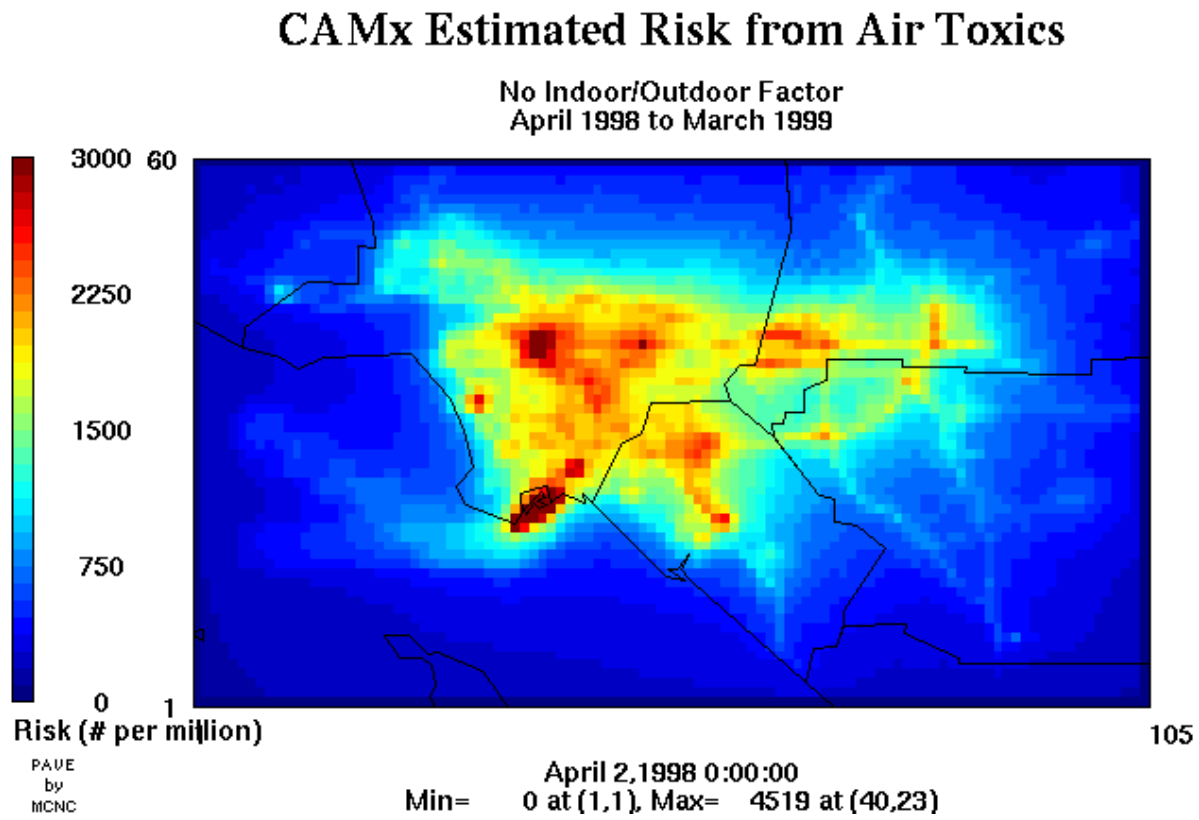


Figure 4-1a. Spatial distribution of estimated risk (out of a million) not accounting for indoor/outdoor effects.

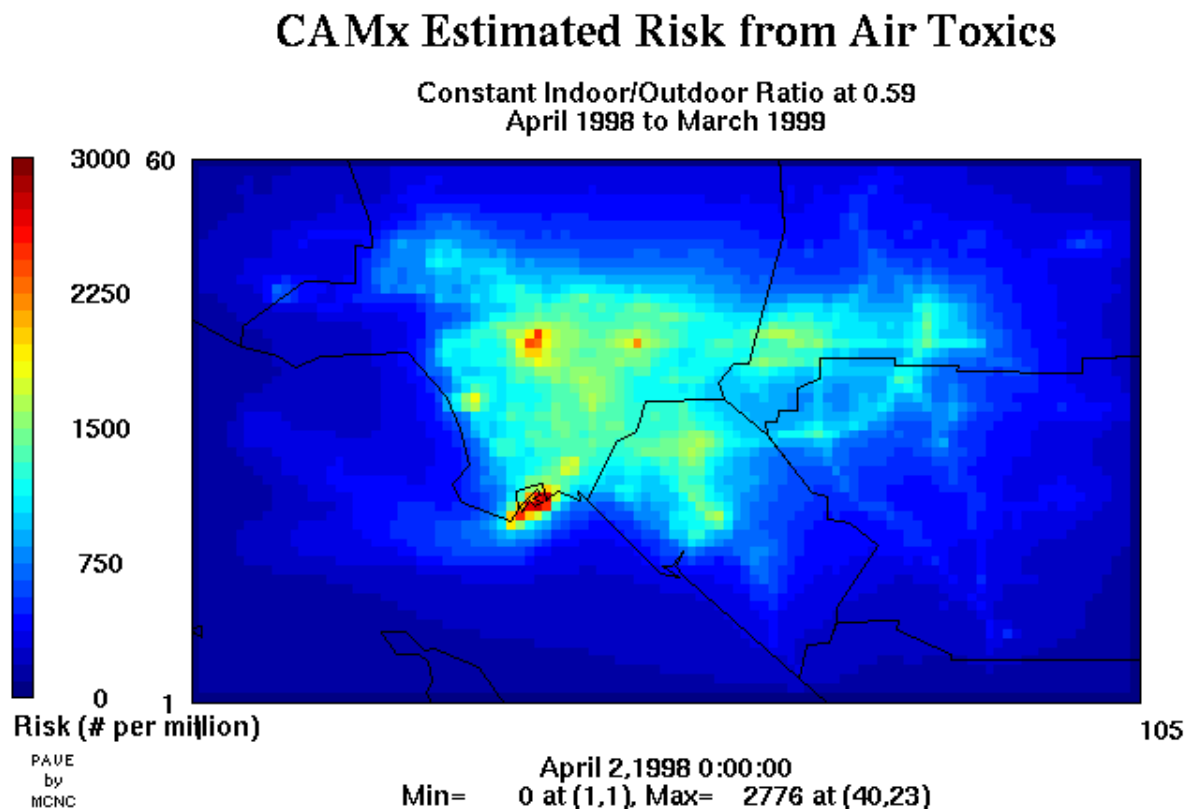


Figure 4-1b. Spatial distribution of estimated risk (out of a million) accounting for indoor/outdoor effects on an annual basis.

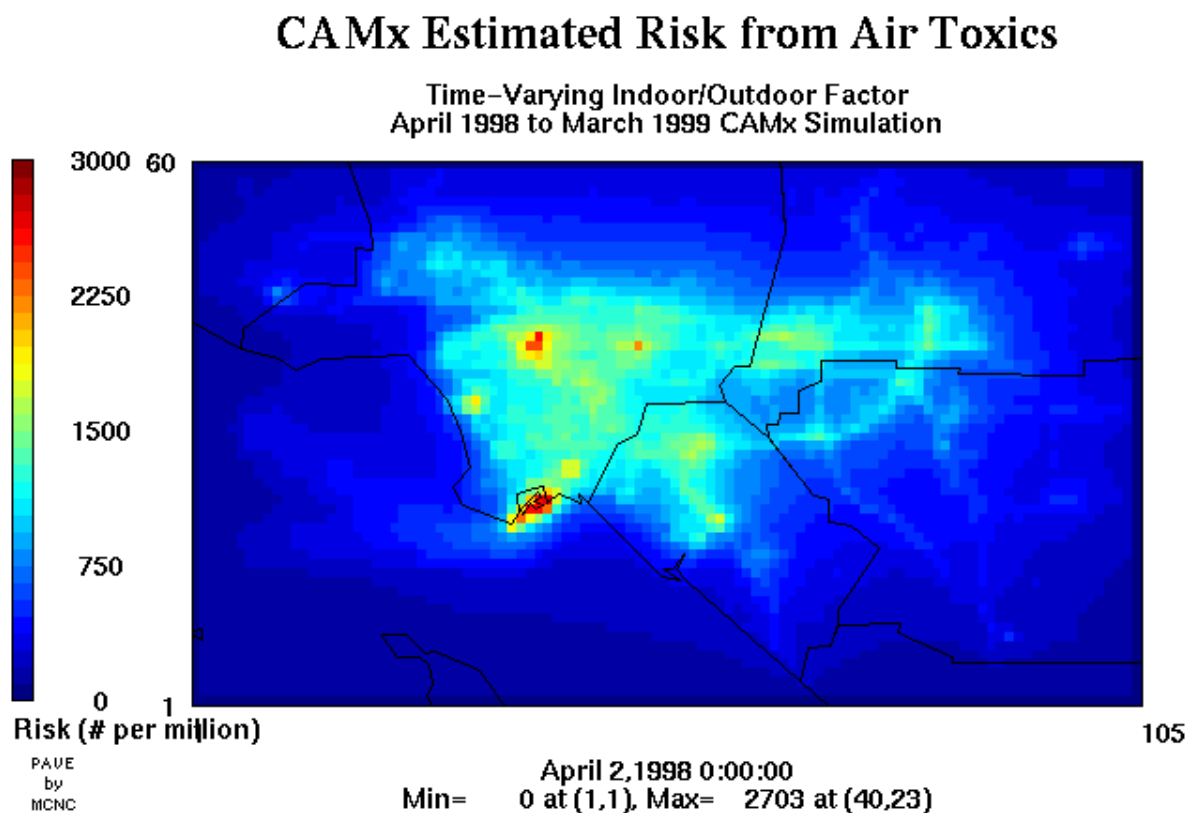


Figure 4-1c. Spatial distribution of estimated risk (out of a million) accounting for indoor/outdoor effects on an hourly basis.

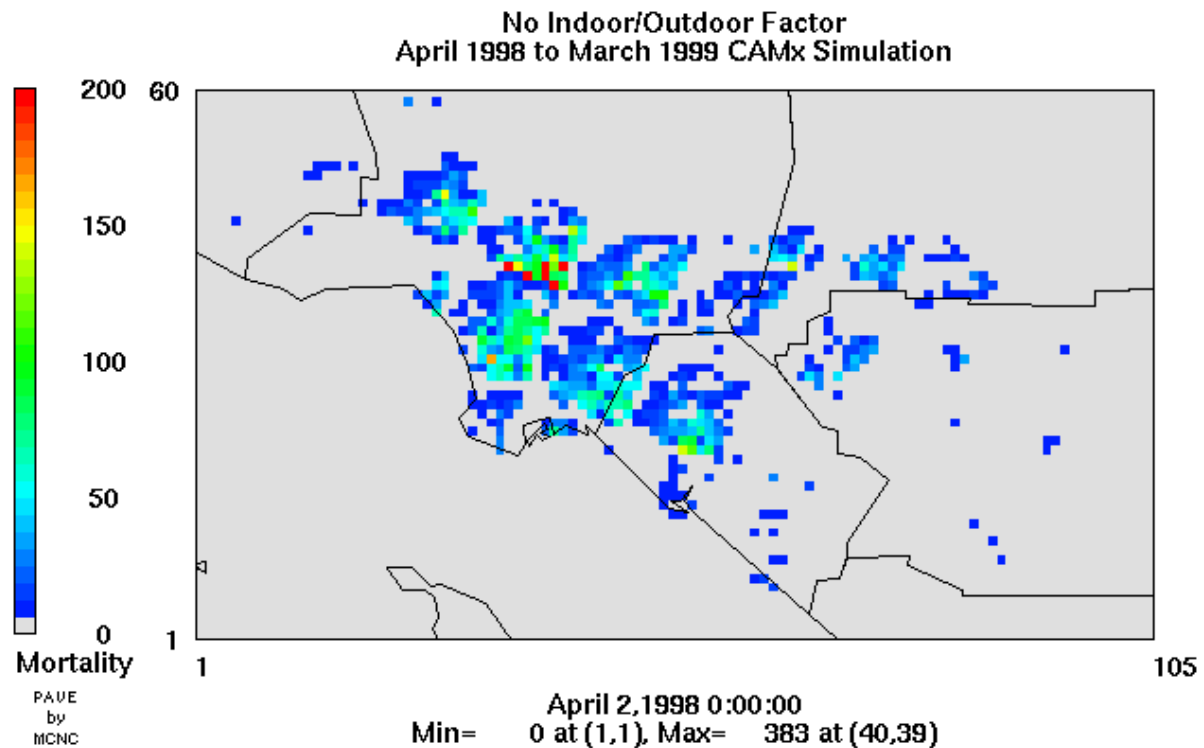


Figure 4-2a. Spatial distribution of exposure using gridded population and annual average risk but not accounting for indoor/outdoor effects.

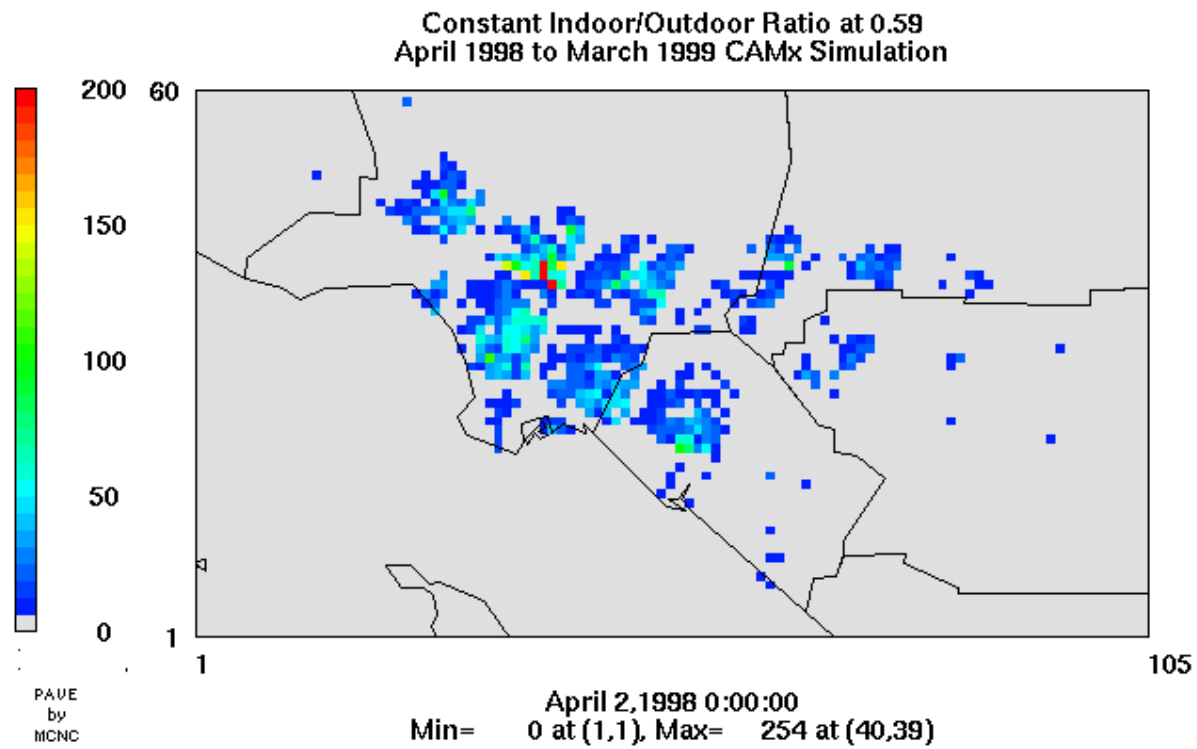


Figure 4-2b. Spatial distribution of exposure using gridded population and annual average risk and accounting for indoor/outdoor effects on an annual basis.

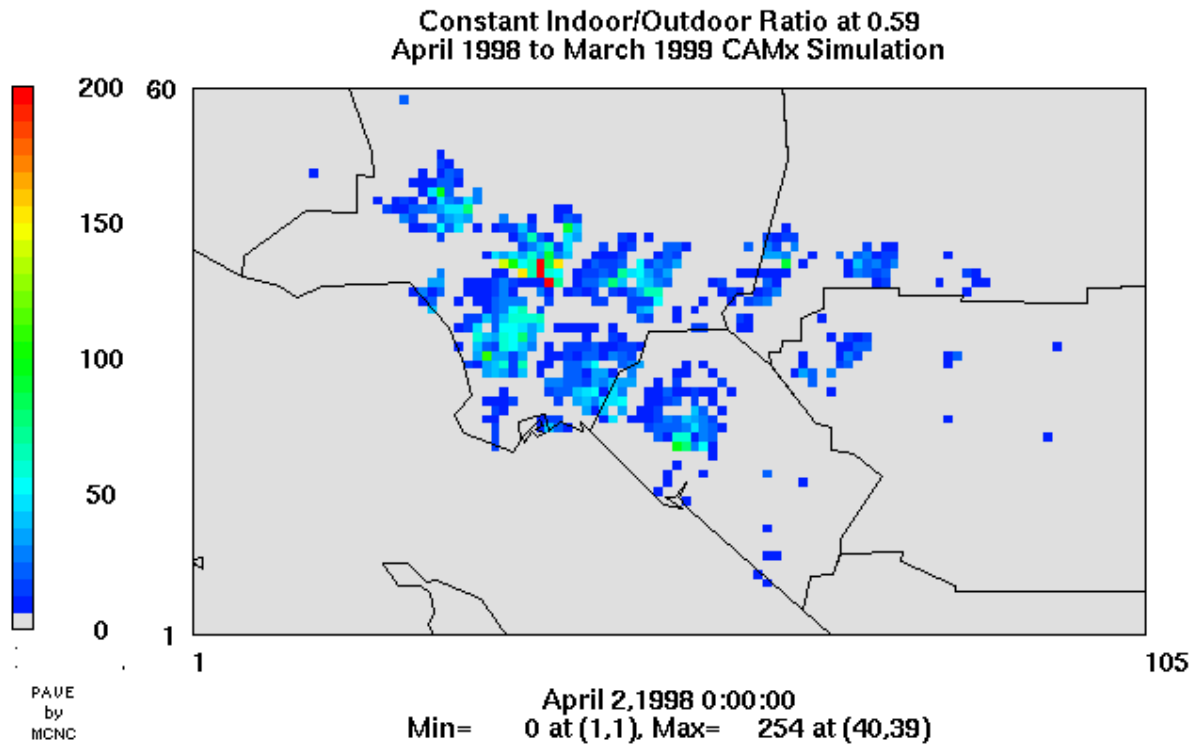


Figure 4-2c. Spatial distribution of exposure using gridded population and hourly risk estimates and accounting for indoor/outdoor effects on an hourly basis.

5. SUBGRID-SCALE NEAR-SOURCE IMPACTS

The implementation of air toxics modeling capability into the CAMx modeling system contained provisions for interfacing with a subgrid-scale near-source model. Originally, the intent was to implement a non-steady-state subgrid-scale near-source model within the CAMx model. However, that approach would not use the latest near-source modeling techniques, such as the PRIME downwash algorithm implemented in ISC and being implemented in AERMOD (two steady-state Gaussian plume models). Furthermore, it would likely become inconsistent with EPA guidance for near-source modeling and therefore limit its usefulness. Instead the CAMx air toxics modeling system subgrid-scale near-source model is run outside of and after the CAMx grid model simulation and is coupled through the CAMx estimated air toxics decay rates. The CAMx/RTRAC formulation and post-processing software are designed to combine the grid model and near-source model estimates in a mass consistent fashion that avoids double counting. In this manner, the users have a choice to use the latest near-source modeling techniques, the EPA-recommended modeling approach, or whatever near-source plume model they desire can be used to obtain near-source fence-line air toxics impacts that are fully consistent with the CAMx air toxics chemistry in a mass conservative fashion (e.g., no double counting).

DEMONSTRATION OF THE SUBGRID-SCALE NEAR-SOURCE TREATMENT USING THE MATES-II DATABASE

The application of the CAMx air toxics modeling system subgrid-scale near-source treatment involves the following activities:

- Identification of the point, area volume, and line to be treated by the subgrid-scale approach into several near-source complexes;
- Separation of the air toxics emissions into separate families of emissions, one for each near-source complex to be treated and then the remainder of the emissions;
- Set up the RTRAC receptor file for extraction of the air toxic decay rates at the locations of the near-source complexes;
- Run the CAMx/RTRAC for the families of air toxics tracers;
- Modification of a near-source plume model to accept the CAMx estimated hourly decay rates;
- Running of the near-source model using a user defined receptor grid; and
- Post-processing and combining of the CAMx/RTRAC gridded air toxics output with the near-source receptor impacts.

It should be noted that the subgrid-scale approach is not just limited to just point sources. The near-source complexes being modeled by the subgrid-scale model could also include area, volume, and line sources.

Setting Up and Running CAMx/RTRAC

The MATES-II emissions databases were analyzed and all point sources that contained emissions for any one of the seven air toxics being analyzed were extracted for use with the subgrid scale near-source algorithm. Surprisingly, there were no point sources with chromium or hexavalent chromium emissions in the MATES-II UAM-Tox modeling database emission inputs. It appears all chromium and hexavalent chromium emissions in the UAM-Tox database were allocated to the 2-km resolution gridded low-level emissions inputs. We suspect that a plume rise cut-off values appropriate for photochemical modeling were used when deciding to allocate point source air toxic emissions to the point sources versus low-level gridded emission inputs. As chromium and hexavalent chromium point sources are not as hot or buoyant as a NO_x source, then using these rules would allocate their emissions to the low-level emissions input file.

There were 13 point sources in the MATES-II modeling emission input files that had air toxics compound emissions. These 13 point sources consisted of five different near-source complex locations as shown in Table 5-1 and Figure 5-1. Emissions from each of the five near-source complexes were treated as a separate family of reactive air toxics tracer emissions in the CAMx RTRAC tracer run using the EMFAC2000 inputs. This results in the model tracking air toxic concentrations for six separate families of tracers, the five near-source complex emissions and the remainder of the emissions. A probing tool receptor input file was prepared with the locations of each of the near-source complexes (see Figure 3-3). The CAMx/RTRAC simulation generated gridded hourly air toxic concentration impacts for each of the six families of tracers, as well as a vertical profile of hourly air toxic compound decay rates extracted from the CAMx chemistry module.

Table 5-1. Location, stack parameters, and emissions for the five near-source complexes in the MATES-II modeling database that continued air toxics emissions.

| Source No. | UTMx (km) | UTMy (km) | Height (m) | Diam (m) | Temp (K) | Vel. (m/s) | ACET (moles/hr) | HCHO (moles/hr) | BENZ (moles/hr) |
|--|-----------|-----------|------------|----------|----------|------------|-----------------|-----------------|-----------------|
| <i>Point Source Complex Location (42,44)</i> | | | | | | | | | |
| 89 | 394.9 | 3777.0 | 18.0 | 3.7 | 694 | 88920 | 0.02 | 0.53 | 0.03 |
| 90 | 394.9 | 3777.0 | 18.0 | 3.7 | 694 | 88920 | 0.02 | 0.53 | 0.03 |
| 93 | 394.9 | 3777.0 | 43.0 | 3.4 | 366 | 25920 | 0 | 125.72 | 24.14 |
| 94 | 394.9 | 3777.0 | 37.0 | 3.0 | 422 | 30240 | 0 | 20.08 | 3.85 |
| 95 | 394.9 | 3777.0 | 37.0 | 3.0 | 422 | 30240 | 0 | 56.84 | 10.92 |
| <i>Point Source Complex Location (50,43)</i> | | | | | | | | | |
| 400 | 409.3 | 3776.8 | 18.3 | 0.5 | 1061 | 34200 | 0 | 2.22 | 0.42 |
| <i>Point Source Complex Location (41,36)</i> | | | | | | | | | |
| 417 | 391.5 | 3762.5 | 41.0 | 1.8 | 591 | 12240 | 0 | 15.48 | 2.98 |
| 418 | 391.5 | 3762.5 | 41.0 | 1.8 | 684 | 19080 | 0 | 12.53 | 2.4 |
| <i>Point Source Complex Location (39,38)</i> | | | | | | | | | |
| 461 | 388.3 | 3762.5 | 18.0 | 1.4 | 1366 | 33840 | 0 | 9.24 | 1.78 |
| 462 | 388.3 | 3762.5 | 18.0 | 1.4 | 1366 | 33840 | 0 | 9.24 | 1.78 |
| 464 | 388.3 | 3762.5 | 18.0 | 1.1 | 1366 | 25200 | 0 | 3.84 | 0.74 |
| <i>Point Source Complex Location (34,48)</i> | | | | | | | | | |
| 518 | 378.9 | 3785.2 | 17.0 | 1.5 | 625 | 28080 | 0 | 0.89 | 0.17 |
| 519 | 378.9 | 3785.2 | 17.0 | 1.5 | 625 | 28080 | 0 | 0.89 | 0.17 |
| Total Air Toxics Emissions in MATES-II Near-Source Modeling | | | | | | | 0.04 | 258.03 | 49.41 |

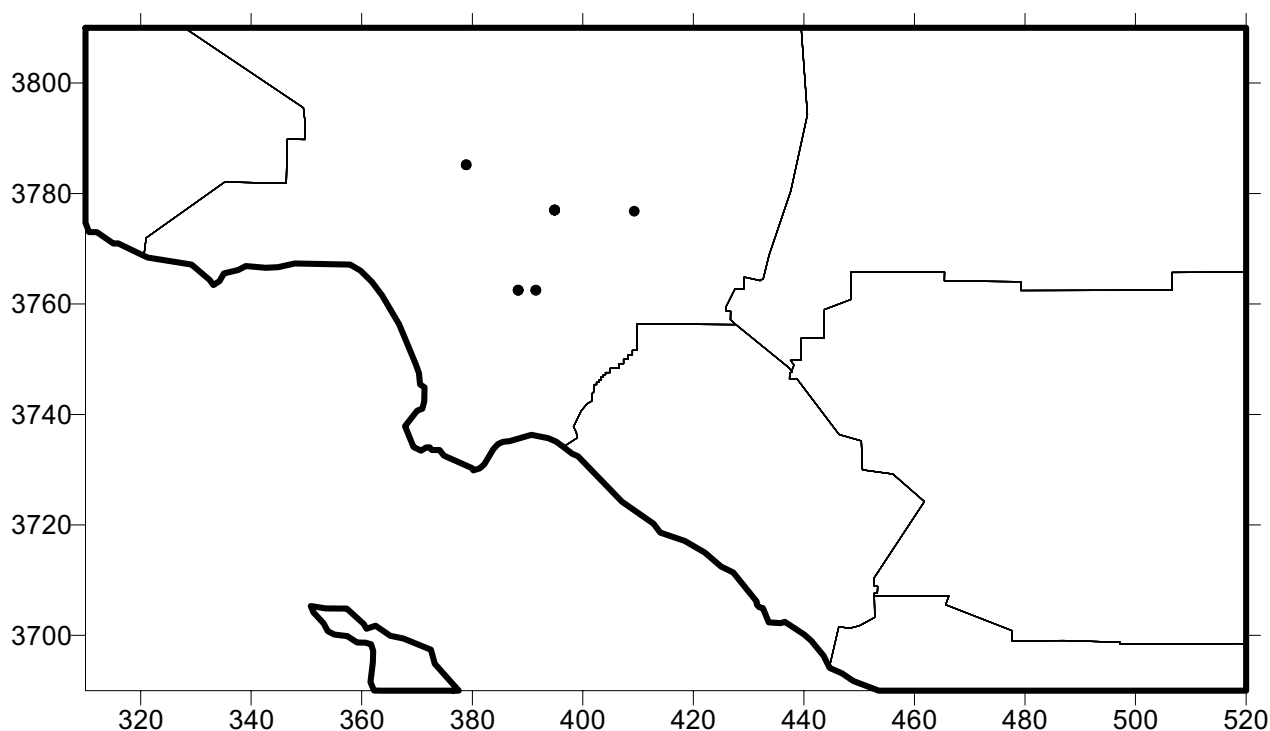


Figure 5-1. Location of near-source complexes treated by the subgrid-scale plume model.

Subgrid-Scale Plume Modeling

The ISC steady-state Gaussian plume model was selected for the subgrid-scale plume model as it is the current near-source model recommended in EPA's UATMG (EPA, 1999).

Modification of ISC to Use CAMx/RTRAC Decay Rates

ISC treats the chemical decay of pollutants through input of a constant half-life decay factor. The ISC model was modified to read in the CAMx/RTRAC vertical sounding of hourly decay rates for the April 1998 through March 1999 year. Different air toxic compound decay rates were used for each hour of each day of the year and potentially for each point source in the near-source complex being modeled. After calculation of the point source plume rise, the air toxic decay rate at the effective stack height of the source is extracted from the array of CAMx estimated decay rates for the day and hour being simulated and used in the ISC near-source impact calculation.

Development of ISC Meteorological Inputs

For each near-source complex location (see Figure 5-1), the CALMET output was processed to generate an ISC-formatted meteorological input file that included hourly surface wind speed, wind direction, temperature, and mixing height.

Development of ISC Emission Inputs

The MATES-II air toxic point source emission inputs (Table 5-1) were reformatted for the formats and units used by the ISC model. Each ISC run simulated only one near-source complex and only one air toxic compound at a time. This resulted in 11 ISC simulations to be performed, five for benzene, five for formaldehyde, and one for acetaldehyde (see Table 5-1).

Receptor Input

Each ISC point source complex was run using a ring of receptors around the point source complex under study at two degree increments and distances of 100-m, 200-m, 300-m, 400-m, 500-m, 600-m, 700-m, 800-m, and 1,000-m. That is, the hybrid CAMx air toxics modeling system near-source plume model is designed to obtain the maximum near-source subgrid-scale impacts. Impacts greater than a grid cell (>2 -km) are obtained from the CAMx grid model.

Subgrid-Scale Point Source Modeling Results

Software has been developed to combine the CAMx/RTRAC regional-scale hourly gridded 2-km resolution concentration impacts with the subgrid-scale near-source receptor concentration impacts. To test whether the CAMx/RTRAC hourly decay rates had any effect on the point source estimated impacts, ISC was also run assuming no decay rates (i.e., inert).

Table 5-2 presents summary results for the subgrid-scale near-source modeling using the MATES-II database. The first two columns (IX, IY) identify the grid cell where the near-source complex resides (see Table 5-1 and Figure 5-1). The next column identifies the species, either benzene, formaldehyde, or acetaldehyde. The fourth column (CAMx Total) is the total CAMx estimated air toxic annual concentration due to all sources in the 2-km by 2-km grid cell containing the near-source complex. The fifth column (CAMx Point) is the CAMx-estimated annual average concentrations due to just the near-source complex under study (identified by IX and IY). The next two columns (ISC Point) are the ISC-estimated maximum concentrations anywhere on the receptor grid with and without using the CAMx/RTRAC chemistry decay rates. The eighth column is the regional background (Backgrnd) that is defined as the CAMx/RTRAC air toxic tracer concentrations due to all sources except the near-source complex under study. The final two columns are the combined CAMx/RTRAC grid model background concentrations plus the maximum impact from the subgrid-scale near-source module with and without accounting for decay. A couple comments on Table 5-2:

- The only point sources with air toxics emissions in the MATES-II emissions file have small impacts compared to the regional “background” concentration estimated by the grid model;
- With one exception, the ISC maximum estimated air toxic concentration is greater than the CAMx/RTRAC grid cell average value;
- The ISC estimated maximum value with decay is either the same or less than the maximum estimated value without decay; and

- The ISC estimated maximum near-source benzene and formaldehyde concentrations due to a near-source complex are as much as 20 and 10 times higher than the corresponding CAMx grid cell volume estimate, respectively.

Table 5-2. Summary of CAMx/RTRAC subgrid-scale near-source modeling annual results for the MATES-II air toxics point sources.

| IX | IY | Species | CAMx Total ($\mu\text{g}/\text{m}^3$) | CAMx Point ($\mu\text{g}/\text{m}^3$) | ISC Point W/ Decay ($\mu\text{g}/\text{m}^3$) | ISC Point No Decay ($\mu\text{g}/\text{m}^3$) | CAMx Total – Point (Backgrnd) ($\mu\text{g}/\text{m}^3$) | ISC Point w/ Decay + Backgrnd ($\mu\text{g}/\text{m}^3$) | ISC Point No Decay + Backgrnd ($\mu\text{g}/\text{m}^3$) |
|----|----|---------|---|---|--|--|--|--|--|
| 34 | 48 | BENZ | 3.879316 | 0.000063 | 0.000090 | 0.000090 | 3.879253 | 3.879343 | 3.879343 |
| 39 | 36 | BENZ | 5.282383 | 0.001360 | 0.001710 | 0.001720 | 5.281023 | 5.282733 | 5.282743 |
| 41 | 36 | BENZ | 5.799652 | 0.002099 | 0.003900 | 0.003900 | 5.797553 | 5.801453 | 5.801453 |
| 42 | 44 | BENZ | 5.865131 | 0.001506 | 0.007010 | 0.007010 | 5.863625 | 5.870635 | 5.870635 |
| 50 | 43 | BENZ | 5.978545 | 0.000071 | 0.001360 | 0.001360 | 5.978474 | 5.979834 | 5.979834 |
| 34 | 48 | FORM | 3.502453 | 0.000107 | 0.000170 | 0.000180 | 3.502346 | 3.502516 | 3.502526 |
| 39 | 36 | FORM | 5.617651 | 0.002453 | 0.003260 | 0.003430 | 5.615198 | 5.618458 | 5.618628 |
| 41 | 36 | FORM | 5.655835 | 0.003790 | 0.007130 | 0.007800 | 5.652045 | 5.659175 | 5.659845 |
| 42 | 44 | FORM | 5.001340 | 0.002465 | 0.013410 | 0.014020 | 4.998875 | 5.012285 | 5.012895 |
| 50 | 43 | FORM | 4.982802 | 0.000270 | 0.002730 | 0.002730 | 4.982532 | 4.985262 | 4.985262 |
| 42 | 44 | ACET | 1.277799 | 0.000000 | 0.000000 | 0.000000 | 1.277799 | 1.277799 | 1.277799 |

The CAMx air toxics modeling system use of the subgrid-scale near-source impacts module using the MATES-II database demonstrates that the coupled hybrid plume/grid approach is working and providing reasonable answers. However, the limited number of point sources in the MATES-II modeling database does not fully demonstrate this capability. But it does clearly show the need for a subgrid-scale model when looking at near-source impacts.

6. CAMx AIR TOXICS TESTS USING THE AUGUST 1997 SCOS EPISODE

A CAMx photochemical modeling database has been developed for the August 3-7, 1997 Southern California Ozone Study (SCOS) episode (Morris et al., 2001; 2002; Yarwood et al., 2002). The CAMx meteorological inputs were based on the MM5 prognostic meteorological model that was exercised using analysis nudging to the Eta analysis fields and observation nudging to the SCOS observed upper-air meteorological data. An all-new complete emissions modeling set up developed by the California Air Resources Board (ARB) using the latest emissions information, including EMFAC2000, was used in this analyses. Although the August 1997 database only contained five simulation days and did not occur during the MATES-II air toxics observation network operation period, the testing of the new CAMx/RTRAC air toxics modeling capability using this database was believed to be a useful exercise for the following reasons:

- The MM5 dynamically balanced meteorological fields are far superior to the CALMET fields used in modeling the MATES-II period (April 1998 – March 1999) whose physical inconsistencies are undoubtedly introducing spurious vertical velocities that are affecting the CAMx estimates.
- A complete emissions modeling system is available so that the emissions can be more easily manipulated rather than the model-ready fully merged UAM-formatted emissions for the TOX chemical mechanism species that were obtained from the SCAQMD for the MATES-II April 1998-March 1999 period. This allows us to:
 - Perform air toxics modeling using different families of tracers to estimate air toxics concentrations due to major source categories (i.e., on-road mobile, point, and other anthropogenic);
 - Generate photochemical modeling inventories for both the CB-IV and SAPRC99 chemical mechanism to evaluate the sensitivity of the air toxic compound estimates to the choice of chemical mechanism and assure that the CAMx air toxics implementation is fully tested with the SAPRC99 mechanism; and
 - To directly speciate the raw air toxics emissions so that when unusual modeling results are seen (e.g., spikes), they can be traced back to the inventory.
- The CAMx ozone and precursor model performance for the August 1997 SCOS episode are some of the best that has ever been achieved in the SoCAB which gives the results more credibility.
- There are several PAMS sites operating in the SoCAB during the SCOS 1997 episode that can provide measured concentrations for some air toxics (organic species) to provide a limited but useful evaluation database.

The development of the August 1997 SCOS episode CAMx/MM5 episode is described in detail elsewhere (e.g., Morris et al., 2001;2002; Yarwood et al., 2002). Thus, below we just discuss the updates made for air toxics modeling.

PAMS OBSERVATIONS DATABASE

There were six PAMS sites operating in the SoCAB during summer of 1997 listed in Table 6-1 and shown in Figure 6-1. However, not all of these sites were collecting data during the August 1997 SCOS episode and not all-organic air toxic species were collected (e.g., 1,3-butadiene data are not present and aldehydes were measured only at one site). The following observed data were available for the CAMx/RTRAC air toxics model performance evaluation using the August 1997 SCOS episode:

- Benzene at all six PAMS sites (Azusa, Banning, Hawthorne, Los Angeles – North Main, Pico Rivera, and Upland);
- Acetaldehyde at Pico Rivera; and
- Formaldehyde at Pico Rivera.

Table 6-1. Locations of the six PAMS sites operating in the SoCAB during summer 1997.

| | <u>Latitude/Longitude</u> | | <u>UTM Coordinates</u> | | <u>Grid Coordinates</u> | |
|------|---------------------------|----------------------------|------------------------|----------------------|-------------------------|------------|
| | Latitude (deg) | Longitude (deg) | UTMx (km) | UTMy (km) | IXX | IYY |
| AZUS | 34.1538 | -117.923 | 414.9136 | 3779.387 | 28 | 22 |
| BANN | 33.9278 | -116.874 | 511.6459 | 3753.952 | 47 | 17 |
| HAWT | 33.9306 | -118.369 | 373.4657 | 3755.099 | 20 | 17 |
| LANM | 34.0672 | -118.225 | 386.9573 | 3770.077 | 22 | 20 |
| PICO | 34.015 | -118.058 | 402.3089 | 3764.117 | 25 | 19 |
| UPLA | 34.1036 | -117.628 | 442.0743 | 3773.614 | 33 | 21 |

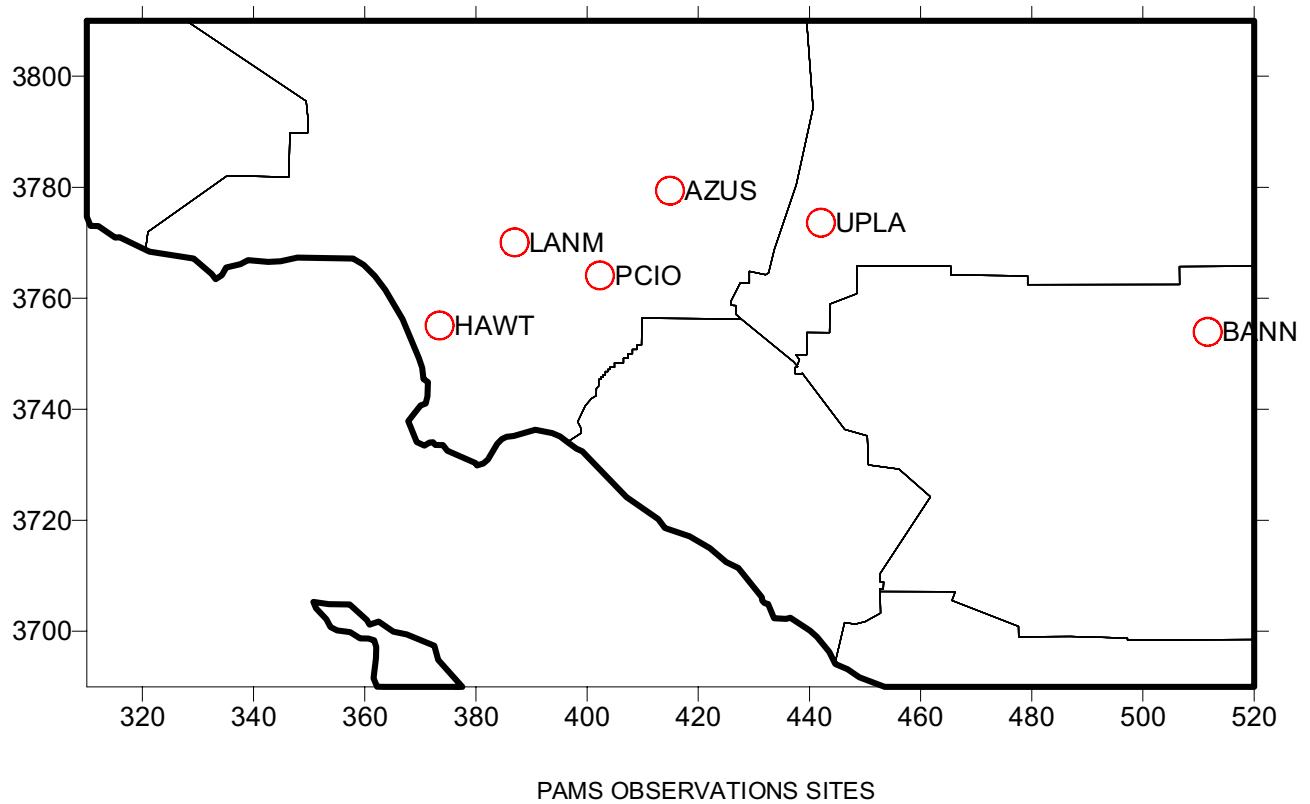


Figure 6-1. Location of PAMS monitors in the SoCAB operating during the August 1997 SCOS episode.

AUGUST 1997 CAMx/RTRAC AIR TOXICS SIMULATION

The ARB emissions data and emissions modeling software were used to generate three types of modeling emission inventories. These emissions were based on the EMFAC2000 on-road mobile source emissions models. The three inventories generated were as follows:

- A photochemical modeling inventory for the CB-IV chemical mechanism;
- A photochemical modeling inventory for the SAPRC99 chemical mechanism; and
- A RTRAC air toxics modeling inventory for benzene, 1,3-butadiene, acetaldehyde, and formaldehyde.

The RTRAC air toxics emissions were separated into three families of emission inputs for separate tracking:

- On-road mobile sources;
- Point sources; and
- Remainder (other) anthropogenic emissions (i.e., area and non-road sources).

MODEL PERFORMANCE EVALUATION

The CAMx/RTRAC air toxics model simulation was conducted for the August 3-7, 1997 SCOS episode using the CB-IV and SAPRC99 chemical mechanism. The air toxic modeling results were compared with the available observed air toxics concentrations at the six PAMS sites.

Benzene

Time series of predicted and observed benzene concentrations at the six PAMS sites for the CAMx/CB-IV (green) and CAMx/SAPRC99 (red) RTRAC air toxics simulations are shown in Figure 6-2. The CAMx/CB-IV (CB4) and CAMx/SAPRC99 (S99) benzene estimates are almost identical with the two time series super-imposed on top of each other most of the time. In the afternoon hours, the CAMx/CB-IV benzene predictions at some sites are slightly higher than the CAMx/SAPRC99 benzene predictions. This effect is most pronounced at the further downwind Banning site in Riverside County (Figure 6-2a), but is also apparent at the downwind Upland site in San Bernardino County (Figure 6-2c), and is barely evident at the Azusa site in eastern Los Angeles County (Figure 6-2a). At the three upwind sites in the middle of Los Angeles County (Los Angeles, Pico Rivera, and Hawthorne), the CAMx/CB-IV and CAMx/SAPRC99 estimate identical benzene concentrations. The differences in the CAMx/CB-IV and CAMx/SAPRC99 benzene concentrations are based solely on the differences in the host model oxidant fields (ozone, OH, and NO₃ concentrations) that are used to define the reaction (decay) rates of the RTRAC benzene tracers. The SAPRC99 is a “hotter” chemical mechanism so estimates higher ozone and radical (OH and NO₃) concentrations, which in turn results in higher benzene decay rates. As benzene is not a very reactive species and photochemical oxidant activity in the western portion of the SoCAB is relative low, then the effect of the hotter SAPRC99 chemistry on the benzene concentrations

are not seen at those sites. However, as one moves downwind and inland toward the east, we begin to see the effects of the hotter SAPRC99 chemistry on the CAMx/CB-IV and CAMx/SAPRC99 RTRAC benzene estimates; very small differences at Azusa, slightly larger ones at Upland, and the largest differences at the Banning site in the far east of the domain.

Note that although the CAMx/CB-IV and CAMx/SAPRC99 host models use different chemistry, the RTRAC air toxics chemistry module is the same in both models as it is based on chemistry for the specific air toxic compounds (Harley and Cass, 1995) rather than a lumped chemical mechanism designed for ozone formation that has been “tuned” to match smog chamber data.

At the farthest west Hawthorne site (Figure 6-2b top), CAMx/RTRAC does a good job in reproducing the diurnal variations in the observed benzene concentrations. Excellent agreement in the predicted and observed benzene concentration at Hawthorne is seen on August 3-5, 1997 (Julian days 97215-97217), with the only discrepancy being a slight underestimation of the observed peak on August 5. On August 6th, the model fails to pick up the occurrence of higher than normal afternoon observed benzene concentrations. By August 7, the model performance for benzene returns to being very good.

The benzene model performance at the Los Angeles – North Main (Figure 6-2b bottom) and Pico Rivera (Figure 6-2c top) sites in the center of the SoCAB is also very good. There are only two observed benzene values at the Los Angeles site on August 5th that show a large drop in the observed benzene from 3.2 ppb in the early morning to 0.8 ppb in the late morning that is reproduced very well by the model. At Pico Rivera the model underestimates the high morning observed benzene concentrations on August 4th and then does a good job in replicating the diurnal variations for the remainder of the episode (August 5-7, 1997).

At the Azusa monitor in eastern Los Angeles County (Figure 6-2a top), the model underestimates the observed benzene concentrations. These underestimations are most pronounced on August 5-6 with good agreement seen on August 4 and August 7.

At the Banning monitor (Figure 6-2a bottom) in the far eastern portion of the modeling domain, the observed benzene concentrations of 0.1-0.9 ppb are underestimated by the model whose benzene concentrations range from 0.0 to 0.3 ppb. Due to the spatial inhomogeneity of emissions in the vicinity of Banning that is a mixture of urban and rural land use types (as compared to the other urban-oriented sites), we suspect this underprediction is due to differences in more urban-oriented point observations verses the 2-km by 2-km grid cell volume-averaged model predictions.

In summary, the benzene model performance of the CAMx/CB-IV and CAMx/SAPRC99 simulations for the August 1997 SCOS episode are fairly good given uncertainties in emissions, meteorology, and measurements and superior to that seen in the MATES-II 98/99 simulation. We suspect that this improved model performance is due to better meteorological fields (MM5) and a better emissions inventory.

Acetaldehyde

Observed acetaldehyde concentrations during the August 1997 SCOS episode were available only at the Pico Rivera PAMS site. The CAMx/CB-IV and CAMx/SAPRC99 estimate substantially different acetaldehyde concentrations (Figure 6-3). The model estimated acetaldehyde concentrations exhibit reasonable to fairly good agreement with the observed values, with the CAMx/CB-IV exhibiting superior performance to CAMx/SAPRC99. Surprisingly, the CAMx/SAPRC99 estimates higher acetaldehyde concentrations than CAMx/CB-IV. This is surprising because the CB-IV "ALD2" species, whose formation in CAMx is allocated to the secondary acetaldehyde RTRAC tracer (SACET), is a lumped species that represents not just acetaldehyde but all higher aldehydes. Whereas the SAPRC99 has an explicit acetaldehyde species. One would expect that an explicit aldehyde species concentration would be lower than the lumped ALD2 species that includes acetaldehyde as well as other higher aldehydes. The fraction of acetaldehyde to the lumped ADL2 CB-IV species can vary. However, it appears that the higher reactivity of the SAPRC99 chemical mechanism forms more acetaldehyde than CB-IV that more than makes up for the additional mass in the CB-IV ALD2 lumped species.

Formaldehyde

The predicted and observed formaldehyde time series are shown in Figure 6-4. As seen for acetaldehyde, the CAMx/SAPRC99 estimates higher formaldehyde concentrations than the CAMx/CB-IV. The CB-IV formaldehyde species (FORM) is also a lumped species; however, it is almost entirely (>95%) formaldehyde so this is not as big of an issue as for acetaldehyde. The CAMx/CB-IV estimated diurnal variations in formaldehyde concentrations track the observed values fairly well, with a slight overestimation tendency. The CAMx/SAPRC99 formaldehyde performance is not as good as CAMx/CB-IV exhibiting a worse overprediction tendency.

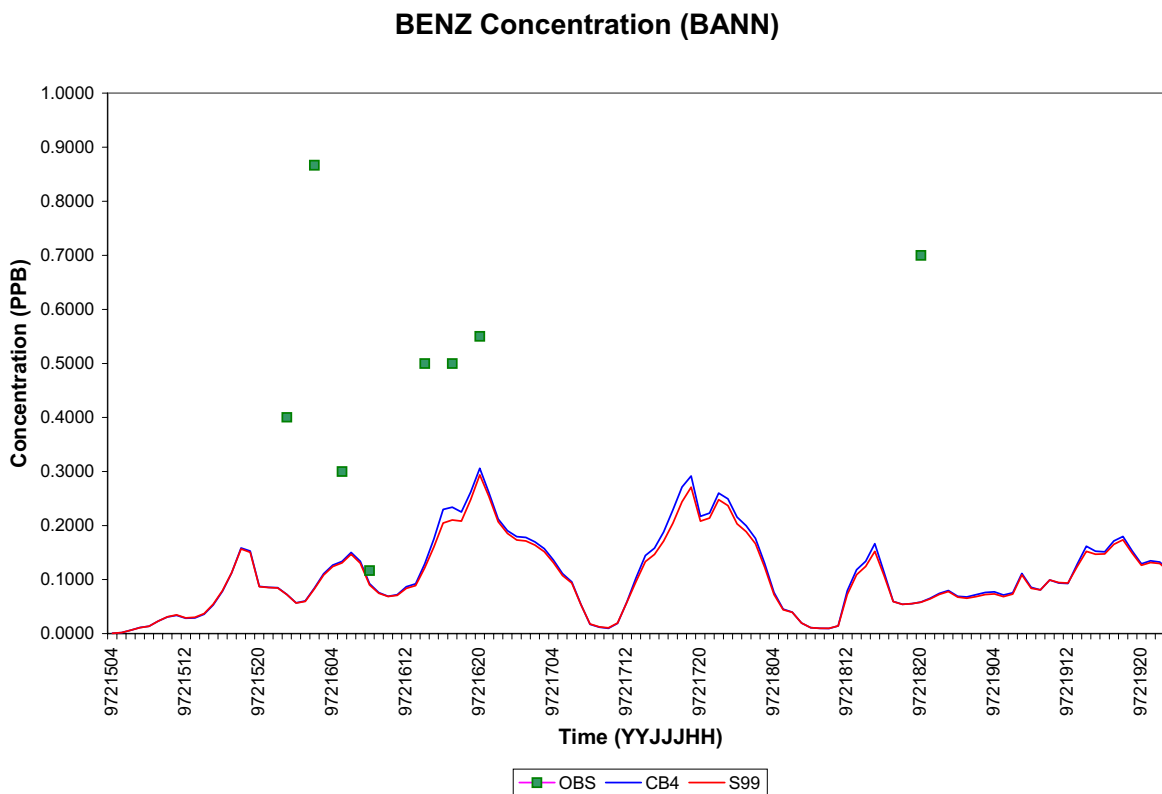
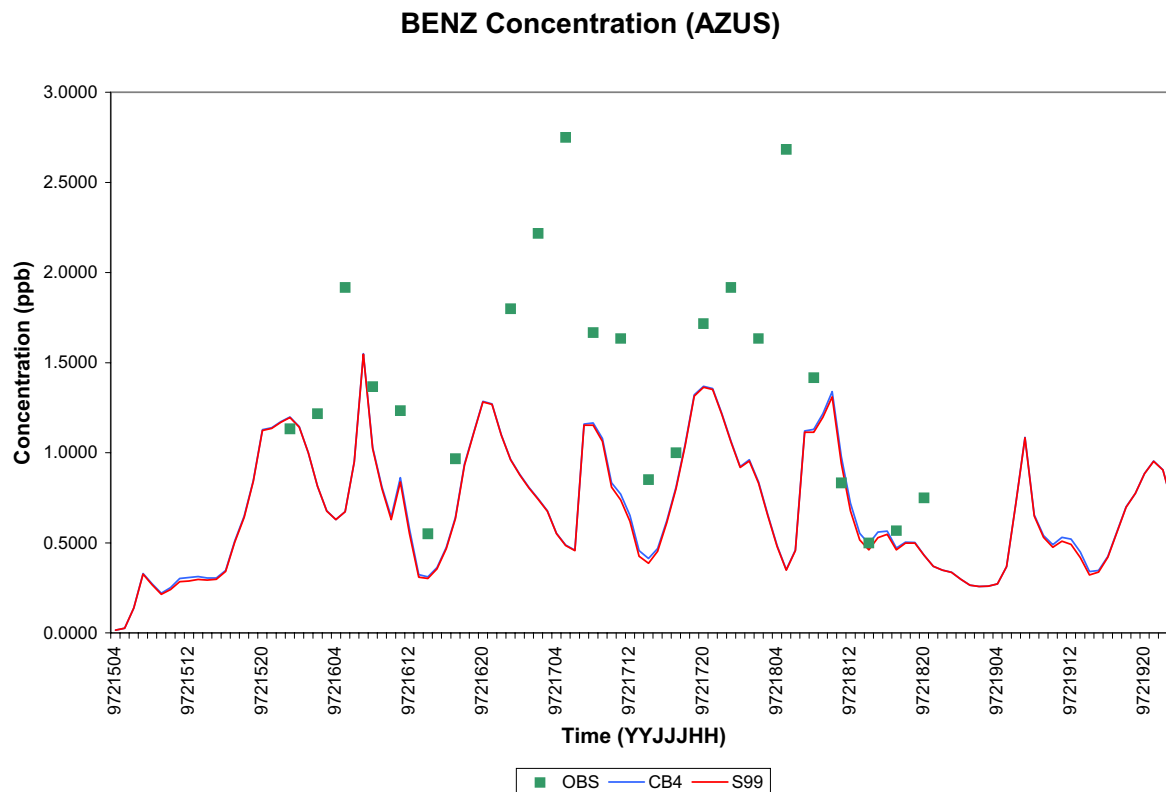


Figure 6-2a. Comparison of predicted and observed benzene concentrations on August 3-7, 1997 at the Azusa (top) and Banning (bottom) PAMS sites using CAMx/CB4 and CAMx/SAPRC99 (S99) model configurations.

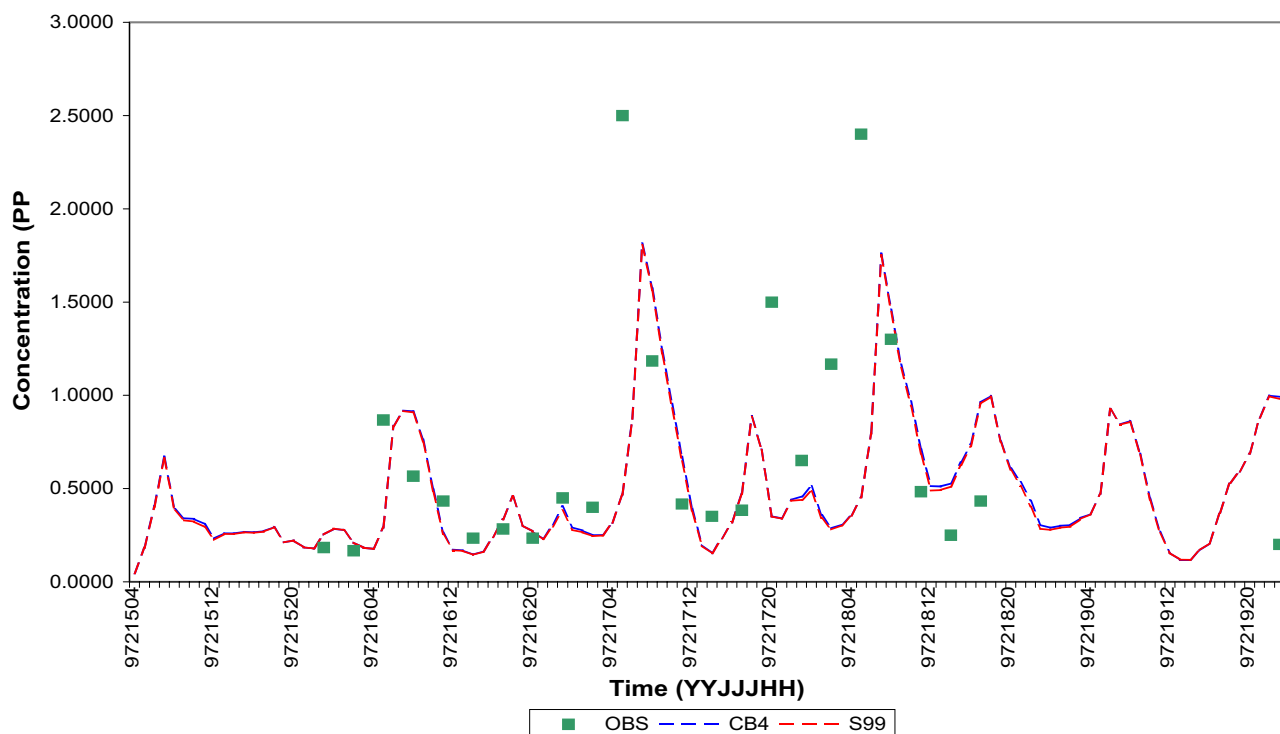
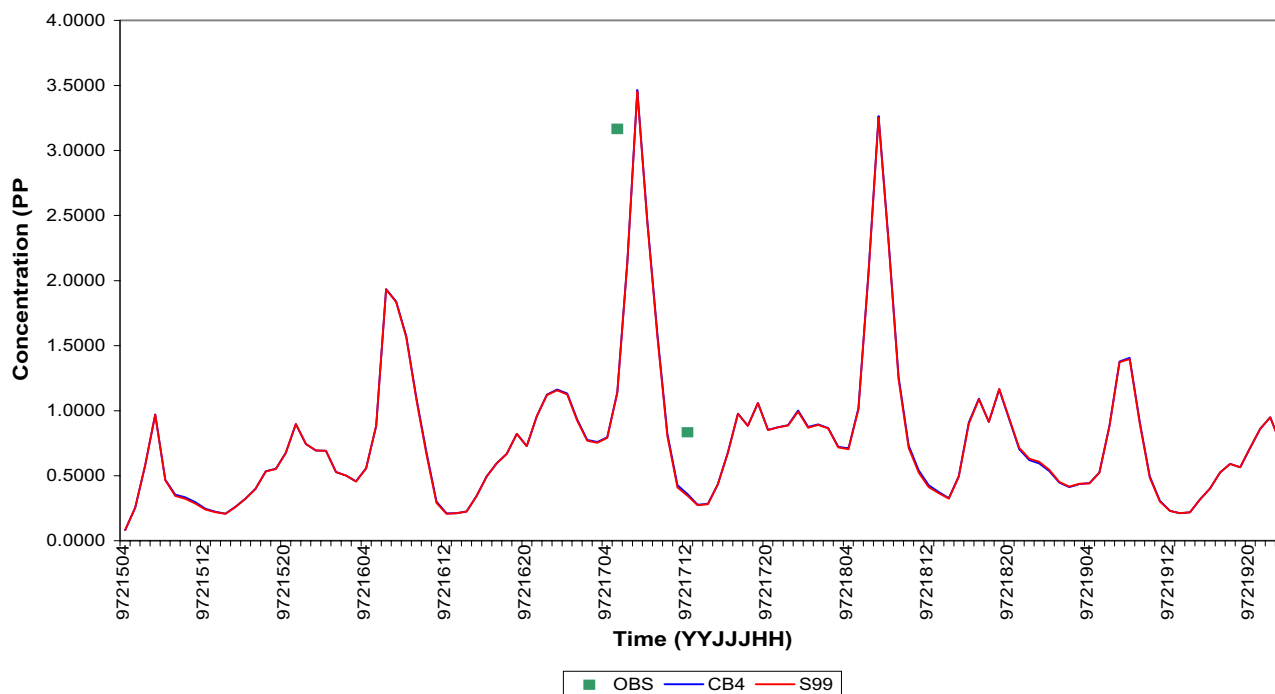
BENZ Concentration (HAWT)**BENZ Concentration (LANM)**

Figure 6-2b. Comparison of predicted and observed benzene concentrations on August 3-7, 1997 at the Hawthorne (top) and Los Angeles – North Main (bottom) PAMS sites using CAMx/CB4 and CAMx/SAPRC99 (S99) model configurations.

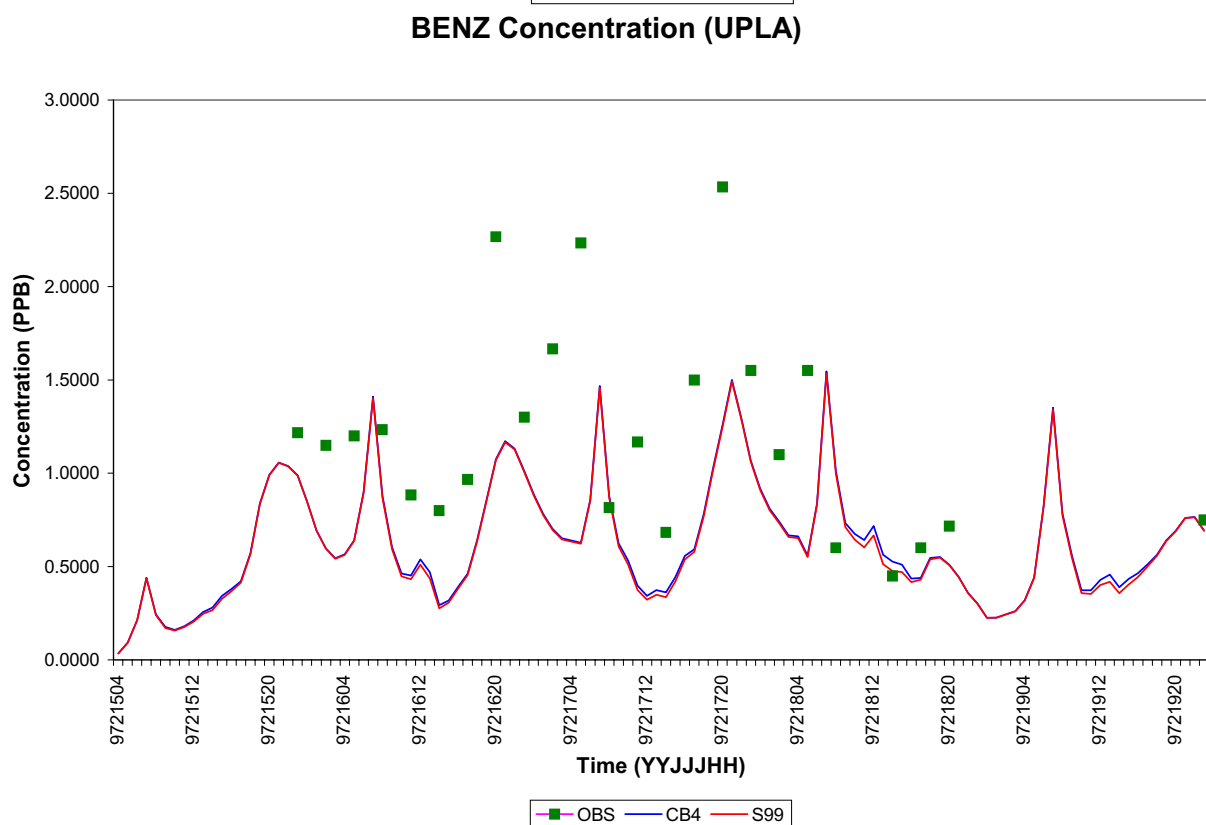
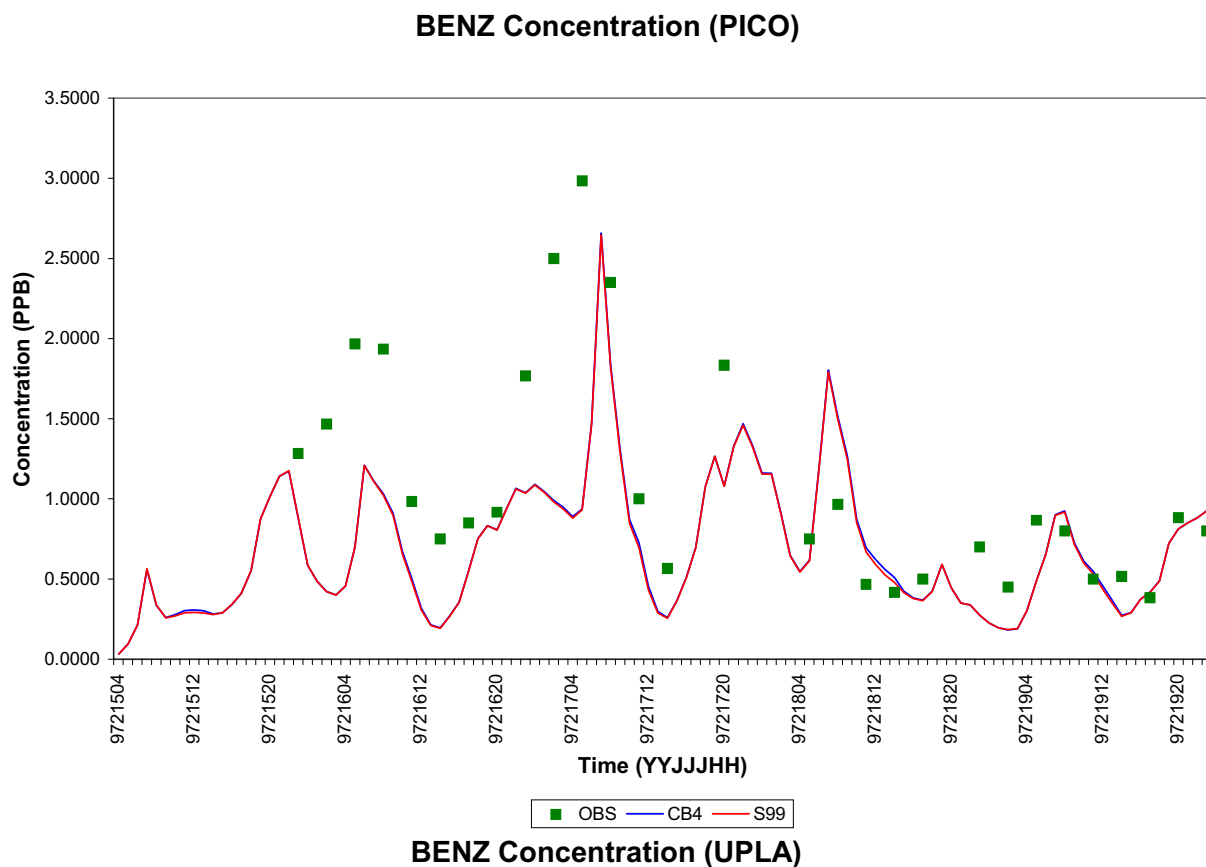


Figure 6-2c. Comparison of predicted and observed benzene concentrations on August 3-7, 1997 at the Pico Rivera (top) and Upland (bottom) PAMS sites using CAMx/CB4 and CAMx/SAPRC99 (S99) model configurations.

ACET Concentration (PICO)

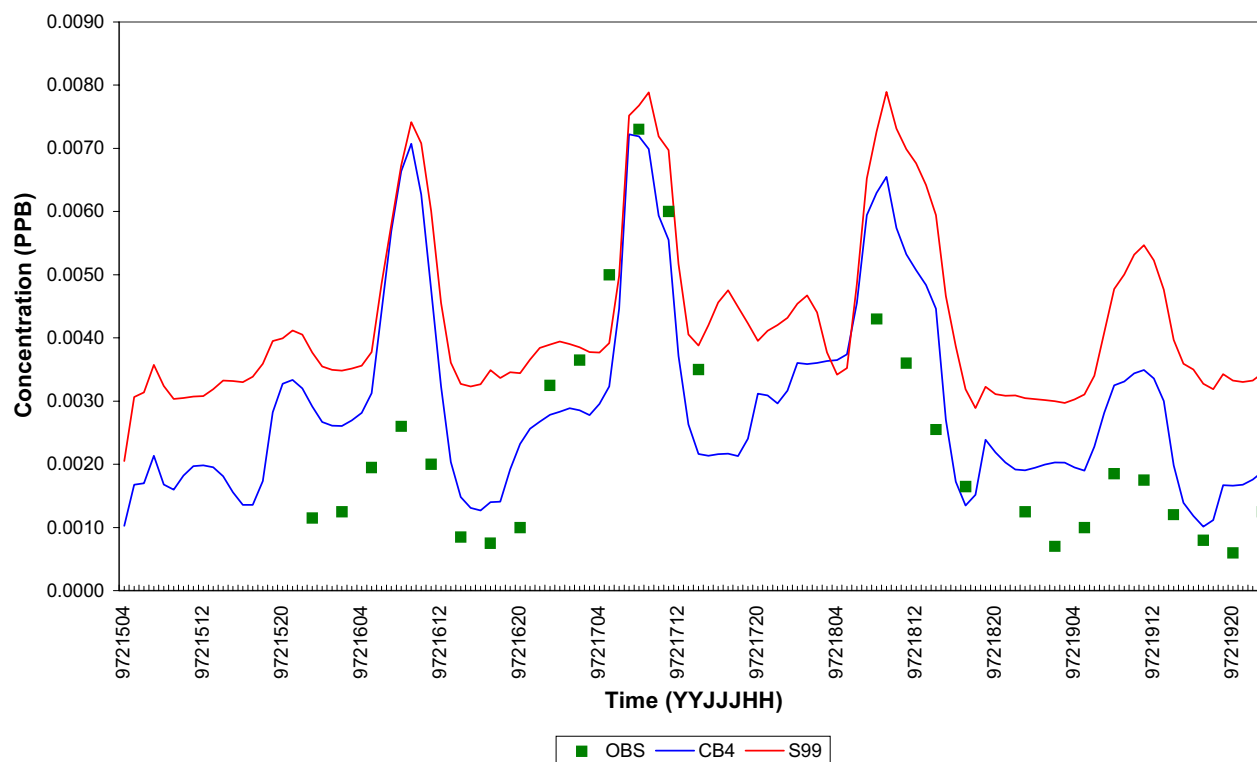


Figure 6-3. Comparison of predicted and observed acetaldehyde concentrations on August 3-7, 1997 at the Pico Rivera PAMS site using CAMx/CB4 and CAMx/SAPRC99 (S99) model configurations.

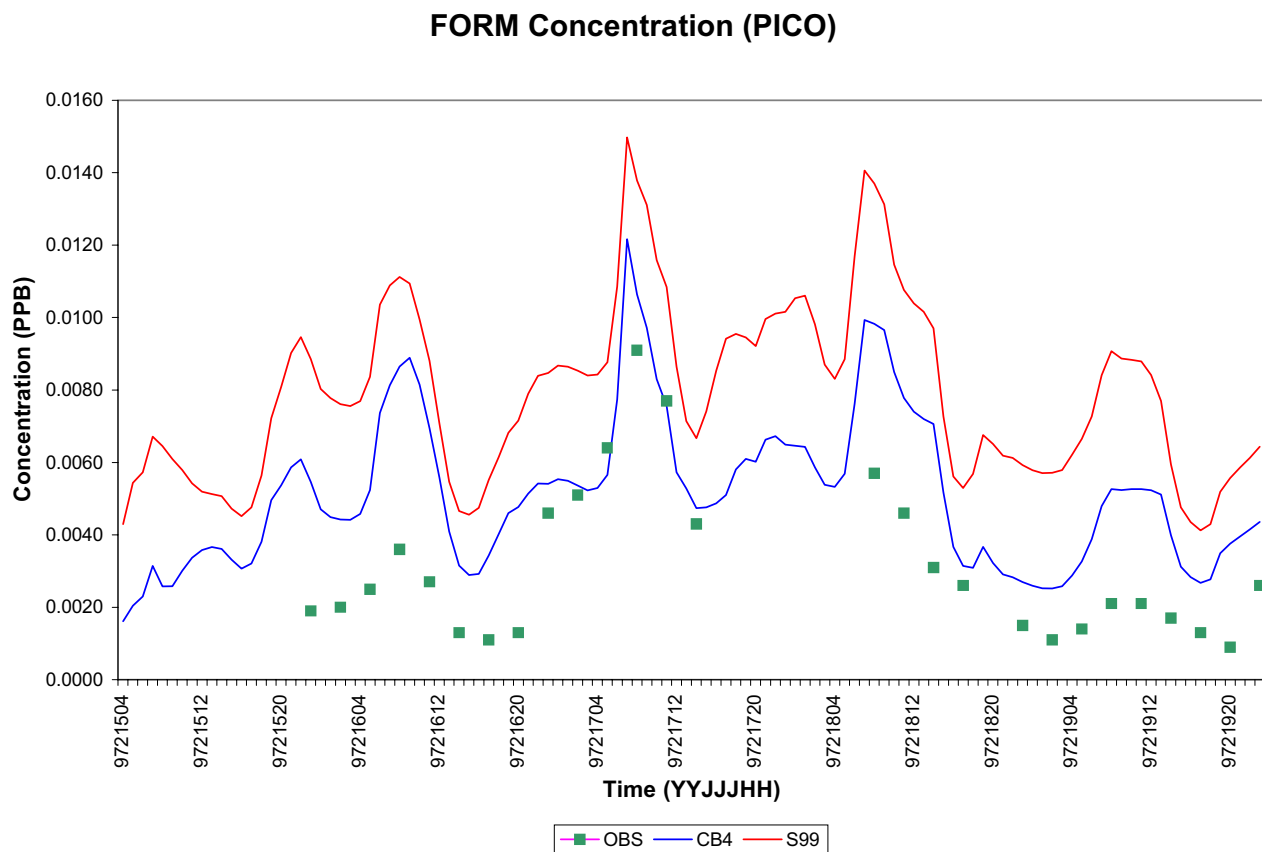


Figure 6-4. Comparison of predicted and observed formaldehyde concentrations on August 3-7, 1997 at the Pico Rivera PAMS site using CAMx/CB4 and CAMx/SAPRC99 (S99) model configurations.

CB-IV VERSUS SAPRC99 CHEMISTRY COMPARISONS

Figure 6-5 compares the CAMx/CB-IV (CB4) and CAMx/SAPRC99 (S99) RTRAC air toxics 24-hour predictions at the 10 MATES-II sites for the August 3-7, 1997 SCOS episode (see Figure 2-2 for MATES-II monitor locations). For benzene (BENZ), CB4 and S99 predict nearly identical concentrations with the CB4 values sometimes being slightly higher (Figure 6-5a). As noted previously, these differences are due to the hotter SAPRC99 chemistry that decays the benzene faster than the CB-IV chemistry.

The comparison of the CB4 and S99 estimated 1,3-butadiene (BUTA) concentrations in Figure 6-5b reveals that the CB4 predictions are always higher than the S99 predictions. 1,3-butadiene is very reactive so the hotter S99 chemistry decays it much faster than the CB4 chemistry resulting in higher 1,3-butadiene concentrations with CB4.

The results for primary acetaldehyde (ACET) and primary formaldehyde (FORM) (Figure 6-5c and 6-5d) also show the effects of the hotter S99 chemistry that decays them faster resulting in higher CB4 estimates than S99 estimates.

For secondary acetaldehyde (SACET) and secondary formaldehyde (SFORM), the S99 simulation predicts higher concentrations than the CB4 simulation (Figure 6-5e and 6-5f). Again this is believed to be due to the more reactive SAPRC99 chemistry that produces more secondarily formed species. The S99 secondary formaldehyde 24-hour concentrations are approximately a factor of two higher than the CB4 counterparts at all sites and days. However, the S99 secondary acetaldehyde estimates are approximately the same as the CB4 values at higher concentrations to a factor of two higher than the CB4 estimates at the lower values. The comparisons of the S99 and CB4 secondary acetaldehyde and secondary formaldehyde concentrations provide new information and insight into the reasons the SAPRC99 chemistry is hotter than CB4. It appears that the aldehyde yields for the SAPRC99 chemistry are approximately twice as large as for the CB-IV chemical mechanism. Which one is more correct is difficult to determine. For the one site comparison in this study (Pico Rivera in Figures 6-3 and 6-4) the CB4 aldehyde estimates better matched the observed values than the S99 estimates. However, this is an extremely limited comparison at a location influenced by both primary and secondary aldehydes. This comparison is also complicated by the fact that the SAPRC99 SACET RTRAC air toxics species is pure acetaldehyde whereas the CB-IV SACET species comes from the CB-IV lumped ALD2 species that includes acetaldehyde as well as other "higher aldehydes" (i.e., not formaldehyde). The percentage of SACET that is acetaldehyde will vary spatially and temporally.

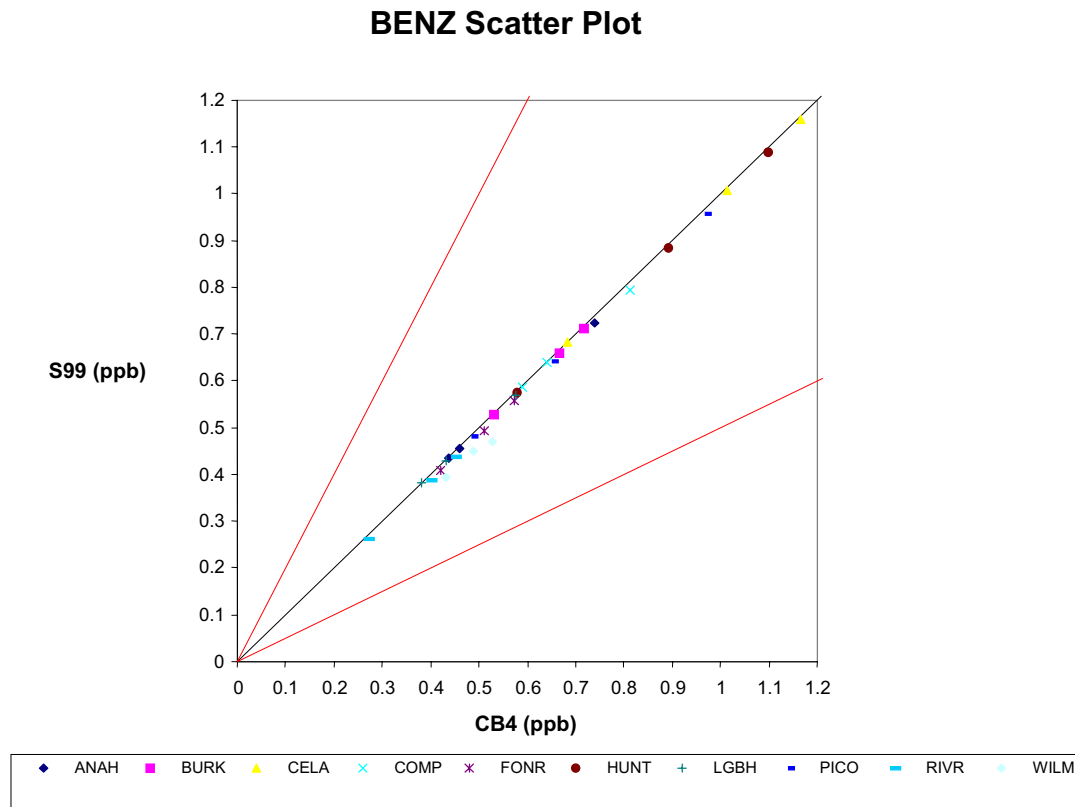


Figure 6-5a. Scatter plot of CAMx/CB-IV (CB4) and CAMx/SAPRC99 (S99) predicted 24-hour average benzene concentrations (ppb) on August 5-7, 1997 at the 10 MATES-II monitoring sites (see Figure 2-2 for locations).

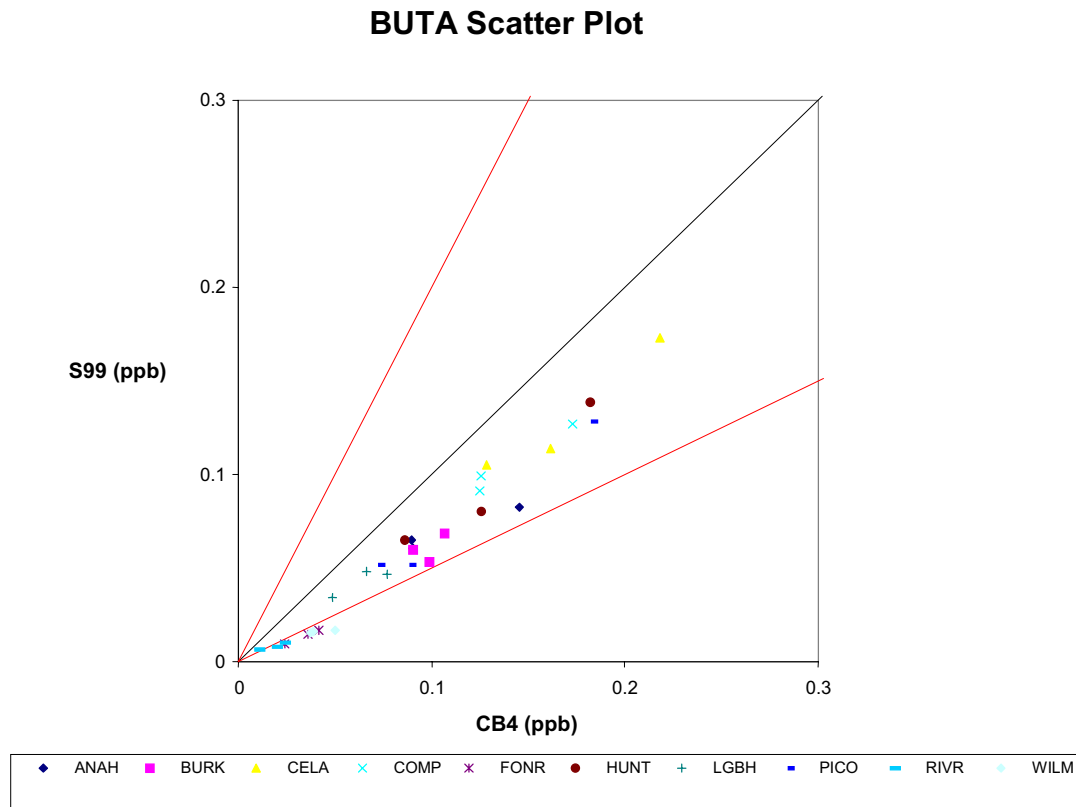


Figure 6-5b. Scatter plot of CAMx/CB-IV (CB4) and CAMx/SAPRC99 (S99) predicted 24-hour average 1,3-butadiene concentrations (ppb) on August 5-7, 1997 at the 10 MATES-II monitoring sites (see Figure 2-2 for locations).

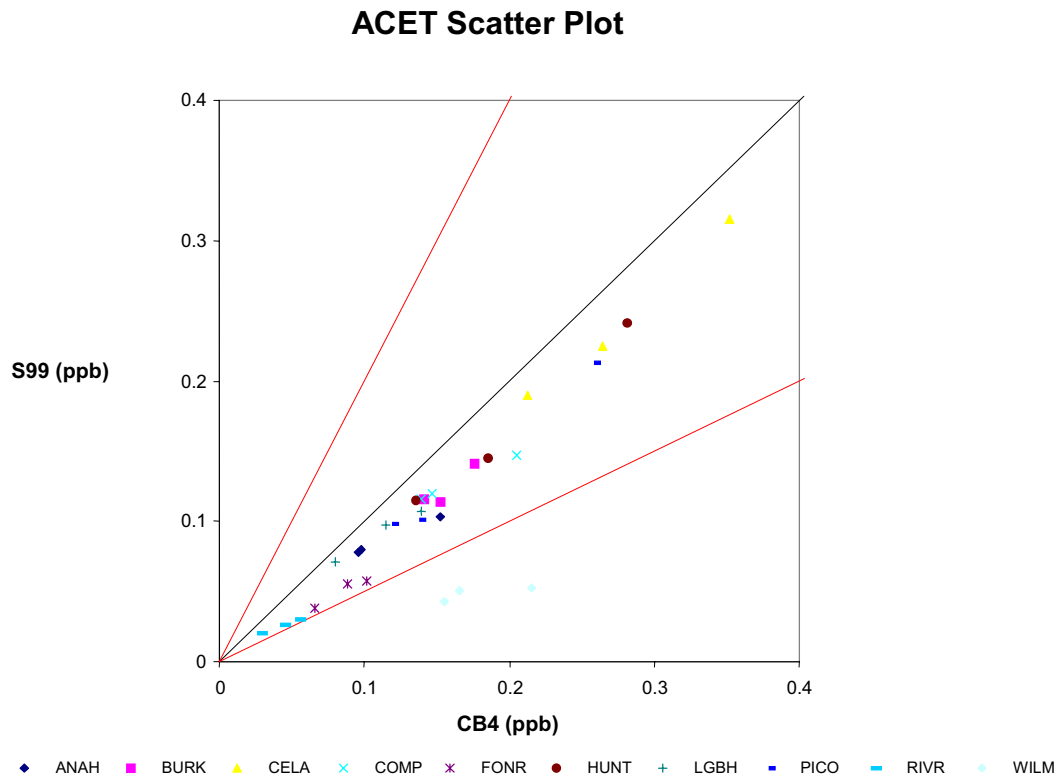


Figure 6-5c. Scatter plot of CAMx/CB-IV (CB4) and CAMx/SAPRC99 (S99) predicted 24-hour average primary acetaldehyde concentrations (ppb) on August 5-7, 1997 at the 10 MATES-II monitoring sites (see Figure 2-2 for locations).

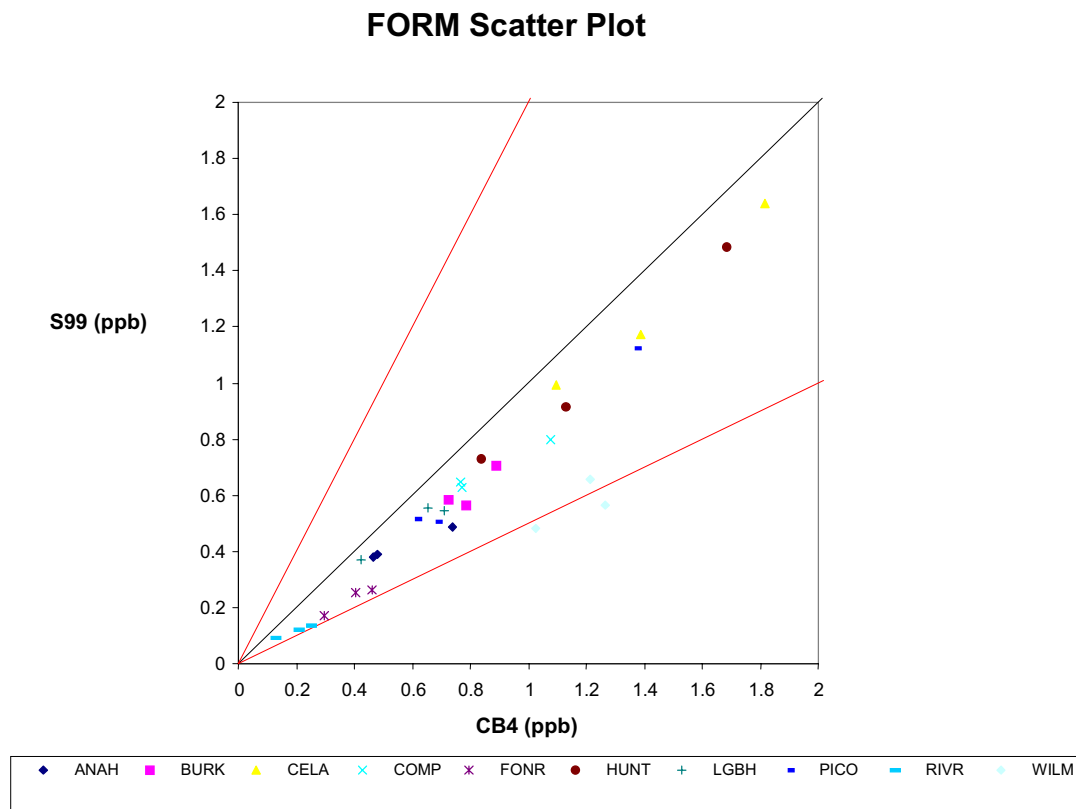


Figure 6-5d. Scatter plot of CAMx/CB-IV (CB4) and CAMx/SAPRC99 (S99) predicted 24-hour average primary formaldehyde concentrations (ppb) on August 5-7, 1997 at the 10 MATES-II monitoring sites (see Figure 2-2 for locations).

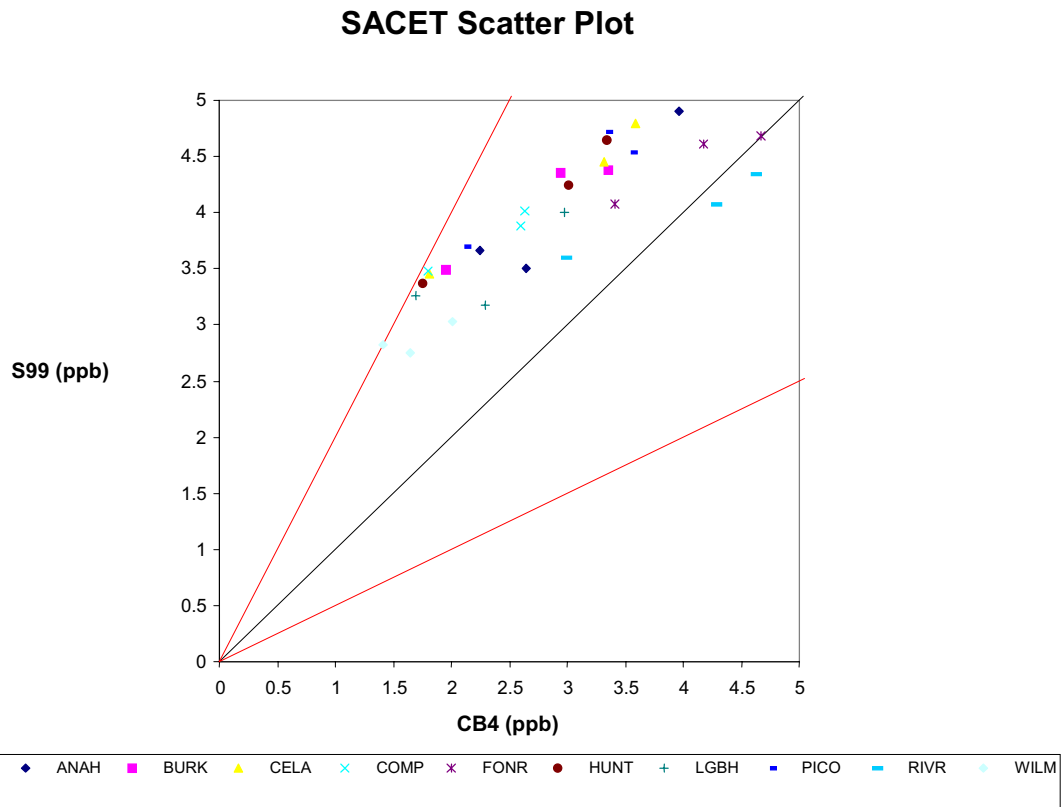


Figure 6-5e. Scatter plot of CAMx/CB-IV (CB4) and CAMx/SAPRC99 (S99) predicted 24-hour average secondary acetaldehyde concentrations (ppb) on August 5-7, 1997 at the 10 MATES-II monitoring sites (see Figure 2-2 for locations).

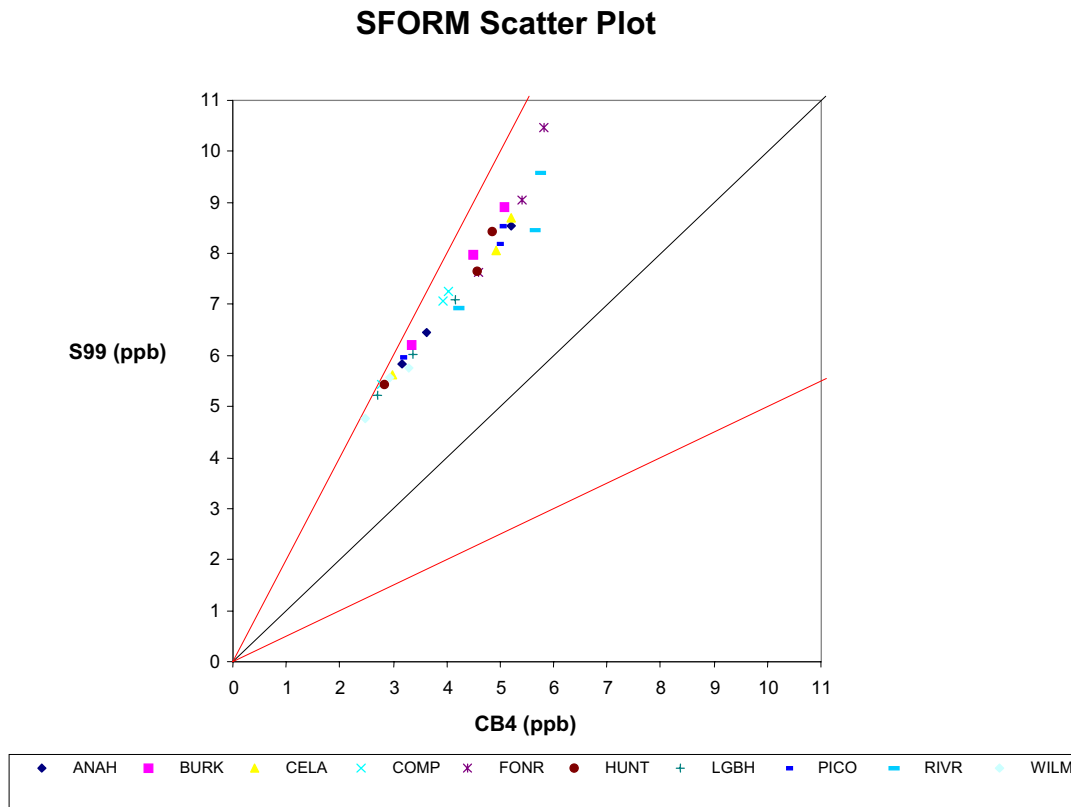


Figure 6-5f. Scatter plot of CAMx/CB-IV (CB4) and CAMx/SAPRC99 (S99) predicted 24-hour average secondary formaldehyde concentrations (ppb) on August 5-7, 1997 at the 10 MATES-II monitoring sites (see Figure 2-2 for locations).

RISK COMPARISONS USING CB-IV AND SAPRC99 CHEMICAL MECHANISMS

The MATES-II used unit risk factors (URFs) were used to estimate the potential long-term risk associated to exposure to the estimated air toxics concentrations in the SoCAB from the simulations of the August 1997 SCOS episode. The URFs are in units of $(\mu\text{g}/\text{m}^3)^{-1}$ and when applied to an air toxic concentration provides the potential probability out of a million people that cancer incidence would occur due to long-term exposure to that level of air toxic concentration. To better understand the effects the CB-IV and SAPRC99 chemical mechanisms would have on risk estimates, the URFs were applied to the episode average air toxic concentrations for the four organic air toxic compounds simulated for the August SCOS episode at the 10 MATES-II sites. The risks from the air toxic concentrations estimated by the CAMx/CB4 and CAMx/S99 were compared to determine whether the use of different chemical mechanisms has a significant effect on the resultant estimated risks. The following URFs were used for the four organic air toxics simulated using the two chemical mechanisms:

- Benzene: $2.9 \times 10^{-5} (\mu\text{g}/\text{m}^3)^{-1}$
- 1,3-Butadiene: $1.7 \times 10^{-4} (\mu\text{g}/\text{m}^3)^{-1}$
- Acetaldehyde: $2.7 \times 10^{-6} (\mu\text{g}/\text{m}^3)^{-1}$
- Formaldehyde: $6.0 \times 10^{-6} (\mu\text{g}/\text{m}^3)^{-1}$

Note that these risk calculations were performed solely for comparing the differences in the risk calculation using the CB-IV versus the SAPRC99 chemical mechanisms to model air toxics. The URFs should be applied to annual average or greater time period air toxic concentrations, not just a multi-day episode average.

Figure 6-6 displays the one in a million risk estimate due to the long term exposure to the episode average of four organic air toxic compounds simulated by the CAMx/CB4 and CAMx/S99 modes. There are many air toxic compounds that affect the risk calculations, so calculation of risk using just four of them is done solely for comparison purposes. The MATES-II study estimated that approximately 70% of the cancer risk due to air toxics exposure in the SoCAB is due to diesel particles. Another approximately 20% of the risk was due to exposure due to the four organic air toxic compounds, which the MATES-II study assumes are “associated with mobile sources”. Thus, the risk calculations presented below represent about 20% of the total risk due to air toxics in the SoCAB based on the MATES-IV study.

The largest risk at any MATES-II site, at over 200 in a million, occurs at the downtown Los Angeles site followed by the Huntington site (Figure 6-6). The lowest risk, at around 100-125 in a million, occurs at the Wilmington, Rubidoux, and Long Beach sites. S99 always estimates higher risks than CB4; however, there is a lot of variation in how much higher it is due to competing effects. CB4 estimates higher risk from primary emitted compounds, whereas S99 estimates higher risk due to secondarily formed species. Thus, at farther downwind sites where secondary formed species are higher (e.g., Rubudoux), the S99 risk is substantially larger than the CB4 risk. Whereas, at upwind sites (e.g., Wilmington) the S99 risk is only slightly higher than the CB4 risk.

The MATES-II study estimated SoCAB wide risks from measurements and modeling by averaging the 10 MATES-II sites (SCAQMD, 2000). These results are presented in Table 6-2 for the CAMx/CB4 and CAMx/S99 RTRAC simulation organic air toxic compound simulations. Although the total risk due to the four organic air toxics estimates by S99 (157 in a million) is only 10% higher than that estimated by CB4 (144 in a million), there are significant differences in the contributions of the different organic compounds to the total risk. The CB4 simulation estimates that primary benzene (40%), and primary 1,3-butadiene (24%) are the two biggest contributors, with secondary formaldehyde (21%) and secondary acetaldehyde (12%) being next most important. The S99 simulation also estimates that primary benzene is the most important contributor to total risk (36%), but secondary formaldehyde is now comparable (34%), followed by 1,3-butadiene (15%) and secondary acetaldehyde (12%) whose risks are also now comparable using S99. Table 6-2 clearly shows the competing effects of the higher reactive S99 simulation that decays the primary emitted air toxics faster than CB4 (e.g., a 33 percent reduction in risk due to 1,3-butadiene), yet forms more secondary air toxic compounds (e.g., 74% increase in risk due to secondary formaldehyde).

Table 6-2. Comparison of the 10 station average one in a million risks using the benzene, 1,3-butadiene, acetaldehyde, and formaldehyde average concentration estimates by the CAMx/CB4 and CAMx/S99 RTRAC modeling of the August 1997 SCOS episode.

| Species | CB-IV Chemistry | | SAPRC99 Chemistry | | % Difference S99-CB4 |
|--------------------|-----------------|-----|-------------------|-----|-------------------------|
| | Risk | (%) | Risk | (%) | |
| Benzene | 57.5 | 40 | 56.4 | 36 | -2 |
| 1,3-Butadiene | 34.7 | 24 | 23.3 | 15 | -33 |
| Prim. Acetaldehyde | 0.7 | 0 | 0.5 | 0 | -28 |
| Prim. Formaldehyde | 6.0 | 4 | 4.5 | 3 | -25 |
| Sec. Acetaldehyde | 14.0 | 10 | 19.1 | 12 | +36 |
| Sec. Formaldehyde | 30.6 | 21 | 53.3 | 34 | +74 |
| Total | 143.5 | | 157.1 | | +10 |

The CAMx/CB4 and CAMx/S99 RTRAC air toxics simulations separately tracked the contributions of air toxics due to point sources, on-road mobile source, other anthropogenic emissions, and secondarily formed air toxics. These results were used to evaluate the contributions of these major source categories to risk due to the organic air toxic species and demonstrate the RTRAC air toxics capability for source apportionment. Note that the MATES-II report attributed all risks associated with these organic air toxic compounds to “mobile sources” (SCAQMD, 2000).

Figure 6-7 displays the contributions by major source categories to total risk due to organic air toxic compounds at each MATES-II monitoring site. At most sites, on-road mobile sources and secondarily formed air toxics are the largest contributors to the total risk. However, which is the single largest contributor varies from site-to-site, with the contribution to total risk from primary air toxic emissions from mobile sources being greater at upwind sites (e.g., Los Angeles) and secondarily formed organic air toxics being greater at downwind sites (e.g., Rubidoux). In addition, there is significant site-to-site variability in the source category contributions, for example:

- At the Wilmington site, there is a significant point source contribution to risk, whereas there is a very small point source contribution at the Compton and Long Beach sites and no point source contribution at the other 7 sites.
- The other anthropogenic emissions contribution (i.e., area, non-road, and low-level points) is insignificant at downwind sites (e.g., Fontana and Rubidoux) and more significant at some upwind sites (e.g., Compton, Huntington, and Wilmington).

Table 6-3 displays the 10-site average risks by source category, an approach used in MATES-II study to estimate basin-wide average risk. The CB4 and S99 simulations both estimate that air toxics emitted from on-road mobile sources and formed as secondary species are the highest contributors to the total risk due to organic air toxic compounds. However, the CB4 simulation estimates that primary emissions from mobile sources (55%) contribute substantially more risk than secondary species (31%), whereas S99 estimates they are about equivalent contributions (44% and 46%). Both simulations estimate that other low-level anthropogenic emissions are minor contributors to total risk due to organic air toxics (~10%) and the point source contribution is negligible (~1%). It is likely that much of the secondarily formed air toxics in the SoCAB are due to mobile sources (either on-road or non-road mobile sources), but in more rural areas and in other areas the contributions of non-mobile sources to organic air toxic cancer risk could be greater. For example, a study on biogenic isoprene products in the eastern U.S. found that, except in the major cities, a vast majority of the formaldehyde in the atmosphere was due to oxidation of isoprene, not mobile sources (Morris, Lee, and Yarwood, 1997). Thus, care should be taken in assuming that all secondary air toxics are due solely to mobile sources.

Table 6-3. Comparison of the 10 station average one in a million risks by major source category from the 4-day average organic air toxic concentration estimates by the CAMx/CB4 and CAMx/S99 RTRAC modeling of the August 1997 SCOS episode.

| Species | CB-IV Chemistry | | SAPRC99 Chemistry | | % Difference S99-CB4 |
|---------------|-----------------|-----|-------------------|-----|-------------------------|
| | Risk | (%) | Risk | (%) | |
| Mobile | 79.6 | 55 | 69.6 | 44 | -13 |
| Point | 3.2 | 2 | 1.5 | 1 | -55 |
| Other Anthro. | 16.0 | 11 | 13.7 | 9 | -15 |
| Secondary | 44.5 | 31 | 72.4 | 46 | +63 |
| Total | 143.5 | | 157.1 | | +10 |

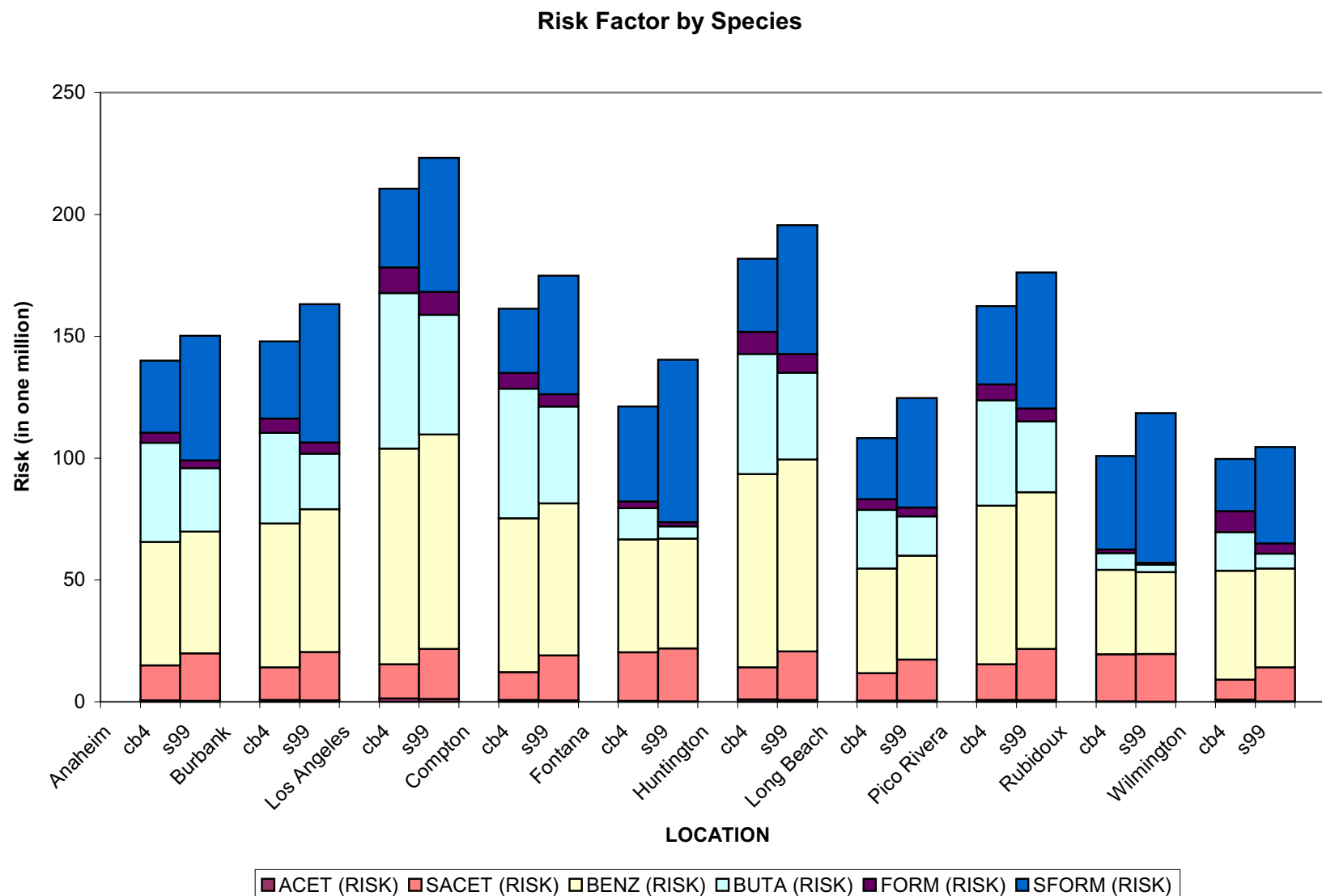


Figure 6-6. Estimated risk due to organic air toxic compounds at the 10 MATES-II sites (see Figure 2-2 for locations), by species estimated by the CAMx/CB-VI (CB4) and CAMx/SAPRC99 (S99) simulations of the August 1997 SCOS episode.

Risk Factor by Source Category

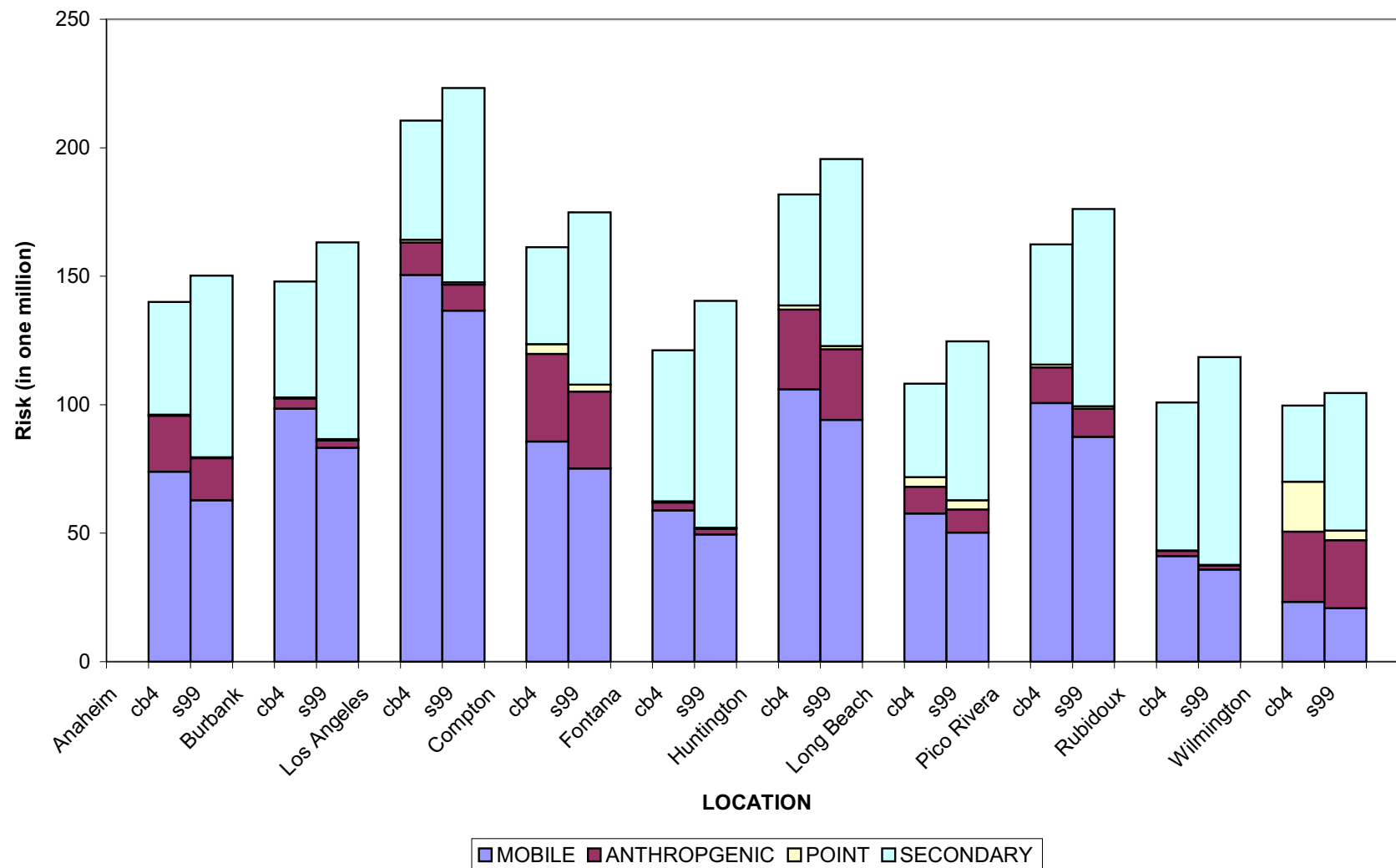
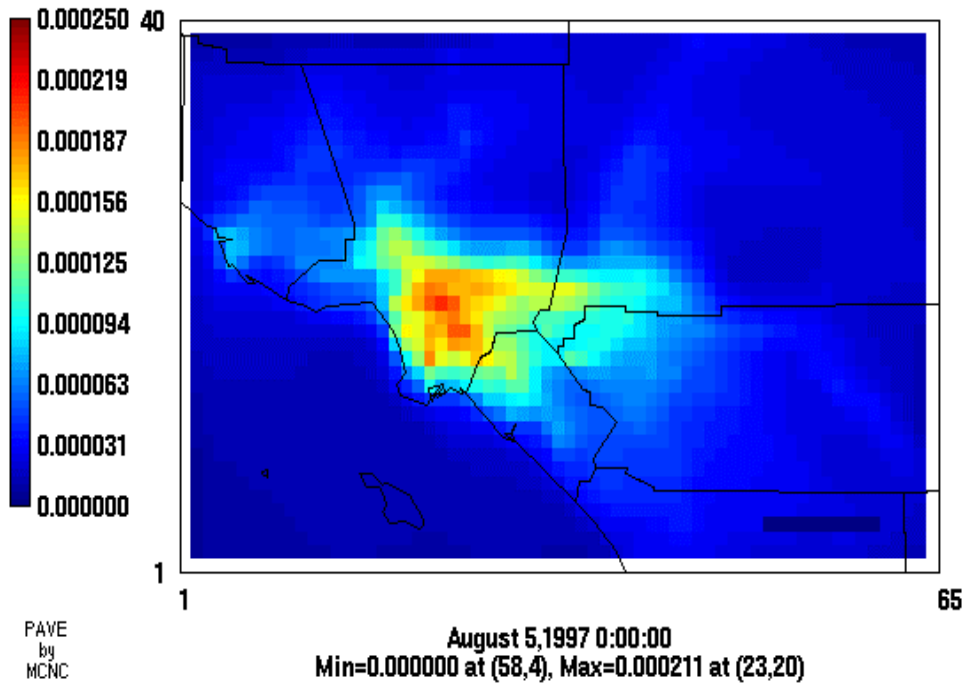


Figure 6-7. Estimated risk due to organic air toxic compounds at the 10 MATES-II sites (see Figure 2-2 for locations), by major source categories estimated by the CAMx/CB-VI (CB4) and CAMx/SAPRC99 (S99) simulations of the August 1997 SCOS episode.

Figure 6-8 displays the spatial distribution of annual risk estimated by the CAMx/CB-IV (CB4) and CAMx/SAPRC99 (S99), whereas Figure 6-9 displays their differences. The S99 estimated risk is higher (maximum of 223 in a million) and more widespread than estimated by CB4 (maximum of 211 in a million). The difference plot clearly shows that the largest differences in the CB4 and S99 estimated risks occur in downwind regions where secondary acetaldehyde and formaldehyde are greatest. Within the center of the SoCAB the CB4 and S99 estimated risk appears to be within approximately 10% of each other.

RISK FACTOR

CB4
Aug 5 - Aug 7 Average



RISK FACTOR

S99
Aug 5 - Aug 7 Average

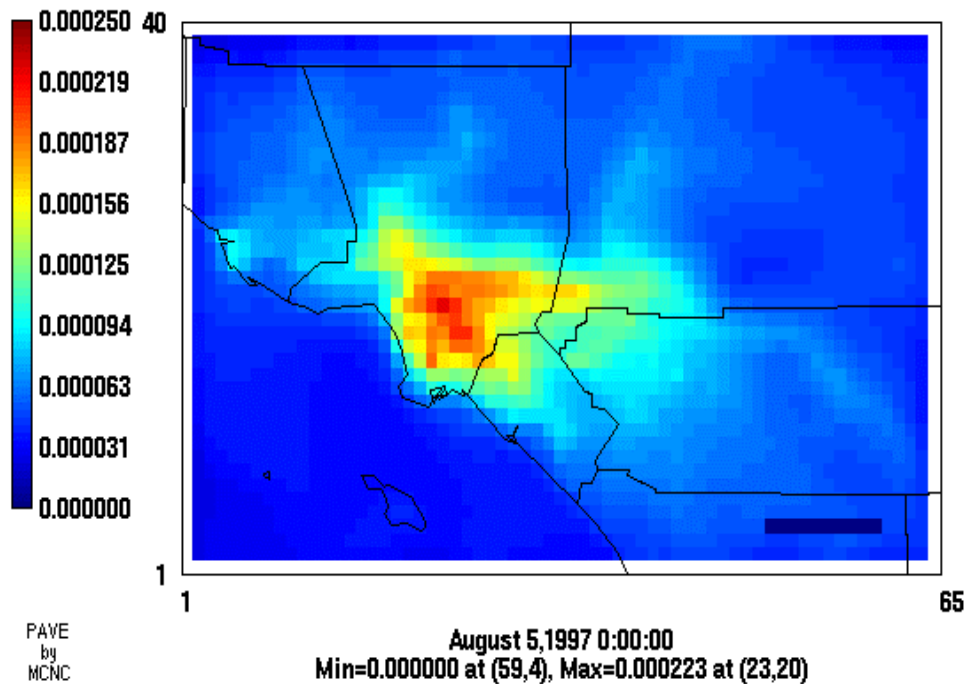


Figure 6-8. Spatial distribution of risks in the SoCAB (in millions) estimated by CAMx/CB-IV (top) and CAMx/SAPRC99 (bottom).

Differences in Risk Factor

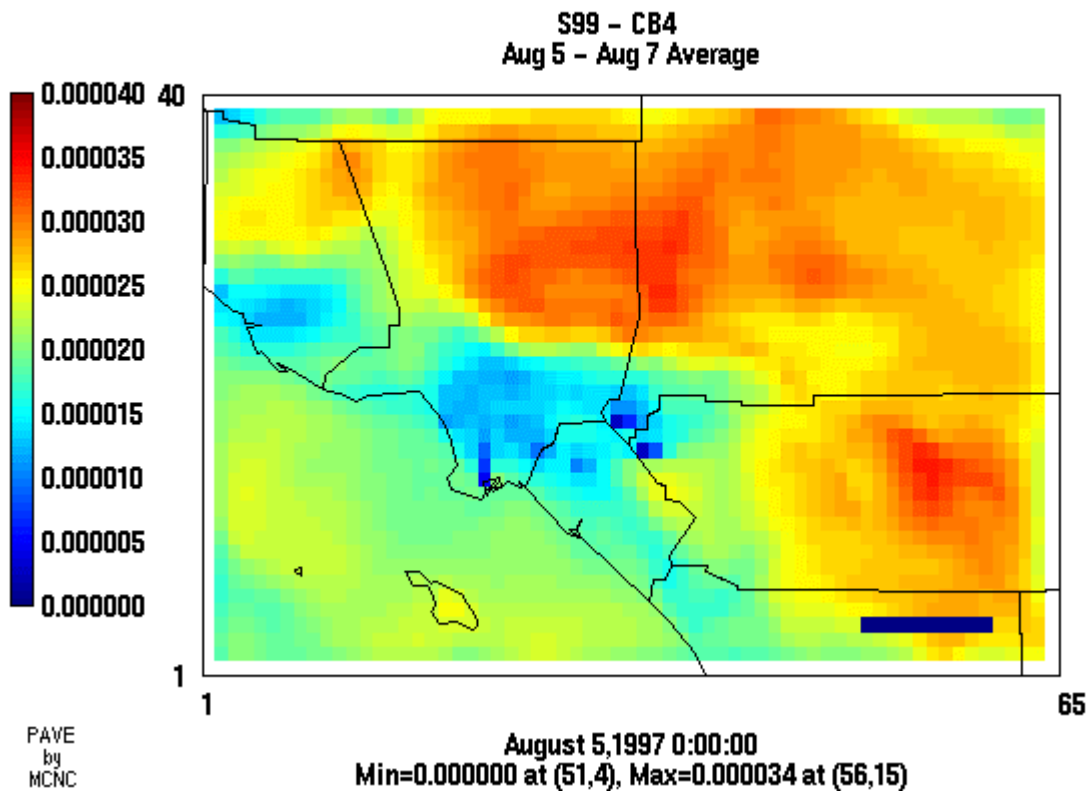


Figure 6-9. Differences in risk (in millions) between the CAMx/CB-IV (CB4) and CAMx/SAPRC99 (S99) air toxics simulations (S99 - CB4).

7. SUMMARY, CONCLUSIONS, AND RECOMMENDATIONS

SUMMARY

An air toxics modeling capability has been implemented in the Comprehensive Air-quality Model with extensions (CAMx) photochemical grid model that includes full chemistry of organic air toxic compounds, the treatment of both gas and particulate phase air toxics, and the treatment of the near-source impacts of air toxics using a subgrid-scale plume model. The hybrid CAMx air toxics modeling system was demonstrated using the April 1998 through March 1999 annual database from the Multiple Air Toxics Exposure Study (MATES-II) in the South Coast Air Basin (SoCAB) for a subset of air toxic compounds. The MATES-II mobile source emissions were updated from EMFAC7G to EMFAC2000. The CAMx estimated air toxics concentrations using the EMFAC7G and EMFAC2000 emissions were compared against the 24-hour observed values at the 10 MATES-II sites in a model performance evaluation. The performance of the MATES-II UAM-Tox modeling application was also evaluated. The subgrid-scale treatment of point sources was also demonstrated using air toxics point source emissions from the MATES-II database. The CAMx air toxics modeling system was also demonstrated using the August 3-7, 1997 Southern California Ozone Study (SCOS) episode using both the CB-IV and SAPRC99 chemical mechanisms. Finally, risk and exposure estimates were made several different ways both accounting for and not accounting for a simple representation indoor/outdoor effects and using both gridded and basin-wide population estimates.

CONCLUSIONS

The following are the major conclusions from the CRC/DOE A-42-2 Air Toxics Modeling Study:

MATES-II Databases

- The MATES-II emissions inventories are suspect and have allocated too many point source air toxics to the low-level gridded emissions rather than leaving them in the point source files.
- The CALMET generated hourly meteorological fields for the SoCAB are highly suspect and likely introduce spurious vertical velocities.
- For several species (e.g., chromium and hexavalent chromium) the MATES-II measured concentrations were frequently below the detection limit so were set to half of the detection limit which affected the model performance evaluation.
- Chromium and hexavalent chromium were measured only in the fine PM mode (PM_{2.5}), yet the emissions inventory and modeling suggest a majority of these compounds are in the coarse mode so the model performance evaluation for these species is incomplete and limited.

CAMx Air Toxics Modeling System

- The CAMx reactive tracer (RTRAC) treatment of air toxics has been demonstrated to be an effective, accurate, flexible, and efficient methodology for treating both inert and reactive, gaseous and particulate, and primary and secondary air toxic compounds.
- The near-source subgrid-scale plume treatment, that is coupled with CAMx through the CAMx chemistry and RTRAC reactive tracers as background concentrations, has proven to be an efficient and flexible approach for estimating maximum fence-line or hot-spot air toxics impacts in a mass consistent fashion with a grid model.
- The CAMx air toxics modeling system is applicable to many scales, from local plume impacts using the subgrid-scale plume models, to the urban-scale and region-scale using the CAMx two-way nested-grid formulation.
- The CAMx air toxics modeling approach is an efficient and flexible approach with ease of addition of other air toxics important for urban and regional air toxics issues.
- The update of the MATES-II emissions from EMFAC7G to EMFAC2000 results in substantial increases (approximately 50%) in on-road mobile source organic air toxics emissions (e.g., benzene, 1,3-butadiene, and aldehydes).
- The use of the subgrid-scale plume model produced maximum concentrations due to the point sources near the source that were as much as 10-20 times greater than the CAMx/RTRAC estimated 2-km by 2-km grid cell average concentration.

Model Performance Evaluation using the MATES-II Annual Database

- The UAM-Tox and CAMx models both exhibit some skill in estimating the MATES-II observed benzene concentrations with UAM-Tox exhibiting almost zero bias on average and CAMx exhibiting a slight (20%) overprediction bias. When the emissions are updated with EMFAC2000, the CAMx overprediction bias is increased. However, both UAM-Tox and CAMx are reproducing the observed benzene concentrations to within the uncertainties of the emissions inventory that is approximately a factor of 2 (Seigneur, Lohman, and Pun, 2002). The spatial distribution of the estimated benzene concentrations in the SoCAB follow the major roadways in the region.
- CAMx and UAM-Tox both underestimate the observed 1,3-butadiene by approximately a factor of 2 on average. The very highest annual average estimated 1,3-butadiene concentrations occur over the LAX airport, with lower 1,3-butadiene concentrations in the remainder of the domain that follow the roadways in the SoCAB.
- The UAM-Tox underestimates the observed acetaldehyde concentrations by approximately a factor of 3, whereas CAMx is within a factor of 2 with an overestimation bias on average of 60% (EMFAC7G) and 80% (EMFAC2000). There are two hot spots of primary acetaldehyde estimates, one over the LAX airport and the other over the port area near Long Beach. Secondary acetaldehyde increases from west to east with maximum values in the Riverside and San Gabriel Mountains areas. Except for the LAX airport and port areas, secondary acetaldehyde contributes over 70% to the total acetaldehyde, exceeding a 90% contribution over most of the domain.

- Both UAM-Tox and CAMx estimate the average observed formaldehyde concentrations within a factor of 2 with UAM-Tox exhibiting a 30% underprediction tendency and CAMx exhibiting a 50% (EMFAC7G) and 90% (EMFAC2000) overprediction tendency. LAX and the port areas are also two hot spots in the primary formaldehyde spatial distributions. Away from these two areas, secondary formaldehyde dominates (50-90%) the total formaldehyde concentrations.
- Both models overestimate the observed chromium and hexavalent chromium concentrations with the UAM-Tox overestimation being quite severe (factor of 4 to 4.5), whereas the CAMx overestimation tendency being not as severe (factor of 2 to 2.5). The spatial distribution of chromium follows the roadways with the coarse mode chromium being much higher than the fine mode chromium. The spatial distribution of the hexavalent chromium is very spotty. The coarse mode hexavalent chromium concentrations are greater than their fine mode counterparts. The MATES-II monitoring only measured fine mode chromium and hexavalent chromium, this as a majority of these species are in the coarse mode the evaluation for these two species is incomplete.

Model Evaluation Using the August 1997 SCOS Episode Database

- The observed benzene concentrations during the August 3-7, 1997 SCOS episode are reproduced by the CAMx model fairly well using both the CB-IV and SAPRC99 chemical mechanisms.
- The observed formaldehyde and acetaldehyde concentrations are also replicated fairly well by the CAMx model, with much better model performance being exhibited by the CAMx using the CB-IV chemistry then using the SAPRC99 chemistry.
- The SAPRC99 chemistry is more reactive than the CB-IV chemistry, thus SAPRC99 decays primary emitted air toxic species much faster (e.g., 1,3-butadiene) and forms more secondary air toxic compounds (e.g., formaldehyde and acetaldehyde) than CB-IV.

Risk and Exposure Calculations

- The CAMx air toxics modeling in this study estimated higher risk than by UAM-Tox in the MATES-II due to increased concentration estimates of primary air toxics, which was partly due to the EMFAC2000 update, and increased concentrations in the secondary air toxics due to higher aldehyde estimates.
- Accounting for indoor/outdoor effects on the risk and exposure calculations reduced the risk and exposure by approximately one-third.
- Very similar risk and exposure estimates were obtained whether an annual composite indoor/outdoor ratio was used with annual average air toxics concentrations or whether hourly indoor/outdoor factors and concentrations were used.

- Use of the SAPRC99 chemistry decreases the risk due to primary air toxics and increases the risk due to secondary air toxics for a net increase in total toxic risk of approximately 10% over using the CB-IV chemistry.
- The two highest areas of risk are the port area near Long Beach and downtown Los Angeles, whereas downtown Los Angeles has much higher exposure due to the higher population.

RECOMMENDATIONS

The study applied the CAMx air toxics modeling system for two applications to the South Coast Air Basin (SoCAB). The study has raised several interesting findings that should be investigated more fully.

The South Coast Air Quality Management District (SCAQMD) research plan includes conducting a MATES-III study in the 2003-2004 time frame. The use of the CAMx air toxics modeling system and performance of some of the recommendations below would enhance the analysis over what was performed previously.

The following is a summary of recommendations:

- New emissions should be generated for the MATES-II period using the latest ARB emissions modeling software and updated VOC and PM speciation profiles.
- An emissions reconciliation of air toxics emissions is needed for the photochemical modeling emissions inventories, the ARB's AB2588 air toxics emissions inventory, and the latest release of the EPA's Toxics Release Inventory (TRI).
- The MATES-II CAMx air toxics modeling analysis should be performed again using the new emissions inventory including treatment of point source impacts for more point sources.
- Procedures for performing cost-effective annual MM5 modeling of the SoCAB should be developed so that it can be used routinely for annual air toxics, PM, and other modeling.
- Application and evaluation of the CAMx air toxics modeling system to other urban areas with adequate air toxics emissions and measurements should be performed (e.g., Houston and/or Phoenix).
- A CAMx RTRAC air toxics input file for all important urban air toxic compounds should be developed.
- Extension of the CAMx RTRAC module to treat regional air toxics such as mercury, cadmium, dioxin, atrazine, and POMs with appropriate chemistry and gas/aerosol partitionary schemes is desired.
- Application and evaluation of CAMx RTRAC on the regional-scale (e.g., eastern or continental U.S.) to estimate the deposition of air toxics onto the Great Waters and provide regional air toxics impacts assessment like in the EPA Cumulative Exposure Project (CEP).
- Development and application of an exposure modeling component of the CAMx air toxics modeling system that takes into account population activity, building types and local effects should be done.

- Integration of an indoor air quality model with the CAMx air toxics modeling system is desired.

8. REFERENCES

- Calvert, J.G., R. Atkinson, J.A. Kerr, S. Madronich, G.K. Moortgat, T.H. Wallington and G. Yarwood. 2000. "The Mechanisms of Atmospheric Oxidation of the Alkenes." Oxford University Press, New York, New York.
- Calvert, J.G., R. Atkinson, K.H. Becker, R.M. Kamens, J.H. Seinfeld, T.H. Wallington and G. Yarwood. 2002. "The Mechanisms of Atmospheric Oxidation of the Aromatic Hydrocarbons." Oxford University Press, New York, New York.
- ENVIRON. 2002. User's Guide - Comprehensive Air Quality Model with Extensions (CAMx). Version 3.1. April.
- EPA. 1999. Air Dispersion Modeling of Toxic Pollutants in Urban Areas – Guidance, Methodology, and Example Applications. Office of Air Quality Planning and Standards. U.S. Environmental Protection Agency, Research Triangle Park, North Carolina. (EPA-454/R-99-021) July.
- EPA. 1991. "Guidelines for the Regulatory Application of the Urban Airshed Model". U.S. Environmental Protection Agency, Research Triangle Park, North Carolina.
- Harley R. A., and G. R. Cass. 1995, Modeling the Atmospheric Concentrations of Individual Volatile Organic Compounds. *Atmos. Environ.* Vol. 29, No. 8, pp. 905-922.
- Hayes, S.R. et al. 1994. Toward Greater Realism in Air Toxics Exposure Assessment. Presented at 88th Annual Meeting of Air & Waste Management Association, San Antonio, TX June 1994
- ICF. 2001. "User's Guide to the Regional Modeling Systems for Aerosols and Deposition". ICF Consulting, Fairfax, VA. November.
- IUPAC. 2001. "Evaluated kinetic and photochemical data for atmospheric chemistry." IUPAC Subcommittee for Gas Kinetic Data Evaluation. Available at <http://www.iupac-kinetic.ch.cam.ac.uk/index.html>. December, 2001.
- JPL. 2001. "Chemical Kinetics and Photochemical Data for Stratospheric Modeling -- Evaluation 13." NASA Jet Propulsion Laboratory publication 00-3. Available at <http://jpldataeval.jpl.nasa.gov>. February, 2001.
- Madronich, S. 2002. The Tropospheric visible Ultra-violet (TUV) model web page. <http://www.acd.ucar.edu/TUV/>.
- Morris, R.E., K. Lee, and G. Yarwood. 1997. "Comparison of OTAG UAM-V/BEIS2 Modeling Results with Ambient Isoprene and Other Related Species Concentrations". ENVIRON International Corporation, Novato, CA. October.

- Morris, R.E. et al. 2001. Evaluation of the Air Quality Impacts of Zero Emission Vehicles (ZEVs) and a No ZEV Alternative in the South Coast Air Basin of California. Final Report. Prepared for C.A.T. Committee, General Motors Corporation and Toyota Motor Company. November 2001.
- Morris, R.E. et al. 2002. Evaluation of the Air Quality Impacts of Zero Emission Vehicles (ZEVs) and a No ZEV Alternative in the South Coast Air Basin of California. Paper presented at Air & Waste Management Association 95th Annual Meeting and Exhibition, Baltimore, Maryland.
- SAI. 1999. Modeling Cumulative Outdoor Concentrations of Hazardous Air Pollutants. Systems applications International, Inc. San Rafael, CA, SYSAPP-99-96/33r.2. February.
- Scire, J.S. et al. 1999. A User's Guide for the CALMET Meteorological Model (Version 5). Earth Tech, Concord, MA. January.
- SCAQMD. 2000. Multiple Air Toxics Exposure Study in the South Coast Air Basin-MATES-II. South Coast Air Quality Management District, Diamond Bar, CA. November.
- Seigneur, Lohman, and Pun. 2002. "Critical Review of Air Toxics Modeling – Lurent Status and Keg Issues". Atmospheric and Environmental Research, Inc. San Ramon, CA. September.
- Slinn, S.A. and W.G.N. Slinn. 1980. Predictions for particle deposition on natural waters. *Atmos. Environ.* 24, 1013-1016.
- Wesely, M.L. 1989. Parameterization of Surface Resistances to Gaseous Dry Deposition in Regional-Scale Numerical Models. *Atmos. Environ.* 23, 1293-1304.
- Yarwood, G., et al. 2002. Proximate Modeling of Weekday/Weekend Ozone Differences for Los Angeles. Draft. Prepared for Coordinating Research Council, Alpharetta, GA. May.

9. GLOSSARY OF ABBREVIATIONS/ACRONYMS

| | |
|----------------------------|--|
| ARB | California Air Resources Board |
| CALMET | CALifornia METeorological model |
| CAMx | Comprehensive Air-quality Model with extensions |
| CB-IB or CB4 | Version IV of the Carbon Bond chemistry mechanism |
| CRC | Coordinating Research Council |
| CrIV | Hexavalent Chromium |
| DDM | Decoupled Direct Method |
| DOE | U.S. Department of Energy |
| DTIM | Direct Traffic Impact Model |
| EC | Elemental Carbon |
| EMFAC2000 | 2000 version of the CA on-road mobile source emissions model |
| EMFAC7G | Version 7G of the CA on-road mobile source emissions model |
| EPA | U.S. Environmental Protection Agency |
| GEM | Gridded Emissions Model |
| ISC | Industrial Source Complex Gaussian plume model |
| MATES-II | Multiple Air Toxics and Exposure Study II |
| MM5 | Mesoscale Model version 5 a prognostic meteorological model |
| OSAT | Ozone Source Apportionment Technology |
| PAMS | Photochemical Assessment Monitoring Stations |
| PM ₁₀ | Particulate Matter of 10 µm diameter or less |
| PM _{2.5} | Particulate Matter of 2.5 µm diameter or less |
| PM _{2.5-10} or CM | Coarse Particulate Matter of 2.5-10 µm diameter |
| RTRAC | Reactive TRACer modeling approach |
| SAPRC99 | 1999 version of the SAPRC chemistry mechanism |
| SCAQMD | South Coast Air Quality Management District |
| SCOS | Southern California Ozone Study |
| SoCAB | South Coast Air Quality Management District |
| UAM-Tox | Air toxics version of the Urban Airshed Model |
| UATMG | Urban Air Toxics Modeling Guidance |
| VMT | Vehicle Miles Traveled |

APPENDIX A

Scatter Plots of Predicted and Observed
24-Hour Concentrations from the MATES-II Database for:

UAM-Tox/EMFAC7G

CAMx/EMFAC7G

CAMx/EMFAC2000

and

Benzene ($\mu\text{g}/\text{m}^3$)

1,3-Butadiene ($\mu\text{g}/\text{m}^3$)

Acetaldehyde ($\mu\text{g}/\text{m}^3$)

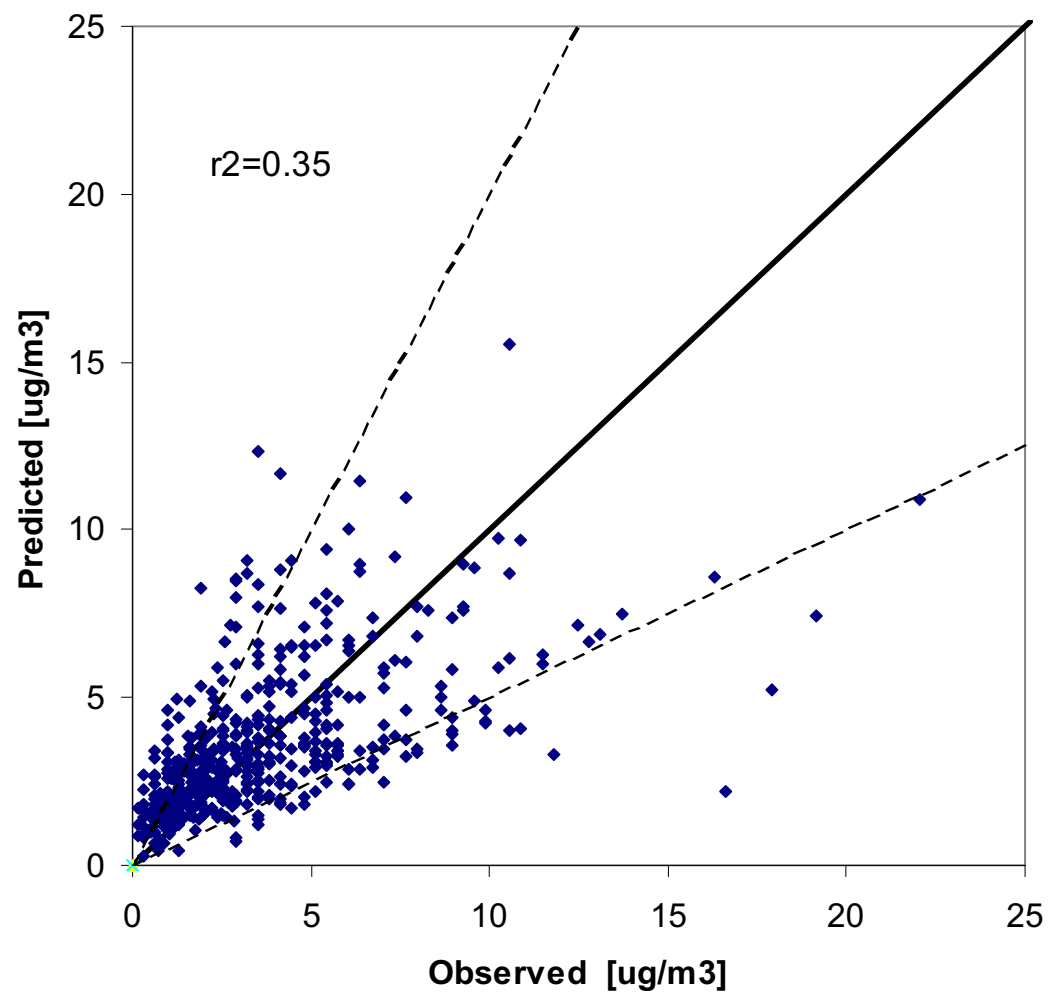
Formaldehyde ($\mu\text{g}/\text{m}^3$)

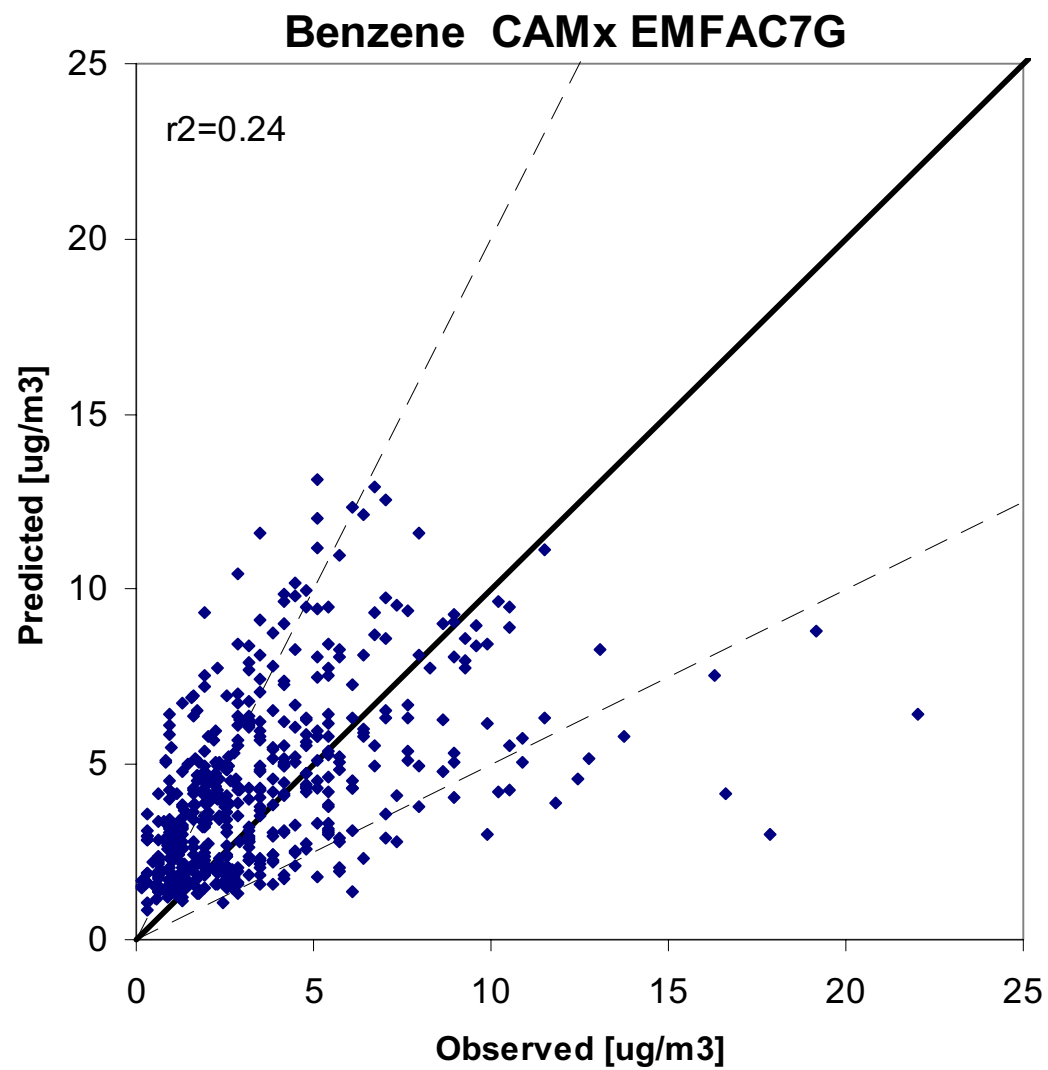
Chromium (ng/m^3)

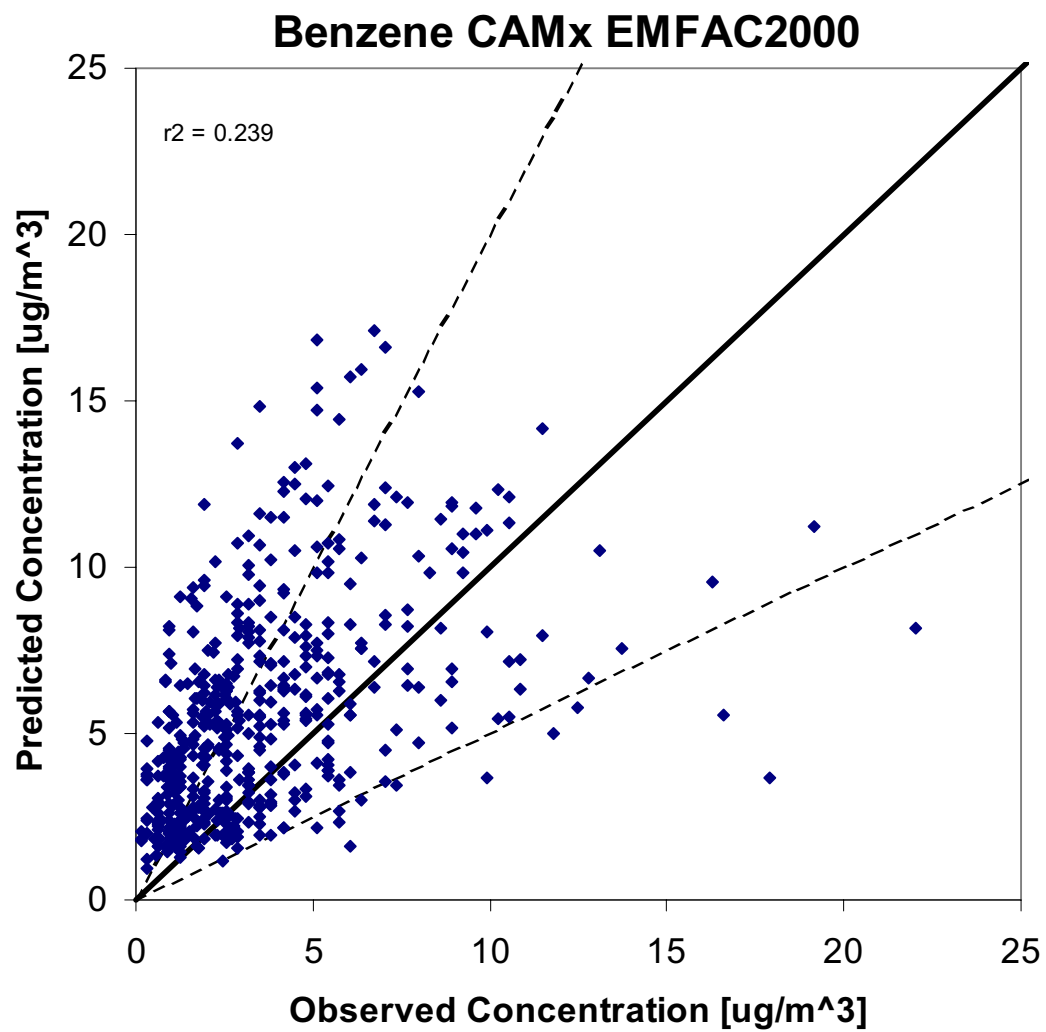
Hexavalent Chromium (ng/m^3)

“Elemental” Carbon ($\mu\text{g}/\text{m}^3$)

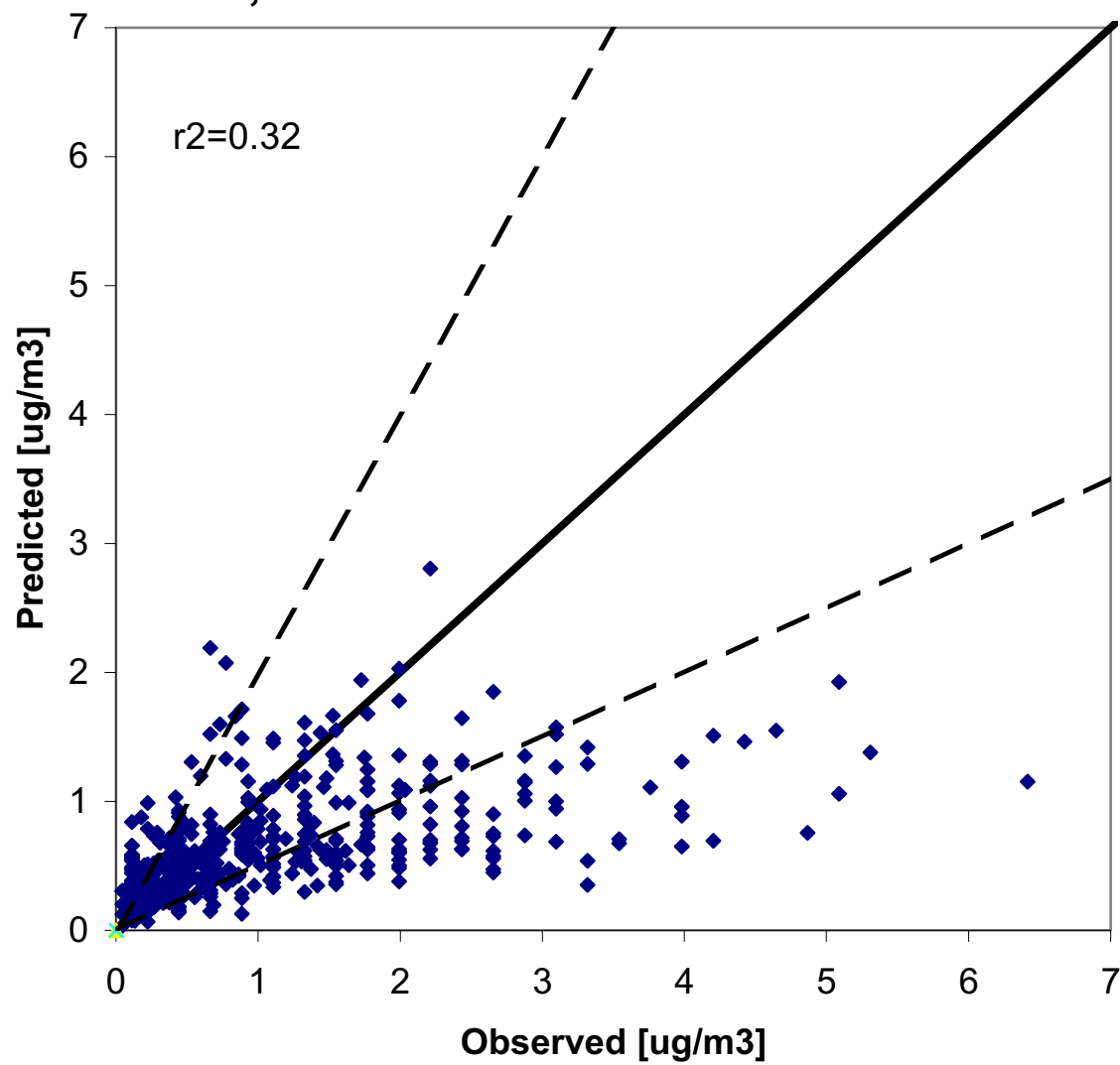
Benzene - UAM-tox EMFAC7G

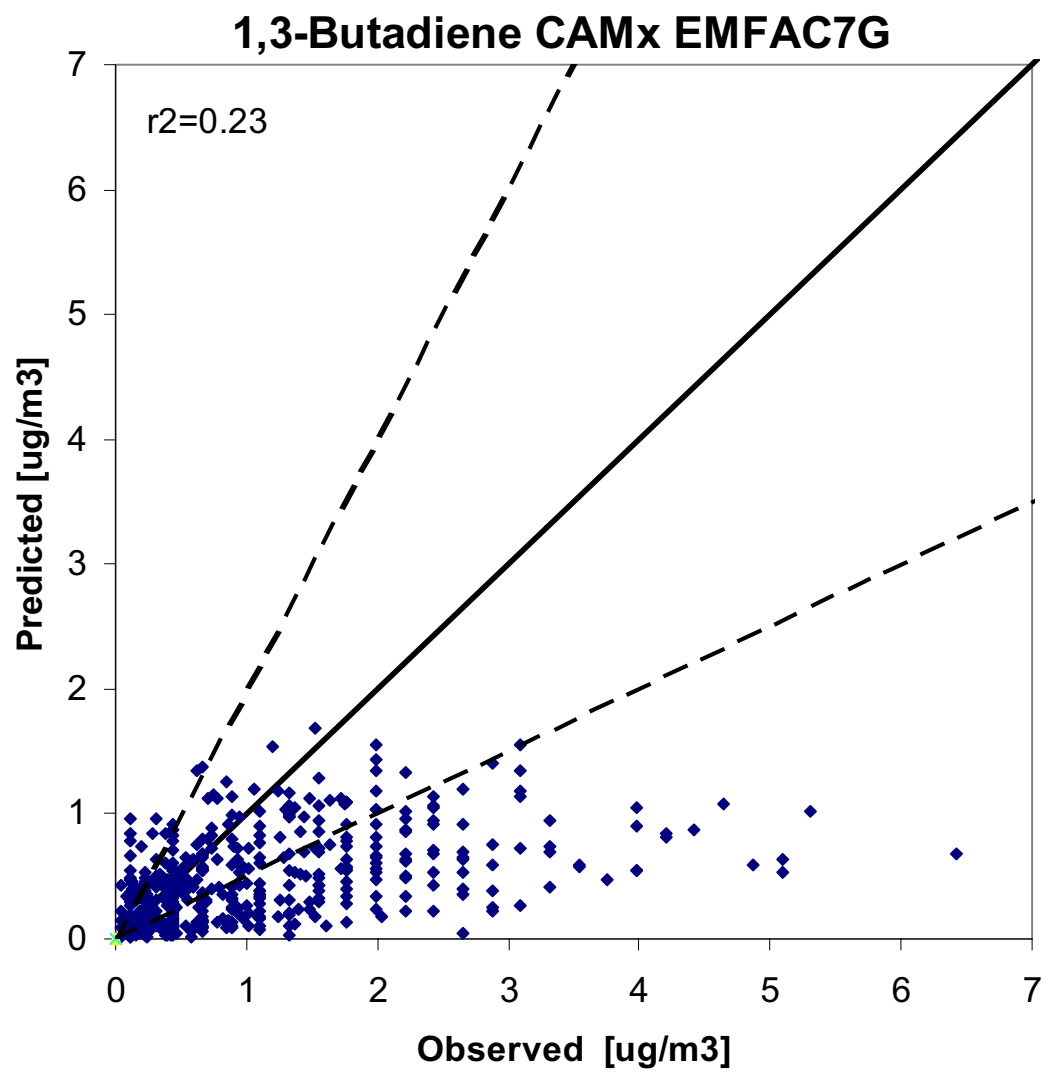




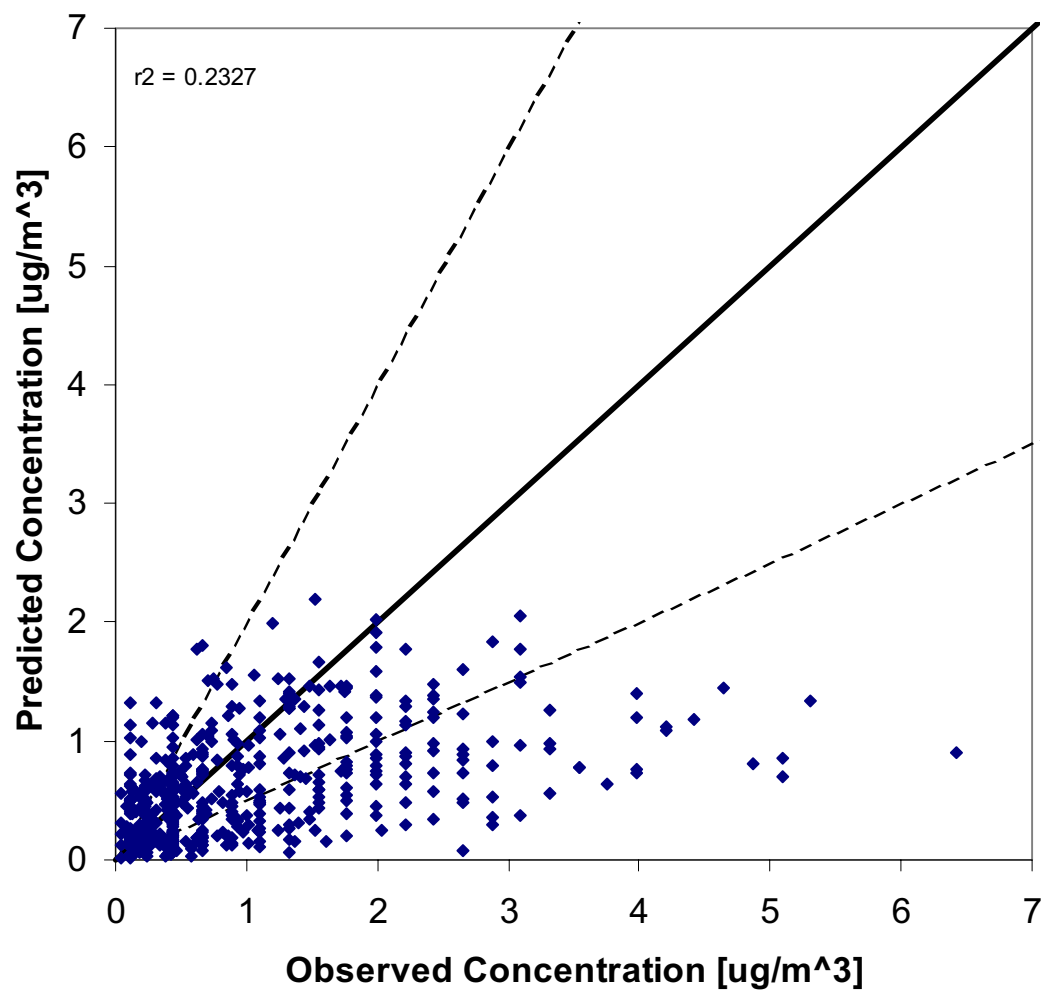


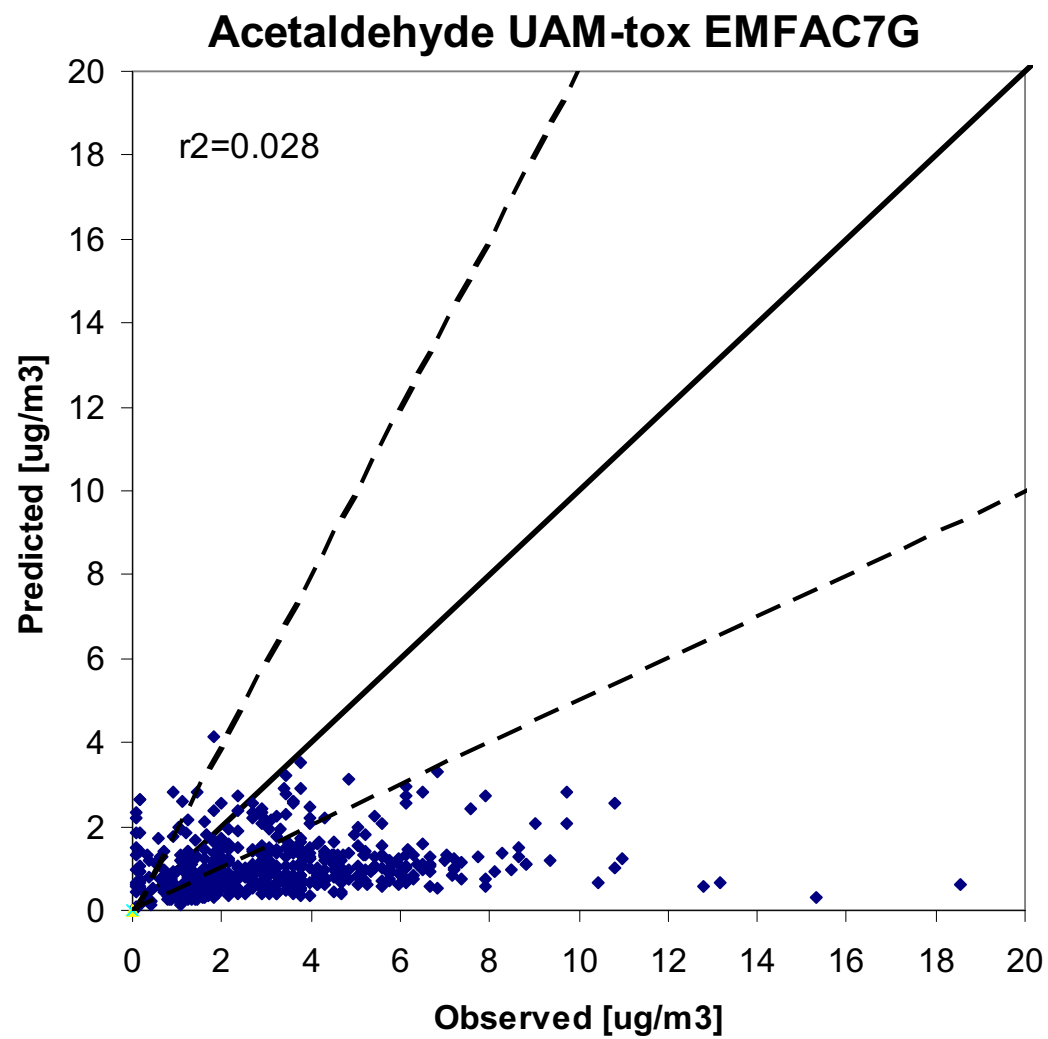
1,3-Butadiene UAM-tox EMFAC7G



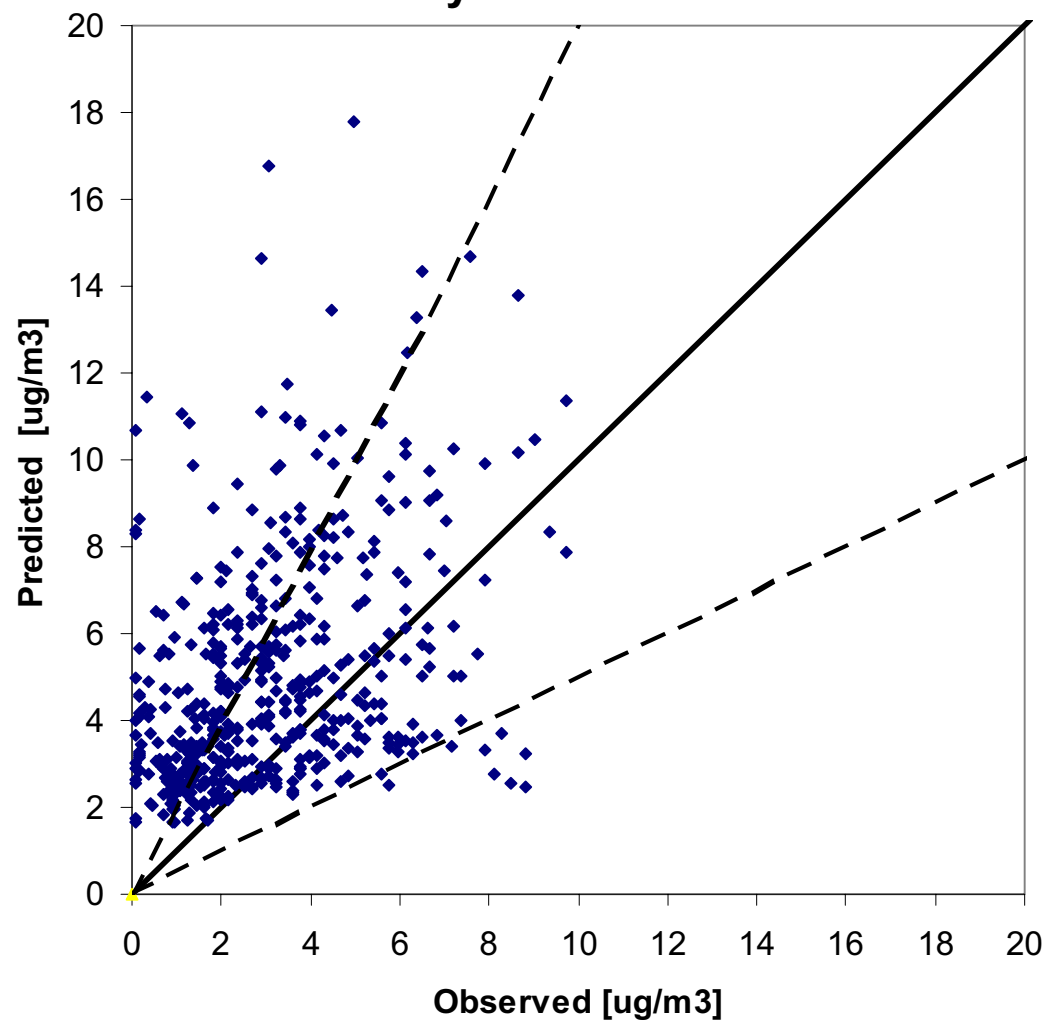


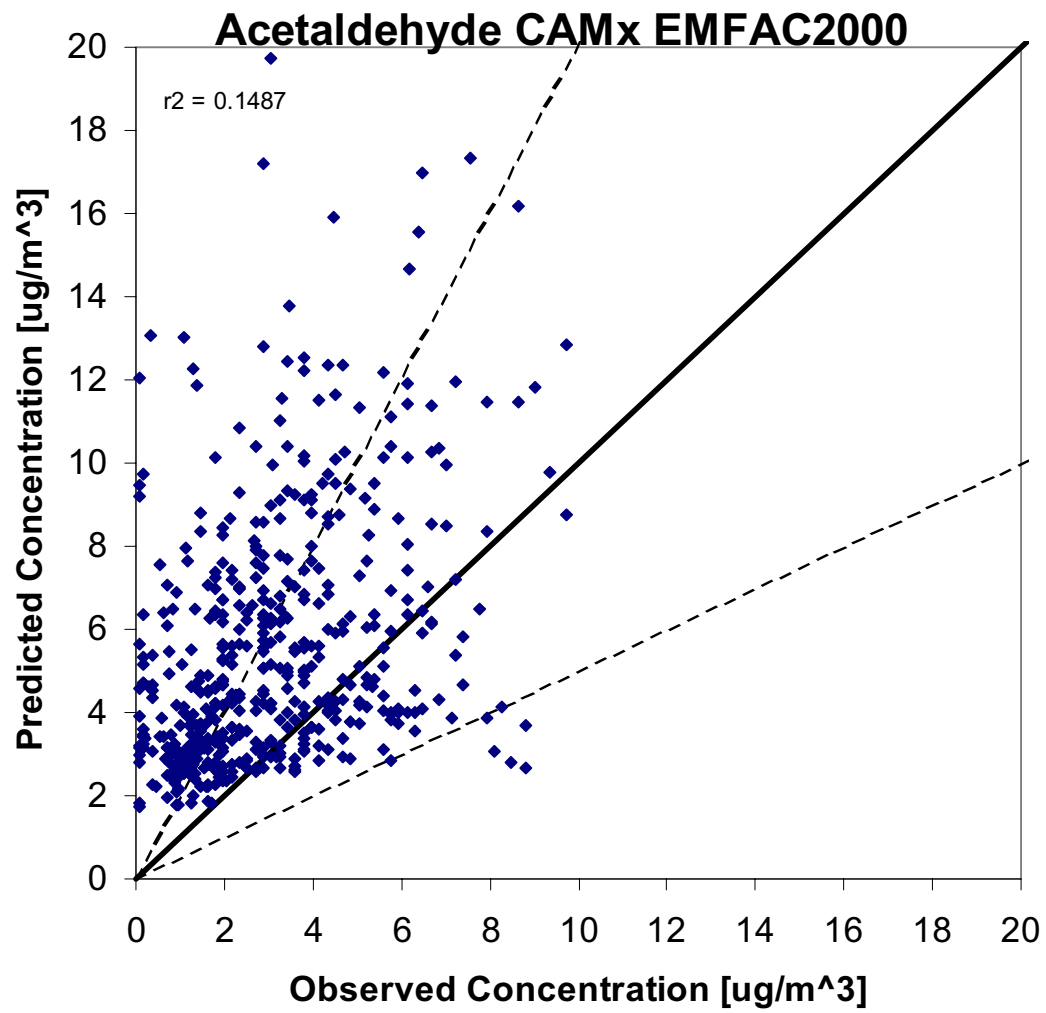
1,3-Butadiene CAMx EMFAC2000

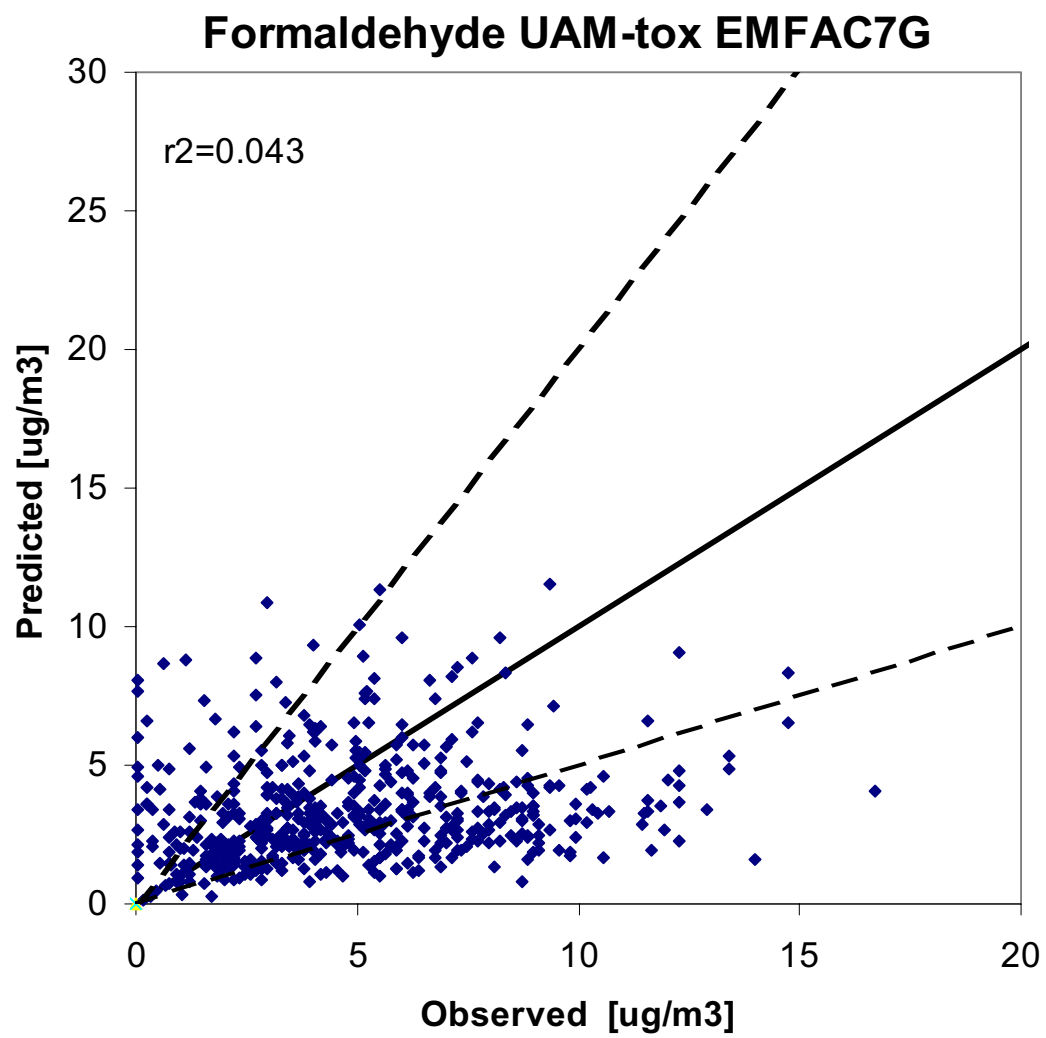


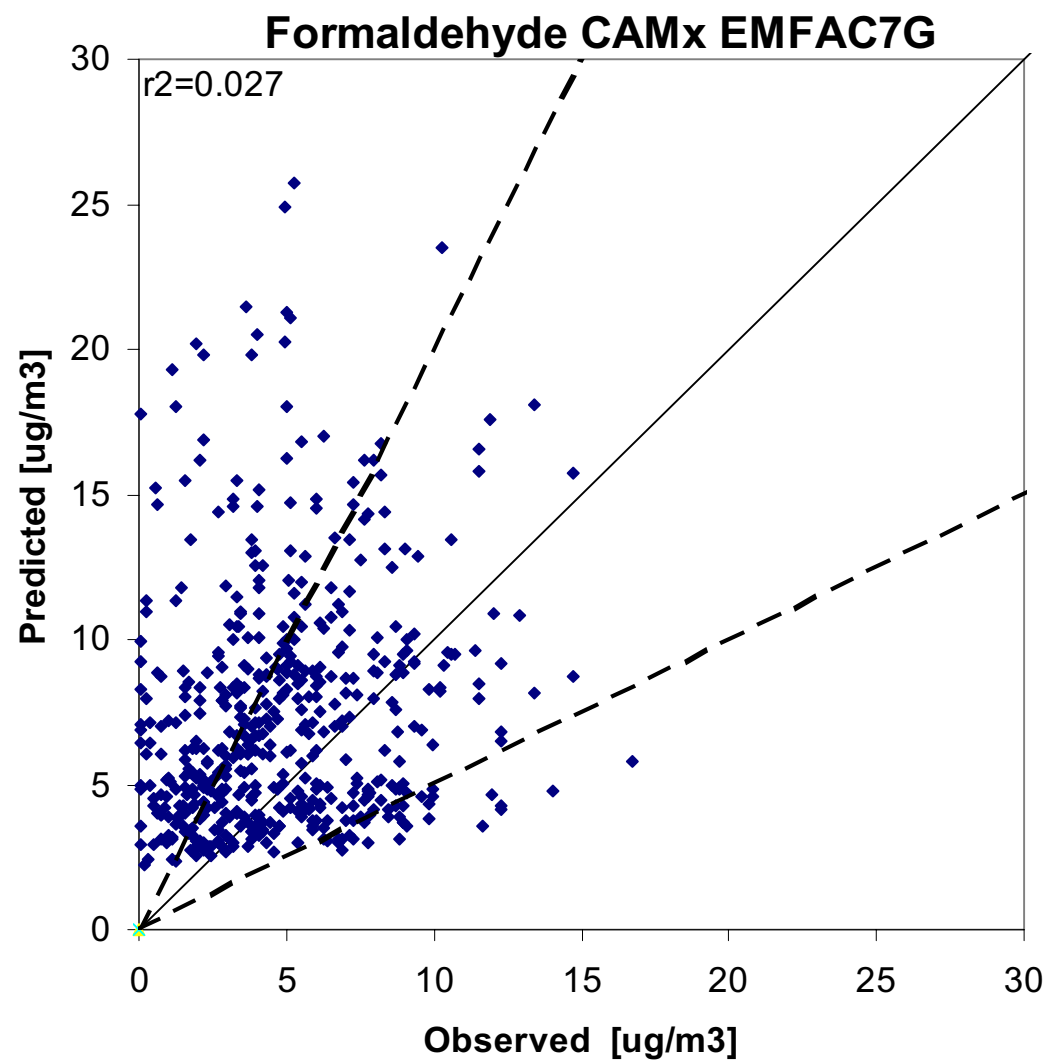


Acetaldehyde CAMx EMFAC7G

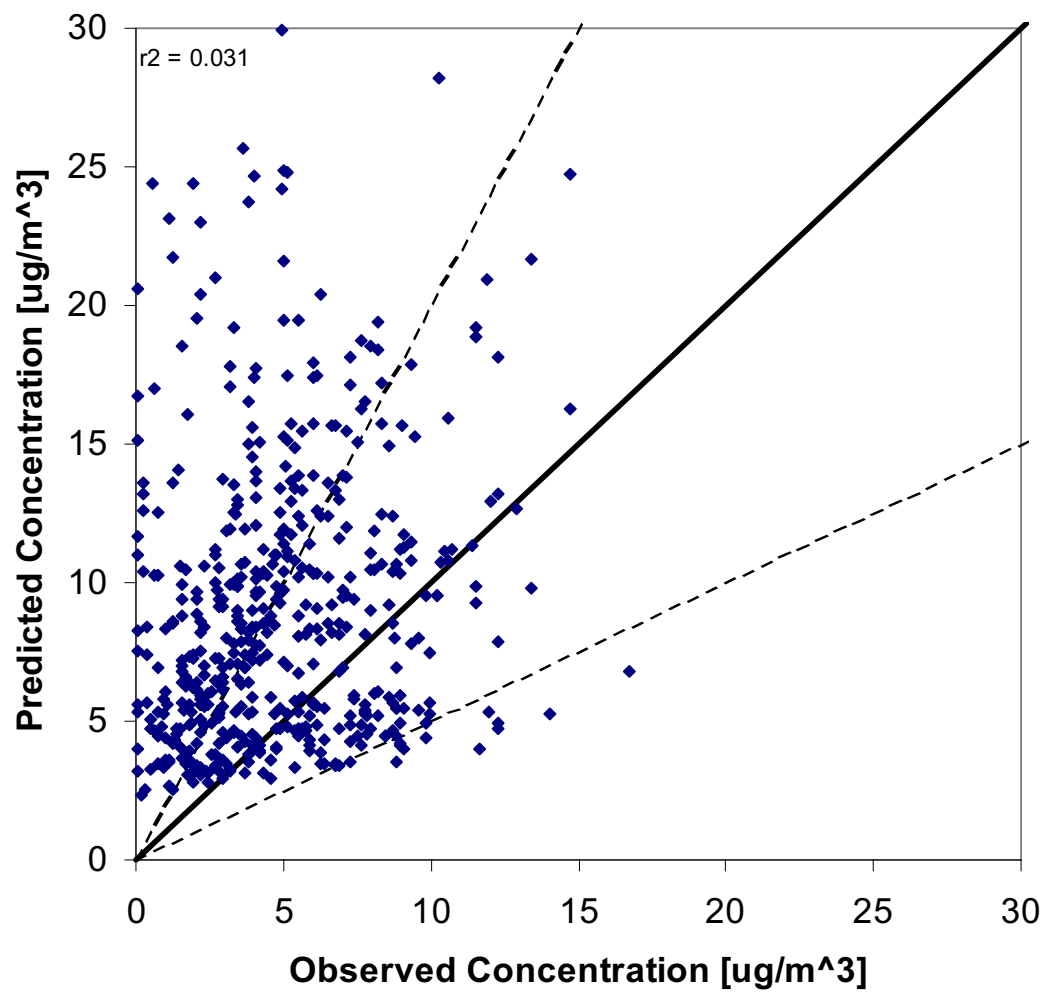


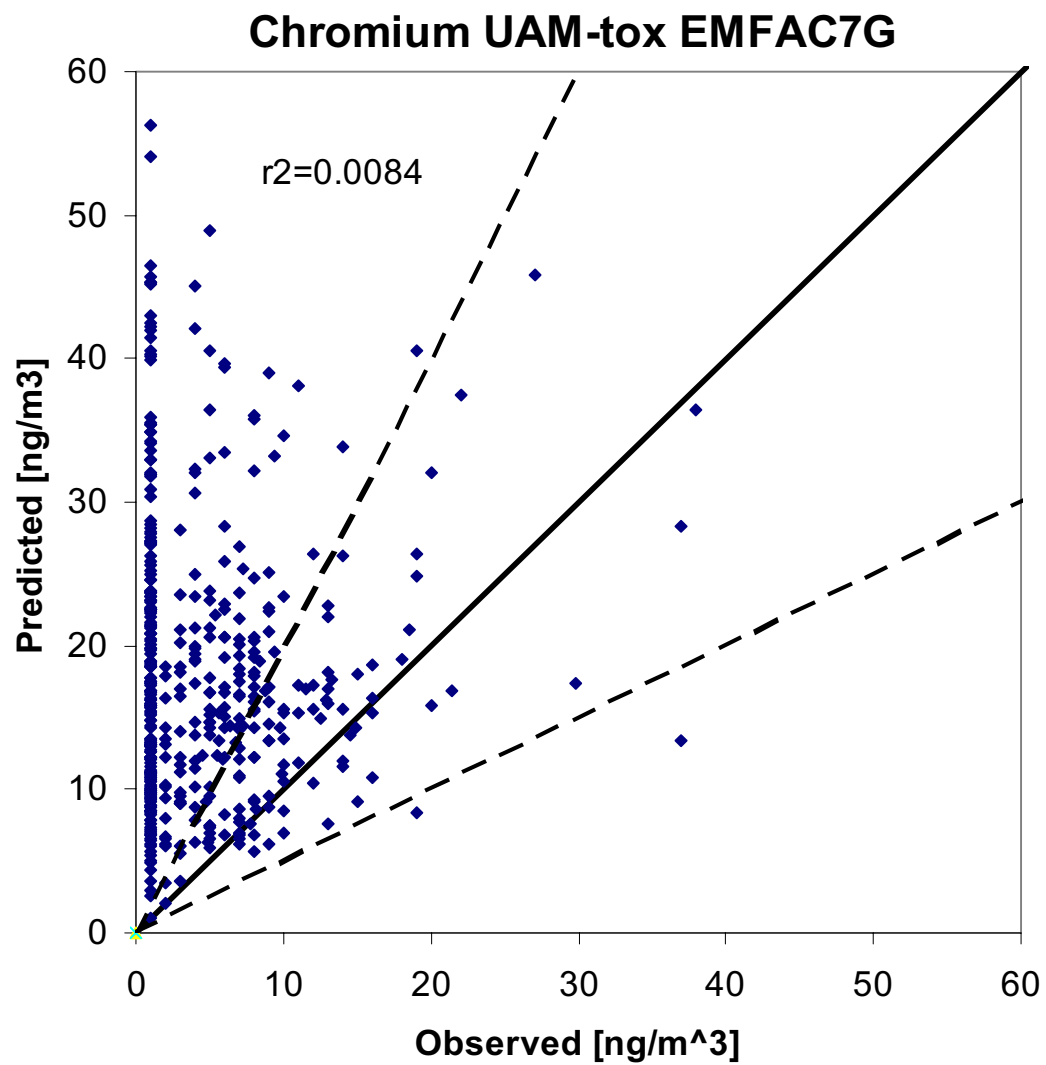




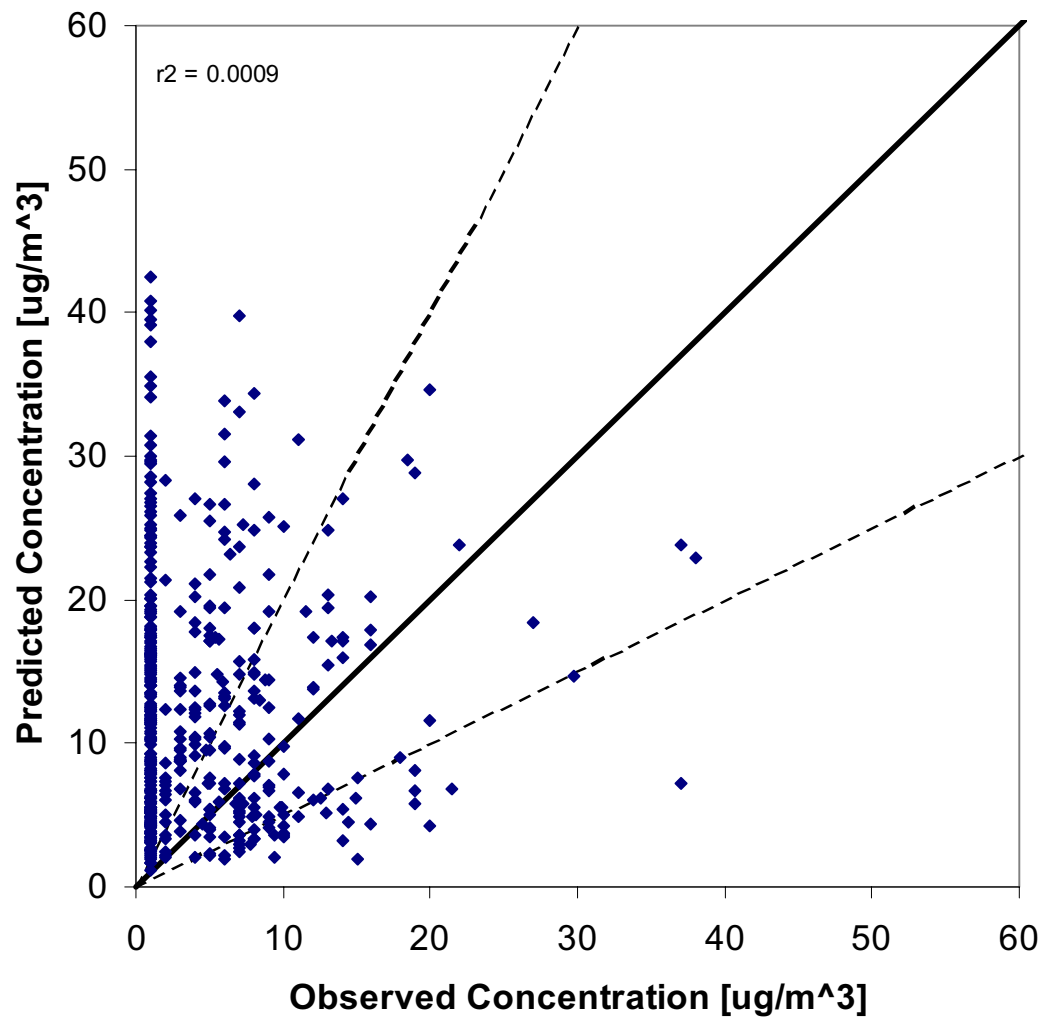


Formaldehyde CAMx EMFAC2000

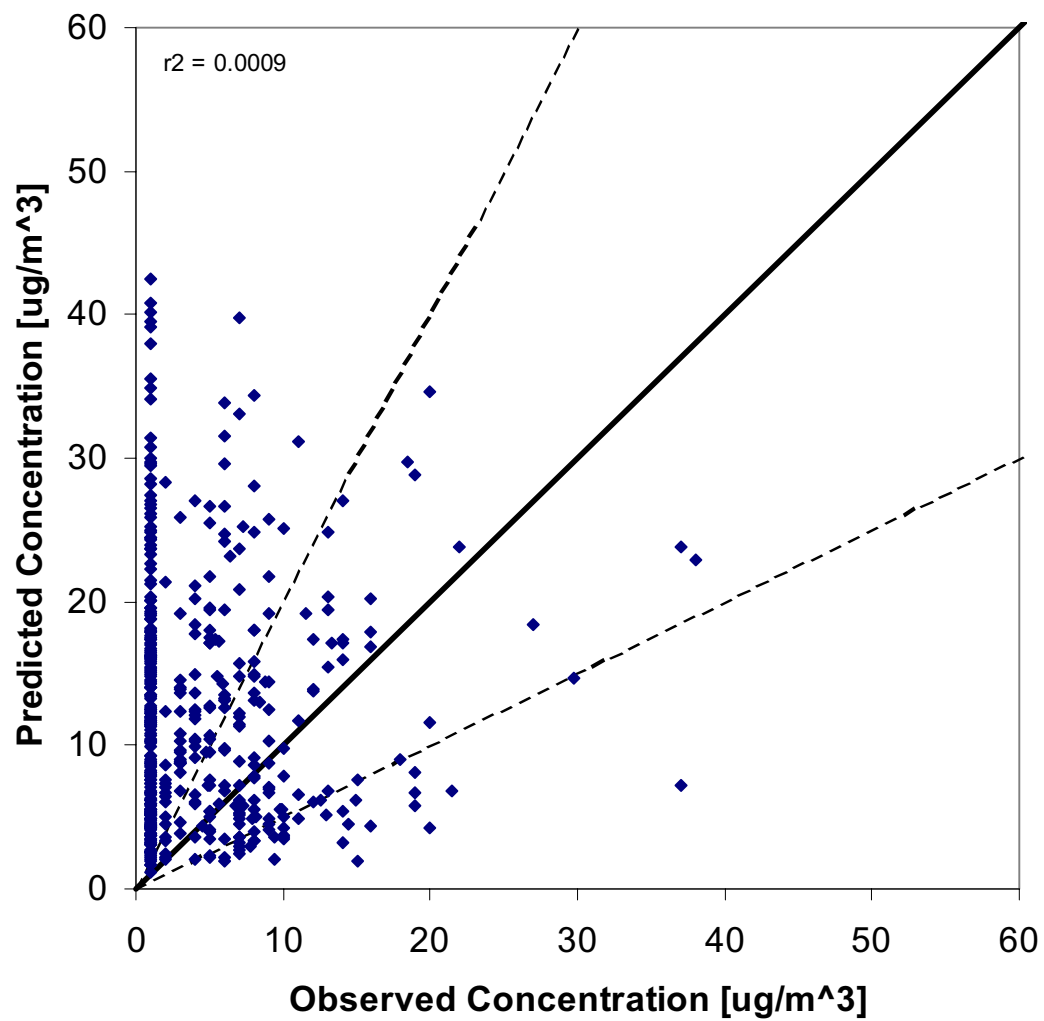


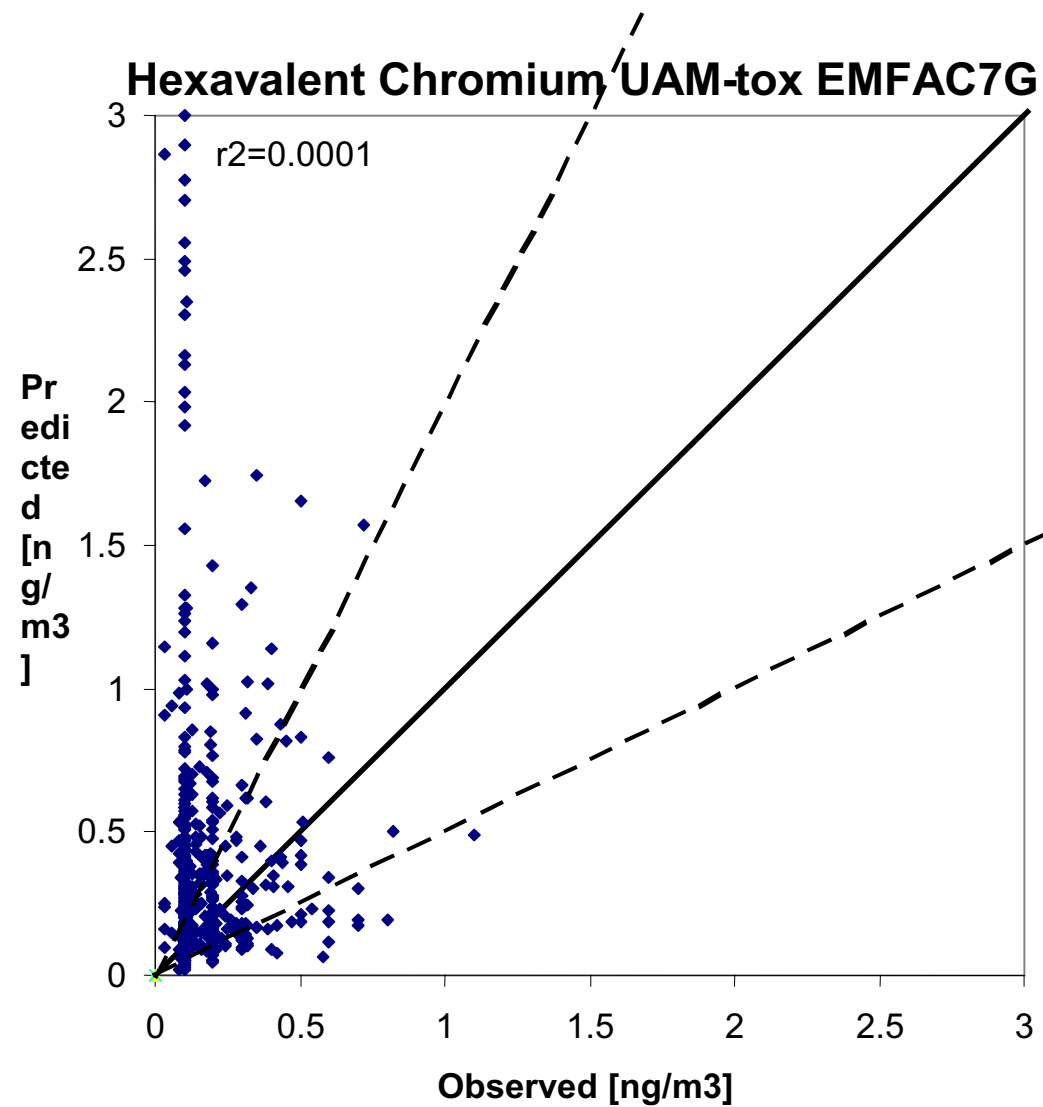


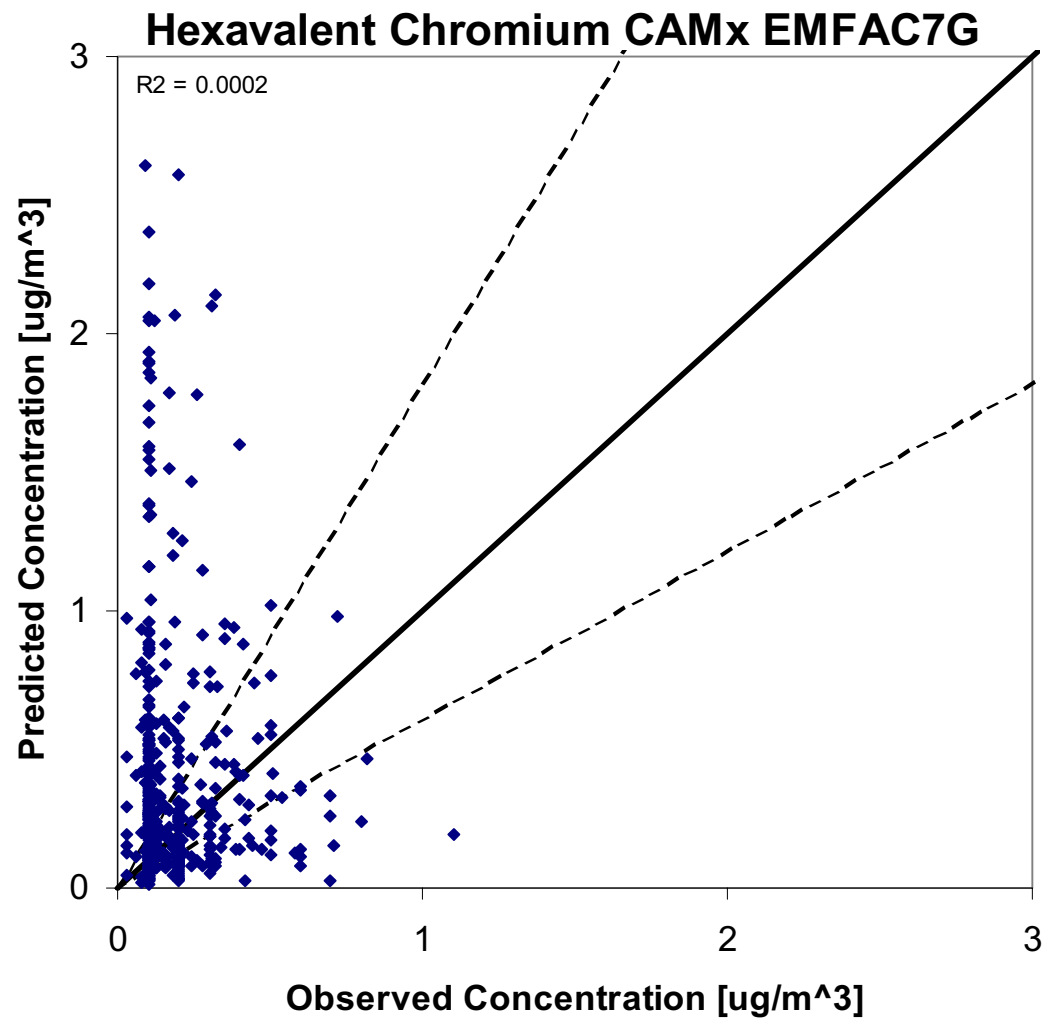
Chromium CAMx EMFAC7G

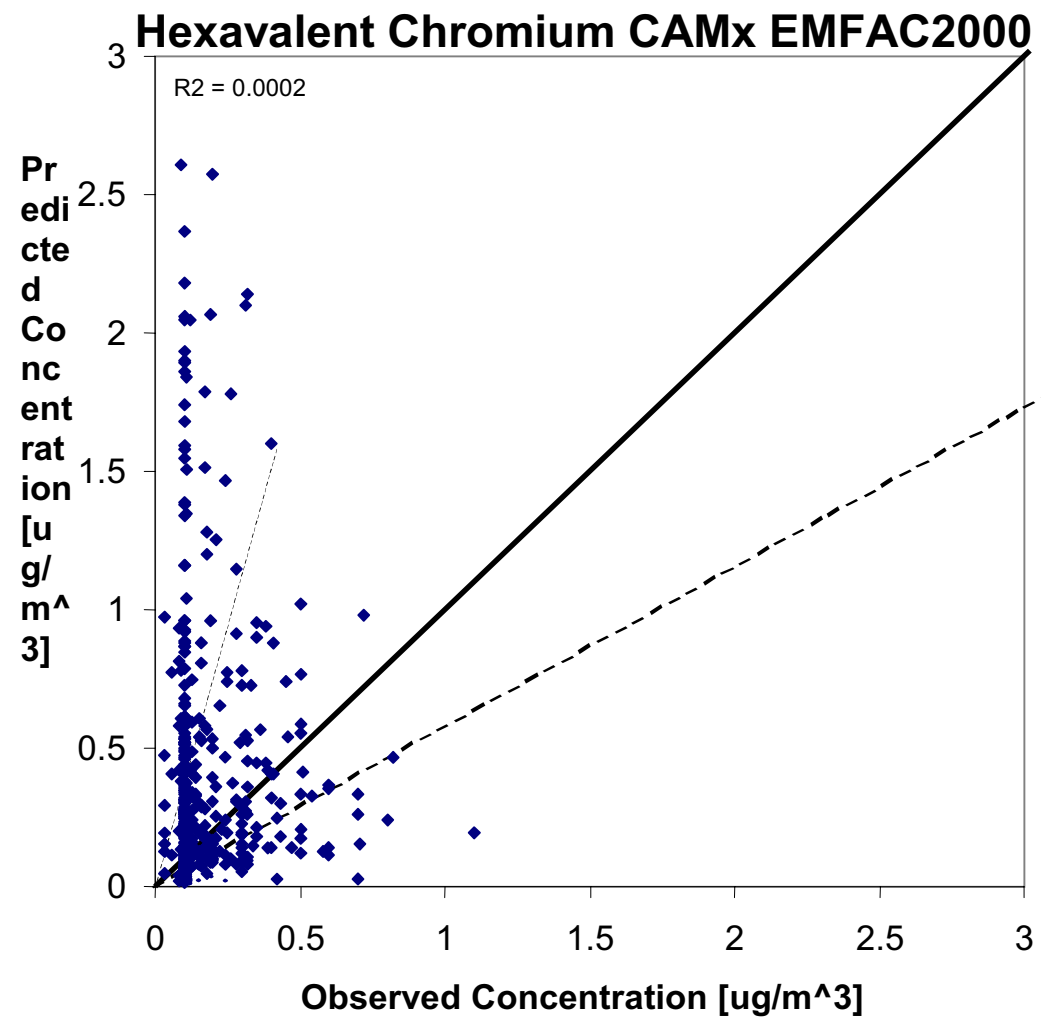


Chromium CAMx EMFAC2000

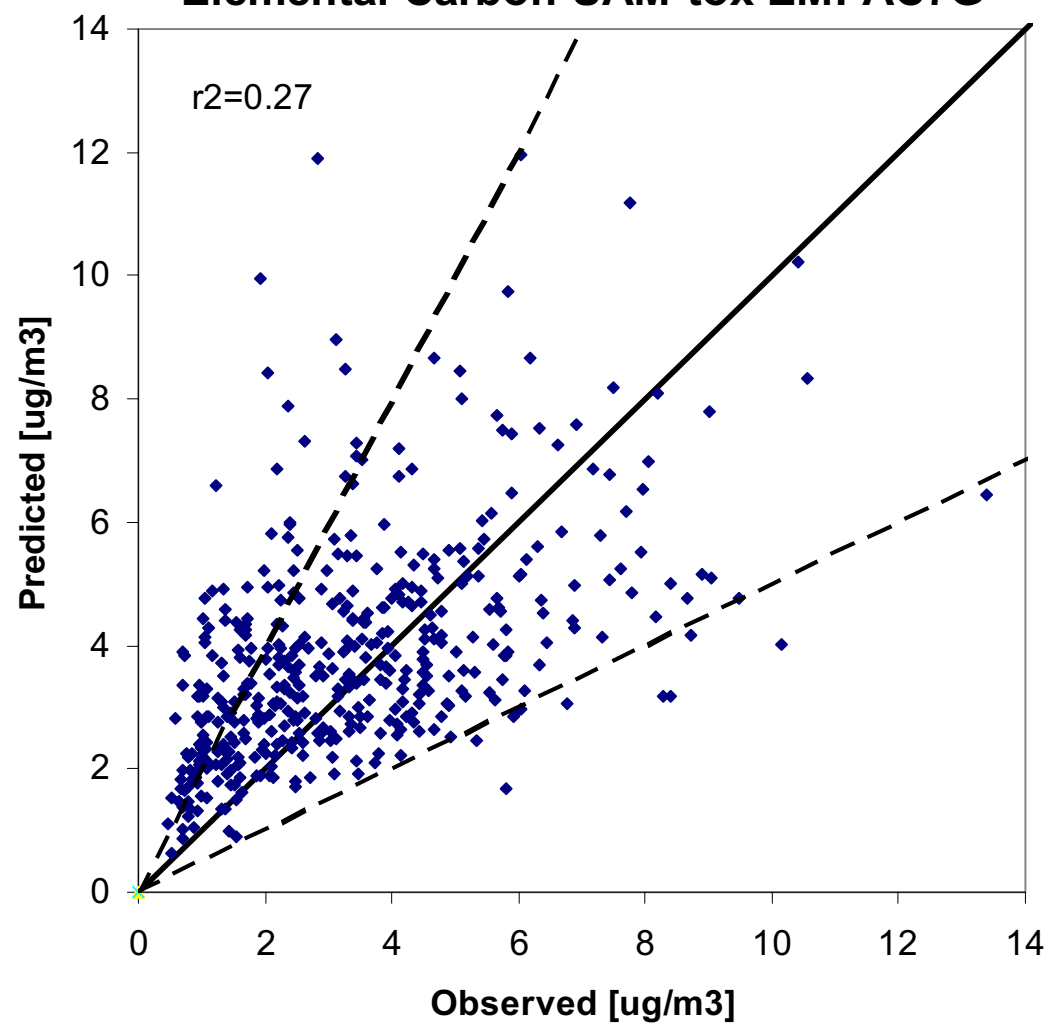




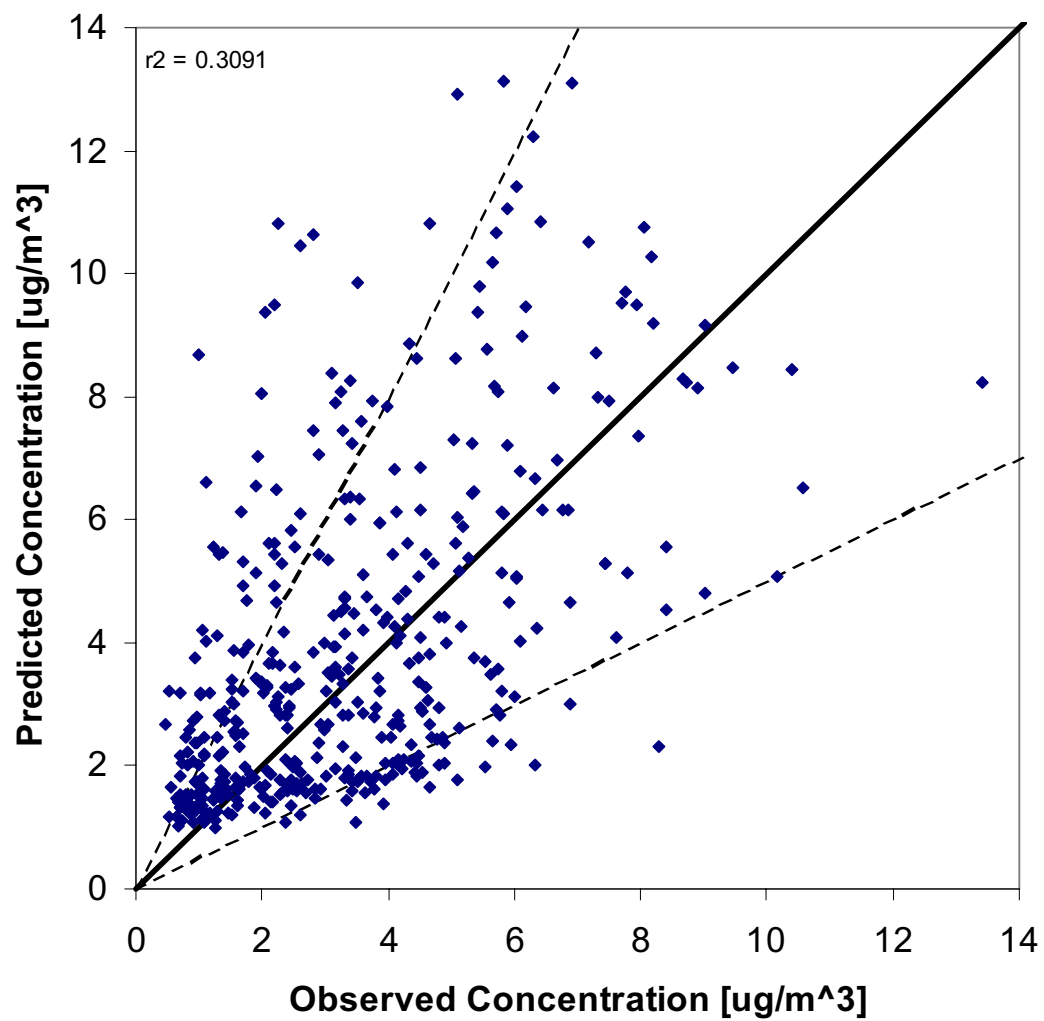




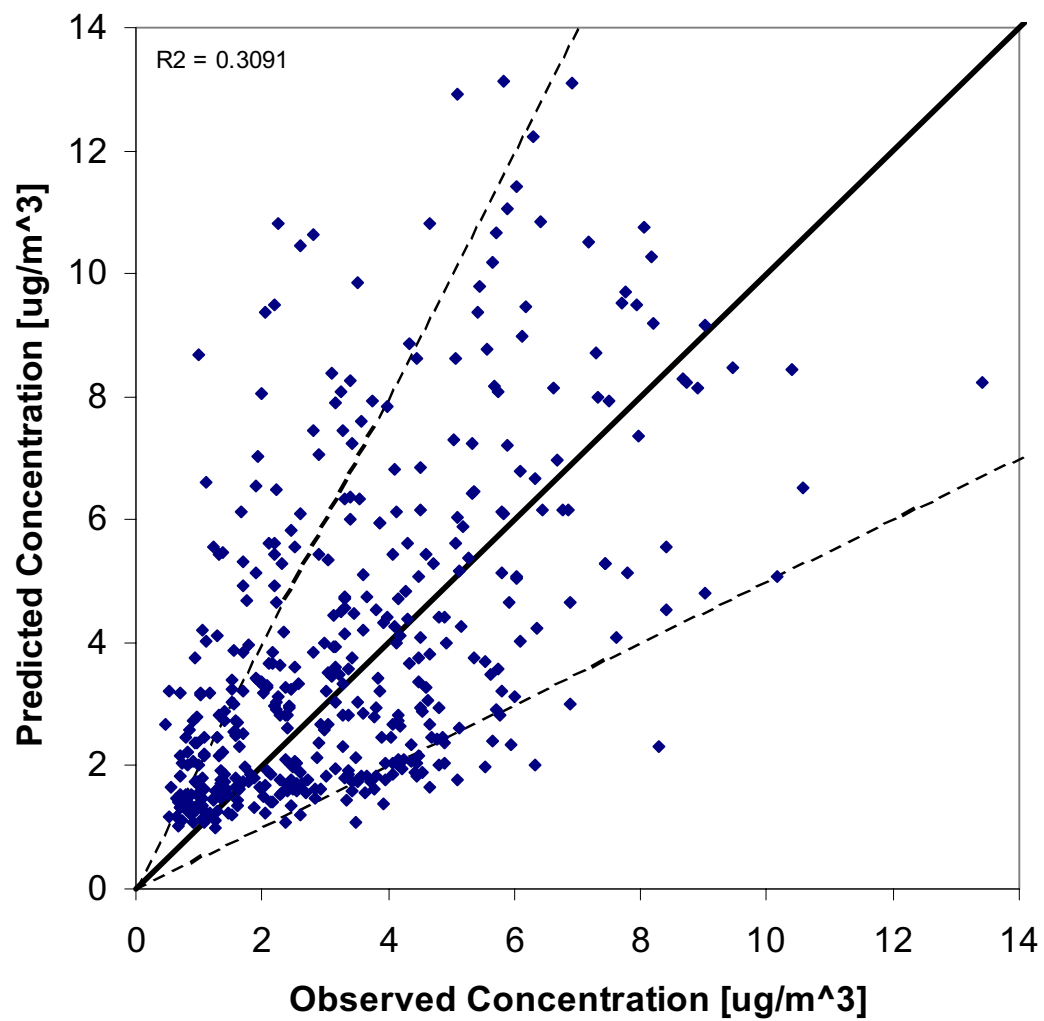
Elemental Carbon UAM-tox EMFAC7G



Elemental Carbon CAMx EMFAC7G



Elemental Carbon CAMx EMFAC2000



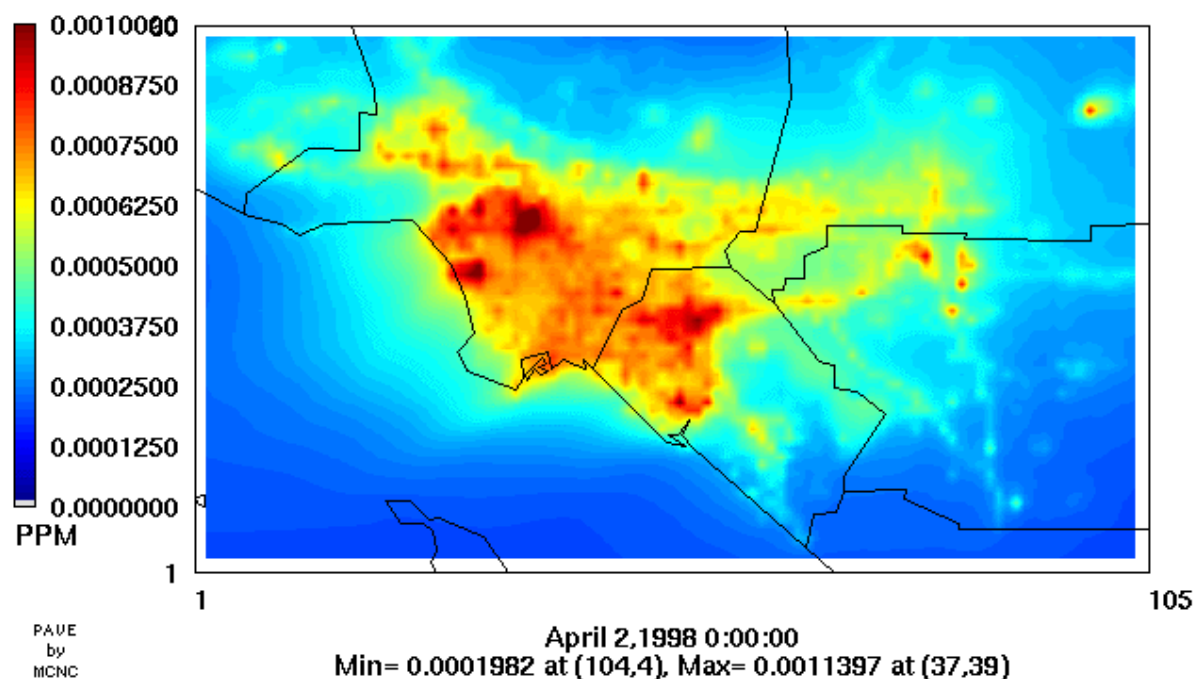
APPENDIX B

Spatial Distribution of Annual Average Concentrations
Estimated by CAMx/EMFAC2000 for:

Benzene (ppm)
1,3-Butadiene (ppm)
Primary Acetaldehyde (ppm)
Secondary Acetaldehyde (ppm)
Primary Formaldehyde (ppm)
Secondary Formaldehyde (ppm)
Ratio of Primary to Total Acetaldehyde
Ratio of Primary to Total Formaldehyde
Chromium PM_{2.5} (µg/m³)
Chromium PM_{2.5-10} (µg/m³)
Hexavalent Chromium PM_{2.5} (µg/m³)
Hexavalent Chromium PM_{2.5-10} (µg/m³)
Diesel PM_{2.5} (µg/m³)
Diesel PM_{2.5-10} (µg/m³)
“Elemental” Carbon PM_{2.5} (µg/m³)
“Elemental” Carbon PM_{2.5-10} (µg/m³)

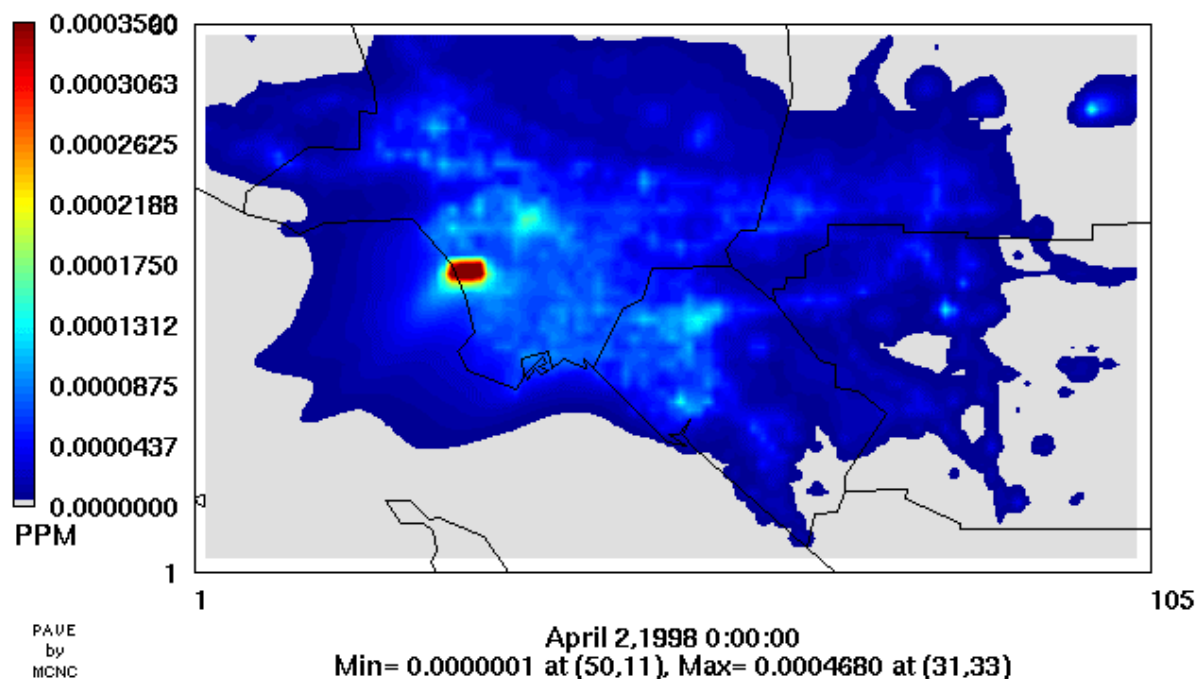
CAMx_Annual_Average

EMFC2000
Benzene



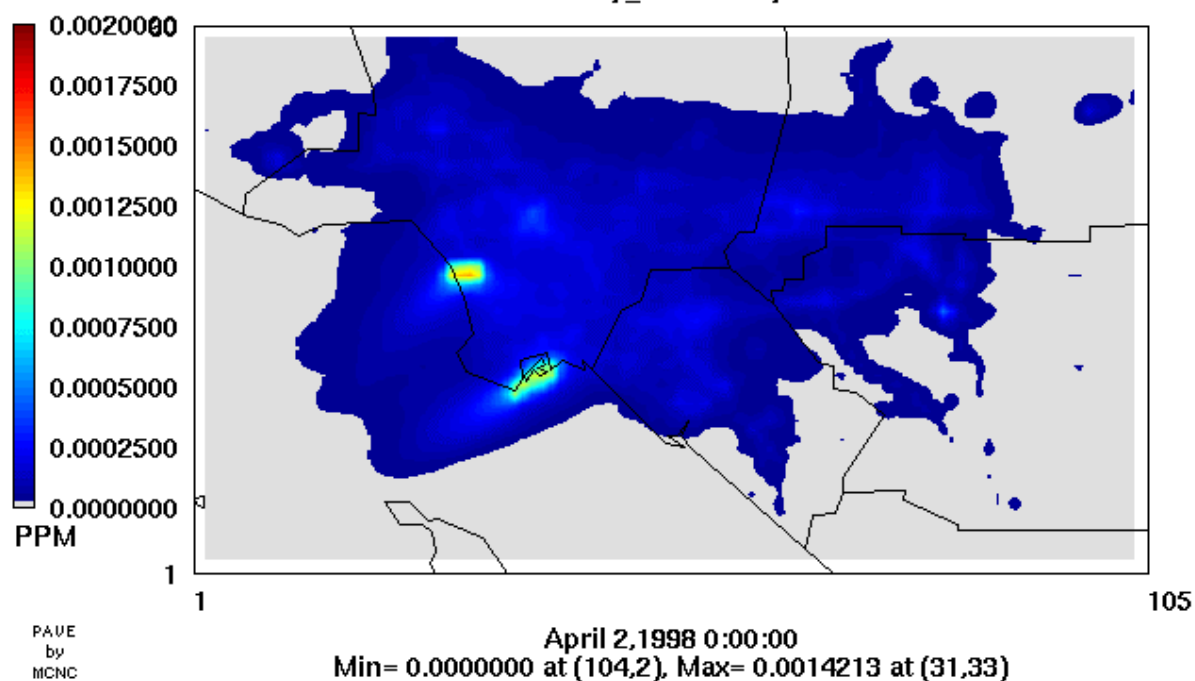
CAMx_Annual_Average

EMFC2000
1,3-Butadiene



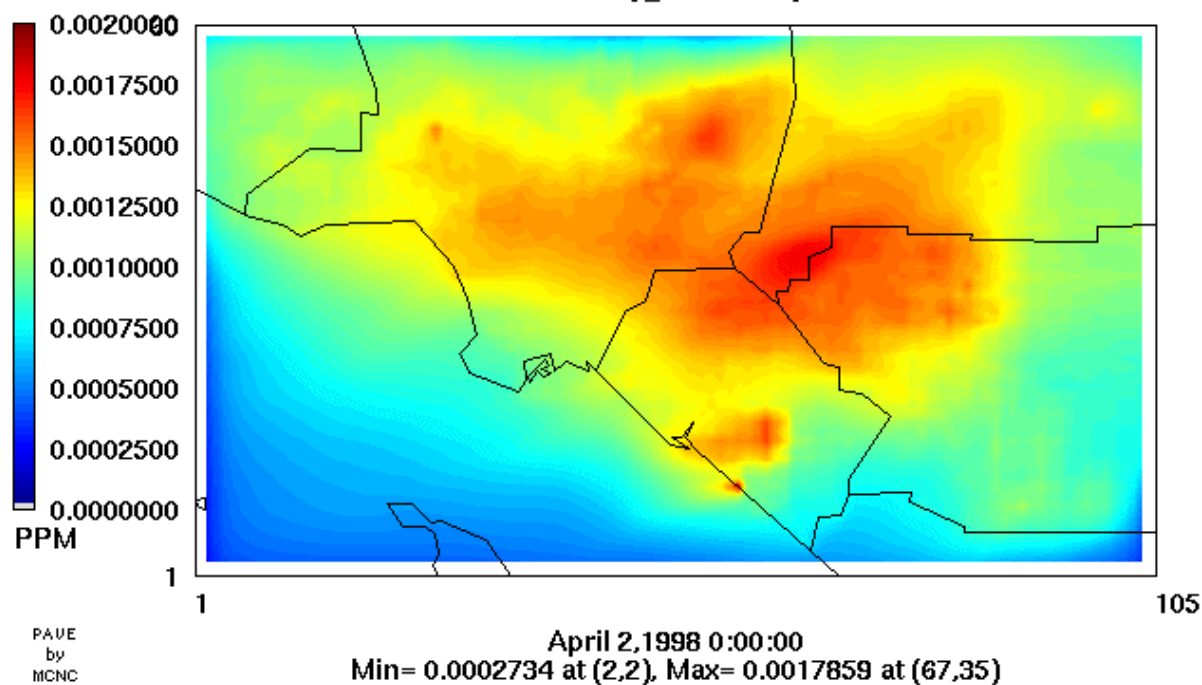
CAMx_Annual_Average

EMFC2000
Primary_Acetaldehyde



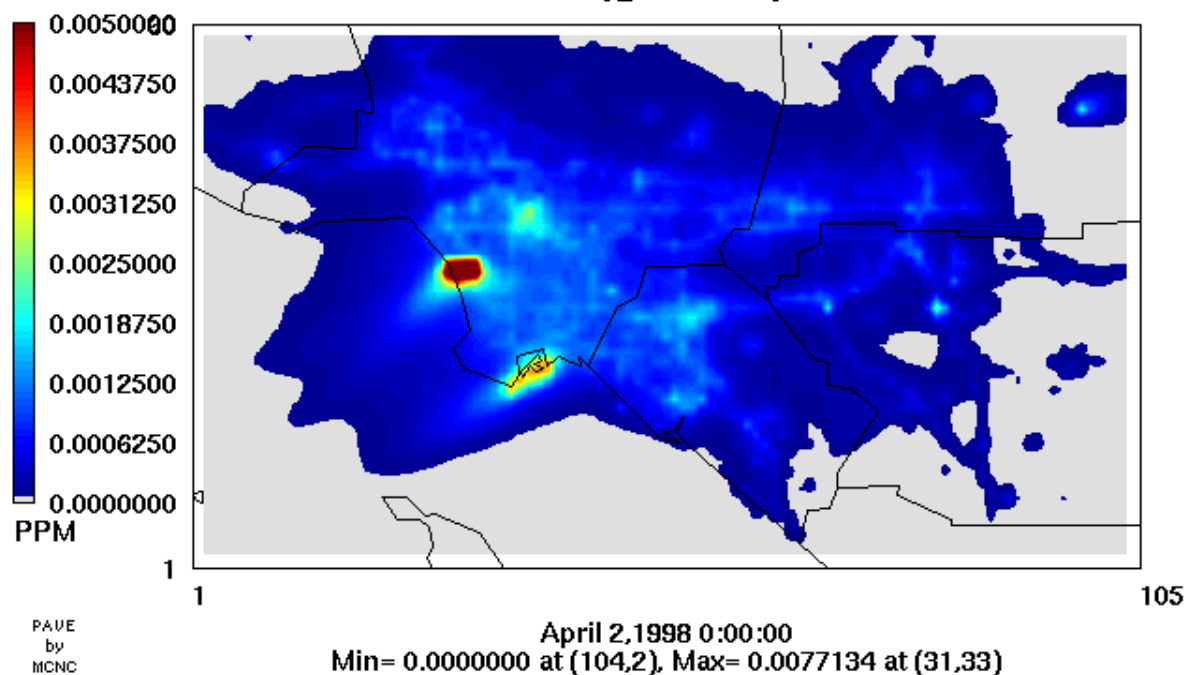
CAMx_Annual_Average

EMFC2000
Secondary_Acetaldehyde



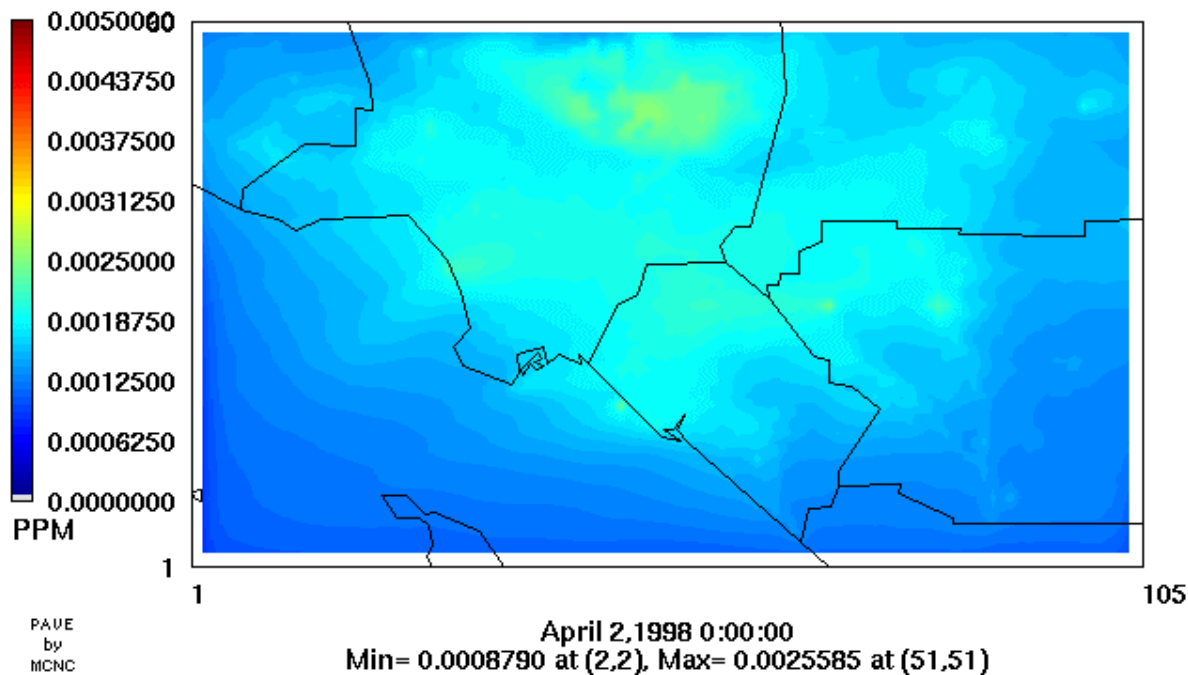
CAMx_Annual_Average

EMFC2000
Primary_Formaldehyde

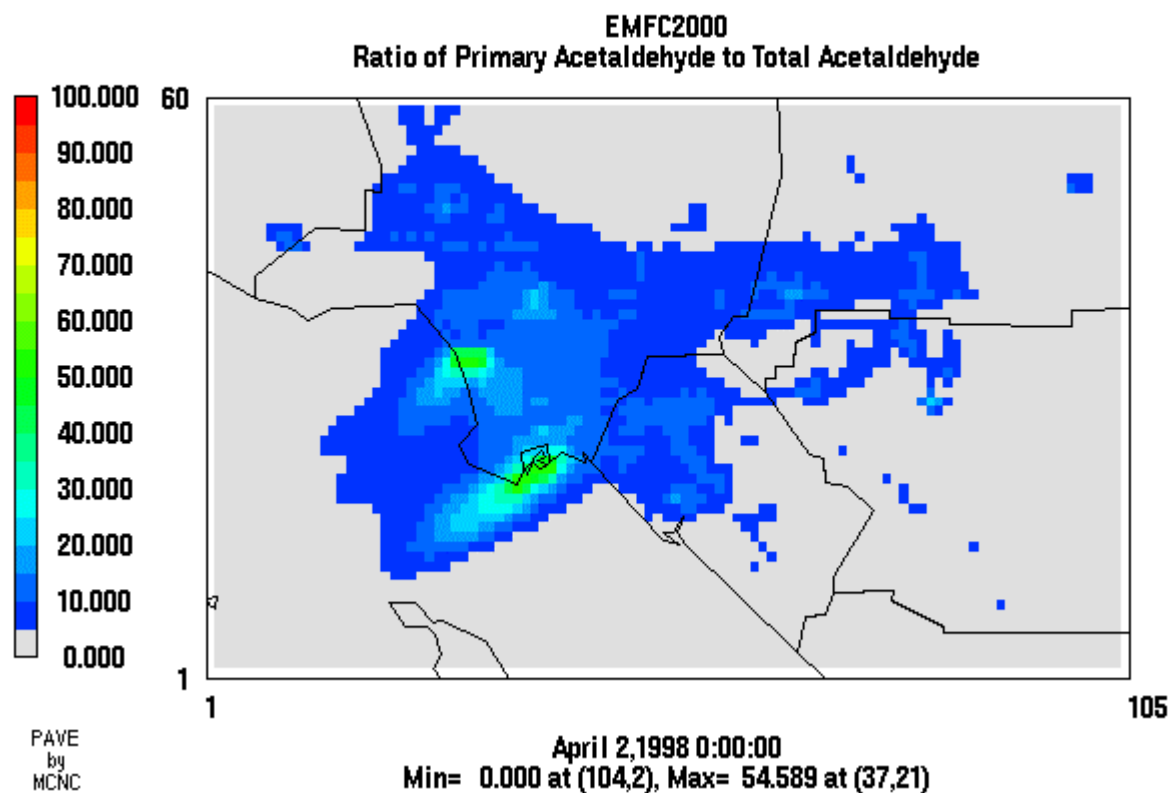


CAMx_Annual_Average

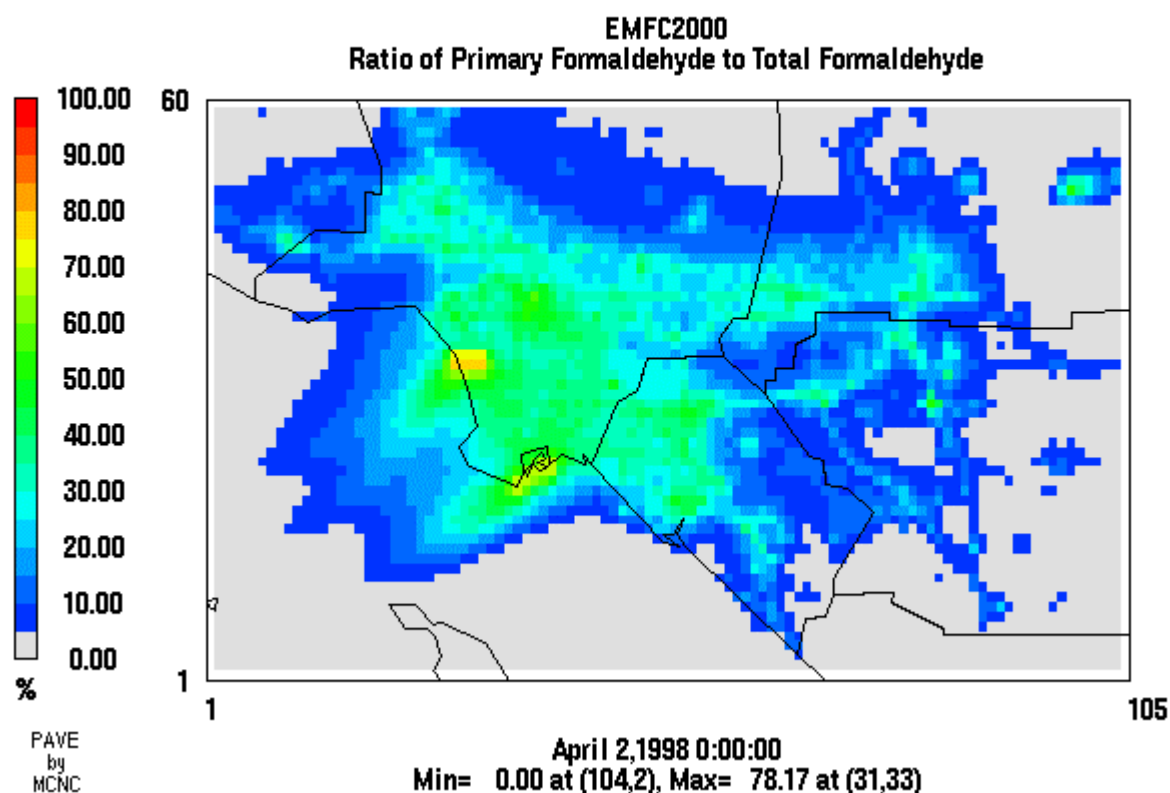
EMFC2000
Secondary_Formaldehyde



CAMx Annual Average

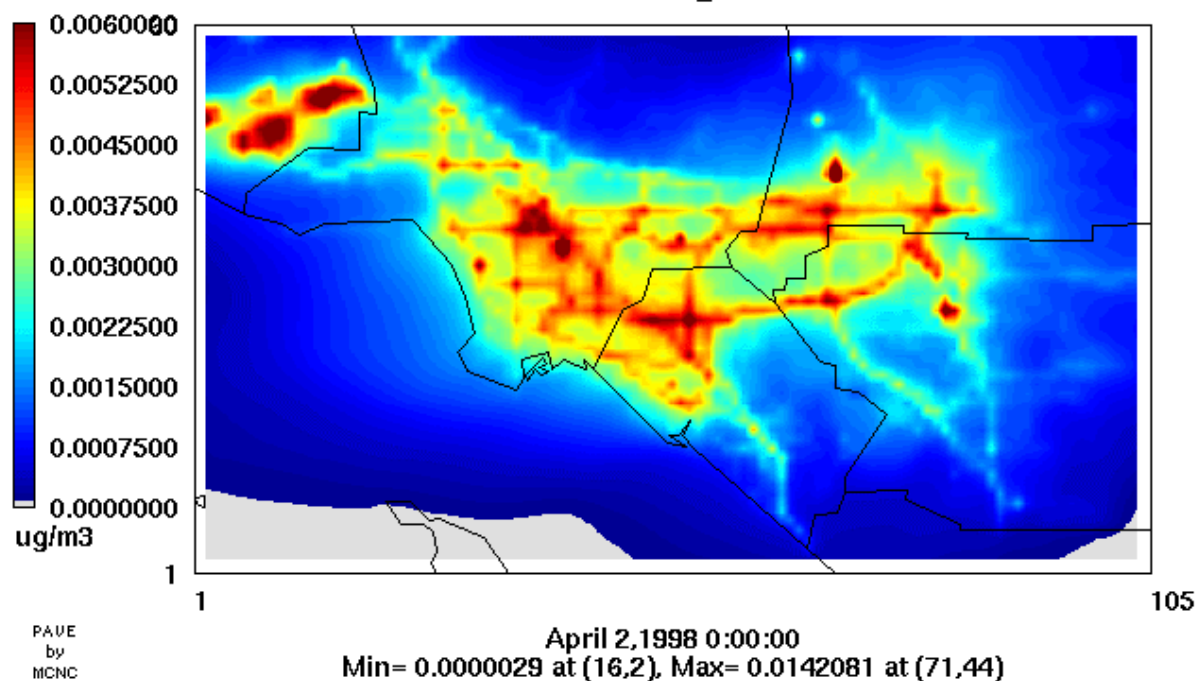


CAMx Annual Average



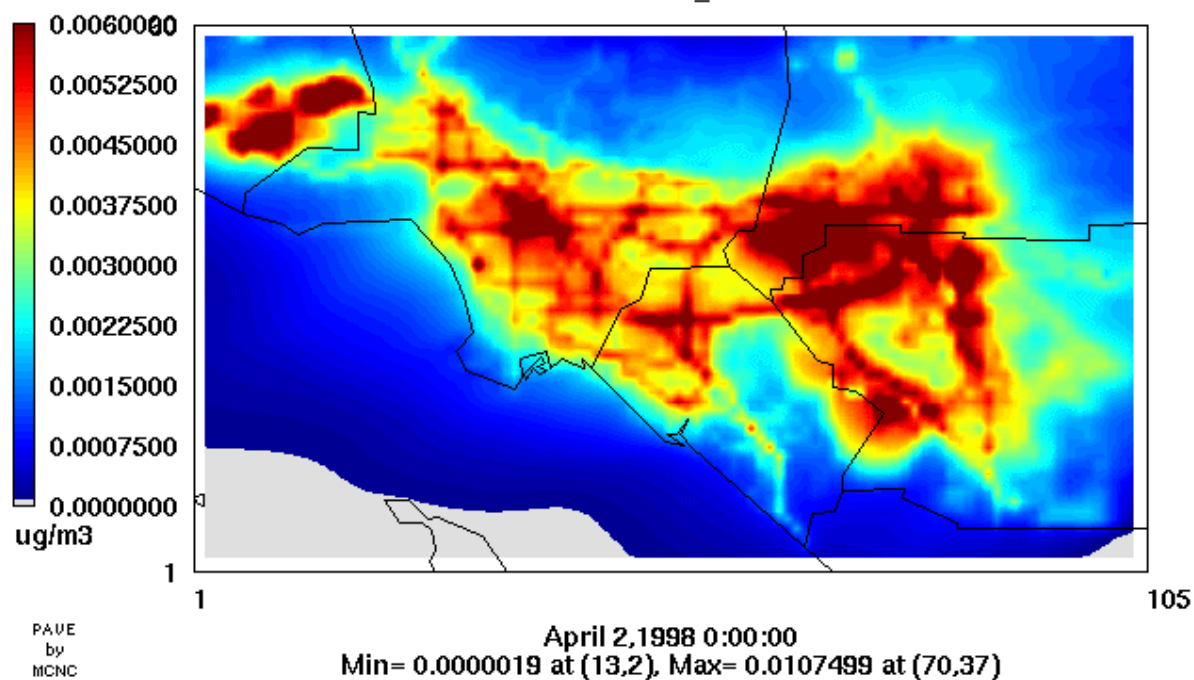
CAMx_Annual_Average

EMFC2000
Chromium_PM25



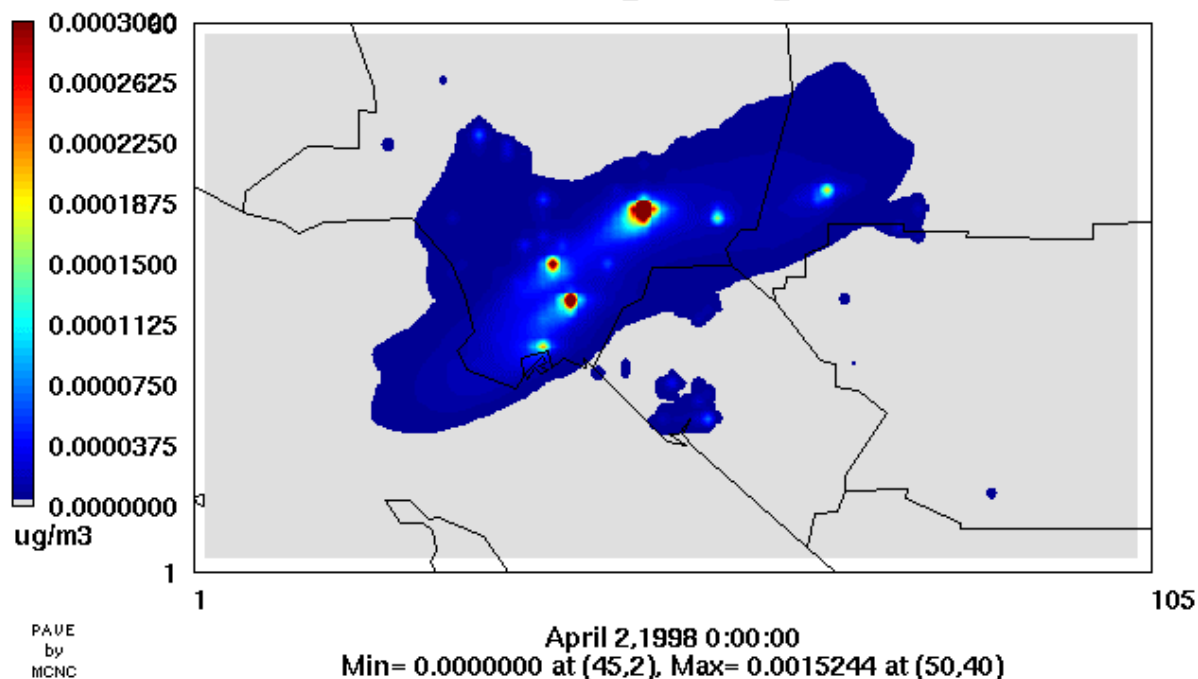
CAMx_Annual_Average

EMFC2000
Chromium_PM10



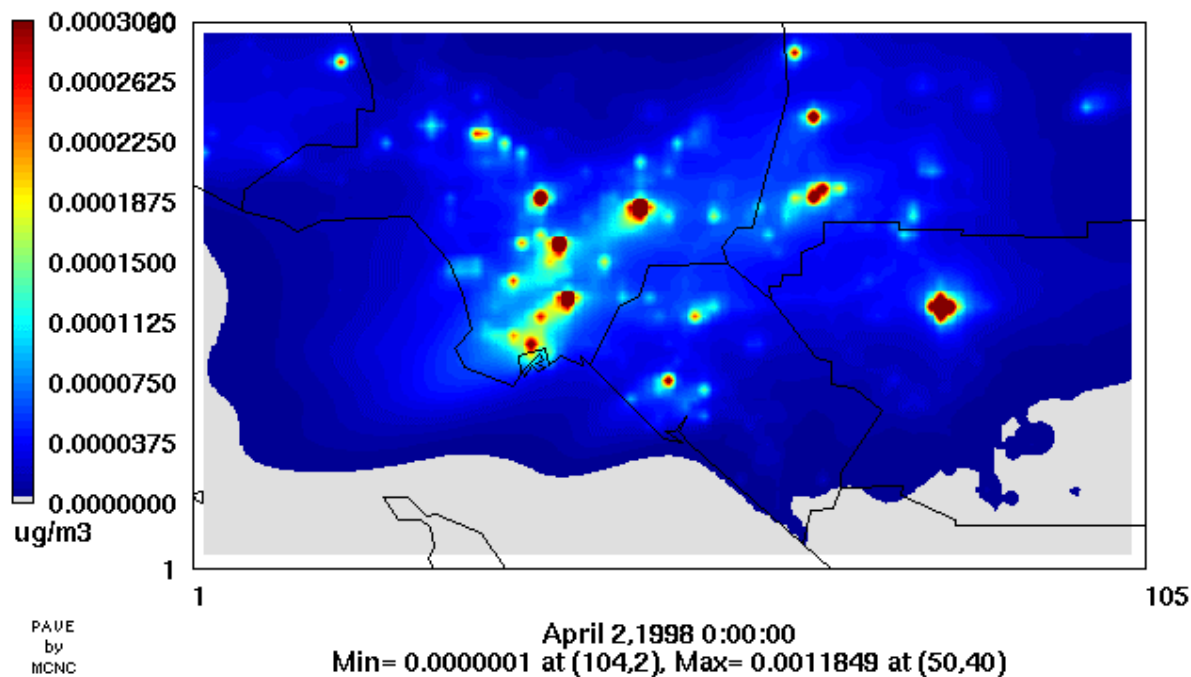
CAMx_Annual_Average

EMFC2000
Hexavalent_Chromium_PM10



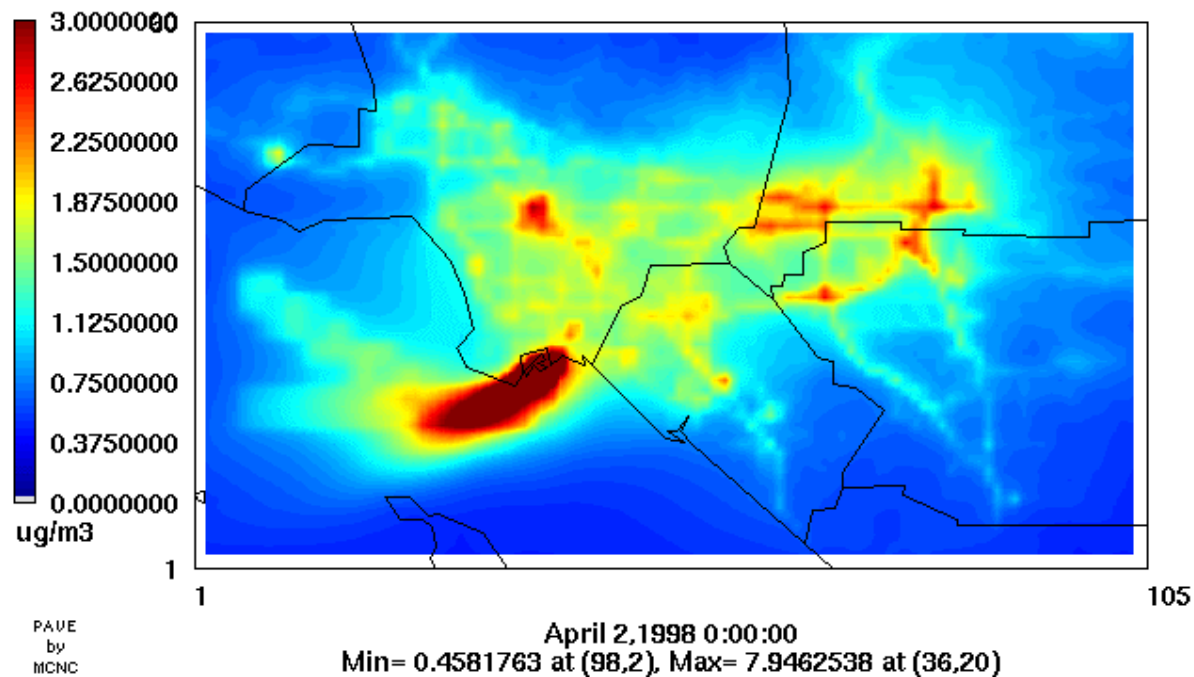
CAMx_Annual_Average

EMFC2000
Hexavalent_Chromium_PM25



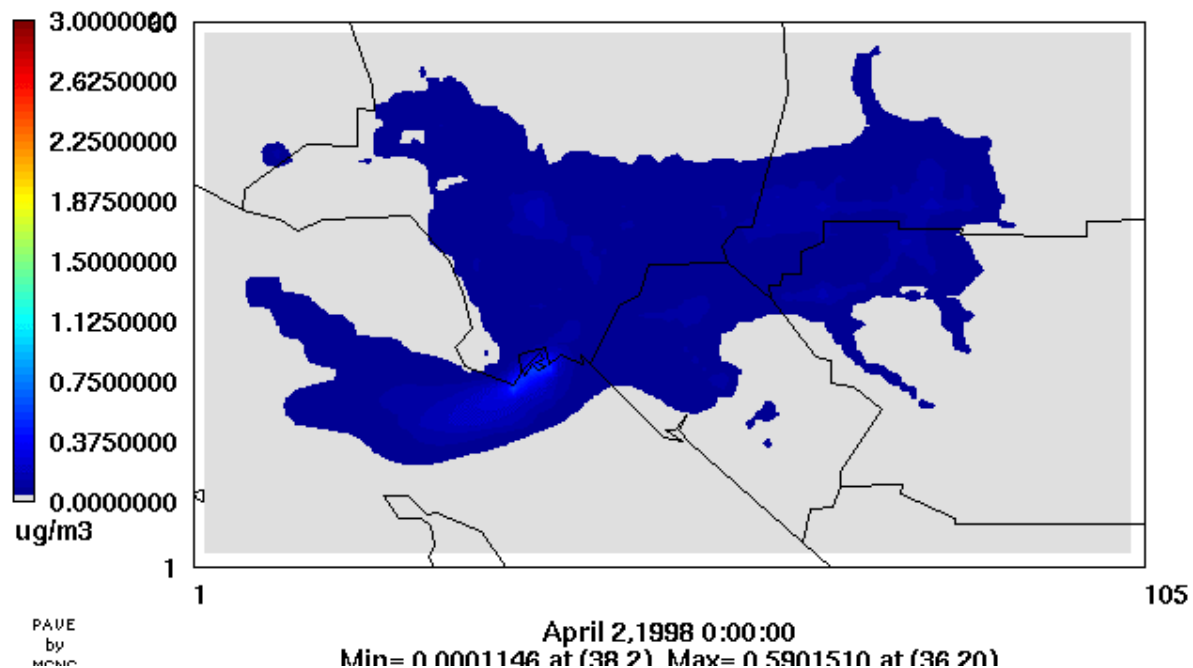
CAMx_Annual_Average

EMFC2000
Diesel_PM25



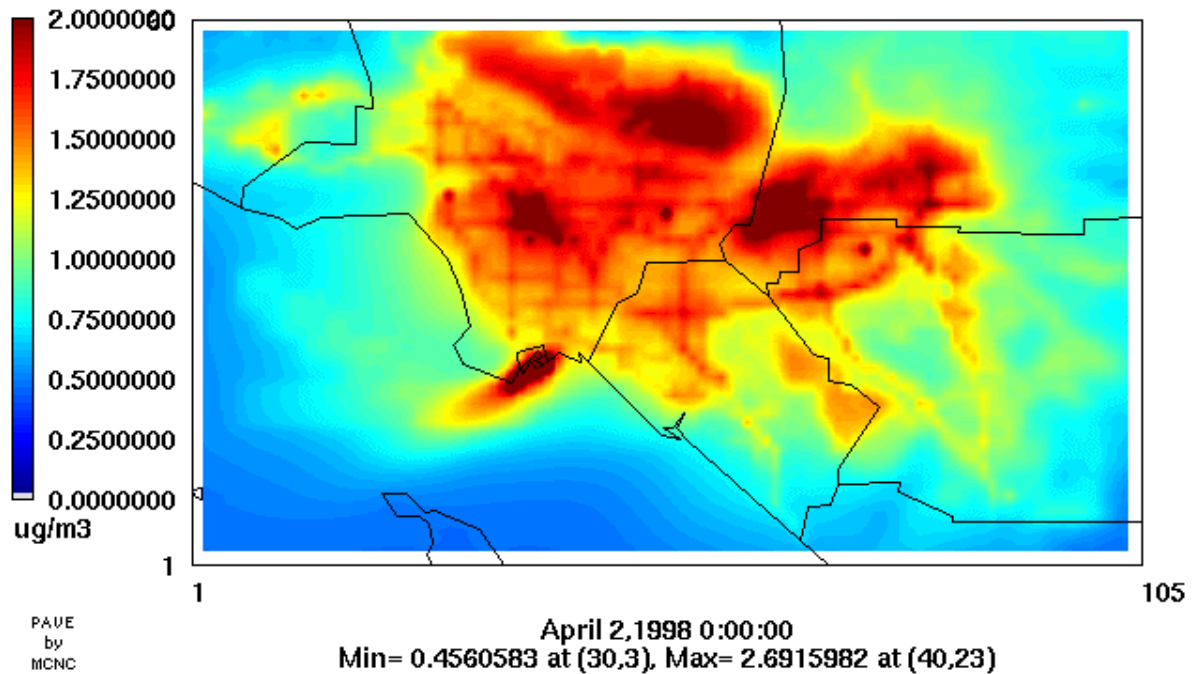
CAMx_Annual_Average

EMFC2000
Diesel_PM10



CAMx_Annual_Average

EMFC2000
Elemental_Carbon_P25



CAMx_Annual_Average

EMFC2000
Elemental_Carbon_PM10

